DETERMINATION OF BENT-CAP AND STRINGER DEFLECTIONS FOR TIMBER RAILWAY BRIDGES UNDER LIVE LOAD

A Thesis

by

LISA NOEL RACHAL

Submitted to the Office of Graduate and Professional Studies of
Texas A&M University
in partial fulfillment of the requirements for the degree of

MASTER OF SCIENCE

Chair of Committee,	Gary Fry
Committee Members,	W. Lynn Beason
	Anastasia H. Muliana
Head of Department,	Robin Autenrieth

May 2016

Major Subject: Civil Engineering

ABSTRACT

Many aging timber railroad bridges are currently in use throughout the United States, and these bridges are being exposed to increasingly heavy loads from rolling stock and other harsh conditions. This could lead to flexural failure or horizontal shear cracking of the stringers, which could result in a split stringer. The maximum flexural stress in a split stringer is two times larger than that of an unimpaired stringer when exposed to the same load. This thesis outlines the instrumentation and analysis of a small-scale timber bridge model and two large-scale bridges in order to better understand a timber railroad bridge's response to a live load. String potentiometers were used to measure bent-cap and stringer deflections, and wheel path position sensors were created and installed in order to determine vehicle speed and position as it traversed the bridge. Each test included different experimental parameters, such as different vehicle speeds and vehicle types.

During the course of each experiment, the bent-caps experienced very little deflection when under live load. It was also determined that vehicle speed did not significantly affect bent-cap deflection, total stringer mid-span deflection, or net stringer mid-span deflection. In the past, it has been assumed that stringers comprising a chord acted as one member. However, the results of this research demonstrated that each stringer in a chord experienced extremely different deflections in response to a vehicle traversing the bridge. This research also demonstrated a significant difference between the magnitude of the maximum total mid-span stringer deflections and the maximum net mid-span stringer deflections. The total mid-span stringer deflections were anywhere from 36% to 80% higher than the net deflections. It was also concluded that the maximum mid-span stringer deflection that occurred as a freight train traversed a bridge were due to the trucks that were on each side of the couplings connecting the rolling stock. In addition, the mid-span deflections of a split stringer were found to be four times larger than that of an unimpaired stringer when exposed to the same live load.

ACKNOWLEDGEMENTS

I would like to extend my gratitude to numerous individuals whom, without their guidance and support, this research would not have been possible. First of all, I would like to express my sincere appreciation for my committee chair, Dr. Gary Fry. I am extremely grateful and indebted to him for his expert guidance and genuine encouragement throughout my academic development.

I thank my committee members, Dr. W. Lynn Beason and Dr. Anastasia Muliana, for their guidance and support. I would also like to express appreciation for my research group. They have provided invaluable support and advice throughout the course of this research. Mrs. Amy White has provided extensive support for my research, and for that, I would like to express my extreme gratitude. I would also like to thank Dr. David Allen for his guidance and review of my thesis.

Union Pacific Railroad has been instrumental in the process of this research. In particular, I would like to thank Mr. Jeff Mancuso for his support of this work and for the opportunity to instrument and gather data from an open deck bridge. I would also like to thank Mr. Sandro Scola with Canadian National Railway Company for his support and the opportunity to instrument and gather data from a ballast deck bridge.

Lastly, I would like to thank my parents. They provided a warm, encouraging environment for me to dream big and flourish. They have extended unconditional love and support throughout my entire academic experience, and for that I am forever grateful.

NOMENCLATURE

AAR	Association of American Railroads
c	the distance from the neutral axis to the extreme fiber of the beam
C_1, C_2	constants of integration
CN	Canadian National Railway Company
$\frac{d^2y}{dx^2}$	the curvature of the beam's neutral surface
E	modulus of elasticity
EI	flexural rigidity
GVW	gross vehicle weight
I	the moment of inertia of the cross-section with respect to the neutral axis
L_i	the center-to-center distance of a wheel path proceeding wheel path 1 to wheel path 1
L_{ms}	the distance from the bent-cap prior to the span of interest to the middle of the span of interest
L_s	length of the span of interest
M	bending moment
$M(x)$	bending moment as a function of the distance x
t_1	the time that wheel path 1 crossed the middle of the span of interest
t_i	the time that a wheel path proceeding wheel path 1 crossed the mid-span of interest
t_s	the time it took the vehicle to cross the span of interest
t_{wp1}	the time that wheel path 1 crossed the bent-cap prior to the span of interest
UP	Union Pacific Railroad
V_s	the velocity of the vehicle while traversing a span of interest
x	the distance of the observation point from the left end of the beam
y	the deflection of the beam at the observation point x
δ_{avg}	the average of the deflection at the south end of the stringer and the deflection at the north end of the stringer

δ_n	the deflection at the north end of a stringer
δ_{net}	the net mid-span deflection of a stringer
δ_s	the deflection at the south end of a stringer
δ_{total}	the total maximum deflection at the middle of a stringer
σ_m	maximum flexural stress
σ_{ms}	maximum flexural stress in the split stringer

TABLE OF CONTENTS

Page

LIST OF FIGURES

Page

LIST OF TABLES

Page

CHAPTER I
INTRODUCTION

1.1 Introduction

A significant number of aging timber railway bridges have been in continuous use for many years. These bridges comprise piles, bent-caps, stringers, and cross ties, shown in Figure 1.1. Each round timber pole, or a pile, is installed deep in the ground using a pile driver. The exterior piles are usually installed at an angle for increased stability. A bent, which consists of 3 to 5 piles with lateral bracing, supports a bent-cap. Bents are typically spaced about 15 feet apart, and they support several stringers, which are the main structural element of the timber bridge and the focus of this research. The stringers provide support for the shorter cross ties, which, in turn, provide direct support for the rails.

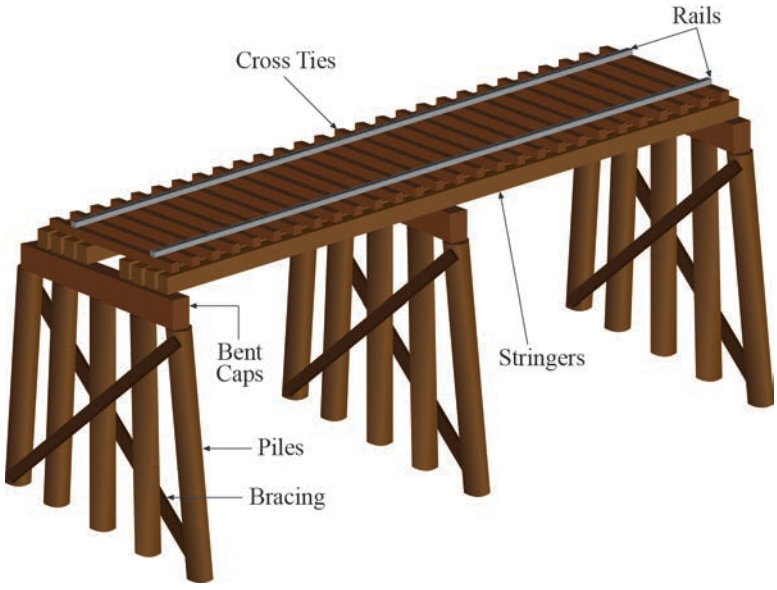

Figure 1.1: Timber Railway Bridge Configuration

Throughout their lifespan, timber bridges are exposed to increasingly heavy loads from trains, harsh weather conditions, and insects that destroy wood. These exposures can cause the timber to lose its strength over time, which in turn can cause increased deflections in the stringers and crushing of the bent caps. The increased stringer deflections could lead to flexural failure or shear cracking, which results in split stringers. Shear cracking can significantly reduce the stringer's flexural strength due to a reduction in the area available to resist load.

While the failure of another element in the timber bridge, such as a cross tie, would be serious, the failure of a stringer would be a much more severe event. As seen in Figure 1.1, the stringer spans long distances between each bent. This makes the stringers subject to higher deflections. Because they support the weight of the train, rails, and cross ties, the entire structural system could collapse if only one stringer were to fail, which would be catastrophic and could possibly lead to fatalities. For these reasons, it is crucial that each stringer's flexural behavior is thoroughly understood and monitored to guarantee that the respective timber bridge is safe and efficient.

1.2 Objective

The goal of this research is to obtain and analyze bent cap and stringer deflections of a timber railway bridge under live load. The analysis of this data will provide a better understanding of how aging bent caps and stringers behave while in service. In order to obtain these deflections from the timber bridge, the following objectives must be met:

1. Develop a data acquisition system and sensor network for testing,
2. Develop and implement a wheel path position sensor system,
3. Design and conduct experiments on a small-scale bridge, and
4. Conduct large-scale experiments to collect bent cap and stringer deflections as a railcar traverses a timber railway bridge.

1.3 Background on Timber Railway Bridges

During the late 19th century, the United States experienced an industrial revolution that was heavily influenced by the building of the transcontinental railroads. Approximately 45,000 miles of railroad track were constructed before 1871, and then an additional 170,000 miles of track were added between 1871 and 1900 (Library of Congress 2014). This growth created a tremendous demand for timber railway bridges. By the mid-1950's, approximately 1,800 miles of timber bridges had been built to serve our nation's railroad system (Ritter 1990). Although they only have design life span of approximately 40 years, most of these timber bridges and trestles are still in service today (Ritter 1990).

In addition to the timber's natural aging process, a desire to increase productivity has caused a significant increase in axle loadings over the past 50 years (Martland 2013). Most railroads were originally developed to withstand a 200,000 lb. gross vehicle weight (GVW). During the 1970s, a 263k GVW car was introduced that demanded stronger materials, better designs, and improved maintenance techniques (Martland 2013). In 1991, the railroad industry began accepting railcars with 286k GVW (Martland 2013). By 2010, nearly 100% of coal traffic and 30% of general freight were moved by 286k GVW cars (Martland 2013). This is a 70% increase in axle loadings over the course of 40 years. Currently, most major lines are allowing 315k GVW railcars to operate on their rail systems (Figure 1.2).

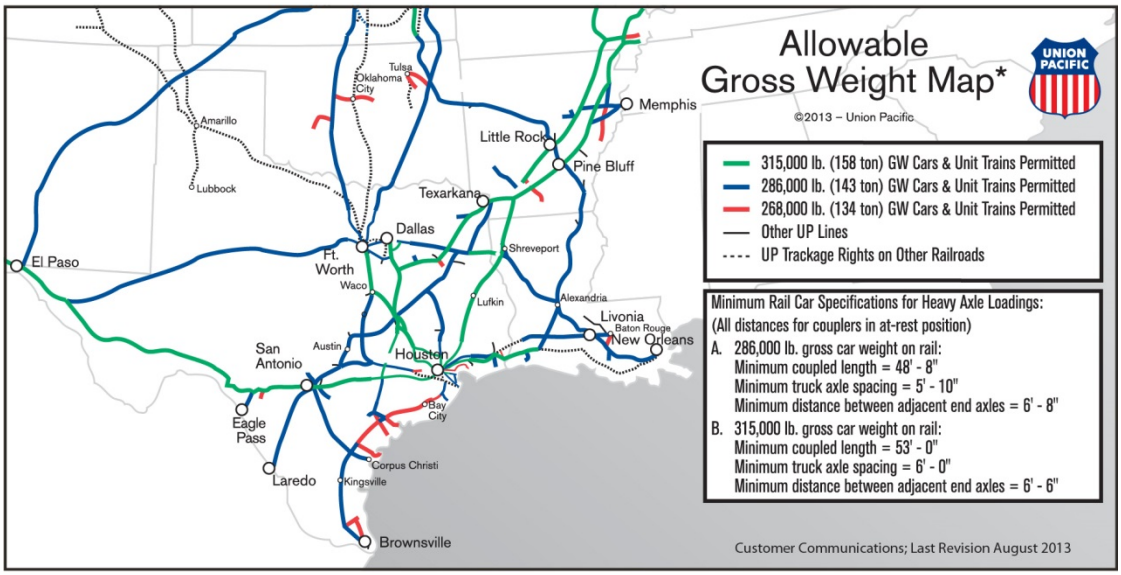

Figure 1.2: Union Pacific Gross Allowable Weight Map (Union Pacific 2013)

According to the National Bridge Inventory, out of the 41,743 total timber bridges currently in use, 19,738 of those bridges are considered structurally deficient (Duwadi and Wood 2006). While this inventory takes all bridges into account, one can assume that many of these timber bridges are a part of the US railroad system. This means that within the United States railroad network, there are thousands of aging timber bridges that require inspection and that a large percentage of those need rehabilitation.

1.4 Theoretical Effect of Loading Timber Stringers

Horizontal cracking can significantly reduce the stringer's flexural strength due to a reduction in the area available to resist load. A crack can continue to form along the entire length and width of the stringer. When this happens, the stringer is referred to as "split". A split stringer can be considered two separate beams, as shown in Figure 1.3. Usually, this occurs at the neutral surface of the stringer.

Figure 1.3: Split Stringer Caused by Shear Cracking

The maximum flexural stress in a beam with a rectangular cross-section in pure bending is given by:

$$\sigma_m = \frac{Mc}{I} \qquad \textbf{Equation 1.1}$$

where σ_m is the maximum stress, M is the moment, c is the distance from the neutral axis to the extreme fiber of the beam, and I is the moment of inertia of the cross-section with respect to the neutral axis (Figure 1.4a).

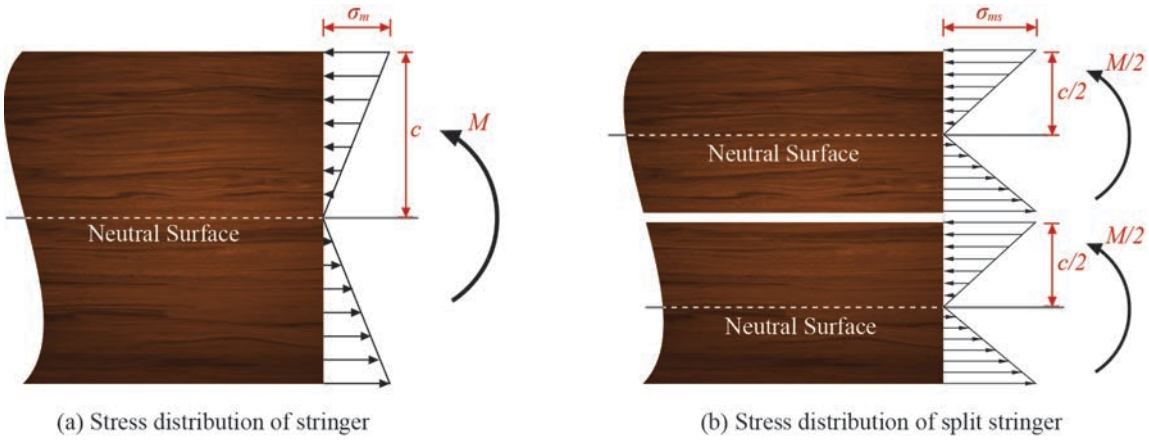

Figure 1.4: Flexural Stress Distributions

When a stringer is split, half the moment, M, acts on each section, the moment of inertia, I, of each section is $1/8^{th}$ of its previous value, and c of each section is half of its previous value (Figure 1.4b). These changes lead to a new equation for a split beam with a rectangular cross-section in pure bending:

$$\sigma_{ms} = \frac{\left(\frac{M}{2}\right)\left(\frac{c}{2}\right)}{\left(\frac{I}{8}\right)} = \frac{2Mc}{I} = 2\sigma_m \qquad \textbf{Equation 1.2}$$

Equation 1.2 shows that the maximum flexural stress in the split stringer, σ_{ms}, is two times larger than the maximum flexural stress in the original stringer, σ_m.

The deflection in a statically determinate, elastic beam in pure bending can be found using the equation for the elastic curve of the beam:

$$\frac{d^2y}{dx^2} = \frac{M(x)}{EI} \qquad \textbf{Equation 1.3}$$

where $\frac{d^2y}{dx^2}$ is the curvature of the beam's neutral surface, x is the distance of an observation point from the left end of the beam, $M(x)$ is the moment as a function of the distance x, E is the modulus of elasticity of the stringer, and EI is the flexural rigidity of the stringer. When integrated with respect to x twice, the equation for deflection can be written as:

$$EI\ y = \int_0^x \left[\int_0^x M(x)\,dx + C_1\right] dx + C_2 \qquad \textbf{Equation 1.4}$$

where y is the deflection of the beam at an observation point x, and C_1 and C_2 are two constants of integration that can be determined from the boundary conditions imposed on the beam by its supports.

When a beam is split, the flexural rigidity (EI), in Equation 1.4 is affected. Because the moment of inertia, I, of each section in the split stringer is $1/8^{th}$ of the original value, the total moment of inertia for the split sections acting together is I/4. Therefore, the theoretical flexural rigidity of the split stringer is EI/4, which means that there is a 75% reduction in flexural rigidity of the stringer. The deflection of a statically determinate, elastic split stringer in pure bending is given by:

$$\frac{EI}{4}\, y = \int_0^x \left[\int_0^x M(x)\, dx + C_1 \right] dx + C_2 \qquad \textbf{Equation 1.5}$$

Equation 1.5 demonstrates that, theoretically, the deflections of the split stringer are four times as large as the unimpaired stringer (Figure 1.5).

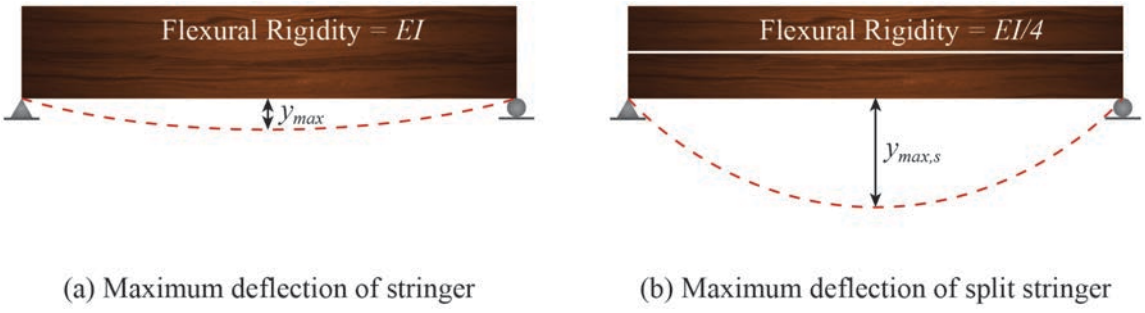

(a) Maximum deflection of stringer (b) Maximum deflection of split stringer

Figure 1.5: Maximum Stringer Deflection

Because this is a large difference, the serviceability of the stringer might be compromised or, even worse, horizontal cracking or failure due to flexure may occur.

1.5 Fatigue Analysis of Timber Railway Bridge Stringers

Field observations have revealed that stringers are susceptible to fatigue damage caused by increasingly heavy axle loads. Research on timber fatigue has been developing since the 1940s, but the initial tests were extremely limited (Jones and Fry 1997). The Forest Products Laboratory added 11 bending machines in order to test for fatigue in timber in 1942 and then conducted a series of static bending tests on full-size timber stringers. Around the same time, clear specimens were being tested for fatigue and block shear at Purdue University (Leggett 1954).

In 1959, the Association of American Railroads (AAR) attempted to relate the experimental data gathered from testing of full size stringers with that of small model specimens in four-point bending. It was observed that all the initial fatigue failures for the full size stringers originated from pre-existing cracks and occurred in horizontal shear near the neutral axis. Two small specimens were taken from the failed full size stringers, one from the tension zone and one from the compression zone, and tested for block shear. These tests revealed that the values of ultimate shearing strength were higher in the small specimens than in the full size stringers, and that there was a correlation between net horizontal shear and cycles to failure. Test results were also acquired from static bending tests on small clear specimens. These results suggested that the full size stringer could resist at least 30 million cycles if the bending stress of the full size stringers did not surpass 50% of the flexural strength of the small clear specimens.

W.C. Lewis conducted tests to investigate the fatigue behavior in four-point bending of approximately 300 quarter-scale southern pine and Douglas fir stringers (Lewis 1962). Specimens were put in groups of green wood, air-dried wood, and treated wood, and could have straight grain or 1:12 slope of grain. Artificial checks, with depths of approximately 20% of the specimen thickness, were produced at mid-depth of the air-dry and treated woods. Four-point bending and static bending tests were performed, and the data suggested that the repeated load strength of treated specimens was approximately

half of the static strength in bending. The estimated fatigue strength was approximately 30% of the static strength in the southern pine specimens. Also, tests revealed that the artificially checked specimens failed in horizontal shear when subjected to repeated loading.

Between 1962 and 1967, AAR conducted a series of static and fatigue tests in four-point bending on full-scale glue laminated and solid-sawn southern pine and Douglas fir stringers in order to determine the ultimate and fatigue timber strength in each type of timber (Bartell 2003). The results revealed that approximately 60% of all fatigue failures occurred in horizontal shear. A separate study in 1974 showed that the shear strength of timber beams is higher when the span-to-depth ratio is smaller (Keenan 1974). In 1990, Tsai and Ansell tested small clear specimens of Khaya ivorensis laminates, solid Sitka spruce, and laminated and densified beech laminates in flexural fatigue and four-point bending (Tsai and Ansell 1990). While the main focus of this research is railroad timber, the results from Tsai and Ansell's research provide an important insight into the behavior of timber in fatigue. Their results indicated that the overall failure modes were compression on the top surface of the specimen and tension cracks on the bottom that appeared just before failure.

More recent tests were implemented due to collaboration between Transportation Technology Center, Inc., a subsidiary of AAR, and Texas A&M University as a part of the AAR's Bridge Life Extension program from 1998 to 2000 (AAR 2001). This program focused on static and dynamic 4-point bending tests on different types of full-size timber stringers: 21 solid sawn, creosote-treated, southern pine and 24 solid sawn, creosote-treated, Douglas fir. These tests enabled researchers to generate fatigue data on the stringers, which could then be used to estimate the remaining stringer life and to assess the stringer's performance under heavy axle loads. One of the most predominant modes of failure in the timber stringers was horizontal shear cracking at approximately

mid-depth of the stringer. Test results also allowed researchers to establish a minimum value for allowable horizontal shear strength.

Texas A&M University elaborated on these efforts in 2000 by performing a static analysis on single-span and two-span continuous timber bridge models based on an existing bridge (Comardo 2000). This research focused on the use of solid sawn, creosote-treated, southern pine stringers and how they performed when subjected to heavy axle load operations. Three different trains were modeled to pass over the bridges: Train A – (3) 400k locomotives followed by (100) 263k hopper cars, Train B - (3) 400k locomotives followed by (100) 286k hopper cars, and Train C - (4) 400k locomotives followed by (100) 315k hopper cars. One important conclusion noted was that the estimated service lives for the two-span continuous stringer models were significantly less than those for the single-span stringer models.

In 2002, research was conducted at Texas A&M University on the fatigue life of under-strength timber railway bridge stringers (Borchers 2002). Nineteen southern pine solid-sawn stringers that were 7 in. wide by 14 in. deep by 16 ft. long were tested. The commercial grade of the stringers ranged from below No. 3 to No. 2, and they had all been pressure treated “to refusal” with creosote. Results from these tests indicated that large seasoning checks can predispose an under-strength member to fail in horizontal shear under fatigue loading. The resulting S-N curve suggested a natural fatigue limit against tensile failure at about 60% of the ultimate bending strength of the stringer. However, the resistance to shear failure appeared to be strongly dependent upon the pre-existing horizontal shear cracks in the stringer.

CHAPTER II
EXPERIMENTAL PROCEDURES

2.1 Instrumentation Selection and Layout

The main objective of this research is to obtain bent cap and stringer deflections for a timber railway bridge under live load. In order to acquire this data, a timber railway bridge that is currently in use needs to be instrumented. Any instrumentation used in this field test needs to be implemented in a non-destructive manner so that no part of the bridge or locomotive is damaged. Therefore, non-destructive methods of measuring deflection, identifying locomotive wheel position, and acquiring data will need to be implemented.

2.1.1 Deflection Measurement

Vertical deflection can be measured using many different methods that can range from using a yardstick to using electronic devices. This particular research demands not only accuracy and precision, but also a high sample rate because of the velocity of a traversing locomotive. Because of these stipulations, string potentiometer-based displacement transducers were used to measure bent cap and stringer deflection.

A string potentiometer-based displacement transducer, commonly referred to as a "string pot", is used to measure the linear displacement of on object. They are generally precise, durable, and inexpensive. These transducers comprise four main parts: a displacement cable, threaded spool, torsion spring, and rotational sensor (Figure 2.1).

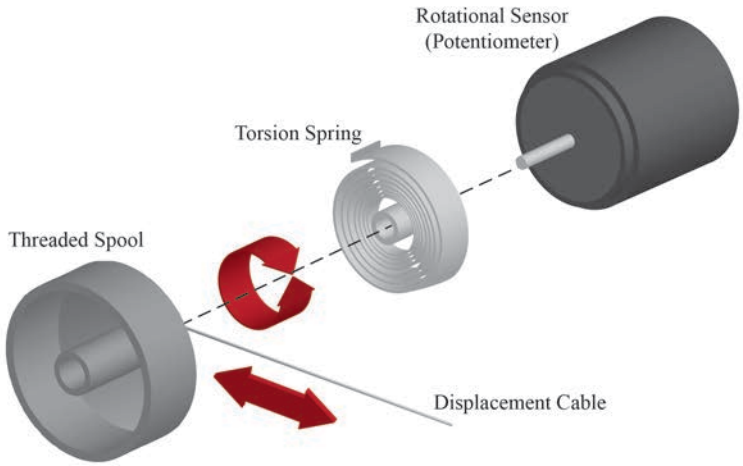

Figure 2.1: String Potentiometer-Based Displacement Transducer Configuration

The stainless steel displacement cable is wound on the threaded spool so that it turns as the cable moves. The spool is connected to both a torsion spring, so that the cable will remain tensioned, and to the shaft of a rotational sensor, or potentiometer.

A potentiometer is a resistor with three nodes: a voltage input, a ground, and a movable element, called a wiper (Figure 2.2). The wiper makes contact with a resistive metal wire, called the slidewire, at any point during its displacement. As the cable is pulled in or out of the string pot, it turns the threaded spool, the torsion spring, and the shaft of the potentiometer, which causes the wiper to move along the slidewire.

Figure 2.2: Potentiometer Configuration

Figure 2.3 shows a basic circuit of a potentiometer. The wiper moves along the resistor, causing a change in the resistance between the reference voltage node and node connected to the wiper.

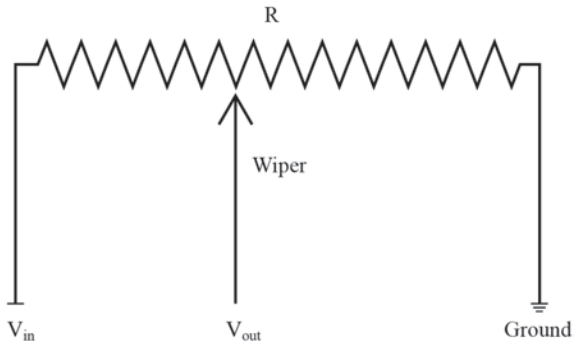

Figure 2.3: Basic Potentiometer Circuit

This variable resistance is proportional to the displacement cable's linear extension. Therefore, a moving object's displacement can be easily calculated if the cable is connected directly to the object.

The Celesco SM2-7 Miniature String Potentiometer was chosen due to its compact size, rugged design, cycle life, and accuracy. The external dimensions of the sensor are 1.7 x 2.5 x 1.8 in. (WxHxD), so it can fit in tight spaces. The SM2-7 also has a cable range of 7.5 inches and an accuracy of 0.25 percent at 500,000 cycles. This will allow for a wide range of deflection and accurate measurements.

2.1.2 Wheel Path Position Sensors

As a railroad vehicle crosses a timber railway bridge, the vehicle transmits its moving wheel forces, axle forces, and inertia actions onto the bridge. The bridge responds by deflecting because of the vehicular movement and the parameters corresponding to the vehicle such as frequency characteristics, damping, and velocity (Fryba 1996). In order to understand the bridge's response to the railway vehicle, the vehicle's wheel path position needs to be known. For the purposes of this research, the vehicle's wheel paths are labeled as shown in Figure 2.4.

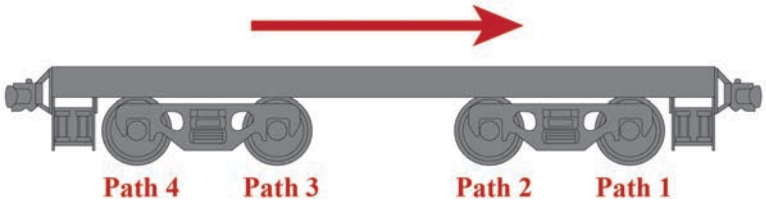

Figure 2.4: Wheel Path Identification

A photoresistor, shown in Figure 2.5, is a resistor that decreases its resistance in a circuit when exposed to increasing amounts of light. The resistor has two prongs that are connected to a photosensitive plate. Bound electrons in the device are stimulated when light shines on this plate. The stimulation causes the bonds to break, which results in the flow of electricity through the photoresistor and a decreased resistance.

Figure 2.5: Photoresistor

Photoresistor sensors were assembled in the lab to determine the vehicle's position over the bridge with respect to time. The photoresistors were placed in dark, hollow tubes where they were supported with foam (Figure 2.6).

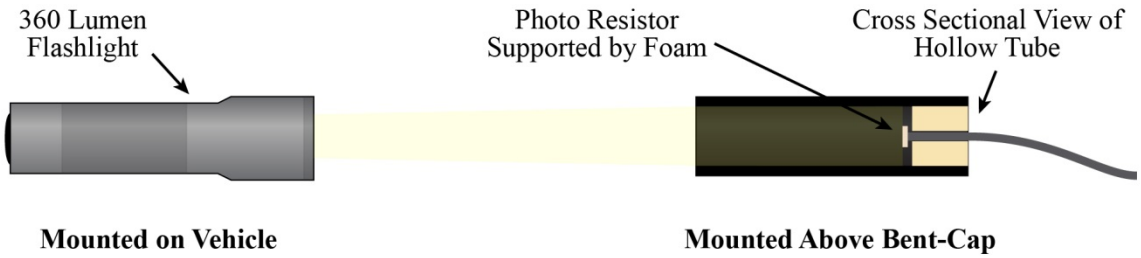

Figure 2.6: Wheel Path Position Sensors

One wheel path position sensor comprised a photo resistor inside a hollow tube and a 360-lumen flashlight, as shown in Figure 2.6. The flashlight mounted on the vehicle passes by the photoresistors mounted above the bent-caps, therefore causing a decrease in resistance in the photoresistors.

2.1.3 Data Acquisition System

A data acquisition system was used to receive the signals from the string potentiometer-based transducers and the signals from the wheel path position sensors. An IOTech StrainBook/616 was used as the primary module. Seven expansion modules were attached on top of the StrainBook/616. Each module had eight built-in channels, so there were 64 available channels. These eight modules were responsible for measuring the changes in voltage that occurred in both the string potentiometers and the wheel path position sensors and sending these voltage values to an on-site laptop.

A Wheatstone bridge circuit was used with the modules to measure the changes in voltage in both sets of sensors. A typical configuration of a Wheatstone bridge circuit is shown in Figure 2.7.

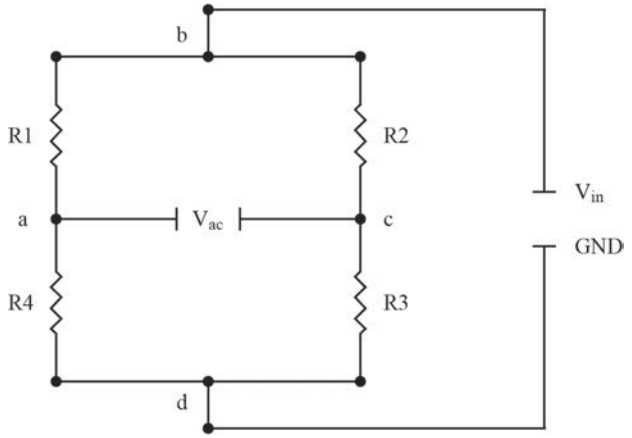

Figure 2.7: Wheatstone Bridge Circuit

When all four resistors are equal, the bridge is balanced and there is no voltage produced between points (a) and (c). If there is a change in resistance in any of the four resistors by only a fractional amount, the bridge becomes unbalanced and a measurable voltage is produced between points (a) and (c).

The cable extending from each string potentiometer was wired to a 6-pin connector (Figure 2.8). This connector was wired to a 125 feet extension cable. The other end of this extension cable was wired to a 9-pin connector that could plug straight into the data acquisition system.

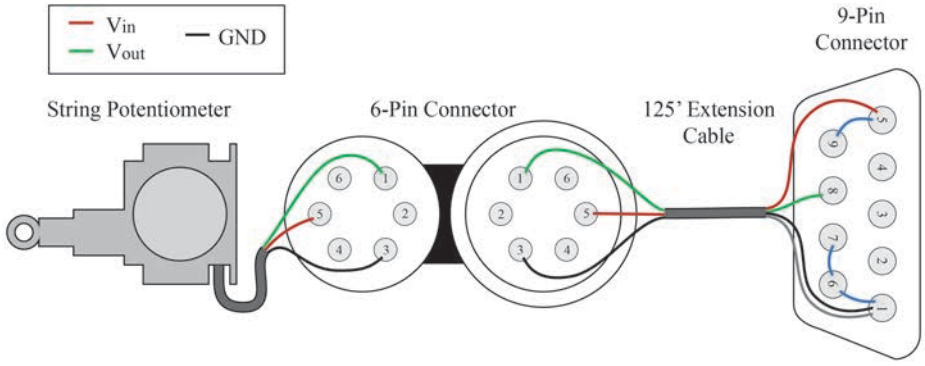

Figure 2.8: String Potentiometer Wiring Diagram

When the cable of a string potentiometer is either extended or contracted, there is a change in resistance. A quarter-bridge circuit was configured using the string potentiometer and StrainBook/616 so that when a change in resistance occurred, the bridge would produce a change in voltage. The StrainBook/616 was programmed to read the change in voltage between pin 7 and pin 8 of the 9-pin connector (Figure 2.9).

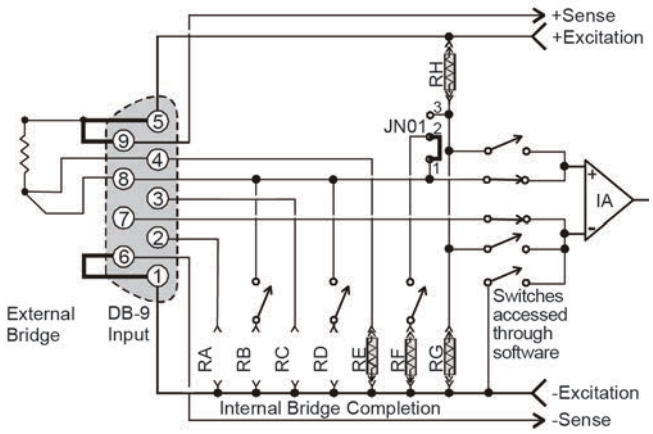

Figure 2.9: Three-Quarter Bridge Circuit (IOTech, 2005)

The photoresistor was wired with 3 bridge completion resistors in an exterior Wheatstone bridge circuit. This component was then wired directly to a 125 feet extension cable. The other end of the extension cable was then wired to a 9-pin connector, which could plug directly into the data acquisition system.

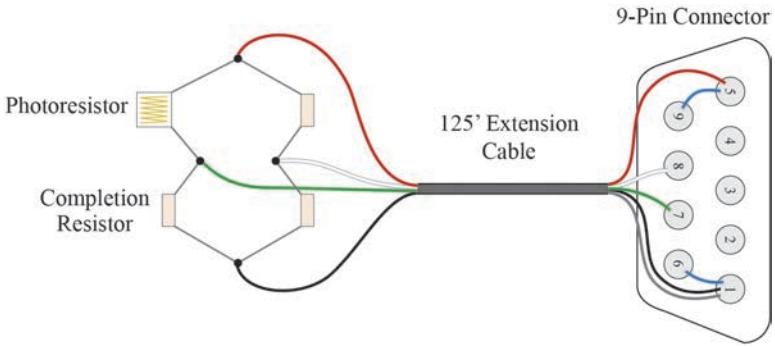

Figure 2.10: Photoresistor Wiring Diagram

When excited by light, the photoresistor experienced a change in resistance. A full-bridge circuit was configured so that when a change in resistance occurred, the bridge would produce a change in voltage. Points (a) and (c) on the circuit were wired into pins

7 and 8 of the 9-pin connector, respectively. The StrainBook/616 was programmed to read the change in voltage between these two pins (Figure 2.11).

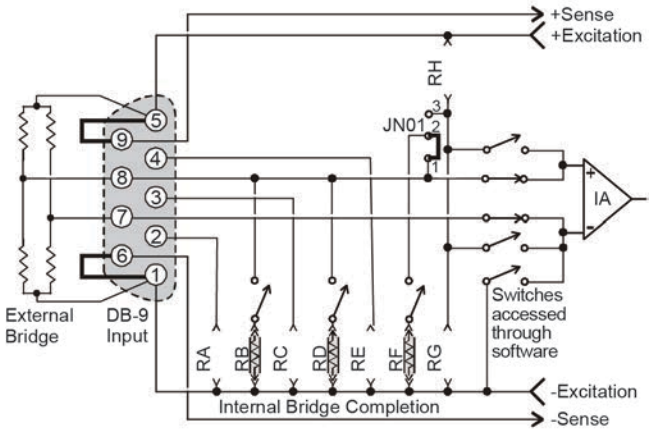

Figure 2.11: Full Bridge Circuit (IOTech, 2005)

The StrainBook/616 module was connected directly to a laptop's Ethernet port in order to import the data. DASYLab is a data acquisition software that was used to import the voltage values from the StrainBook/616, convert the voltage values to engineering units, and store both sets of data to designated files. DASYLab was also used to set a sampling rate for both sets of sensors. Because a railway vehicle will be traveling at a high velocity, the sampling rate for all of the sensors was set at 1000 Hz so no essential data would be missed.

2.2 Small-Scale Experiment

A large-scale experiment comprising a vehicle traversing a timber railway bridge presents a less controlled environment with a small margin for error and a limited amount of time for testing. Therefore, a small-scale experiment was conducted prior to this test in a controlled environment where an unlimited amount of tests could be

performed. This allowed for all of the sensors, cables, and data acquisition system to be tested in the lab to ensure a smooth, quick process during the large-scale experiment.

2.2.1 Description of Small-Scale Testbed

The small-scale experiment was assembled and conducted at Texas A&M University Riverside Lab during the months of January 2015 through July 2015. A Radio Flyer Classic Red Metal Wagon was used to represent a railway vehicle 3-piece truck. A truck is a framework attached underneath the vehicle that secures two wheel-sets using bearings (Figure 2.12).

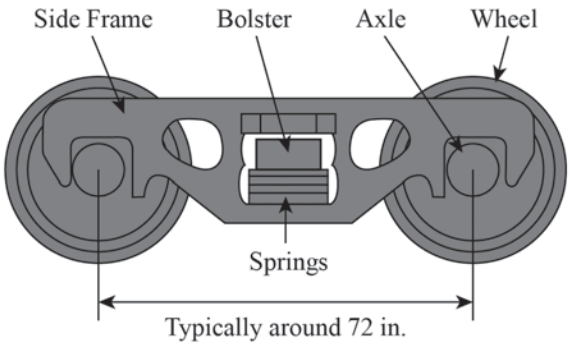

Figure 2.12: Typical 3-Piece Truck

The axles of the wagons were installed so that both the front and rear axles were fixed (Figure 2.13).

Figure 2.13: Radio Flyer Classic Red Metal Wagon

After the distance between the front and rear axles of the wagons was measured to be 26 inches, the ratio of the span length of the railway bridge to the axle center spacing of the trucks was multiplied by the wagon axle spacing to find the small-scale span length. A typical span of a timber railway bridge is 180 inches, and the typical axle center spacing of a truck is 72 inches.

$$\frac{Span\ Length\ of\ Small\ Scale\ Bridge}{Axle\ Spacing\ of\ Wagon\ (26\ in.)} = \frac{Span\ Length\ of\ Bridge\ (180in.)}{Axle\ Spacing\ of\ Truck\ (72\ in.)} \qquad \textbf{Equation 2.1}$$

Using Equation 2.1, the span length of the small-scale bridge was found to be 65 inches. Kiln-dried yellow pine 2in. x 4in. studs were used to construct the frame for the small-scale bridge, whose dimensions can be seen in Figure 2.14.

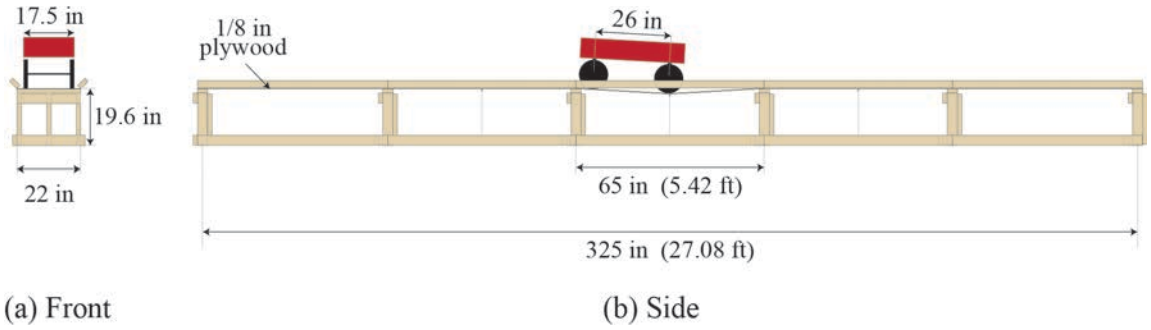

Figure 2.14: Small-Scale Experiment Configuration

Five equally spanned bays were constructed so that there would be an adequate amount of length for the wagon to gain speed while crossing the bridge. Sheets of hardwood, non-treated plywood were used to represent a bridge deck. The sheets of plywood were only attached to the frame at each bent-cap so that they would deflect under a load (Figure 2.14). A plywood thickness of 5mm (0.197 in) was chosen so that the plywood sheets would experience larger, visible deflections.

2.2.2 Instrumentation of Small-Scale Testbed

Six string potentiometers were used to measure the deck deflections of the small-scale bridge. Each of the string potentiometers was mounted to a 4 in. x 6 in. x 0.25 in. steel plate, as shown in Figure 2.15.

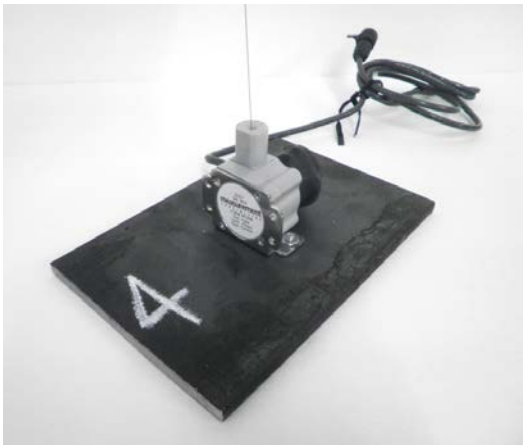

Figure 2.15: Small-Scale Experiment String Potentiometer on Steel Plate

As shown in Figure 2.16, span 2, span 3, and span 4 were instrumented. Two string potentiometers were placed under the middle of each of the three spans approximately 1 foot apart.

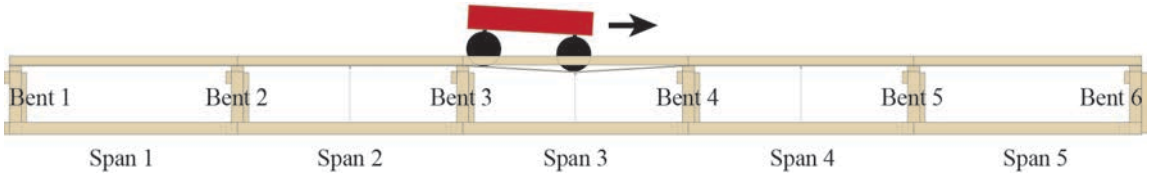

Figure 2.16: Small-Scale Bridge Nomenclature

The string potentiometers' cables were attached to the bottom of each deck using 3/4 in. brass-plated steel cup hooks (Figure 2.17). A 5/64 in. drill bit was used to predrill into the bottom of the deck. Then, the cup hooks were screwed in by hand.

Figure 2.17: String Potentiometer Installation on Small-Scale Bridge

Four wheel path position sensor photoresistors were secured to posts and set up at bent 2, bent 3, bent 4, and bent 5 of the small-scale bridge. One wheel path position flashlight was secured to a magnet and placed on the lead axle of the wagon.

The data acquisition system was set up on a folding table in the lab near the small-scale bridge. The string potentiometers were connected to channels 1-6, and the wheel path position sensors were connected to channels 9-12 (Figure 2.18).

Figure 2.18: Small-Scale Experiment Data Acquisition System

DASYLab was programmed so that an average deflection was calculated using the deflections from each set of string potentiometers under each span. In addition, DASYLab was programmed to display gauges reflecting the real-time deflections of each set of string potentiometer, as shown in Figure 2.18.

2.2.3 Small-Scale Experimental Parameters

Several load cases were considered by adding sandbags into the wagon. A difference in velocity was not considered because the wagon was being pushed by hand from one side of the small-scale bridge to the other, which made it difficult to reach significantly different velocities. The parameters of each load case are listed in Table 2.1.

Table 2.1: Small-Scale Experiment Load Cases

Case No.	Vehicle Weight (lbs)
1	40
2	60
3	80

Four sets of data were obtained for each load case. Table 2.2 presents each test number with its corresponding load case number.

Table 2.2: Small-Scale Experimental Parameters

Test No.	Case No.
1	1
2	1
3	1
4	1
5	2
6	2
7	2
8	2
9	3
10	3
11	3
12	3

For each test, the wagon was first placed on top of span 1. The data acquisition system was set to record data. Then, the wagon was pushed across the bridge at an approximate velocity of 5 mph until the wagon reached the end of span 5. The data acquisition system was stopped at this time. This process was repeated for each test.

2.3 Large-Scale Open Deck Experiment

After the small-scale experiment was completed and all data had been analyzed, preparation began in order to move forward with a large-scale experiment on an open deck timber railroad bridge. An open deck bridge comprises rails that are anchored directly to the cross ties, which are supported directly by the bent-caps. Figure 1.1 is an example of an open deck bridge. The test needed to be performed on a bridge that had experienced fatigue damage so that the effects of impaired structural members could be

analyzed. Also, the bent-caps and stringers of the bridge needed to be easily accessible to ensure adequate access for instrumentation.

2.3.1 Description of Large-Scale Open Deck Testbed

On August 11, 2015, Texas A&M University conducted testing for the Union Pacific Railroad (UP) on Bridge 17.14 south of Mumford, Texas. Bridge 17.14 was chosen due to its deck, condition, and its accessibility. As Figure 2.19 shows, Bridge 17.14's short height provided easy access to the bent-caps and stringers. Also, the ground was dry and flat beneath each span, which made it easy to work underneath.

Figure 2.19: Bridge 17.14

Figure 2.20 shows that a bent-cap comprised a solid-sawn timber beam mounted on top of a glue laminate beam. The bent-caps were experiencing various amounts of crushing, as Figure 2.20 shows.

Figure 2.20: Bridge 17.14 Bent-Cap Detail

In addition to these impairments, several of Bridge 17.14's stringers were split (Figure)., Some of the stringers were not visible because of the configuration of the bridge, so it is unclear during a visual inspection if any of those members were split.

Figure 2.21: Bridge 17.14 Stringer Detail

This research focused on two of Bridge 17.14's spans: span 7 and span 8. Specific labels were used in reference to Bridge 17.14, which is displayed in Figure 2.22. Stringers were labeled by their span, chord, and ply. Bents were labeled according to the cardinal direction and bent number, such as Bent 9 East or Bent 7 West (Figure 2.22).

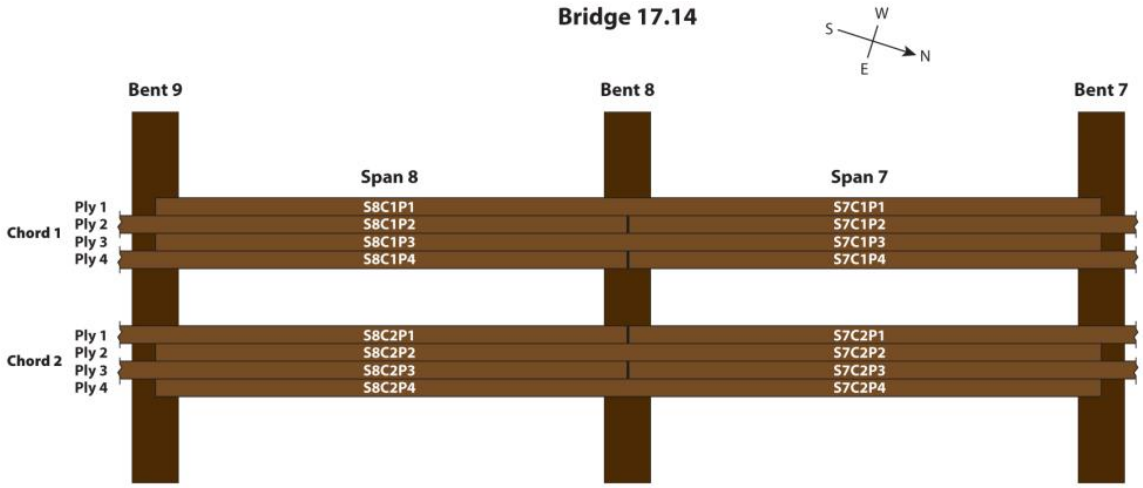

Figure 2.22: Bridge 17.14 Nomenclature

Bridge 17.14 had two chords which each comprised 4 plys. Eight stringers extended across each span. Each span was 15 feet wide. As Figure 2.22 shows, each stinger extended across two spans, although they alternated in continuity. Bridge 17.14 also had steel grating mounted to the cross ties on each side of the rails. This grating created a walkway deck on each side of the bridge.

A DE-650 locomotive crane was used to pass over Bridge 17.14 during the experiment (Figure 2.23).

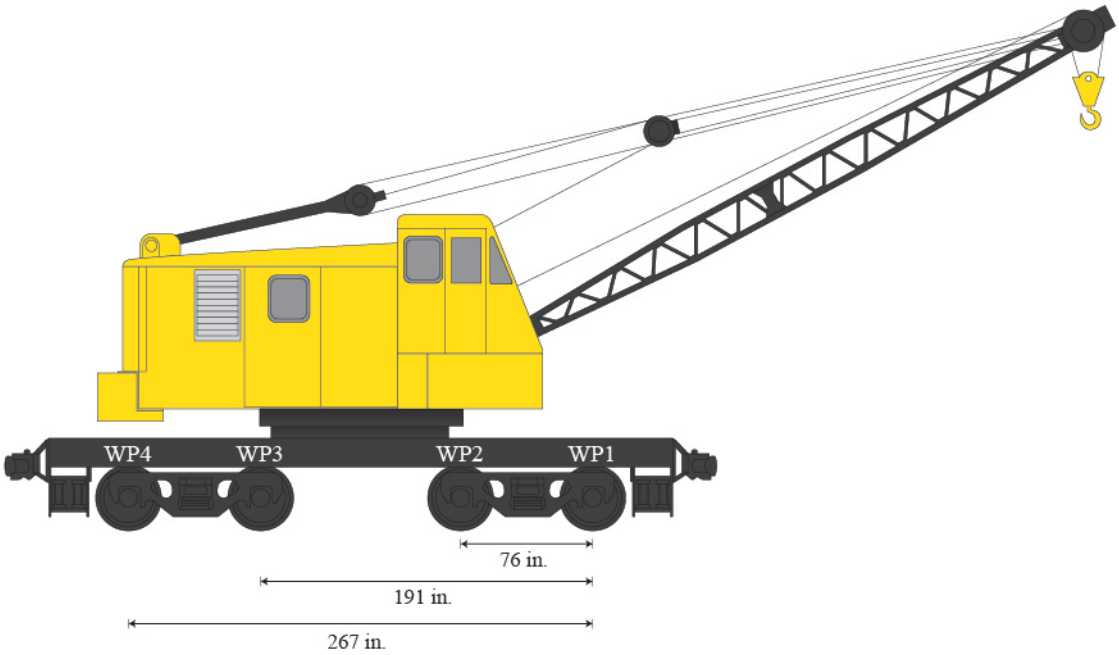

Figure 2.23: DE-650 Locomotive Crane

The locomotive crane's maximum speed was 30 mph, and it weighed approximately 300,000 pounds. Each truck weighed approximately 17,400 pounds, and the locomotive crane comprised four trucks. The locomotive crane had four motors located near the rear of the vehicle above wheel path 3 and wheel path 4. Dimensions of the wheel path positions can be seen in Figure 2.23.

2.3.2 Instrumentation of Large-Scale Open Deck Testbed

Forty-eight string potentiometers were used to measure the stringer deflections of span 7 and span 8. Six string potentiometers were used to measure the deflections of bent-caps 7, 8, and 9. Each string potentiometer was secured to a 4 in. x 6 in. x 1/4in. steel plate. The layout of these string potentiometers can be seen in Figure 2.24.

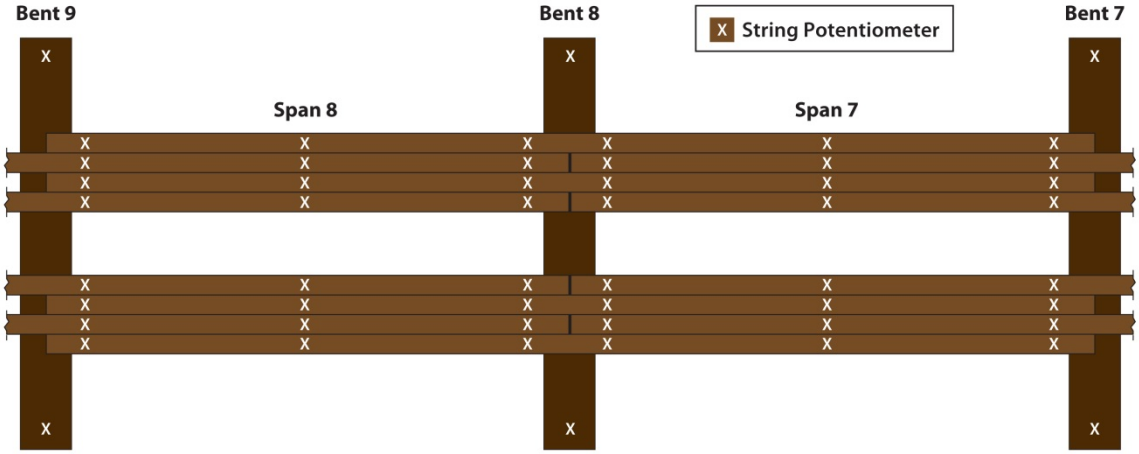

Figure 2.24: Bridge 17.14 Sting Potentiometer Layout

Although the methods used to instrument the bridge needed to be nondestructive, the string potentiometer's cable needed to be secured to the stringer. Applying the same method used in the small-scale experiment, a 5/64 in. drill bit was used to predrill into the bottom of each stringer of span 7 and span 8. Then, steel cup hooks were screwed into these holes by hand.

The bottom of a stringer was approximately 5 feet off of the ground. Therefore, the 7.5 in. displacement cable would not reach from the string potentiometer on the ground to the bottom of the stringer. A stainless steel fishing leader wire was used to span this distance. A loop was created at each end of the leader wire by crimping a single barrel sleeve over the wire. The displacement cable of the string potentiometer was pulled out approximately 5 inches. Then, one loop of the leader wire was connected to a cup hook at the stinger's surface, and the other loop was connected to the extended displacement cable. Figure 2.25 shows the string potentiometers set up at the mid-span and the north end of span 7.

Figure 2.25: String Potentiometers Under Span 7 of Bridge 17.14

Three wheel path position photoresistors were secured to posts and set up at bents 7, 8, and 9 of Bridge 17.14. The posts were secured to the steel walkway using nondestructive, ratcheting straps. One wheel path position flashlight was secured to a magnet and placed above wheel path 1 on the locomotive crane (Figure 2.26). The wheel path position photoresistors were vertically aligned with the wheel path position flashlight at each bent, as shown in Figure 2.26.

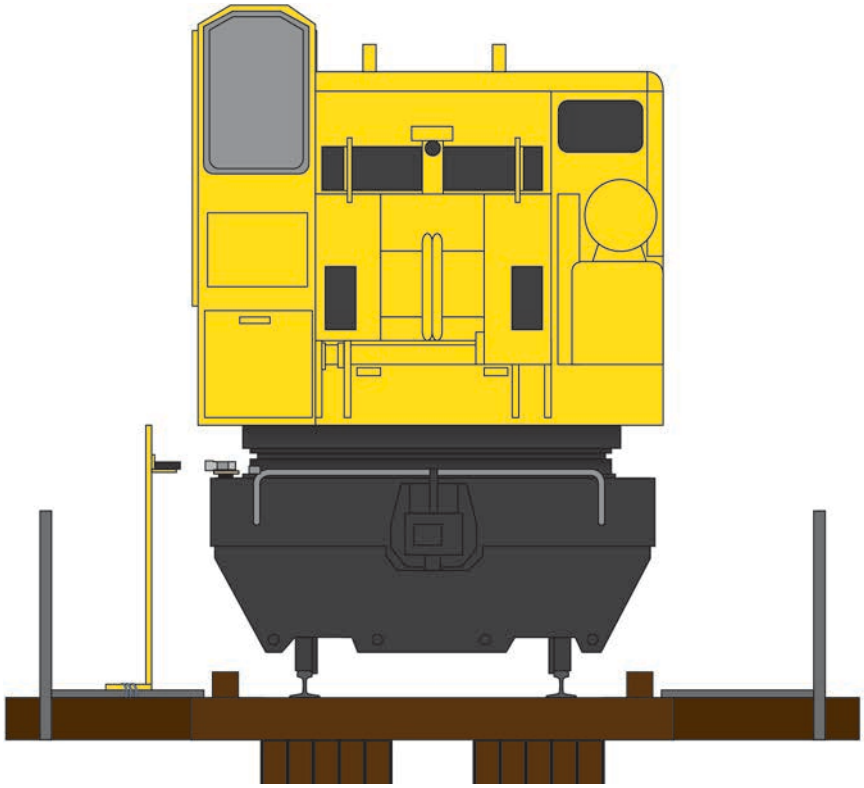

Figure 2.26: Wheel Path Position Sensor Setup

The data acquisition system was set up on a folding table approximately 30 feet from Bridge 17.14. The string potentiometers measuring stringer deflections were connected to channels 1-48, the string potentiometers measuring bent-cap deflections were connected to channels 49-54, and the bridge wheel path position sensors were connected to channels 62-64.

Figure 2.27: Bridge 17.14 Data Acquisition System

Approximately 7,000 feet of cable was used to connect all of the sensors to the data acquisition system. A portable generator was set up onsite and was used to supply power to the data acquisition system. Similar to the small-scale experiment, DASYLab was programmed to display gauges reflecting the real-time deflections of each set of string potentiometer, as shown in Figure.

2.3.3 Large-Scale Open Deck Experimental Parameters

After the string potentiometers were completely setup, a southbound freight train was allowed to pass over Bridge 17.14 (Figure). The wheel path position sensors were not in place on the bridge or on the freight train, though, so no position data was collected.

Once all of the sensors were set up, including the wheel path position sensors, the locomotive crane was used to pass over Bridge 17.14 at various speeds. Table 2.3 lists each test number, the vehicle type, the vehicle direction, and the vehicle speed.

Table 2.3: Open Deck Bridge Experimental Parameters

Test No.	Vehicle Type	Vehicle Direction	Vehicle Speed (mph)
1	Freight Train	S	-
2	Locomotive Crane	N	2.1
3	Locomotive Crane	N	1.8
4	Locomotive Crane	N	11.2
5	Locomotive Crane	N	11.2
6	Locomotive Crane	N	19.2
7	Locomotive Crane	N	19.4
8	Locomotive Crane	N	25.3
9	Locomotive Crane	N	27.4
10	Locomotive Crane	S	5.5

The data acquisition system would be set to record data, and then the locomotive crane would pass over Bridge 17.14. Once the locomotive crane had passed across the last bent that was instrumented, the data acquisition system would be stopped. Once the crane had come to a complete stop, the engineer would reverse the crane back across the bridge to a distance where the crane could gain adequate speed. Then the process would repeat for each test.

2.4 Large-Scale Ballast Deck Experiment

The open deck bridge experiment comprised a single locomotive crane passing over an open deck bridge at speeds varying from 1.8 mph to 27.4 mph. Maximum authorized speeds vary by the type of track, but some freight trains may run at speeds over 60 mph. Also, there are two types of decks that can be used in the construction of a timber railway bridge: open decks and ballast decks. An experiment comprising a freight train passing over a ballast deck bridge was conducted in order to analyze the effects of these parameters.

2.4.1 Description of Large-Scale Ballast Deck Testbed

On a ballast deck bridge, the rails are anchored to cross ties, which are supported by ballast. The ballast rests on a timber floor, which is supported by stringers. Figure 2.28 shows an example of a ballast deck bridge.

Figure 2.28: Ballast Deck Bridge

On September 2, 2015 through September 3, 2015, Texas A&M University conducted testing on a Canadian National Railway Company (CN) ballast deck bridge. Bridge 816.9, which was located just south of Magnolia, Mississippi, consisted of two adjacent timber bridges. The experiment was performed on the east bridge. Bridge 816.9 had experienced less fatigue damage than Bridge 17.14. Similar to Bridge 17.14, Bridge 816.9 was also easily accessed due to its height being less than 10 feet. The ground underneath each span was also dry and flat. Figure 2.29 shows a broad view of Bridge 816.9.

Figure 2.29: Bridge 816.9

Unlike the bridge in the open deck experiment, Bridge 816.9 had concrete bent-caps, as shown in Figure 2.30. In addition to this difference, there were 10 stringers arranged in a completely different configuration (Figure 2.30).

Figure 2.30: Bridge 816.9 Bent-Cap and Stringer Detail

This particular experiment focused only on span 8 of Bridge 816.9. Specific nomenclature was used in reference to Bridge 816.9, which is displayed in Figure 2.31. Stringers were labeled according to their ply, and bent-caps were labeled according to their cardinal direction and bent number (similar to the open deck experiment). Each stringer extended across two spans, but similar to the open deck experiment, they alternated in continuity (Figure 2.31).

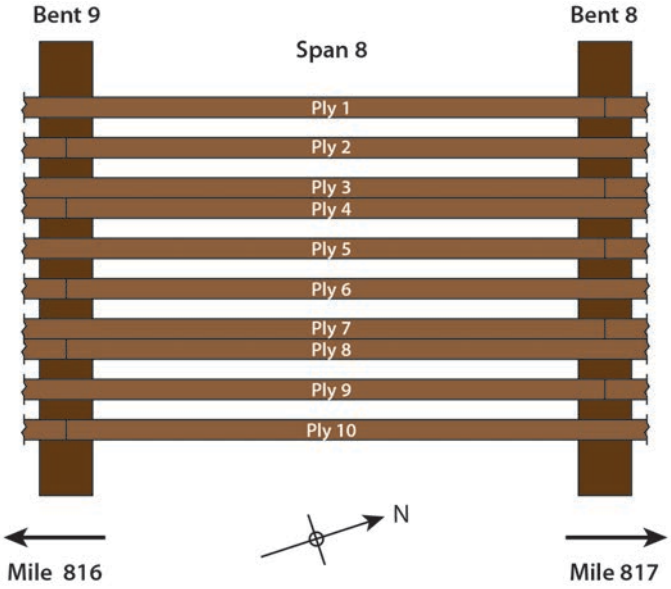

Figure 2.31: Bridge 816.9 Nomenclature

Bridge 816.9 was under construction at the time of the experiment. CN railroad workers were in the process of tearing down the existing bridges and installing new ones. The workers focused on the west bridge, and the east bridge was left intact during the two days of testing.

A CN work train, shown in Figure 2.32, was used to pass over Bridge 816.9.

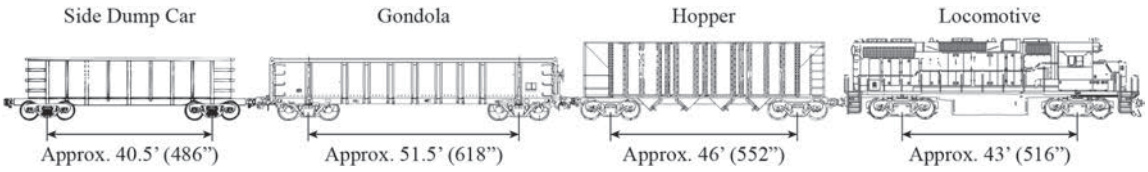

Figure 2.32: Work Train

The train comprised a locomotive hauling a hopper, a gondola, and a side dump car. Each component included two trucks, which meant that the work train had 8 trucks total.

2.4.2 Instrumentation of Large-Scale Ballast Deck Testbed

The stringer deflections of span 8 were measured using 30 string potentiometers, and the deflections of bent-caps 8 and 9 were measured using 4 string potentiometers. As with the other tests, each string potentiometer was secured to a steel plate. The layout of these sensors can be seen in Figure 2.33.

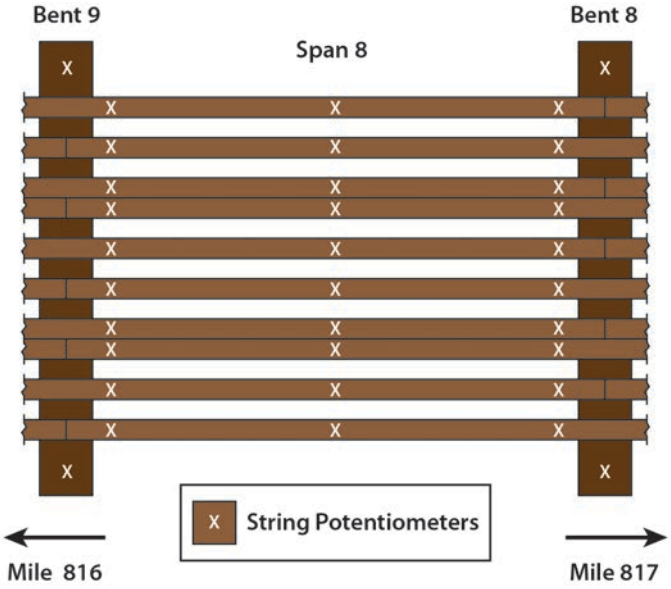

Figure 2.33: Bridge 816.9 String Potentiometer Layout

The same method used with the open deck experiment was implemented when instrumenting the stringers with string potentiometers. Small holes were drilled into the timber, cup hooks were installed, and fishing leader wire was used to connect the hooks to the string potentiometer displacement cables. Figure 2.34 shows string potentiometers installed at the south end of span 9.

Figure 2.34: String Potentiometers Under Span 9 of Bridge 816.9

Because the bent-caps were concrete, a different method had to be used to install four of the string potentiometers. First, four small 1 in. x 1 in. x 3/8 in. wood blocks were cut, and a cup hook was screwed into the center of each block. Each block was attached at the appropriate locations on the bent-caps using an epoxy resin. Then, fishing leader wire was used to connect the cup hooks to the displacement cables of the string potentiometers.

The data acquisition system was again set up on a folding table approximately 20 feet from the bridge (Figure 2.35). The string potentiometers measuring stringer deflections were connected to channels 1-30, and the string potentiometers measuring bent-cap deflections were connected to channels 31-34. The sensors were connected to the data acquisition system using over 4,000 feet of cable. There were no wheel path position sensors used during this experiment.

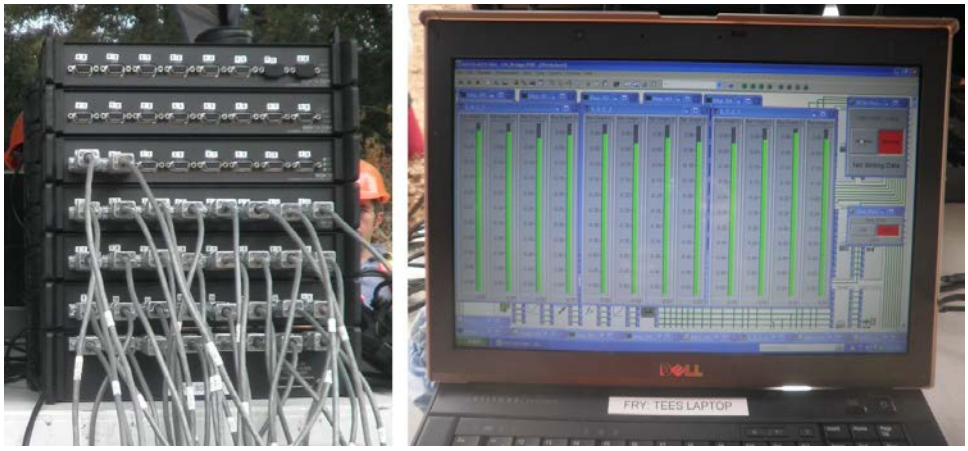

Figure 2.35: Bridge 316.9 Data Acquisition System

As with the open deck experiment, a portable generator was used to supply power the data acquisition system. DASYLab was again programmed to display the real-time deflections of the stringers and bent-caps.

2.4.3 Large-Scale Ballast Deck Experimental Parameters

The objective of this experiment was to have the CN work train pass over Bridge 816.9 at different speeds. Before this could happen, a few other trains were scheduled to pass over the bridge. All of the sensors and the data acquisition system were completely set up, so data was collected for these trains. After the work train tests were completed, two more trains were scheduled to pass over the bridge, so data was collected for those trains

as well. Table 2.4 lists each test number, the vehicle type, the vehicle direction, and the vehicle speed.

Table 2.4: Ballast Deck Bridge Experimental Parameters

Test No.	Vehicle Type	Vehicle Direction	Vehicle Speed (mph)
1	Freight Train	S	-
2	Passenger Train	S	-
3	Work Train	N	5
4	Work Train	S	10
5	Work Train	N	15
6	Work Train	S	20
7	Work Train	N	25
8	Work Train	S	30
9	Work Train	N	35
10	Work Train	S	40
11	Work Train	N	40
12	Work Train	S	45
13	Work Train	N	43
14	Work Train	S	45
15	Work Train	N	5
16	Work Train	N	52
17	Work Train	S	10
18	Work Train	N	54
19	Work Train	S	20
20	Work Train	N	63
21	Passenger Train	S	-
22	Freight Train	S	-

Once the data acquisition system was set to record data, the work train passed over Bridge 816.9 at a designated speed of interest. The train would begin to come to a complete stop after it had completely traversed the bridge. The data acquisition system was then stopped and the file was saved. While the train was still stopped, the data acquisition system was set to record again. While the data was being recorded, the work

train would pass back over the bridge in reverse at the next speed of interest. This process was repeated in order to gather data for all the designated speeds.

CHAPTER III
DATA ANALYSIS

3.1 Scope of Data Analysis

This section discusses the analysis of the data recorded from the small-scale bridge, the open deck bridge, and the ballast deck bridge. Once the experiments had been performed and all data had been recorded and saved, each set of data from each experiment was imported into Microsoft Excel. This program was used to:

- Delete all unnecessary data that was recorded before each vehicle crossed the spans of interest and after the vehicle had passed the spans of interest for each experiment,
- Perform a moving average on large scale data,
- Plot total mid-span deflections from all tests,
- Plot net mid-span deflections from both large scale tests,
- Plot bent-cap deflections from both large-scale tests,
- Calculate vehicle speed for the open deck bridge experiment,
- Calculate and identify the times that each wheel path crossed the middle of each span of interest for the small-scale experiment and the open deck bridge experiment, and
- Calculate and identify the times that each wheel path crossed each bent-cap of interest for the open deck bridge experiment.

The wheel path position sensor data was used to determine the times that each wheel path crossed each mid-span of interest and each bent-cap of interest. The ballast deck bridge was not instrumented with wheel path position sensors, so the times that each wheel path crossed each mid-span of interest or each bent-cap of interest could not be calculated.

3.1.1 Wheel Path Position Analysis

The wheel path position sensors provided a spike in voltage whenever wheel path 1 passed over each bent-cap of interest. Therefore, the times that it took wheel path 1 to cross each span of interest were known. As discussed in Chapter II, the length of each span for both the small-scale bridge and the open deck bridge were known. These times and distances were used to calculate each vehicle's velocity over each span of interest, as shown in Equation 3.1.

$$V_s = \frac{L_s}{t_s} \qquad \textbf{Equation 3.1}$$

where V_s is the vehicle's velocity while traversing a span of interest, L_s is length of the span of interest, and t_s is the time it took the vehicle to cross the span of interest.

The length from the middle of each span of interest to each bent was known for each experiment. Because each vehicle's velocity over each span of interest and the time that wheel path 1 crossed each bent-cap of interest was also known, the specific times that wheel path 1 crossed each mid-span could then be calculated, as shown in Equation 3.2.

$$t_1 = t_{wp1} + \frac{L_{ms}}{V_s} \qquad \textbf{Equation 3.2}$$

where t_1 is the time that wheel path 1 crossed a mid-span of interest, t_{wp1} is the time that wheel path 1 crossed the bent-cap prior to that span, and L_{ms} is the distance from that bent-cap to the middle of that span.

The center-to-center spacing of wheel path 1 to each consecutive wheel path for each vehicle was known, as discussed in Chapter II. With this information, the specific times that each consecutive wheel path crossed each mid-span of interest could then be calculated, as shown in Equation 3.3.

$$t_i = t_1 + \frac{L_i}{V_s} \qquad \textbf{Equation 3.3}$$

where t_i is the time that a wheel path following wheel path 1 crossed a mid-span of interest and L_i is the center-to-center distance of that wheel path to wheel path 1.

As mentioned in Section 2.4, the speed of the work train was known for the ballast deck bridge experiment. The train operator used a speedometer and reported the train speeds after every test was completed.

3.1.2 Moving Average of Large Scale Data

The data acquisition system was set to record the small scale data at 50 Hz; however, it was set to record both of the large scale data at 1000 Hz. This relatively high sampling rate was chosen for the large-scale experiments so that no important data would be missed as a vehicle traversed either bridge at high speeds. A 20 point moving average was performed in Microsoft Excel in order to smooth each set of data so that the general trend in the deflections could be seen.

3.1.3 Small-Scale Deflection Analysis

As mentioned in Chapter II, two string potentiometers were placed under the middle of each span of the small-scale bridge. For the purposes of analysis, an average of these two deflections was taken to reflect a total mid-span deflection. This was done for each set of deflections for all three instrumented spans.

3.1.4 Large-Scale Deflection Analysis

Three separate deflections were recorded for each stringer for both large-scale experiments: the deflection at the south end of a stringer (δ_s), the deflection at the north end of a stringer (δ_n), and the total maximum deflection at the middle of a stringer

(δ_{total}). For the purposes of this research, the total mid-span deflection at the middle of a stringer (δ_{total}) will be referred to as the "total" stringer deflection (Figure 3.1).

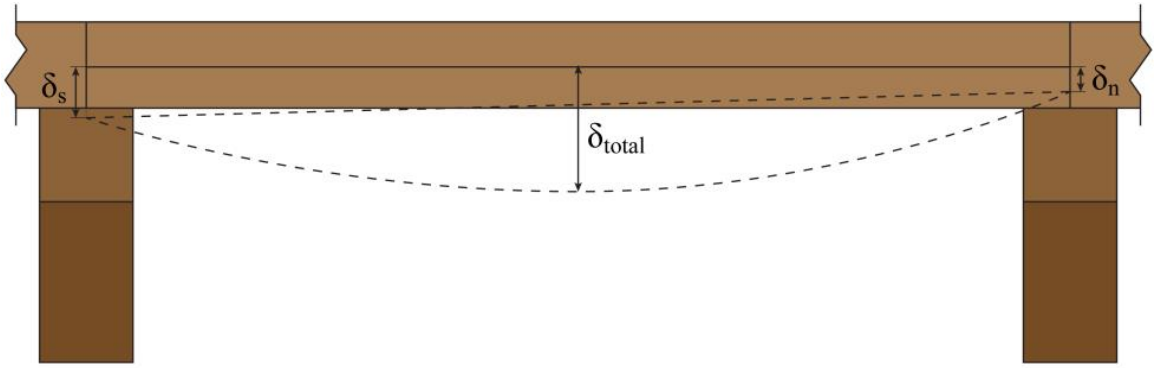

Figure 3.1: Total Bridge Deflection

This total mid-span stringer deflection not only includes the mid-span stringer deflection, but it also includes deflections due to support settlement. The following equation was used in order to account for this settlement:

$$\delta_{avg} = \frac{\delta_s + \delta_n}{2} \qquad \textbf{Equation 3.4}$$

where δ_{avg} is the average of the deflection at the south end of a stringer (δ_s) and the deflection at the north end of a stringer (δ_n).

Using Equation 3.4, the net mid-span deflection of the stringer (δ_{net}) can be found:

$$\delta_{net} = \delta_{total} - \delta_{avg} \qquad \textbf{Equation 3.5}$$

The net stringer deflection is the actual stringer deflection and does not include any support settlement. This is demonstrated in Figure 3.2.

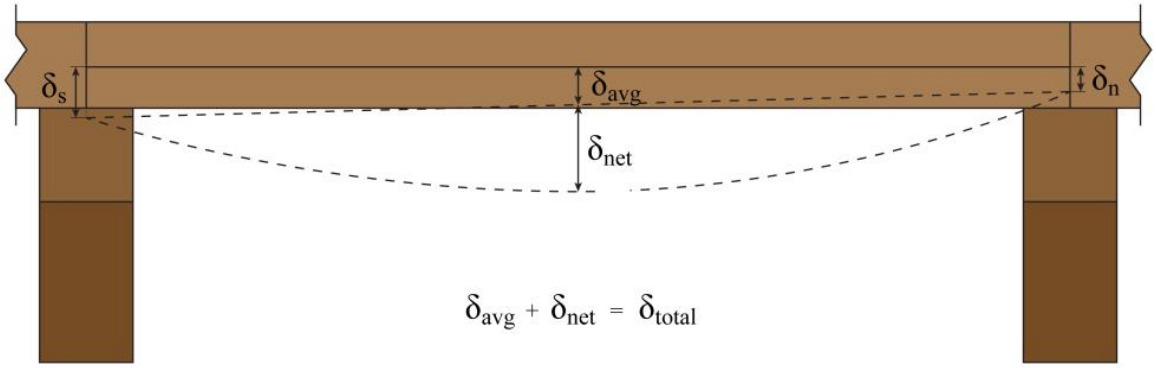

Figure 3.2: Net Bridge Deflection and Support Settlement

The small-scale bridge was built on a rigid, indoor floor, so support settlement was not taken into account during analysis.

CHAPTER IV
RESULTS

4.1 Small-Scale Experiment Results

During this experiment, deflections of three mid-spans were measured under three different load cases. For each test, a wagon was pushed across the bridge in one direction (from Bent 1 to Bent 6). This section highlights key results from each test performed in this experiment.

4.1.1 Small-Scale Mid-Span Deflection Results

Plots of deflection versus time for each span in each test are shown in Appendix A. There are thirty-six plots in total: Three load cases each comprising 4 tests for 3 different spans. Although Appendix A includes plots for the entire experiment, a few select plots will be shown in this section for the purposes of discussion.

Table 4.1 displays the maximum deflections measured for each span during each test.

Table 4.1: Small-Scale Experiment Maximum Deflections (in.)

Load Case No.	Test No.	Span 2	Span 3	Span 4
Case 1 (40 lbs)	1	-0.41351736	-0.44198626	-0.39296284
	2	-0.39586014	-0.37733239	-0.37493348
	3	-0.40619081	-0.40964448	-0.36560577
	4	-0.40041226	-0.41496766	-0.37931535
Case 2 (60 lbs)	5	-0.55182624	-0.5267241	-0.51393503
	6	-0.53409362	-0.54534954	-0.55905187
	7	-0.57538247	-0.53842354	-0.50137711
	8	-0.56338054	-0.5461756	-0.53732038
Case 3 (80 lbs)	9	-0.77894217	-0.70732737	-0.74195838
	10	-0.73272777	-0.69283879	-0.7146641
	11	-0.77827311	-0.69120526	-0.77942264
	12	-0.76456892	-0.71024585	-0.70802671

The maximum deflections for each load case are highlighted in red in Table 4.1. As expected, as more load is added to the vehicle, the larger the average deflections become. According to this table, test 1-span 3 produced the maximum deflection for load case 1, test 7-span 2 produced the maximum deflection for load case 2, and test 11-span 4 produced the maximum deflection for load case 3. There is a 30.2% increase from the case 1 maximum deflection to the case 2 maximum deflection, for which there is a 50% load increase. There is a 35.5% increase from the case 2 maximum deflection to the case 3 maximum deflection, for which there is a 33.3% load increase.

The average maximum deflection for each load case is displayed in Table 4.2. Here, it can be seen that, on average, span 2 experienced larger deflections than span 3 or span 4.

Table 4.2: Small-Scale Experiment Average Maximum Deflections (in.)

Case No.	Span 2	Span 3	Span 4
Case 1	-0.40399514	-0.4109827	-0.37820436
Case 2	-0.55617072	-0.53916819	-0.5279211
Case 3	-0.76362799	-0.70040432	-0.73601796

Considering span 2, there is a 37.7% average increase between case 1 and case 2, and there is a 37.3% average increase between case 2 and case 3. For span 3, there is a 31.2% average increase between case 1 and case 2, and there is a 29.9% average increase between case 2 and case 3. For span 4, there is a 39.6% average increase between case 1 and case 2, and there is a 39.4% average increase between case 2 and case 3.

Figure 4.1 shows a plot of deflection versus time for load case 3, test 9, span 2. This particular test was performed with load case 3, and it had larger than average maximum deflections for each span.

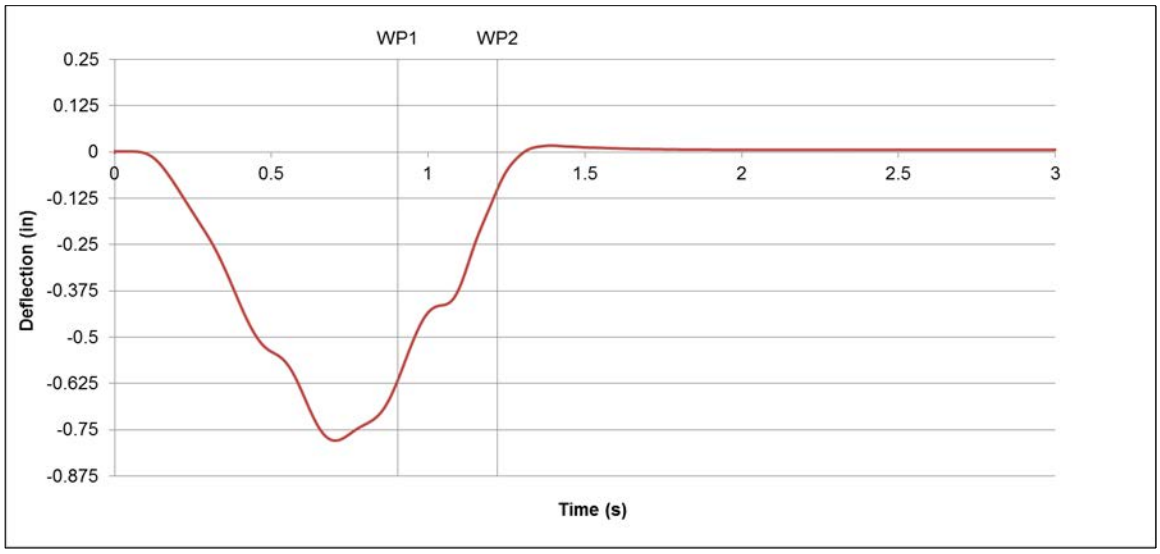

Figure 4.1: Small-Scale Experiment Case 3 Test 9 Span 2 Deflection

Figure 4.2 shows a plot of deflection versus time for load case 3, test 9, span 3.

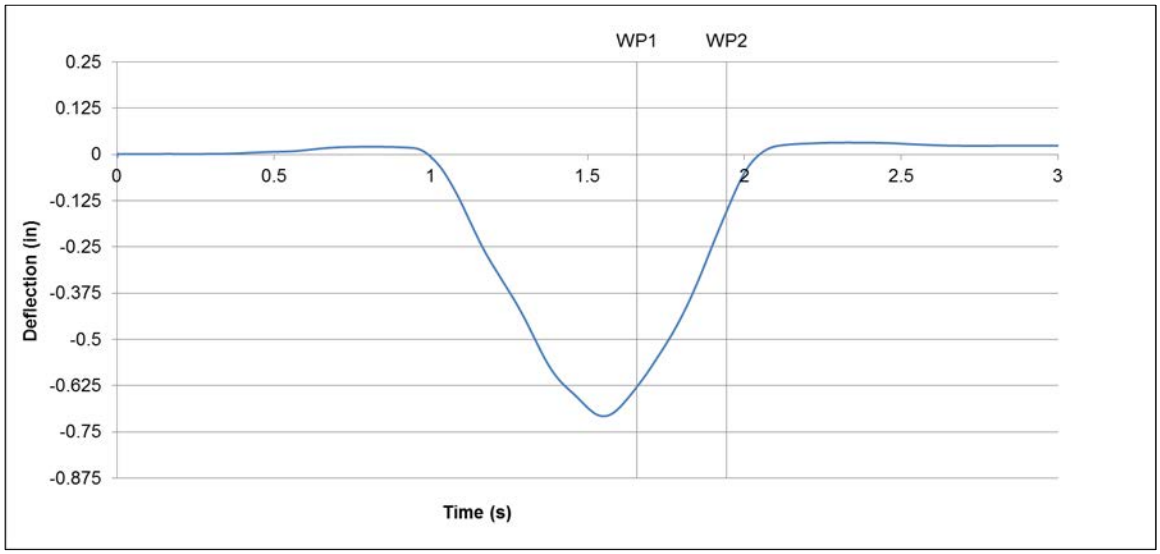

Figure 4.2: Small-Scale Experiment Case 3 Test 9 Span 3 Deflection

Figure 4.3 shows a plot of deflection versus time for load case 3, test 9, span 4.

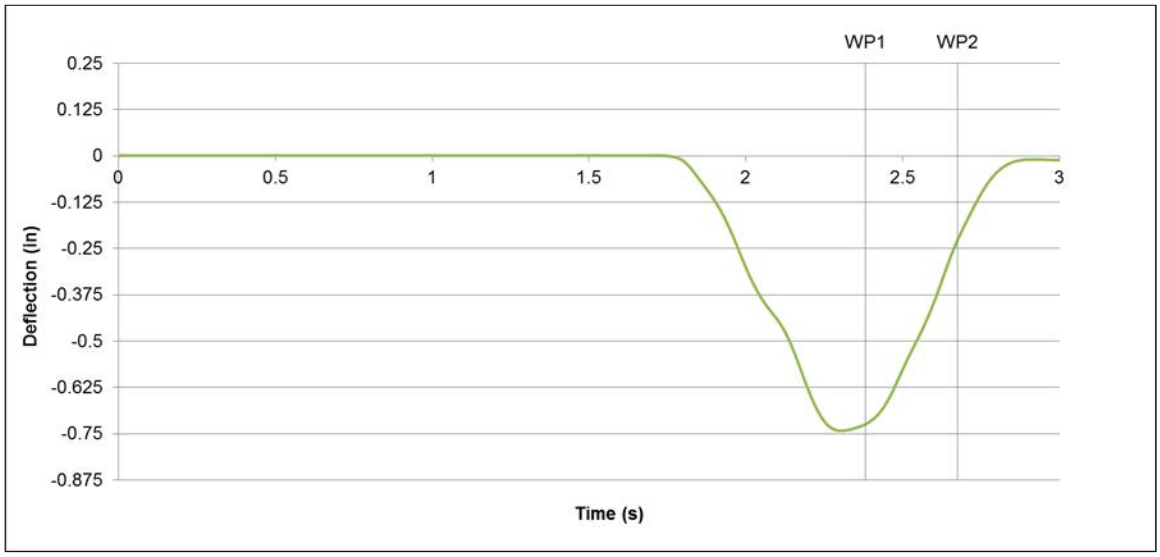

Figure 4.3: Small-Scale Experiment Case 3 Test 9 Span 4 Deflection

For each plot related to the small-scale experiment, two vertical lines have been graphed. The line labeled WP1 reflects the time when wheel path 1 of the wagon crossed the mid-span of the span that has been plotted. The line labeled WP2 reflects the time when wheel path 2 of the wagon crossed the mid-span of the span that has been plotted. The time of a wheel path over each bent was calculated using the velocity of the wagon.

When looking at Figure 4.1, Figure 4.2, and Figure 4.3, it can be seen that the maximum mid-span deflection for each span occurred just before wheel path 1 crossed the middle of that span. This position appears to be constant for all of the spans for each test (Appendix A). Figure 4.4 shows the location of the wagon at the time of the maximum mid-span deflection of Span 2 during Case 3 Test 9.

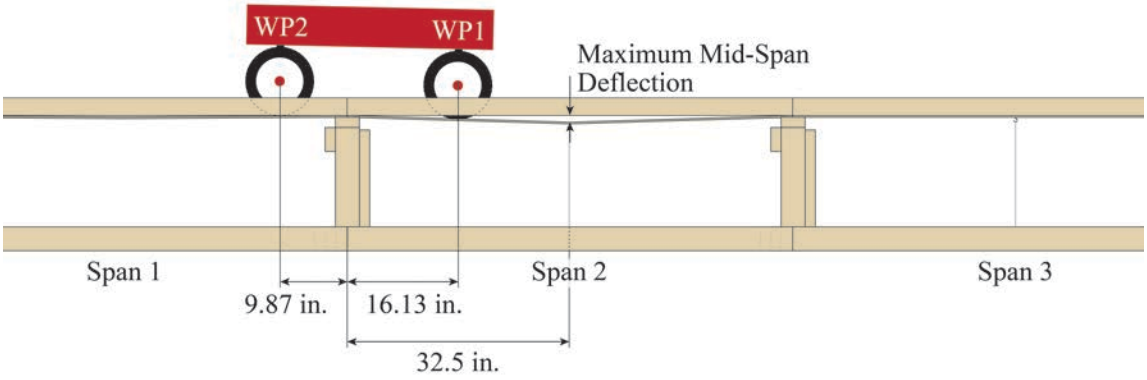

Figure 4.4: Wheel Path Position on Small-Scale Bridge during Maximum Mid-Span Deflection for Case 3 Test 9 Span 2

Figure 4.5 shows the location of the wagon at the time of the maximum mid-span deflection of Span 3 during Case 3 Test 9.

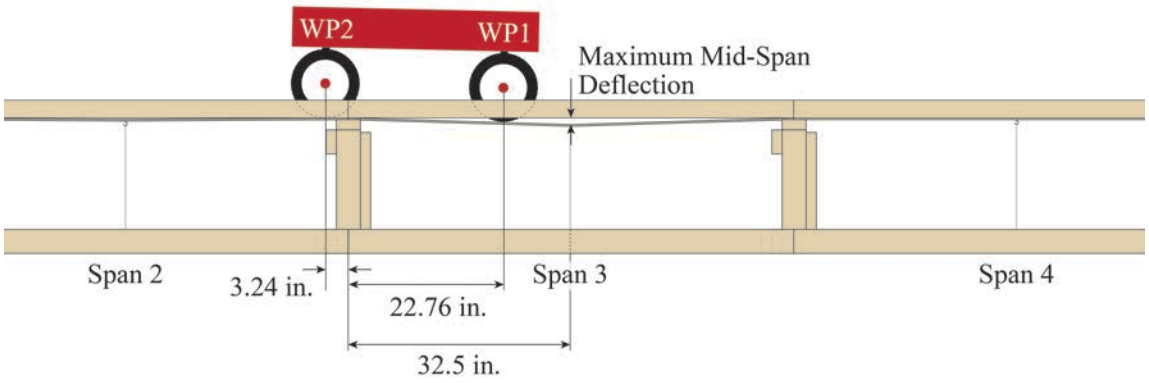

Figure 4.5: Wheel Path Position on Small-Scale Bridge during Maximum Mid-Span Deflection for Case 3 Test 9 Span 3

Figure 4.6 shows the location of the wagon at the time of the maximum mid-span deflection of Span 4 during Case 3 Test 9.

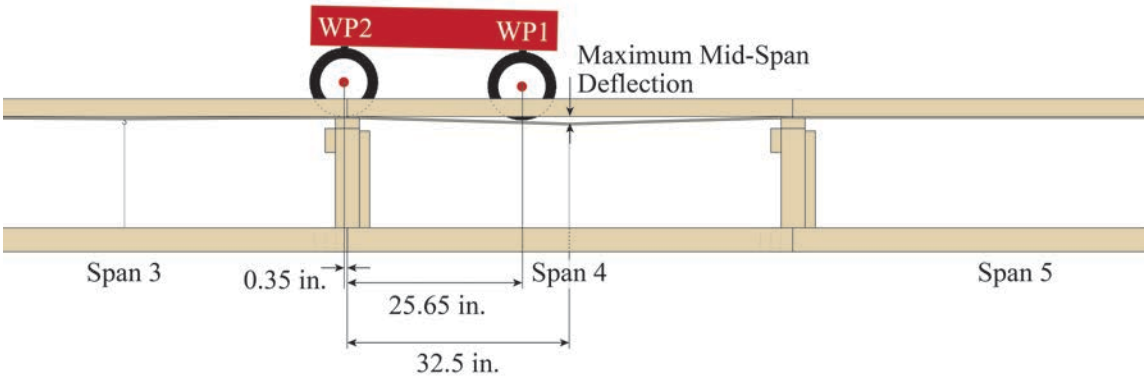

Figure 4.6: Wheel Path Position on Small-Scale Bridge during Maximum Mid-Span Deflection for Case 3 Test 9 Span 4

It is evident that the maximum mid-span deflection of each span occurred just before wheel path 1 reached the mid-span and just before wheel path 2 crossed the bent before that span.

4.2 Large-Scale Open Deck Experiment Results

This section highlights key results from the large-scale open deck experiment. The deflections of stringer for two spans and the deflections of three bent-caps were measured under various parameters, which are listed in Chapter II. A southbound freight train passed over Bridge 17.14 for Test 1. Plots for this test can be found in Appendix B for the bent-cap deflections, total stringer deflections, and net stringer deflections.

4.2.1 Large-Scale Open Deck Bent-Cap Deflection Results

Appendix C contains plots of bent-cap deflection vs. time for the nine tests conducted with the locomotive crane. The maximum deflections for Bent 9 West, Bent 9 East, Bent 8 West, Bent 8 East, Bent 7 West, and Bent 7 East are reflected in Table 4.3.

Table 4.3: Open Deck Bridge Maximum Bent-Cap Deflections (in.)

Test No.	Bent 7 W	Bent 7 E	Bent 8 W	Bent 8 E	Bent 9 W	Bent 9 E
1	-0.01554	-0.04698	-0.08213	-0.02901	-0.03886	-0.04168
2	-0.00181	-0.01484	-0.05124	-0.00869	-0.00869	-0.01421
3	-0.00156	-0.01557	-0.05197	-0.00889	-0.01054	-0.01488
4	-0.00098	-0.01711	-0.05090	-0.00966	-0.01043	-0.01432
5	-0.00069	-0.01517	-0.05063	-0.00878	-0.0105	-0.01445
6	-0.00053	-0.01748	-0.05002	-0.01014	-0.01062	-0.01414
7	-0.00081	-0.01720	-0.04999	-0.01094	-0.00974	-0.01334
8	-0.00072	-0.01830	-0.04842	-0.01231	-0.00872	-0.01228
9	-0.00081	-0.01928	-0.05020	-0.01160	-0.0080	-0.01144
10	-0.00071	-0.01854	-0.04767	-0.01055	-0.00764	-0.00706

It can be seen that for every test, Bent 8 West had the largest deflections of all the bent-cap locations. Although this is true, they are almost negligible deflections. The largest deflection Bent 8 West experienced was during Test 1 when the freight train passed over the bridge. This deflection was approximately 1/12 of an inch, which is not very large, relatively speaking. It is worth noting that all of the bent-caps experienced their largest deflection as the freight train traversed the bridge.

In order to see how speed affected the bent-cap deflections, Table 4.4 shows the average maximum deflection of each bent-cap during each test arranged by ascending vehicle speed.

Table 4.4: Open Deck Bridge Average Maximum Bent-Cap Deflections

Test	Speed (mph)	Avg. B7 (in.)	Avg. B8 (in.)	Avg. B9 (in.)
3	1.8	-0.00856	-0.03043	-0.01271
2	2.1	-0.00833	-0.02996	-0.01145
10	5.5	-0.00962	-0.02911	-0.00735
4	11.2	-0.00905	-0.03028	-0.01237
5	11.2	-0.00793	-0.02971	-0.01248
6	19.2	-0.00901	-0.03008	-0.01238
7	19.4	-0.00900	-0.03046	-0.01154
8	25.3	-0.00951	-0.03036	-0.0105
9	27.4	-0.01004	-0.0309	-0.00972

In general, it appears as the vehicle speed increases, the average bent-cap deflection is consistent. This suggests that vehicle speeds below 30 mph do not have a significant impact on bent-cap deflection.

Figure 4.7 is a plot of bent-cap deflections versus time for bent-cap 9 during Test 6. For this test, the locomotive crane traversed the bridge at 19.2 mph. Because the vehicle was traveling north, it crossed over bent-cap 9 first.

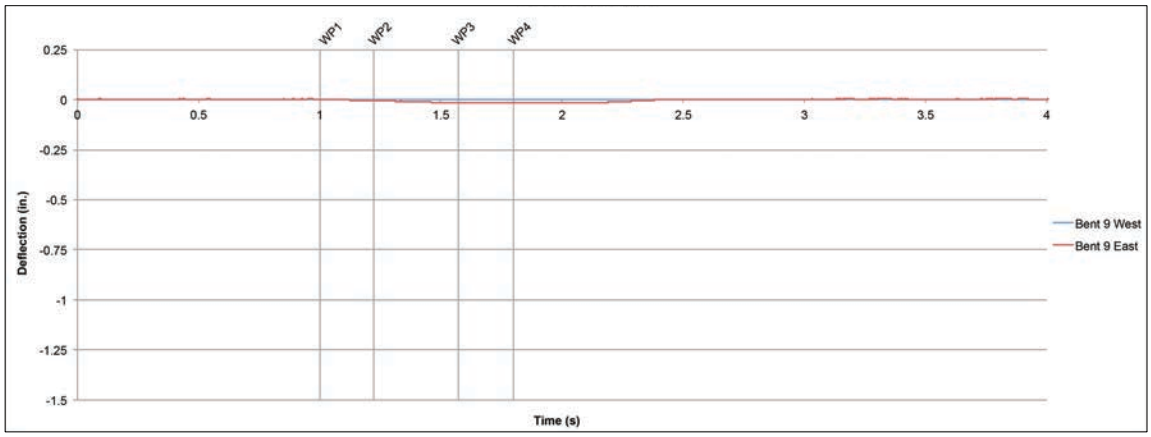

Figure 4.7: Open Deck Bridge Bent-Cap 9 Deflections for Test 6

Figure 4.8 is a plot of bent-cap deflections versus time for bent-cap 8 during Test 6.

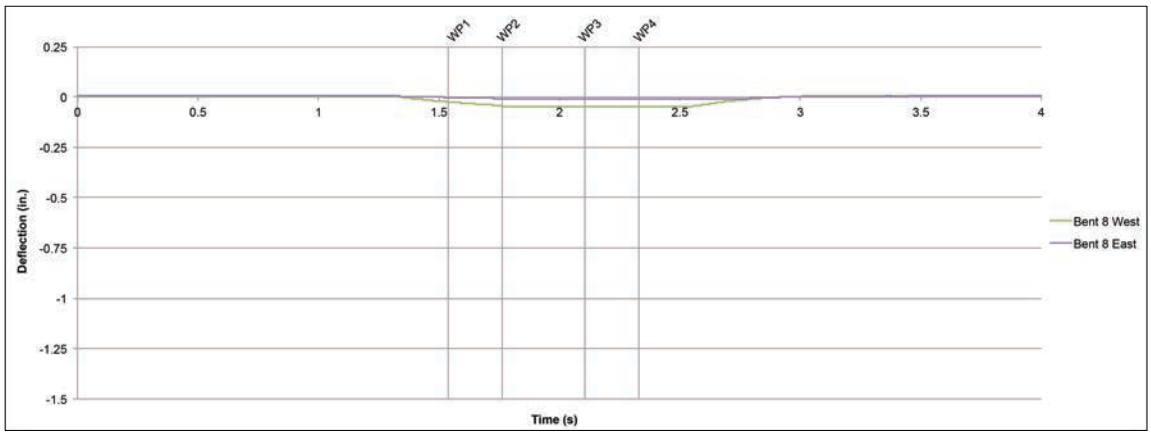

Figure 4.8: Open Deck Bridge Bent-Cap 8 Deflections for Test 6

Finally, Figure 4.9 displays bent-cap 8 deflections versus time during Test 6.

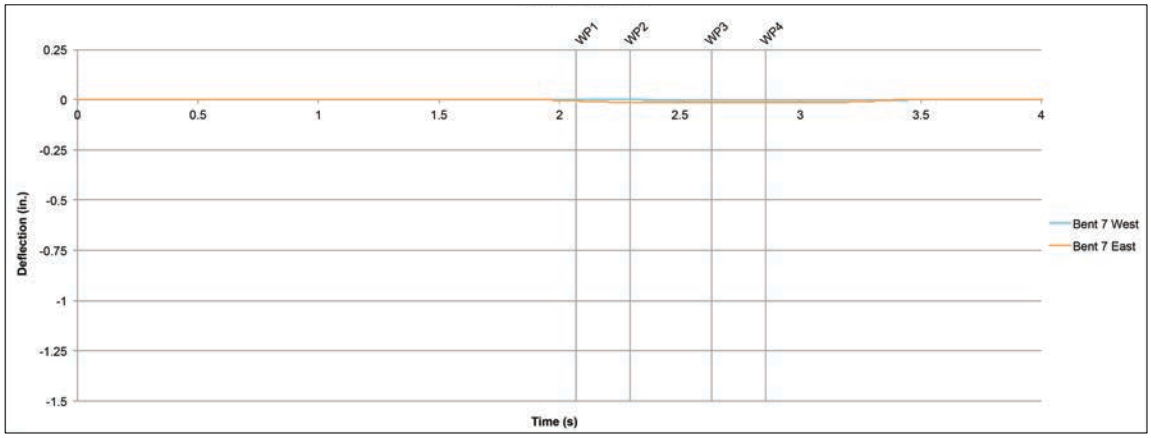

Figure 4.9: Open Deck Bridge Bent-Cap 7 Deflections for Test 6

For each of these plots, there are four vertical lines graphed. These lines indicate the time that a wheel path crossed over the bent-cap of interest. These times were calculated using the velocity of the locomotive crane during the respective test.

The times of wheel path position are difficult to relate to the maximum bent-cap deflection in each of these plots because the bent-cap deflections are so small. However, upon examination of all the bent-cap deflection plots in Appendix C, the time of the wheel path position at the maximum bent-cap deflection appears to be similar. In order to see this relationship more clearly, figures were created showing the positions of the locomotive over the bridge at the times of maximum bent-cap deflection during Test 6. Figure 4.10 shows the position of the locomotive crane at the time of the maximum bent-cap 9 deflection during Test 6.

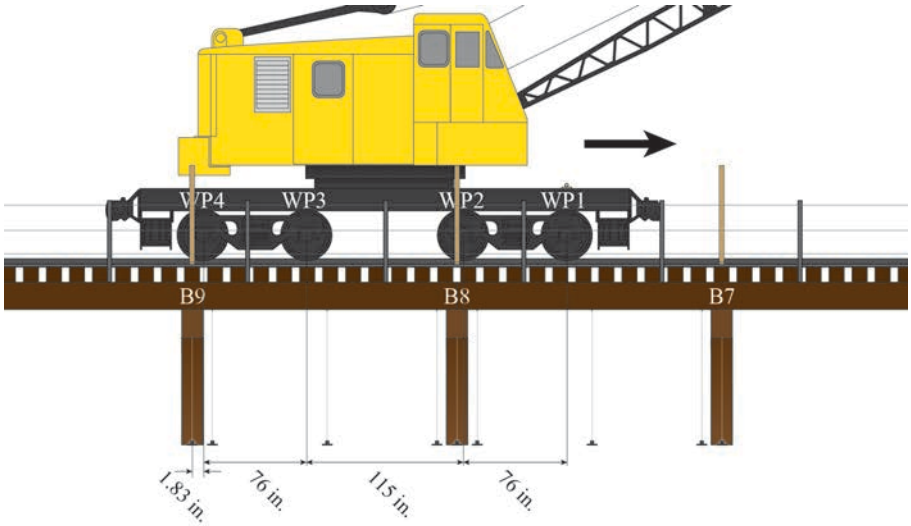

Figure 4.10: Wheel Path Position on Open Deck Bridge during Maximum Bent-Cap 9 Deflection of Test 6

Figure 4.11 shows the position of the locomotive crane at the time of the maximum bent-cap 8 deflection during Test 6.

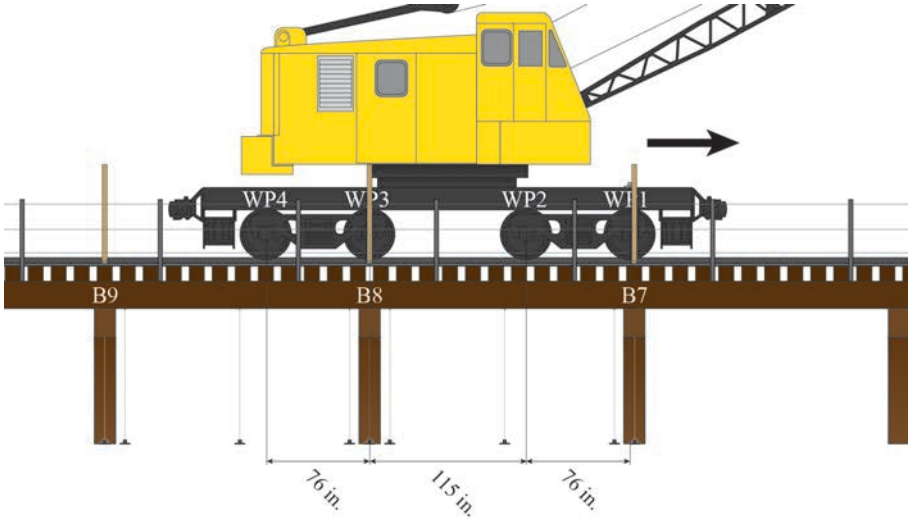

Figure 4.11: Wheel Path Position on Open Deck Bridge during Maximum Bent-Cap 8 Deflection of Test 6

Figure 4.12 shows the position of the locomotive crane at the time of the maximum bent-cap 7 deflection during Test 6.

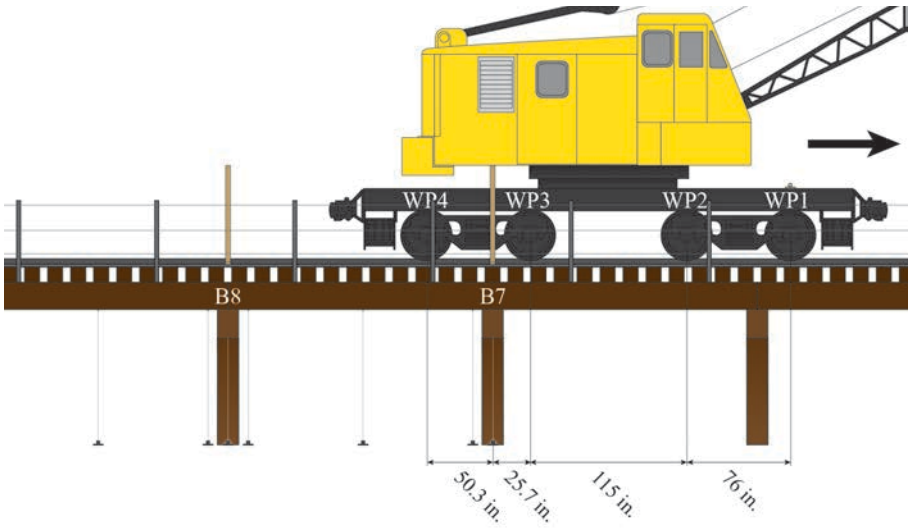

Figure 4.12: Wheel Path Position on Open Deck Bridge during Maximum Bent-Cap 7 Deflection of Test 6

Upon examination of Figure 4.10, Figure 4.11, and Figure 4.12, the maximum bent-cap deflection occurs when the truck comprising wheel path 3 and wheel path 4 is over that respective bent-cap. As stated in Chapter II, this locomotive crane has four engines which are located directly above this truck. This means that a substantial amount of the locomotive crane's weight is being placed on the truck, and that weight is ultimately being transferred to the bent-cap directly underneath the truck.

4.2.2 Large-Scale Open Deck Mid-span Total Deflection Results

Appendix D contains plots of total stringer deflection versus time for tests 2-10 of the large-scale open deck experiment. The maximum total stringer deflections of span 7 during each test (1-10) are shown below in Table 4.5.

Table 4.5: Open Deck Bridge Maximum Total Stringer Deflections of Span 7 (in.)

Test	S7C1P1	S7C1P2	S7C1P3	S7C1P4	S7C2P1	S7C2P2	S7C2P3	S7C2P4
1	-0.4666	-0.4978	-0.5141	-0.5603	-0.8286	-0.9528	-1.0058	-1.099
2	-0.4482	-0.511	-0.5412	-0.5869	-0.8896	-1.0217	-1.0776	-1.1708
3	-0.451	-0.5121	-0.5413	-0.589	-0.8883	-1.019	-1.0772	-1.1678
4	-0.436	-0.4989	-0.5261	-0.5756	-0.8972	-1.0328	-1.0992	-1.1934
5	-0.439	-0.495	-0.5253	-0.5752	-0.8934	-1.0299	-1.0984	-1.1915
6	-0.4559	-0.5209	-0.5515	-0.5994	-0.9073	-1.0412	-1.1019	-1.1942
7	-0.4505	-0.5118	-0.5453	-0.5948	-0.9088	-1.0424	-1.1035	-1.1966
8	-0.4618	-0.5341	-0.5746	-0.6324	-0.9751	-1.1203	-1.1874	-1.2917
9	-0.428	-0.5052	-0.5495	-0.6164	-0.9934	-1.1501	-1.223	-1.3295
10	-0.4362	-0.4914	-0.5174	-0.5658	-0.8418	-0.9718	-1.0315	-1.1198

Chord 2 appears to have the largest total deflections. In particular, Ply 2, Ply 3, and Ply 4 of Chord 2 appear to have extremely high total deflections. A visual examination was performed on the day of testing, and it was noted that Ply 4 was split. Ply 2 and Ply 3 were not visible, but according to this data, they may have been impaired to some degree.

Table 4.6 shows the maximum total stringer deflections of span 8 during Tests 1-10.

Table 4.6: Open Deck Bridge Maximum Total Stringer Deflections of Span 8 (in.)

Test	S8C1P1	S8C1P2	S8C1P3	S8C1P4	S8C2P1	S8C2P2	S8C2P3	S8C2P4
1	-0.3523	-0.4369	-0.4965	-0.5516	-0.9665	-0.8944	-0.9364	-1.0892
2	-0.3492	-0.4408	-0.5075	-0.5588	-0.9911	-0.9271	-0.9462	-1.0852
3	-0.3539	-0.4464	-0.511	-0.5625	-0.9993	-0.9304	-0.9486	-1.0892
4	-0.3329	-0.4199	-0.4919	-0.5358	-1.0082	-0.9441	-0.9729	-1.1181
5	-0.3337	-0.4221	-0.4932	-0.5351	-1.0101	-0.9458	-0.9741	-1.1231
6	-0.3425	-0.4299	-0.5029	-0.5479	-0.9752	-0.9122	-0.9399	-1.0798
7	-0.3507	-0.4372	-0.5103	-0.5545	-0.983	-0.906	-0.9341	-1.0697
8	-0.3399	-0.4296	-0.4982	-0.5446	-0.9719	-0.8906	-0.922	-1.0693
9	-0.393	-0.4766	-0.5434	-0.5915	-1.0382	-0.9266	-0.9521	-1.0861
10	-0.3243	-0.4068	-0.4733	-0.5183	-1.02	-0.9189	-0.9559	-1.1033

Again, Chord 2 appears to have the largest total deflections. All four stringers in Chord 2 appear to have extremely large total deflections. Ply 2 and Ply 4 were continuous across span 7 and span 8, so it is known that Ply 4 was split. Ply 1, Ply 2 and Ply 3 of Chord 2 may have been impaired to some degree, too.

It is important to note that Table 4.5 and Table 4.6 also show that the stringers in each chord do not act as one member. Each stringer in each chord of each span has a different response to the live load. For instance, the smallest deflection that occurred in Span 8 Chord 1 during Test 6 was -0.3425 inches, and the largest deflection was -0.5479 inches. This is a 37.5% increase in deflection. This is because each stringer has a different condition due to fatigue, weather, insects, and a variety of other exposures.

In order to see how speed affected the total stringer deflections, Table 4.7 lists average total maximum stringer deflections of each chord during each test according to ascending speed.

Table 4.7: Open Deck Bridge Average Total Maximum Stringer Deflections of Each Chord and Vehicle Speed

Test	Speed (mph)	S7C1 Avg (in.)	S7C2 Avg (in.)	S8C1 Avg (in.)	S8C2 Avg (in.)
3	1.8	-0.52335	-1.03808	-0.46845	-0.99188
2	2.1	-0.52183	-1.03993	-0.46408	-0.9874
10	5.5	-0.5027	-0.99123	-0.43068	-0.99953
4	11.2	-0.50915	-1.05565	-0.44513	-1.01083
5	11.2	-0.50863	-1.0533	-0.44603	-1.01328
6	19.2	-0.53193	-1.06115	-0.4558	-0.97678
7	19.4	-0.5256	-1.06283	-0.46318	-0.9732
8	25.3	-0.55073	-1.14363	-0.45308	-0.96345
9	27.4	-0.52478	-1.174	-0.50113	-1.00075

It appears that the average total stringer deflection for each chord stays relatively consistent as vehicle speed increases. This suggests that vehicle speeds below 30 mph do not have a significant impact on total stringer deflection.

Figure 4.13 is a plot of total stringer deflection versus time for span 8 during Test 6. For this test, the locomotive crane traversed the bridge at 19.2 mph. Because the vehicle was traveling north, it crossed over span 8 first.

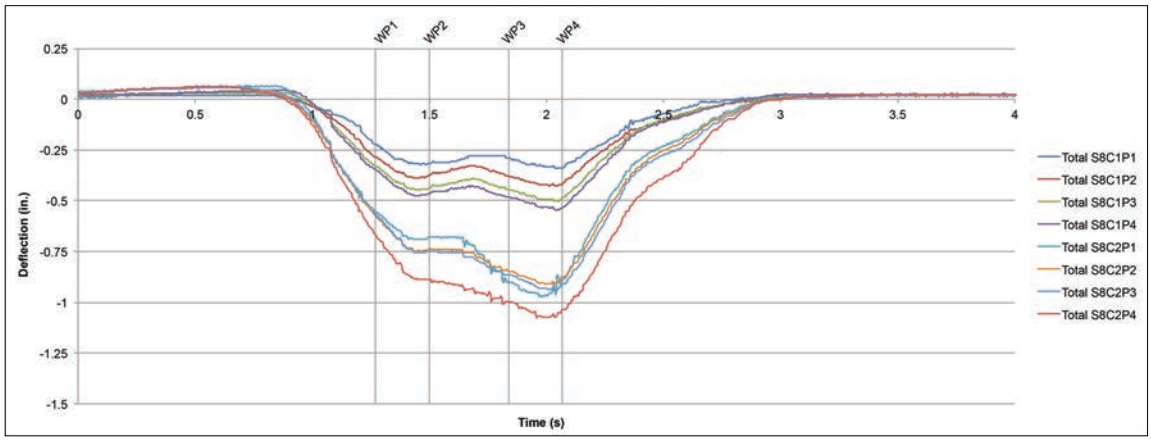

Figure 4.13: Open Deck Bridge Total Span 8 Stringer Deflection during Test 6

Figure 4.14 is a plot of total stringer deflection versus time for span 7 during Test 6.

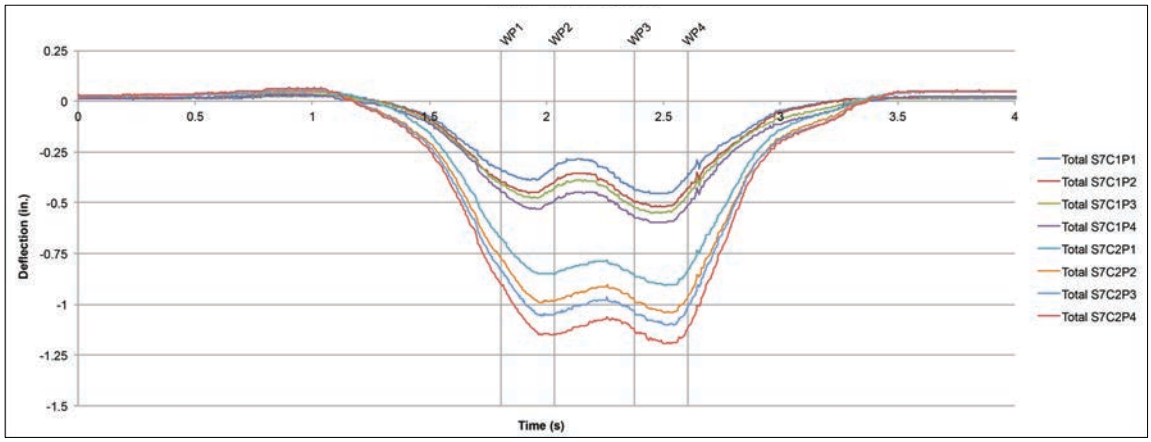

Figure 4.14: Open Deck Bridge Total Span 7 Stringer Deflection during Test 6

For each of these plots, four vertical lines have been graphed. Each line reflects the time that a particular wheel path crossed the mid-span of the span of interest. These times were calculated using the velocity of the locomotive train during the respective test.

Figure 4.13 and Figure 4.14 show that as wheel path 1 approaches mid-span, there is a rapid increase in mid-span total deflection. As the truck comprising wheel path 1 and wheel path 2 is directly above the mid-span, a local maximum deflection occurs. As wheel path 2 crosses the mid-span, an inflection point can be seen as the deflection decreases. As the locomotive crane is centered above the mid-span, a local minimum deflection occurs. This is because concentrated loads are not above the mid-span; they are approximately equidistant from the mid-span. As wheel path 3 approaches the mid-span, an inflection point can be seen as the deflection begins to increase. As this truck is above the mid-span, a maximum deflection occurs. This is due to the extremely heavy engines in the locomotive crane that are enclosed directly above this truck. After wheel path 4 crosses the mid-span, the deflections begin to rapidly decrease until the stringers return to their resting position.

As the truck comprising wheel path 1 and wheel path 2 crosses the mid-span of this ply, it seems to follow the same general pattern of the other plies. As Figure 4.13 and Figure 4.14 display, Ply 1 of the chords has the smallest deflections in response to the live load. Ply 2 has slightly larger deflections, and Ply 3 again sees an increase in deflection. Ply 4 has the largest deflections in response to the live load. Each ply appears to have this response to the live load, except for Span 8 Chord 2 Ply 1. As wheel path 3 approaches the mid-span of Span 8 Chord 2 Ply 1, there is a rapid increase in deflection. As the truck comprising wheel path 3 and wheel path 4 crosses over the mid-span of this ply, the deflection surpasses that of Ply 2 and Ply 3. This could be another indication that this particular ply is critically impaired.

Figure 4.13 and Figure 4.14 also show that there was a slope within the cross-section during total mid-span stringer deflection. To better understand how the stringers were deflecting, a cross-section, A-A, was taken from the mid-span of Span 7, as shown in Figure 4.15.

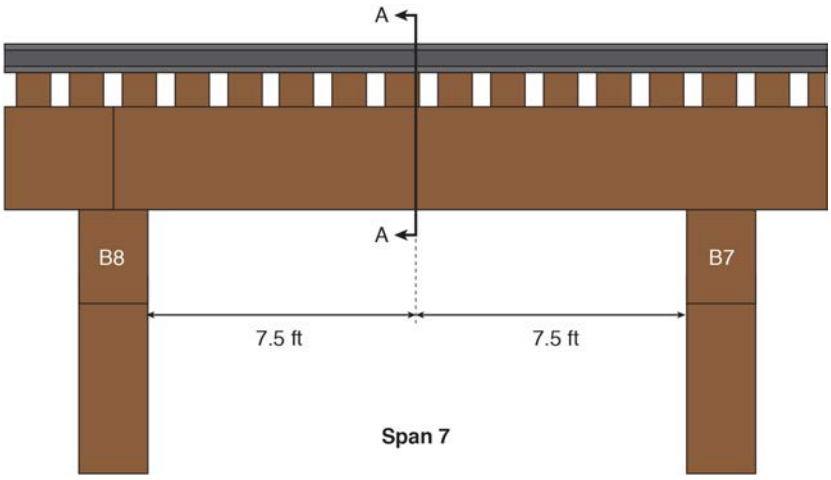

Figure 4.15: Span 7 of Open Deck Bridge Showing Cross-Section A-A

Figure 4.16 shows the cross-section A-A taken from Figure 4.15.

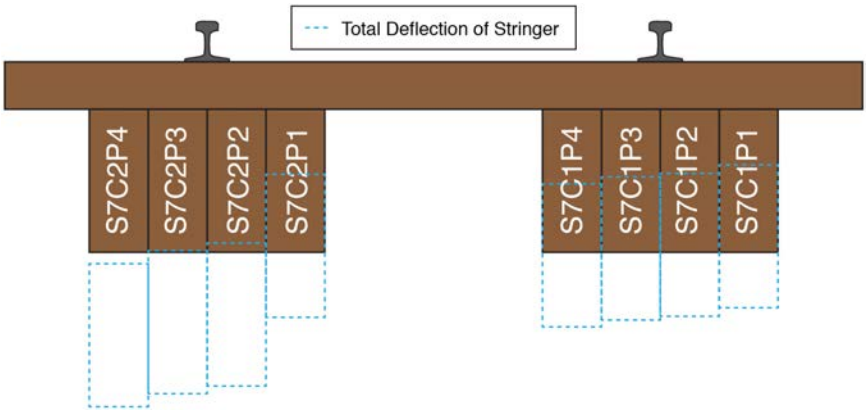

Figure 4.16: Cross-Section A-A Showing Span 7 Maximum Total Mid-Span Deflection During Test 6

Figure 4.16 shows that the stringers of Span 7 were actually sloped as the vehicle traversed the bridge.

Several figures have been created in order to show the wheel path positions when the mid-spans are experiencing a maximum deflection. Figure 4.17 shows the position of the locomotive crane at the time of the maximum Span 8 Chord 1 deflection during Test 6.

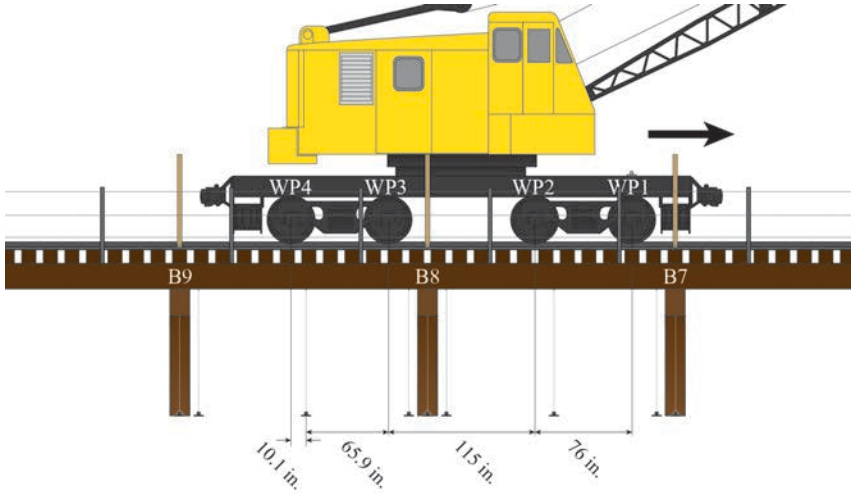

Figure 4.17: Wheel Path Position on Open Deck Bridge during Maximum Total Span 8 Chord 1 Stringer Deflection

Figure 4.18 shows the position of the locomotive crane at the time of the maximum Span 8 Chord 2 deflection during Test 6.

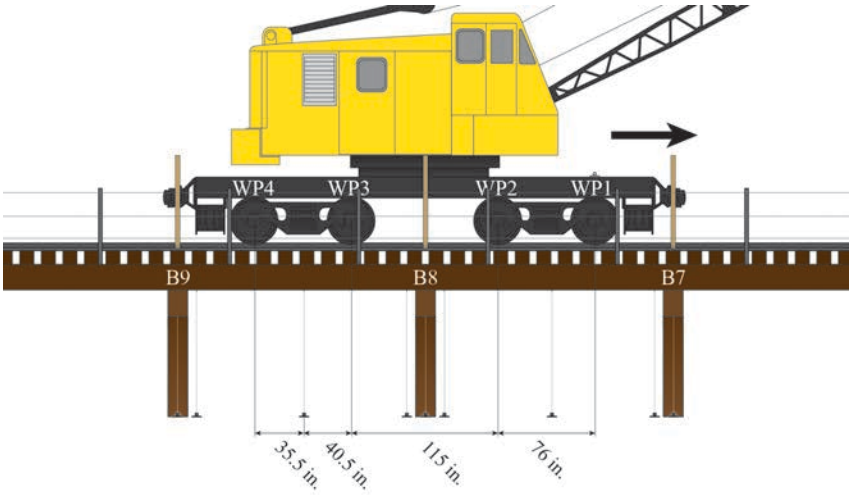

Figure 4.18: Wheel Path Position on Open Deck Bridge during Maximum Total Span 8 Chord 2 Stringer Deflection

Figure 4.19 shows the position of the locomotive crane at the time of the maximum Span 8 Chord 2 deflection during Test 6.

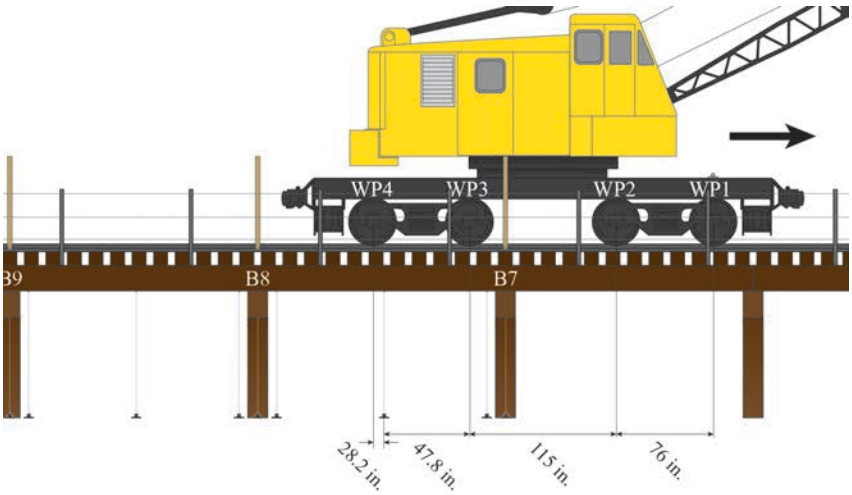

Figure 4.19: Wheel Path Position on Open Deck Bridge during Maximum Total Span 7 Chord 1 Stringer Deflection

Figure 4.20 shows the position of the locomotive crane at the time of the maximum Span 8 Chord 2 deflection during Test 6.

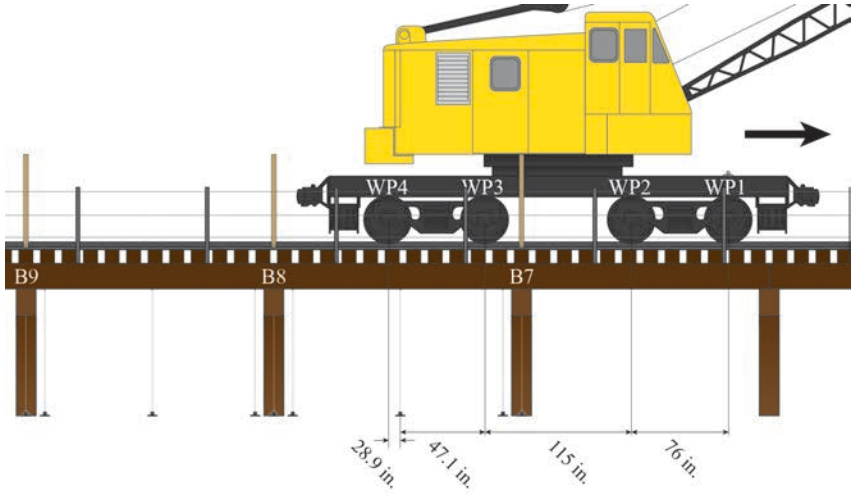

Figure 4.20: Wheel Path Position on Open Deck Bridge during Maximum Total Span 7 Chord 2 Stringer Deflection

Figure 4.17, Figure 4.18, Figure 4.19, and Figure 4.20 clearly show that each chord of each span experienced a maximum total mid-span deflection just before wheel path 4 passed over the mid-span. Again, this is due to the placement of the four engines in the locomotive crane.

4.2.3 Large-Scale Open Deck Mid-span Net Deflection Results

Appendix E contains plots of net stringer deflection versus time for tests 2-10 of the large-scale open deck experiment. The maximum net stringer deflections of span 7 during each test (1-10) are shown below in Table 4.8.

Table 4.8: Open Deck Bridge Maximum Net Mid-Span Stringer Deflections of Span 7 (in.)

Test	S7C1P1	S7C1P2	S7C1P3	S7C1P4	S7C2P1	S7C2P2	S7C2P3	S7C2P4
1	-0.1673	-0.1853	-0.1514	-0.1714	-0.3629	-0.5322	-0.5816	-0.6714
2	-0.1889	-0.2251	-0.1908	-0.2157	-0.4084	-0.5836	-0.6352	-0.7270
3	-0.1906	-0.2258	-0.1917	-0.2159	-0.4062	-0.5847	-0.6336	-0.7258
4	-0.1811	-0.2153	-0.1844	-0.2106	-0.4181	-0.5987	-0.6532	-0.7431
5	-0.1779	-0.2114	-0.1832	-0.2092	-0.4154	-0.5929	-0.6522	-0.7435
6	-0.1937	-0.2293	-0.1996	-0.2224	-0.4241	-0.6041	-0.6576	-0.7519
7	-0.1944	-0.2276	-0.1970	-0.2219	-0.4279	-0.6063	-0.6582	-0.7496
8	-0.2035	-0.2440	-0.2183	-0.2470	-0.4689	-0.6578	-0.7142	-0.8150
9	-0.1922	-0.2308	-0.2111	-0.2413	-0.4763	-0.6729	-0.7348	-0.8302
10	-0.1894	-0.2112	-0.1874	-0.2033	-0.3920	-0.5753	-0.6200	-0.7100

The maximum net stringer deflections of span 8 during each test (1-10) are shown below in Table 4.9.

Table 4.9: Open Deck Bridge Maximum Net Mid-Span Stringer Deflections of Span 8 (in.)

Test	S8C1P1	S8C1P2	S8C1P3	S8C1P4	S8C2P1	S8C2P2	S8C2P3	S8C2P4
1	-0.0958	-0.1379	-0.1885	-0.2729	-0.4366	-0.5043	-0.3618	-0.6245
2	-0.1043	-0.1590	-0.2057	-0.2777	-0.4425	-0.5338	-0.3842	-0.6378
3	-0.1070	-0.1614	-0.2067	-0.2792	-0.4481	-0.5343	-0.3841	-0.6382
4	-0.0930	-0.1475	-0.1993	-0.2662	-0.4630	-0.5484	-0.4029	-0.6627
5	-0.0921	-0.1459	-0.1998	-0.2616	-0.4617	-0.5489	-0.4027	-0.6654
6	-0.1063	-0.1560	-0.2078	-0.2729	-0.4305	-0.5318	-0.3842	-0.6481
7	-0.1119	-0.1623	-0.2112	-0.2738	-0.4491	-0.5305	-0.3808	-0.6434
8	-0.1058	-0.1584	-0.2028	-0.2673	-0.4398	-0.5180	-0.3742	-0.6477
9	-0.1366	-0.1830	-0.2309	-0.3006	-0.4996	-0.5440	-0.3919	-0.6547
10	-0.1024	-0.1436	-0.1945	-0.2523	-0.4869	-0.5380	-0.4024	-0.6728

Section 3.1.15 of Chapter 7 in the 2015 AREMA Manual for Railway Engineering specifies that the measured net chord deflection (in inches) of a bridge under live load should not exceed L/250, where L is the span length in inches (AREMA 2015). Each span length of Bridge 17.14 was 180 inches. This means that net chord deflections should not exceed -0.72 inches. Deflections in excess of the -0.72 inch maximum are highlighted in red in Table 4.8 and Table 4.9. Span 7 Chord 2 Ply 3 only exceeded this limit during Test 9. However, Span 7 Chord 2 Ply 4 exceeded this limit for every test but Test 1 (southbound freight train) and Test 10 (southbound locomotive crane at 5.5 mph). This was the stringer that was obviously split when a visual examination was performed on the day of testing.

It is also apparent when looking at the net deflections that the stringers in each chord do not act as one member. For instance, the smallest deflection of Span 7 Chord 2 Ply 4 is -0.6714 inches, and the largest deflection is -0.8302 inches. This is a 19.1% increase in net deflection. This is larger than the percent increase in the total deflection of the same member, which was 17.3%.

Chapter I suggested that a split stringer would experience deflections 4 times as large as an unimpaired stringer. Chord 1 Ply 1 and Chord 2 Ply 4 are the outermost stringers of Span 7, so they should have experienced similar loads as the vehicle traversed the bridge. It has already been established that Ply 4 was split. Ply 1 consistently has smaller deflections than the rest of the stringers, so it can be assumed that it is in better condition. Table 4.10 shows the deflections of Chord 1 Ply 1 and Chord 2 Ply 4 of Span 7 for each test, and it also describes the increase in deflection.

Table 4.10: Open Deck Bridge S7C1P1 and S7C2P4 Comparison

Test	S7C1P1 (in.)	S7C2P4 (in.)	S7C2P4 / S7C1P1
1	-0.1673	-0.6714	4.01
2	-0.1889	-0.727	3.85
3	-0.1906	-0.7258	3.81
4	-0.1811	-0.7431	4.10
5	-0.1779	-0.7435	4.18
6	-0.1937	-0.7519	3.88
7	-0.1944	-0.7496	3.86
8	-0.2035	-0.815	4.00
9	-0.1922	-0.8302	4.32
10	-0.1894	-0.71	3.75

Table 4.10 demonstrates that the deflections of S7C2P4, which is the split stringer, are approximately 4 times as large as the deflections of S7C1P1 for each test. This supports the theory outlined in Chapter I.

There is a significant difference between the total mid-span stringer deflections and the net stringer deflections. For instance, the maximum net mid-span stringer deflection of Span 7 Chord 2 Ply 4 was -0.8302 inches during test 9. The maximum total mid-span stringer deflection of the same span, chord, and ply during test 9 was -1.3295 inches. This is a 37.6% increase in deflection, which is substantial. Table 4.11 demonstrates the percent increase in deflection in each ply in Span 7 for each test performed.

Table 4.11: Open Deck Bridge Percent Increase from Net Maximum Deflection to Total Maximum Deflection for Span 7

Test	S7C1P1	S7C1P2	S7C1P3	S7C1P4	S7C2P1	S7C2P2	S7C2P3	S7C2P4
1	64.1%	62.8%	70.6%	69.4%	56.2%	44.1%	42.2%	38.9%
2	57.9%	56.0%	64.7%	63.3%	54.1%	42.9%	41.1%	37.9%
3	57.7%	55.9%	64.6%	63.4%	54.3%	42.6%	41.2%	37.9%
4	58.5%	56.9%	65.0%	63.4%	53.4%	42.0%	40.6%	37.7%
5	59.5%	57.3%	65.1%	63.6%	53.5%	42.4%	40.6%	37.6%
6	57.5%	56.0%	63.8%	62.9%	53.3%	42.0%	40.3%	37.0%
7	56.9%	55.5%	63.9%	62.7%	52.9%	41.8%	40.4%	37.4%
8	55.9%	54.3%	62.0%	61.0%	51.9%	41.3%	39.9%	36.9%
9	55.1%	54.3%	61.6%	60.9%	52.1%	41.5%	39.9%	37.6%
10	56.6%	57.0%	63.8%	64.1%	53.4%	40.8%	39.9%	36.6%

Table 4.12 demonstrates the percent increase in deflection in each ply in Span 7 for each test performed.

Table 4.12: Open Deck Bridge Percent Increase from Net Maximum Deflection to Total Maximum Deflection for Span 8

Test	S8C1P1	S8C1P2	S8C1P3	S8C1P4	S8C2P1	S8C2P2	S8C2P3	S8C2P4
1	72.8%	68.4%	62.0%	50.5%	54.8%	43.6%	61.4%	42.7%
2	70.1%	63.9%	59.5%	50.3%	55.4%	42.4%	59.4%	41.2%
3	69.8%	63.8%	59.6%	50.4%	55.2%	42.6%	59.5%	41.4%
4	72.1%	64.9%	59.5%	50.3%	54.1%	41.9%	58.6%	40.7%
5	72.4%	65.4%	59.5%	51.1%	54.3%	42.0%	58.7%	40.8%
6	69.0%	63.7%	58.7%	50.2%	55.9%	41.7%	59.1%	40.0%
7	68.1%	62.9%	58.6%	50.6%	54.3%	41.5%	59.2%	39.9%
8	68.9%	63.1%	59.3%	50.9%	54.7%	41.8%	59.4%	39.4%
9	65.2%	61.6%	57.5%	49.2%	51.9%	41.3%	58.8%	39.7%
10	68.4%	64.7%	58.9%	51.3%	52.3%	41.5%	57.9%	39.0%

It is clear that the support settlement had a large impact on the stringer deflections. The smallest percent increase in deflection was for the Test and Ply already noted (Span 7 Chord 2 Ply 4 during Test 9), which was 37.6%. Even the smallest percent increase is substantial. It appears as though Chord 1 of Span 7 and Span 8 were influenced the most by support settlement. Span 8 Chord 2 Ply 3 and Span 7 Chord 2 Ply 1 also appear to have been significantly affected by support settlement.

In order to see how speed affected the net stringer deflections, Table 4.13 lists average net maximum stringer deflections of each chord during each test ranked by ascending speed.

Table 4.13: Open Deck Bridge Average Net Maximum Stringer Deflections of Each Chord and Vehicle Speed

Test	Speed (mph)	S7C1 Avg (in.)	S7C2 Avg (in.)	S8C1 Avg (in.)	S8C2 Avg (in.)
1	-	-0.1688	-0.5370	-0.17375	-0.4818
3	1.8	-0.2060	-0.5876	-0.18855	-0.50113
2	2.1	-0.2051	-0.2600	-0.18665	-0.49955
10	5.5	-0.1978	-0.5743	-0.17319	-0.52501
4	11.2	-0.1978	-0.6033	-0.17648	-0.51923
5	11.2	-0.1954	-0.6010	-0.17481	-0.51966
6	19.2	-0.2112	-0.6094	-0.18571	-0.4986
7	19.4	-0.2102	-0.6105	-0.18978	-0.50093
8	25.3	-0.2282	-0.6640	-0.18355	-0.49491
9	27.4	-0.2188	-0.6785	-0.21276	-0.52253

It appears that the average net stringer deflection for each chord stays relatively consistent as vehicle speed increases, too. This suggests that vehicle speeds below 30 mph do not have a significant impact on net stringer deflection.

Figure 4.21 is a plot of net stringer deflection versus time for Span 8 during Test 6. This is the same test examined for the bent-cap deflections and the total stringer deflections.

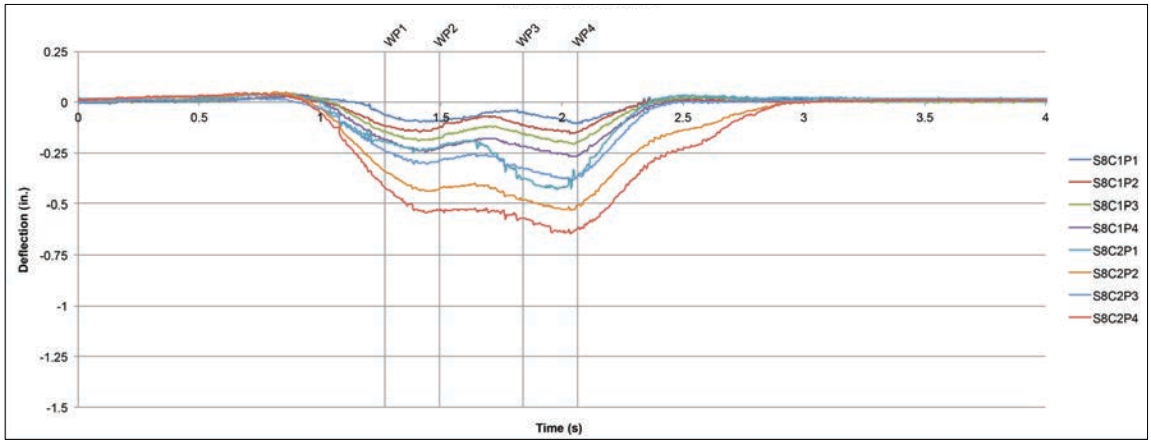

Figure 4.21: Open Deck Bridge Net Span 8 Stringer Deflection During Test 6

Figure 4.22 is a plot of net stringer deflection versus time for span 7 during Test 6.

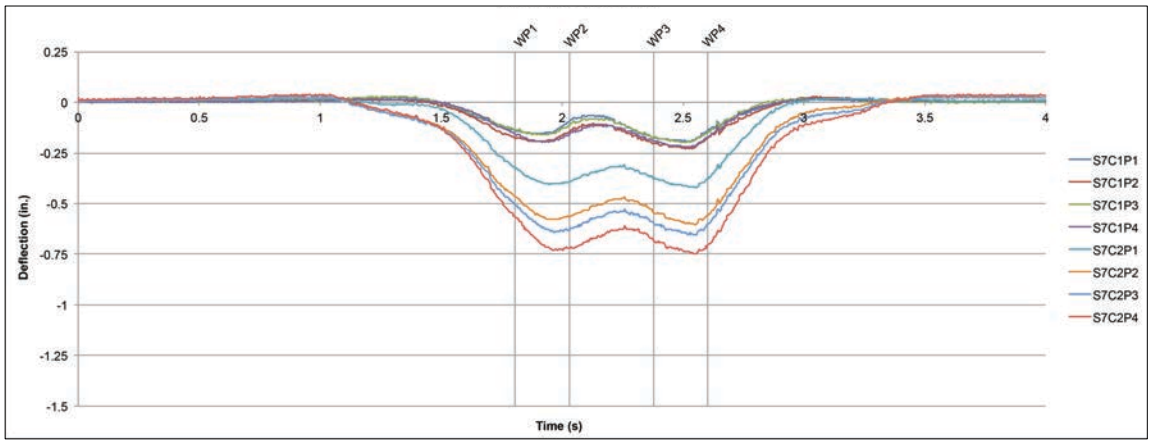

Figure 4.22: Open Deck Bridge Net Span 7 Stringer Deflection During Test 6

The net deflections appear to follow the same pattern as the total deflections. As already noted, there is a significant difference in the magnitude of the deflections, though. When comparing Figure 4.13 with Figure 4.21 (Span 8 total deflections and span 8 net deflections, respectively), it is clear that the support settlement had a large impact on the stringer deflections of Span 8 Chord 1. The total deflections reflect that the maximum mid-span deflections of Chord 1 were all more than 0.25 inches, while the net deflections show that the mid-span deflections were all approximately 0.25 inches or less. It is also clear that the support settlement greatly affected the mid-span deflections of Span 8 Chord 2. Figure 4.13 shows a large increase in total deflection when compared to Chord 1, but Figure 4.21 shows that the deflections of Chord 2 are not that drastically different than the deflections of Chord 1.

When comparing Figure 4.14 with Figure 4.22 (Span 7 total deflections and Span 7 net deflections, respectively), there is also a noticeable difference without the support settlement. Again, the total deflections reflect that the maximum mid-span deflections of Chord 1 were all more than 0.25 inches, while the net deflections show that the mid-span deflections were all less than 0.25 inches. The total Chord 2 Span 7 deflections also have a large increase in deflection when compared to that of Chord 1. However, the net Chord 2 Span 7 deflections do not reflect the drastic increase.

When comparing the plots of net deflection with the plots of total deflection, the time of maximum mid-span deflection appears to be consistent. In addition, the time of the wheel path positions seem to be consistent.

Figure 4.21 and Figure 4.22 also show that, just like during the total deflection, there was a slope within the cross-section during net mid-span stringer deflection. To better understand how the net deflection of the stringers, Figure 4.24 shows the cross-section A-A taken from Figure 4.21 as well as the maximum net mid-span stringer deflection of Span 7 during Test 6.

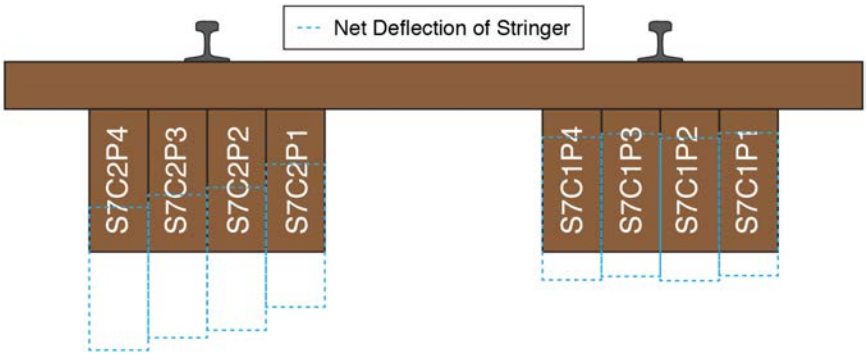

Figure 4.23: Cross-Section A-A Showing Span 7 Maximum Net Mid-Span Deflection During Test 6

Figure 4.24 shows the slope of the stringers during their net mid-span deflection.

4.3 Large-Scale Ballast Deck Experiment Results

This section highlights key results from the large-scale ballast deck experiment. The deflections of stringer for one span and the deflections of two bent-caps were measured under various parameters, which are listed in Chapter II. Wheel path position sensors were not used during this experiment, so wheel path positions were unknown. A southbound freight train and a southbound passenger train passed over Bridge 816.9 for Test 1 and Test 2, respectively. After the tests with the Work Train had been executed, another southbound freight train and a southbound passenger train passed over the bridge. This data was recorded for Test 21 and Test 22, respectively. Plots of bent-cap deflections, total stringer deflections, and net stringer deflections can be found in Appendix F.

4.3.1 Large-Scale Ballast Deck Bent-Cap Deflection Results

Appendix G contains plots of bent-cap deflection versus time for the 18 tests conducted with the work train. The maximum deflections for Bent 9 West, Bent 9 East, Bent 8 West, and Bent 8 East for all 22 tests are reflected in Table 4.14.

Table 4.14: Ballast Deck Bridge Maximum Bent-Cap Deflections

Test	B9W (in.)	B9E (in.)	B8W (in.)	B8E (in.)
1	-0.0561	-0.0254	-0.026	-0.0174
2	-0.0571	-0.0441	-0.0202	-0.0148
3	-0.038	-0.0169	-0.0211	-0.0155
4	-0.0416	-0.018	-0.0212	-0.0163
5	-0.0374	-0.0169	-0.0208	-0.0153
6	-0.0408	-0.0164	-0.0202	-0.0154
7	-0.0363	-0.0182	-0.0216	-0.0159
8	-0.041	-0.0145	-0.0215	-0.0164
9	-0.0348	-0.0164	-0.0222	-0.0173
10	-0.0422	-0.0118	-0.0203	-0.0176
11	-0.0381	-0.0151	-0.0226	-0.018
12	-0.0426	-0.0101	-0.0203	-0.0193
13	-0.0386	-0.0128	-0.0226	-0.0179
14	-0.0426	-0.0079	-0.0209	-0.019
15	-0.0375	-0.0096	-0.025	-0.0199
16	-0.0359	-0.0101	-0.0263	-0.0201
17	-0.0416	-0.018	-0.0212	-0.0163
18	-0.0328	-0.0155	-0.0223	-0.0098
19	-0.0371	-0.0092	-0.02	-0.0111
20	-0.0313	-0.0127	-0.022	-0.0089
21	-0.0188	-0.0064	-0.014	-0.004
22	-0.0387	-0.0264	-0.0209	-0.0141

The average of all of the bent-cap deflections for all of the tests is -0.02303 inches. The deflections that exceed this average are highlighted in red in Table 4.14. Bent 9 West had larger than average deflections for every test except Test 21, which comprised a passenger train traversing the bridge. Bent 9 East experienced a relatively large deflection during Test 2, which comprised a passenger train traversing the bridge. Bent 9 East and Bent 8 West experienced a few more deflections that were slightly higher than average, but not enough to be considered significant. While Table 4.14 shows that Bent 9 West experienced deflections that were larger than average, these deflections are still

extremely small. The largest of the bent-cap deflections was -0.0571 inches, which is less than 1/17 of an inch.

In order to determine the effect of speed on bent-cap deflections in a ballast deck bridge, Table 4.15 shows the average maximum deflections of each bent-cap during each test, which are ranked by ascending vehicle speed.

Table 4.15: Ballast Deck Bridge Average Maximum Bent-Cap Deflections and Vehicle Speed

Test	Speed (mph)	Avg B9 (in.)	Avg B8 (in.)
3	5	-0.0275	-0.0183
15	5	-0.0236	-0.0225
4	10	-0.0298	-0.0188
17	10	-0.0298	-0.0188
5	15	-0.0272	-0.0181
6	20	-0.0286	-0.0178
19	20	-0.0232	-0.0156
7	25	-0.0273	-0.0188
8	30	-0.0278	-0.0190
9	35	-0.0256	-0.0198
10	40	-0.0270	-0.0190
11	40	-0.0266	-0.0203
13	43	-0.0257	-0.0203
12	45	-0.0264	-0.0200
14	45	-0.0253	-0.0200
16	52	-0.0230	-0.0232
18	54	-0.0242	-0.0161
20	63	-0.0220	-0.0155

As with the large-scale open deck experiment, the results from Table 4.15 suggest that vehicle speed does not have a significant impact on bent-cap deflection.

Figure 4.24 is a plot of bent-cap deflection versus time for both bent-caps during Test 20. This test comprised a northbound work train traversing the bridge at 63 mph. Because the train was traveling north, it would have crossed over Bent-Cap 9 first.

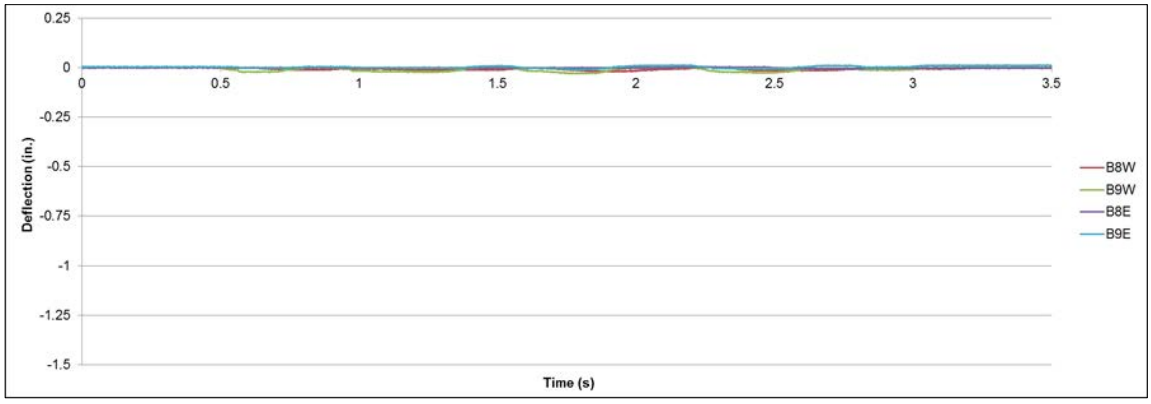

Figure 4.24: Ballast Deck Bridge Bent-Cap Deflections for Test 20

Figure 4.24 clearly demonstrates how small the bent-cap deflections were. The deflections for both Bent-Cap 9 and Bent-Cap 8 remain close to zero at all times.

4.3.2 Large-Scale Ballast Deck Mid-span Total Deflection Results

Appendix H contains plots of total stringer deflection versus time for Test 3 through Test 20 of the ballast deck bridge experiment. The maximum total stringer deflections of Ply 1 through Ply 5 during each test are listed in Table 4.16. During Test 1, the string potentiometer connected to Ply 2 malfunctioned, so the deflection is not known for that test.

Table 4.16: Ballast Deck Bridge Ply 1 through Ply 5 Maximum Total Stringer Deflections

Test	Ply 1 (in.)	Ply 2 (in.)	Ply 3 (in.)	Ply 4 (in.)	Ply 5 (in.)
1	-0.2244	-	-0.2929	-0.2857	-0.2115
2	-0.1689	-0.2162	-0.2230	-0.2148	-0.1459
3	-0.1801	-0.2299	-0.2407	-0.2444	-0.1684
4	-0.1814	-0.2329	-0.2453	-0.2471	-0.1647
5	-0.1811	-0.2325	-0.2440	-0.2452	-0.1654
6	-0.1842	-0.2367	-0.2456	-0.2478	-0.1643
7	-0.1962	-0.2474	-0.2520	-0.2507	-0.1647
8	-0.1790	-0.2335	-0.2434	-0.2465	-0.1614
9	-0.1888	-0.2422	-0.2535	-0.2524	-0.1722
10	-0.1755	-0.2322	-0.2420	-0.2438	-0.1654
11	-0.1746	-0.2251	-0.2391	-0.2401	-0.1677
12	-0.1752	-0.2314	-0.2442	-0.2423	-0.1658
13	-0.1858	-0.2385	-0.2469	-0.2517	-0.1665
14	-0.1747	-0.2330	-0.2424	-0.2450	-0.1638
15	-0.1776	-0.2300	-0.2458	-0.2488	-0.1716
16	-0.1801	-0.2344	-0.2485	-0.2527	-0.1748
17	-0.1814	-0.2329	-0.2453	-0.2471	-0.1647
18	-0.1766	-0.2258	-0.2353	-0.2350	-0.1655
19	-0.1867	-0.2341	-0.2379	-0.2355	-0.1596
20	-0.1618	-0.2122	-0.2323	-0.2313	-0.1688
21	-0.1456	-0.1880	-0.2024	-0.1920	-0.1212
22	-0.1939	-0.2431	-0.2517	-0.2485	-0.1736

The maximum total stringer deflections of Ply 6 through Ply 10 during each test are listed in Table 4.17.

Table 4.17: Ballast Deck Bridge Ply 6 through Ply 10 Maximum Total Stringer Deflections

Test	Ply 6 (in.)	Ply 7 (in.)	Ply 8 (in.)	Ply 9 (in.)	Ply 10 (in.)
1	-0.3099	-0.2454	-0.3448	-0.2936	-0.2149
2	-0.2198	-0.1459	-0.2273	-0.1797	-0.1417
3	-0.2505	-0.1715	-0.2625	-0.2145	-0.1664
4	-0.2458	-0.1575	-0.2476	-0.1971	-0.1505
5	-0.2530	-0.1702	-0.2614	-0.2107	-0.1611
6	-0.2438	-0.1581	-0.2492	-0.2022	-0.1568
7	-0.2513	-0.1655	-0.2576	-0.2064	-0.1577
8	-0.2445	-0.1569	-0.2483	-0.1984	-0.1533
9	-0.2542	-0.1747	-0.2717	-0.2218	-0.1703
10	-0.2451	-0.1578	-0.2445	-0.2012	-0.1566
11	-0.2596	-0.1754	-0.2737	-0.2278	-0.1761
12	-0.2460	-0.1600	-0.2499	-0.2113	-0.1626
13	-0.2618	-0.1750	-0.2732	-0.2243	-0.1722
14	-0.2471	-0.1658	-0.2552	-0.2089	-0.1562
15	-0.2620	-0.1774	-0.2689	-0.2201	-0.1682
16	-0.2714	-0.1941	-0.2894	-0.2422	-0.1882
17	-0.2458	-0.1575	-0.2476	-0.1971	-0.1505
18	-0.2591	-0.1785	-0.2793	-0.2333	-0.1874
19	-0.2384	-0.1498	-0.2455	-0.2007	-0.1614
20	-0.2594	-0.1769	-0.2833	-0.2422	-0.1951
21	-0.2027	-0.1263	-0.2189	-0.1725	-0.1332
22	-0.2725	-0.1912	-0.2966	-0.2487	-0.1911

The average deflection of all the total maximum stringer deflections was -0.2121. Any deflection exceeding this average is highlighted in red in Table 4.16 and Table 4.17. Ply 2, Ply 3, Ply 4, Ply 6, and Ply 8 had larger than average deflections for nearly all the tests. In particular, Ply 6 and Ply 8 had the largest deflections. This could indicate some level of impairment in these stringers.

In order to analyze how speed affected the total stringer deflection, Table 4.18 lists average total maximum stringer deflections during each test by ascending speed for Ply 1 through Ply 5.

Table 4.18: Ballast Deck Bridge Ply 1 through Ply 5 Max Total Stringer Deflections and Vehicle Speed

Test	Speed	Ply 1	Ply 2	Ply 3	Ply 4	Ply 5
3	5	-0.1801	-0.2299	-0.2407	-0.2444	-0.1684
15	5	-0.1776	-0.2300	-0.2458	-0.2488	-0.1716
4	10	-0.1814	-0.2329	-0.2453	-0.2471	-0.1647
17	10	-0.1814	-0.2329	-0.2453	-0.2471	-0.1647
5	15	-0.1811	-0.2325	-0.2440	-0.2452	-0.1654
6	20	-0.1842	-0.2367	-0.2456	-0.2478	-0.1643
19	20	-0.1867	-0.2341	-0.2379	-0.2355	-0.1596
7	25	-0.1962	-0.2474	-0.2520	-0.2507	-0.1647
8	30	-0.1790	-0.2335	-0.2434	-0.2465	-0.1614
9	35	-0.1888	-0.2422	-0.2535	-0.2524	-0.1722
10	40	-0.1755	-0.2322	-0.2420	-0.2438	-0.1654
11	40	-0.1746	-0.2251	-0.2391	-0.2401	-0.1677
13	43	-0.1858	-0.2385	-0.2469	-0.2517	-0.1665
12	45	-0.1752	-0.2314	-0.2442	-0.2423	-0.1658
14	45	-0.1747	-0.2330	-0.2424	-0.2450	-0.1638
16	52	-0.1801	-0.2344	-0.2485	-0.2527	-0.1748
18	54	-0.1766	-0.2258	-0.2353	-0.2350	-0.1655
20	63	-0.1618	-0.2122	-0.2323	-0.2313	-0.1688

Table 4.19 lists average total maximum stringer deflections during each test by ascending speed for Ply 6 through Ply 10.

Table 4.19: Ballast Deck Bridge Ply 6 through Ply 10 Max Total Stringer Deflections and Vehicle Speed

Test	Speed	Ply 6	Ply 7	Ply 8	Ply 9	Ply 10
3	5	-0.2505	-0.1715	-0.2625	-0.2145	-0.1664
15	5	-0.2620	-0.1774	-0.2689	-0.2201	-0.1682
4	10	-0.2458	-0.1575	-0.2476	-0.1971	-0.1505
17	10	-0.2458	-0.1575	-0.2476	-0.1971	-0.1505
5	15	-0.2530	-0.1702	-0.2614	-0.2107	-0.1611
6	20	-0.2438	-0.1581	-0.2492	-0.2022	-0.1568
19	20	-0.2384	-0.1498	-0.2455	-0.2007	-0.1614
7	25	-0.2513	-0.1655	-0.2576	-0.2064	-0.1577
8	30	-0.2445	-0.1569	-0.2483	-0.1984	-0.1533
9	35	-0.2542	-0.1747	-0.2717	-0.2218	-0.1703
10	40	-0.2451	-0.1578	-0.2445	-0.2012	-0.1566
11	40	-0.2596	-0.1754	-0.2737	-0.2278	-0.1761
13	43	-0.2618	-0.175	-0.2732	-0.2243	-0.1722
12	45	-0.2460	-0.1600	-0.2499	-0.2113	-0.1626
14	45	-0.2471	-0.1658	-0.2552	-0.2089	-0.1562
16	52	-0.2714	-0.1941	-0.2894	-0.2422	-0.1882
18	54	-0.2591	-0.1785	-0.2793	-0.2333	-0.1874
20	63	-0.2594	-0.1769	-0.2833	-0.2422	-0.1951

Similar to the large-scale open deck experiment, it appears that the average total stringer deflection remained consistent as the vehicle speed increased. This suggests that speed does not have a significant impact on total stringer deflection.

Figure 4.25 is a plot of total stringer deflection versus time for Span 8 during Test 20. The work train was northbound and traveling 63 mph during Test 20.

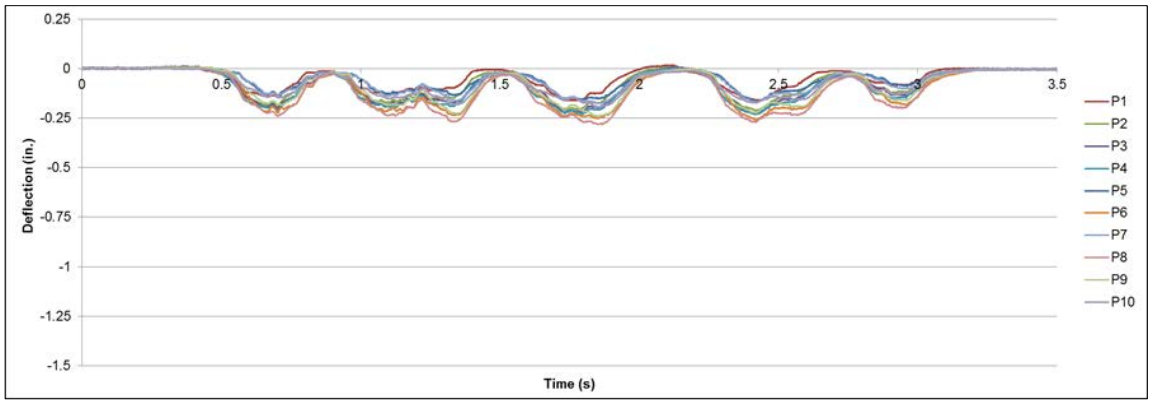

Figure 4.25: Ballast Deck Bridge Total Span 8 Stringer Deflection During Test 20

The work train included 8 trucks, and this can be seen in Figure 4.25 because there are 8 local minimuma that occur in the plot. The trucks that were on each side of the couplings connecting the rolling stock were closer together (Figure 4.32), and this resulted in local minimuma that were very close together in time.

Figure 4.25 and the rest of the total deflection plots for the large-scale ballast deck experiment (Appendix H) show that a maximum total mid-span stringer deflection occurs due to the trucks that were on each side of the couplings connecting the rolling stock.

4.3.3 Large-Scale Ballast Deck Mid-span Net Deflection Results

Appendix I contains plots of net stringer deflection versus time for Test 3 through Test 20 performed during the large-scale ballast deck experiment. The maximum net stringer deflections of Ply 1 through Ply 5 of Span 8 during each test are shown in Table 4.20.

Table 4.20: Ballast Deck Bridge Ply 1 through Ply 5 Maximum Net Stringer Deflections

Test	Ply 1	Ply 2	Ply 3	Ply 4	Ply 5
1	-0.0702	-0.1323	-0.1692	-0.1514	-0.0968
2	-0.0345	-0.1109	-0.1200	-0.1111	-0.0551
3	-0.0455	-0.1276	-0.1384	-0.1264	-0.0686
4	-0.0454	-0.1274	-0.1403	-0.1281	-0.0710
5	-0.0445	-0.1281	-0.1407	-0.1279	-0.0716
6	-0.0460	-0.1295	-0.1416	-0.1292	-0.0705
7	-0.0544	-0.1379	-0.1463	-0.1319	-0.0699
8	-0.0419	-0.1275	-0.1400	-0.1292	-0.0699
9	-0.0495	-0.1336	-0.1463	-0.1323	-0.0739
10	-0.0388	-0.1269	-0.1411	-0.1313	-0.0676
11	-0.0401	-0.1196	-0.1354	-0.1256	-0.0697
12	-0.0396	-0.1279	-0.1398	-0.1320	-0.0654
13	-0.0454	-0.1272	-0.1390	-0.1309	-0.0684
14	-0.0373	-0.1268	-0.1390	-0.1327	-0.0678
15	-0.0409	-0.1199	-0.1362	-0.1281	-0.0698
16	-0.0405	-0.1233	-0.1388	-0.1294	-0.0726
17	-0.0454	-0.1274	-0.1403	-0.1281	-0.0710
18	-0.0384	-0.1242	-0.1325	-0.1204	-0.0732
19	-0.0441	-0.1305	-0.1389	-0.1236	-0.0715
20	-0.0310	-0.1157	-0.1342	-0.1196	-0.0741
21	-0.0305	-0.1062	-0.1227	-0.1142	-0.0572
22	-0.0490	-0.1350	-0.1488	-0.1347	-0.0771

The maximum net stringer deflections of Ply 6 through Ply 10 of Span 8 during each test are shown in Table 4.21.

Table 4.21: Ballast Deck Bridge Ply 6 through Ply 10 Maximum Net Stringer Deflections

Test	Ply 6	Ply 7	Ply 8	Ply 9	Ply 10
1	-0.1679	-0.1289	-0.1950	-0.1703	-0.1178
2	-0.1186	-0.0700	-0.1248	-0.1012	-0.0542
3	-0.1366	-0.0896	-0.1493	-0.1288	-0.0711
4	-0.1366	-0.0831	-0.1441	-0.1199	-0.0646
5	-0.1381	-0.0914	-0.1482	-0.1258	-0.0664
6	-0.1367	-0.0845	-0.1443	-0.1256	-0.0696
7	-0.1375	-0.0866	-0.1491	-0.1267	-0.0690
8	-0.1370	-0.0852	-0.1425	-0.1203	-0.0645
9	-0.1407	-0.0921	-0.1530	-0.1356	-0.0750
10	-0.1322	-0.0786	-0.1412	-0.1269	-0.0708
11	-0.1454	-0.0918	-0.1556	-0.1397	-0.0776
12	-0.1344	-0.0846	-0.1459	-0.1311	-0.0758
13	-0.1466	-0.0931	-0.1614	-0.1390	-0.0763
14	-0.1349	-0.0909	-0.1464	-0.1293	-0.0714
15	-0.1435	-0.0938	-0.1521	-0.1329	-0.0720
16	-0.1522	-0.1051	-0.1709	-0.1495	-0.0856
17	-0.1366	-0.0831	-0.1441	-0.1199	-0.0646
18	-0.1454	-0.0966	-0.1612	-0.1453	-0.0881
19	-0.1329	-0.0820	-0.1419	-0.1248	-0.0741
20	-0.1461	-0.0937	-0.1606	-0.1500	-0.0945
21	-0.1223	-0.0698	-0.1321	-0.1100	-0.0589
22	-0.1467	-0.0919	-0.1639	-0.1472	-0.0830

The average maximum net stringer deflection for all the stringers was -0.10937 inches. Any deflection exceeding this average is highlighted in red in Table 4.20 and Table 4.21. Ply 2, Ply 3, Ply 4, Ply 6, Ply 8, and Ply 9 all have maximum net deflections that are consistently larger than average for each test. All of these stringers also had larger than average maximum total deflections, except for Ply 9.

The span length of Bridge 816.9 was 180 inches. According to the AREMA Chapter 7, the net deflections of the stringers under a live load should not exceed -0.72 inches

(AREMA 2015). Table 4.20 and Table 4.21 show that there were no maximum net stringer deflections that exceeded this limit. In fact, the largest net deflection recorded was -0.1950 inches in Ply 8 during Test 1, which was when a freight train was traversing the bridge (Table 4.21). Ply 8 has over a half of inch of deflection before it reaches the limit that AREMA has recommended. Therefore, it can be assumed that no stringers in Bridge 816.9 were split.

There was a significant difference between the total mid-span stringer deflections and the net stringer deflections of the open deck bridge, and this is also true for the ballast deck bridge. For instance, the maximum net mid-span stringer deflection of Ply 8 was -0.1950 inches during Test 1. The maximum total mid-span deflection of Ply 8 was -0.3448 inches. This is a 43.4% increase in deflection, which is substantial. Table 4.22 demonstrates the percent increase in deflection of Ply 1 through Ply 5 for each test performed.

Table 4.22: Ballast Deck Bridge Ply 1 through Ply 5 Percent Increase from Net Maximum Deflection to Total Maximum Deflection

Test	Ply 1	Ply 2	Ply 3	Ply 4	Ply 5
1	68.7%	-	42.2%	47.0%	54.3%
2	79.6%	48.7%	46.2%	48.3%	62.2%
3	74.8%	44.5%	42.5%	48.3%	59.3%
4	75.0%	45.3%	42.8%	48.2%	56.9%
5	75.5%	44.9%	42.3%	47.9%	56.7%
6	75.1%	45.3%	42.4%	47.9%	57.1%
7	72.3%	44.3%	42.0%	47.4%	57.6%
8	76.6%	45.4%	42.5%	47.6%	56.7%
9	73.8%	44.9%	42.3%	47.6%	57.1%
10	77.9%	45.4%	41.7%	46.2%	59.2%
11	77.1%	46.9%	43.4%	47.7%	58.4%
12	77.4%	44.7%	42.8%	45.5%	60.6%
13	75.6%	46.7%	43.7%	48.0%	58.9%
14	78.6%	45.6%	42.7%	45.8%	58.6%
15	77.0%	47.9%	44.6%	48.5%	59.3%
16	77.5%	47.4%	44.1%	48.8%	58.5%
17	75.0%	45.3%	42.8%	48.2%	56.9%
18	78.3%	45.0%	43.7%	48.8%	55.8%
19	76.4%	44.3%	41.6%	47.5%	55.2%
20	80.9%	45.5%	42.2%	48.3%	56.1%
21	79.1%	43.5%	39.4%	40.5%	52.8%
22	74.7%	44.5%	40.9%	45.8%	55.6%

Table 4.23 demonstrates the percent increase in deflection of Ply 6 through Ply 10 for each test performed.

Table 4.23: Ballast Deck Bridge Ply 6 through Ply 10 Percent Increase from Net Maximum Deflection to Total Maximum Deflection

Test	Ply 6	Ply 7	Ply 8	Ply 9	Ply 10
1	45.8%	47.5%	43.4%	42.0%	45.2%
2	46.1%	52.0%	45.1%	43.7%	61.8%
3	45.5%	47.8%	43.1%	40.0%	57.3%
4	44.4%	47.3%	41.8%	39.2%	57.1%
5	45.4%	46.3%	43.3%	40.3%	58.8%
6	43.9%	46.6%	42.1%	37.9%	55.6%
7	45.3%	47.7%	42.1%	38.6%	56.2%
8	44.0%	45.7%	42.6%	39.4%	58.0%
9	44.7%	47.3%	43.7%	38.9%	56.0%
10	46.1%	50.2%	42.3%	37.0%	54.8%
11	44.0%	47.7%	43.1%	38.7%	56.0%
12	45.4%	47.2%	41.6%	38.0%	53.4%
13	44.0%	46.8%	40.9%	38.0%	55.7%
14	45.4%	45.2%	42.7%	38.1%	54.3%
15	45.2%	47.1%	43.4%	39.6%	57.2%
16	43.9%	45.9%	41.0%	38.3%	54.5%
17	44.4%	47.3%	41.8%	39.2%	57.1%
18	43.9%	45.9%	42.3%	37.7%	53.0%
19	44.3%	45.3%	42.2%	37.8%	54.1%
20	43.7%	47.0%	43.3%	38.1%	51.6%
21	39.7%	44.8%	39.7%	36.2%	55.8%
22	46.2%	52.0%	44.7%	40.8%	56.6%

The smallest percent increase from net maximum deflection to total maximum deflection was 36.2%, which was for Ply 4 during Test 21. Although this is the smallest increase, it is still substantial. Support settlement influenced Ply 1 the most according to Table 4.22 and Table 4.23.

Table 4.24 lists average net maximum stringer deflections of Ply 1 through Ply 5 during each test according to ascending speed.

Table 4.24: Ballast Deck Bridge Ply 1 through Ply 5 Average Net Maximum Stringer Deflections and Vehicle Speeds

Test	Speed	Ply 1	Ply 2	Ply 3	Ply 4	Ply 5
3	5	-0.0455	-0.1276	-0.1384	-0.1264	-0.0686
15	5	-0.0409	-0.1199	-0.1362	-0.1281	-0.0698
4	10	-0.0454	-0.1274	-0.1403	-0.1281	-0.0710
17	10	-0.0454	-0.1274	-0.1403	-0.1281	-0.0710
5	15	-0.0445	-0.1281	-0.1407	-0.1279	-0.0716
6	20	-0.0460	-0.1295	-0.1416	-0.1292	-0.0705
19	20	-0.0441	-0.1305	-0.1389	-0.1236	-0.0715
7	25	-0.0544	-0.1379	-0.1463	-0.1319	-0.0699
8	30	-0.0419	-0.1275	-0.1400	-0.1292	-0.0699
9	35	-0.0495	-0.1336	-0.1463	-0.1323	-0.0739
10	40	-0.0388	-0.1269	-0.1411	-0.1313	-0.0676
11	40	-0.0401	-0.1196	-0.1354	-0.1256	-0.0697
13	43	-0.0454	-0.1272	-0.1390	-0.1309	-0.0684
12	45	-0.0396	-0.1279	-0.1398	-0.1320	-0.0654
14	45	-0.0373	-0.1268	-0.1390	-0.1327	-0.0678
16	52	-0.0405	-0.1233	-0.1388	-0.1294	-0.0726
18	54	-0.0384	-0.1242	-0.1325	-0.1204	-0.0732
20	63	-0.0310	-0.1157	-0.1342	-0.1196	-0.0741

Table 4.25 lists average net maximum stringer deflections of Ply 6 through Ply 10 during each test according to ascending speed.

Table 4.25: Ballast Deck Bridge Ply 6 through Ply 10 Average Net Maximum Stringer Deflections and Vehicle Speeds

Test	Speed	Ply 6	Ply 7	Ply 8	Ply 9	Ply 10
3	5	-0.1366	-0.0896	-0.1493	-0.1288	-0.0711
15	5	-0.1435	-0.0938	-0.1521	-0.1329	-0.0720
4	10	-0.1366	-0.0831	-0.1441	-0.1199	-0.0646
17	10	-0.1366	-0.0831	-0.1441	-0.1199	-0.0646
5	15	-0.1381	-0.0914	-0.1482	-0.1258	-0.0664
6	20	-0.1367	-0.0845	-0.1443	-0.1256	-0.0696
19	20	-0.1329	-0.0820	-0.1419	-0.1248	-0.0741
7	25	-0.1375	-0.0866	-0.1491	-0.1267	-0.0690
8	30	-0.1370	-0.0852	-0.1425	-0.1203	-0.0645
9	35	-0.1407	-0.0921	-0.1530	-0.1356	-0.0750
10	40	-0.1322	-0.0786	-0.1412	-0.1269	-0.0708
11	40	-0.1454	-0.0918	-0.1556	-0.1397	-0.0776
13	43	-0.1466	-0.0931	-0.1614	-0.1390	-0.0763
12	45	-0.1344	-0.0846	-0.1459	-0.1311	-0.0758
14	45	-0.1349	-0.0909	-0.1464	-0.1293	-0.0714
16	52	-0.1522	-0.1051	-0.1709	-0.1495	-0.0856
18	54	-0.1454	-0.0966	-0.1612	-0.1453	-0.0881
20	63	-0.1461	-0.0937	-0.1606	-0.1500	-0.0945

Similar to the open deck bridge experiment, the average net maximum stringer deflection is not significantly affected by vehicle speed.

Figure 4.26 is a plot of net stringer deflection versus time for Span 8 during Test 20. This is the same test examined for the bent-cap deflections and the total stringer deflections of the ballast deck bridge.

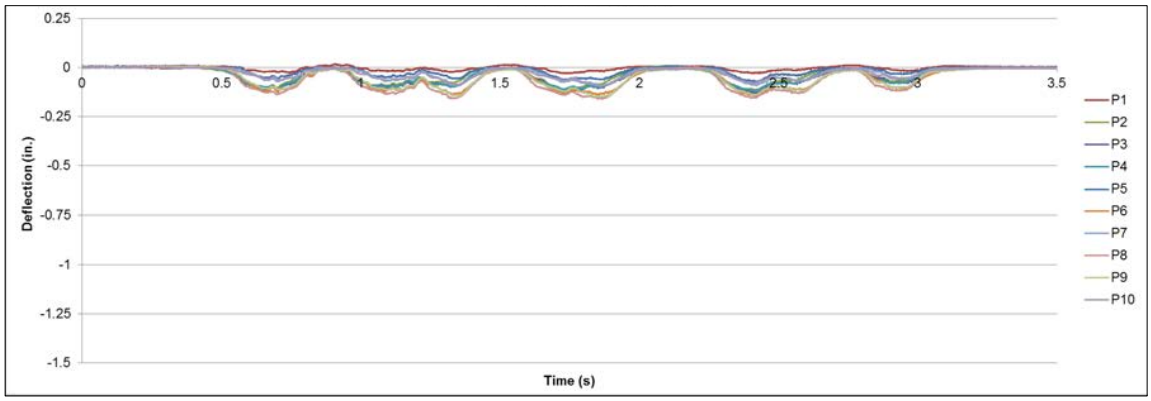

Figure 4.26: Ballast Deck Bridge Net Stringer Deflection during Test 20

Again, there are 8 local minimuma that occur in the plot. These minimuma are due to the 8 trucks that support the work train. Figure 4.25 and Figure 4.26 display an obvious difference between the magnitude of the total stringer deflections and the net stringer deflections. The net deflections appear to follow the same behaviors as the total deflections because the local minimuma and maximuma occur at the same times.

CHAPTER V
CONCLUSIONS

5.1 Conclusions

Deflections of bent-caps and stringers were measured for a small-scale bridge in the lab, a large-scale open deck bridge, and a large-scale ballast deck bridge while under live loads. Each set of data was recorded and analyzed. The following important revelations were made during the analysis:

- Bent-caps experienced very little deflection when under live load.
- Vehicle speed did not significantly affect bent-cap deflection, total stringer mid-span deflection, or net stringer mid-span deflection.
- Stringers comprising a chord did not act as one member. In fact, they experienced extremely different deflections as a vehicle traversed the bridge.
- There was a significant difference between the magnitude of the maximum total mid-span stringer deflections and the maximum net mid-span stringer deflections. During the experiments performed for this research, the total mid-span stringer deflections were anywhere from 36% to 80% higher than the net mid-span stringer deflections.
- When a freight train traversed a bridge, the maximum mid-span stringer deflection occurred due to the trucks that were on each side of the couplings connecting the rolling stock.
- A split stringer experienced approximately 4 times the mid-span deflection that an unimpaired stringer did under the same live load.

5.2 Future Research

Future research should focus on conducting experimental research with a variety of different parameters. Different bridges should be considered: an open-deck bridge in better condition or, perhaps, a ballast deck bridge with more impairment. It would be extremely beneficial to gather data on an impaired bridge that is scheduled to have

stringers replaced. After the repairs, more data could be gathered with the unimpaired stringers. And finally, more experiments with the wheel path position sensors would also be of great benefit. Instrumenting a loaded work train with the sensors would provide more information about the wheel path position at the time of maximum mid-span stringer deflection.

REFERENCES

AAR (2001). "Fatigue Strength of Douglas Fir Railroad Bridge Stringers." Transportation Technology Center, Report No. R-953, Association of American Railroads, Pueblo, CO.

AREMA (2015). Manual for Railway Engineering Vol. 2. American Railway Engineering Association, Washington, DC.

Borchers, C. R. (2002). "Fatigue Tests of Under-Strength Timber Railroad Bridge Stringers." MS Thesis, Department of Civil Engineering, Texas A&M University, College Station, TX.

Duwadi, S. R. and Wood, R. C. (1996). The Federal Highway Administration Timber Bridge Program. In: National Conf. on Wood Transportation in Structures. Oct. 23-25, Madison, WI. M. A. Ritter, S. R. Duwadi, and P. D. H. Lee, eds. pp. 333-339. Gen. Tech. Rep. FPL-GTR-94. USDA Forest Service, Forest Products Laboratory, Madison, WI. www.fpl.fs.fed.us/documnts/pdf1996/duwad96a.pdf.

Emerson, R. N., Pollock, D. G., Kainz, J. A., Fridley, K. J., McLean, D. I., and Ross, R. J. (1998). "Nondestructive Evaluation Techniques for Timber Bridges." Proc., 5th World Conference on Timber Engineering, Monteaux, Switzerland.

Emerson, R. N., Pollock, D. G., McLean, D. I., Fridley, K. J., Pellerin, R., and Ross, R. J. (2002). "Ultrasonic Inspection of Large Bridge Timbers." Forest Products Journal, Vol. 52, No. 9 (September 2002), pp. 88-95.

Fryba, L. (1996). Dynamics of Railway Bridges, T. Telford, London.

IOTech (2005). StrainBook/616 User's Manual, Cleveland, OH: IOTech.

Jones, S. L., and Fry, G. T. (1997). "Review of Fatigue Strength Research for Wood in Flexure." Report No. 909, Association of American Railroads, Transportation Technology Center, Pueblo, CO.

Keenan, F. J. (1974). "Shear Strength of Wood Beams". Forest Products Journal, Vol. 24, No. 9, 63-70.

Leggett, J. L., Jr. (1954). “Investigation of Fatigue Strength of Railroad Timber Bridge Stringers.” Advance Progress Report of Committee 7 – Wood Bridges & Trestles, Proceedings of the 53rd Annual Convention of the AREA, Chicago, IL, Vol. 55, 161-211.

Lewis, W. C. (1962). "Fatigue Resistance of Quarter-scale Bridge Stringers in Flexure and Shear". Forest Products Laboratory Report No. 2236, Madison, WI.

Library of Congress (2014). “Rise of Industrial America, 1876-1900: Railroads in the Late 19th Century”. < http://www.loc.gov/teachers/classroommaterials/presentationsandactivities/presentations/timeline/riseind/railroad/>. 23 Dec. 2014.

Martland, C. D. (2013). “Introduction of Heavy Axle Loads by the North American Rail Industry.” Journal of the Transportation Research Forum, Vol. 52, No. 2 (Summer 2013), pp. 103-125.

Morison, A., VanKarsen, C. D., Evensen, H. A., Ligon, J. B., Erickson, J. R., Ross, J. R., and Forsman, J. W. (2002). “Timber Bridge Evaluation: A Global Nondestructive Approach Using Impact Generated FRFs.” Proc., 20th International Modal Analysis Conference, Los Angeles, CA, USA.

Peterson, M. L., and Gutkowski, R. M. (1997). “Evaluation of the Structural Integrity of Timber Bridges.” NDT&E International, 32(1), 43-48.

Ritter, M. A. (1990). “Timber Bridges: Design, Construction, Inspection, and Maintenance.” United States Department of Agriculture, Forest Service, Washington, DC.

Story, B. (2012). “Structural Impairment Detection Using Arrays of Competitive Artificial Neural Networks.” Ph. D. Dissertation, Department of Civil Engineering, Texas A&M University, College Station, TX.

Tsai, K. T. and Ansell, M. P. (1990). “The Fatigue Properties of Wood in Flexure.” Journal of Material Science, Vol. 25, 865-878.

Union Pacific (2013). “Allowable Gross Weight.” Accessed 2 January 2015. < http://www.up.com/aboutup/reference/maps/allowable_gross_weight/

index.htm>

APPENDIX A
SMALL-SCALE PLOTS

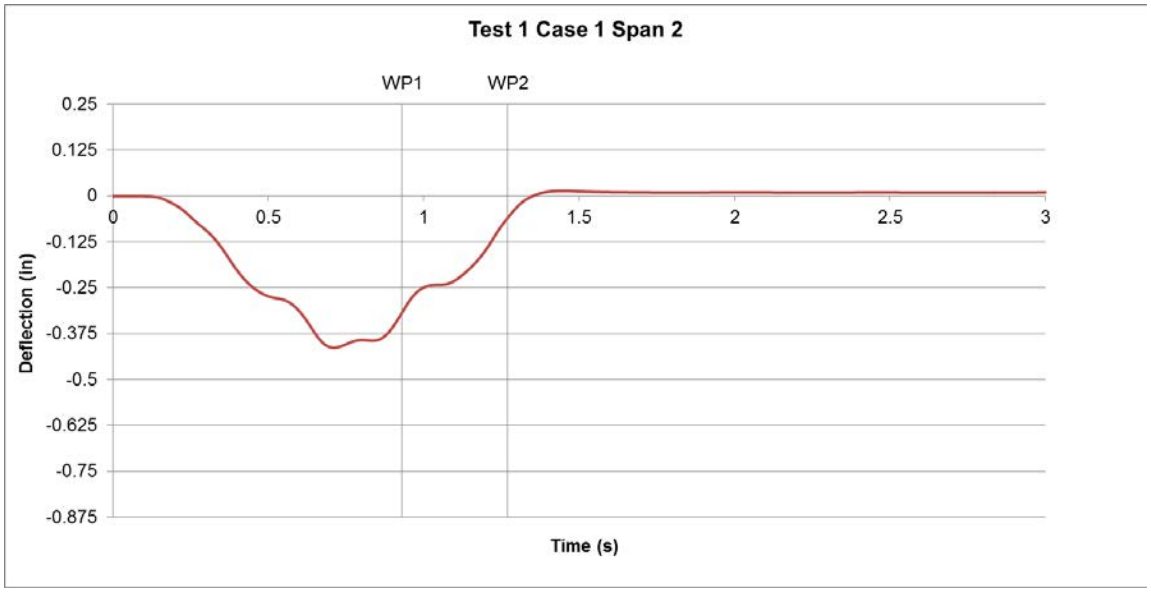

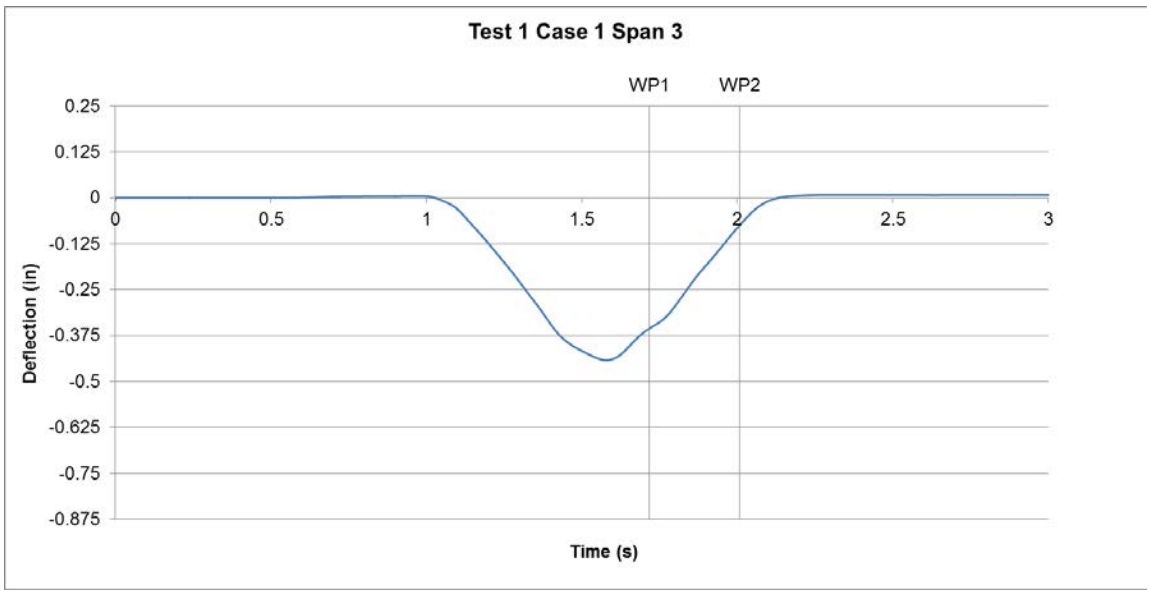

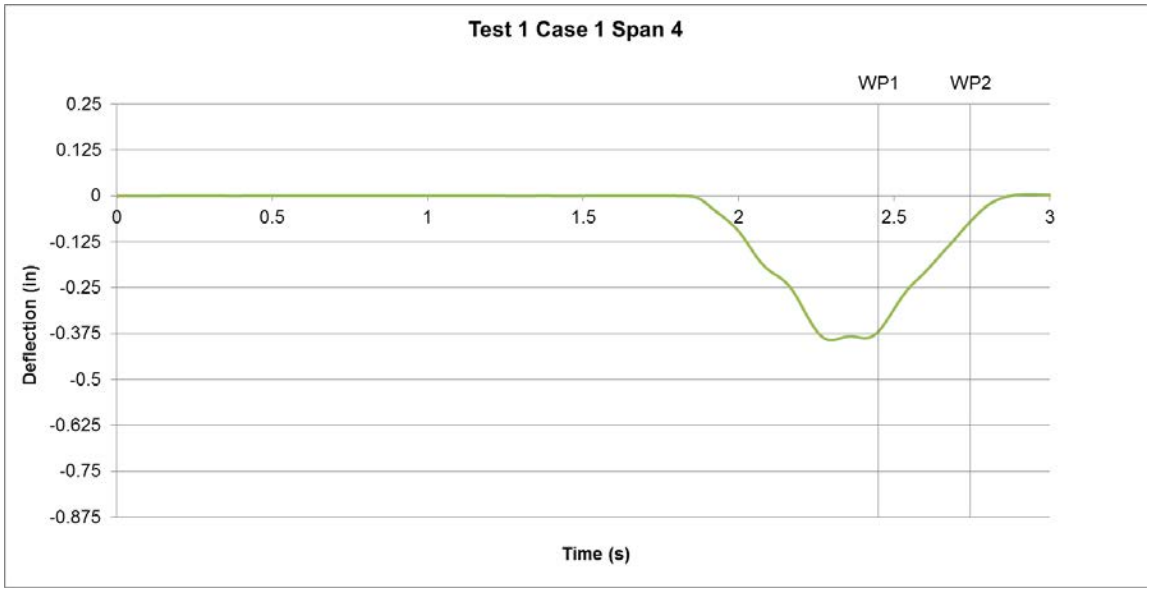
Test 1 Case 1 Span 4
WP1
WP2
0.25
0.125
0
-0.125
-0.25
-0.375
-0.5
-0.625
-0.75
-0.875
0
0.5
1
1.5
2
2.5
3
Deflection (in)
Time (s)

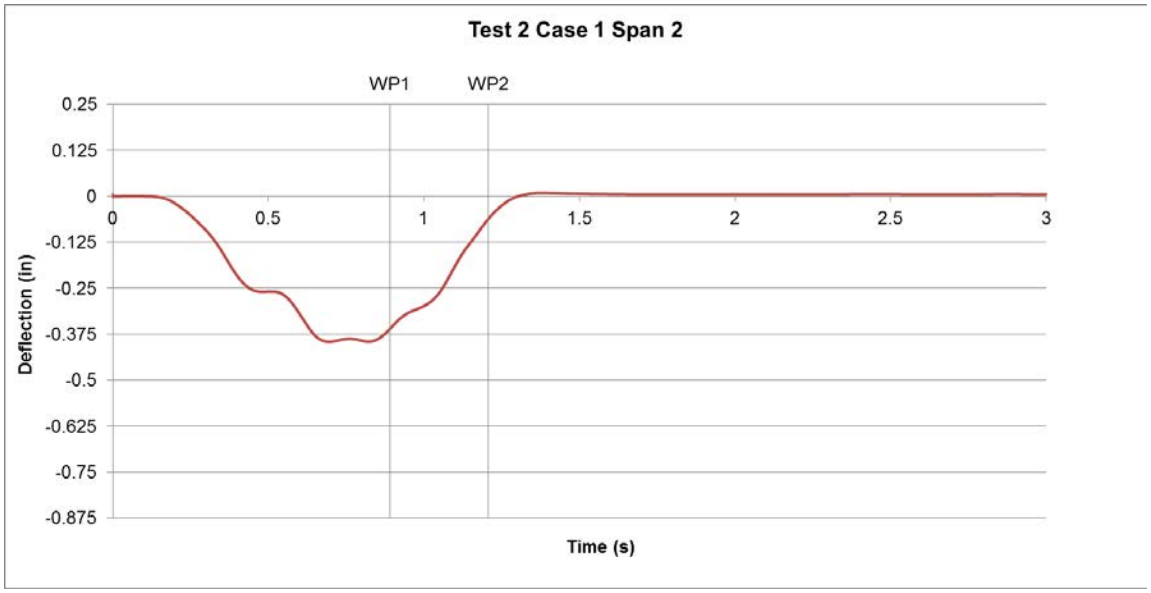
Test 2 Case 1 Span 2
WP1
WP2
0.25
0.125
0
-0.125
-0.25
-0.375
-0.5
-0.625
-0.75
-0.875
0
0.5
1
1.5
2
2.5
3
Deflection (in)
Time (s)

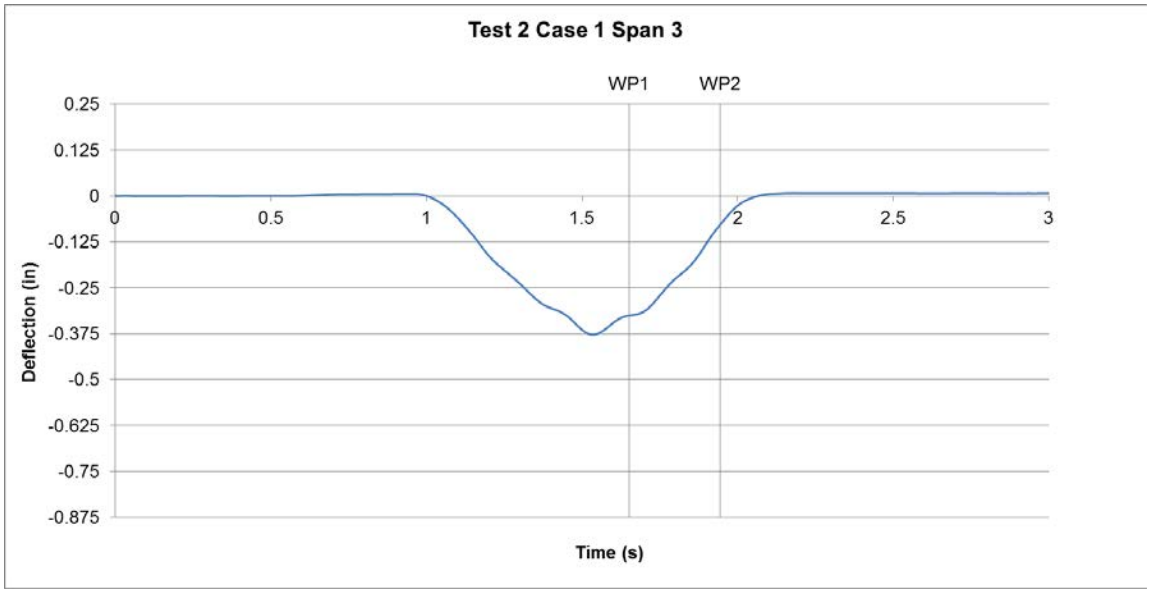
Test 2 Case 1 Span 3
WP1
WP2
0.25
0.125
0
-0.125
-0.25
-0.375
-0.5
-0.625
-0.75
-0.875
0
0.5
1
1.5
2
2.5
3
Deflection (in)
Time (s)

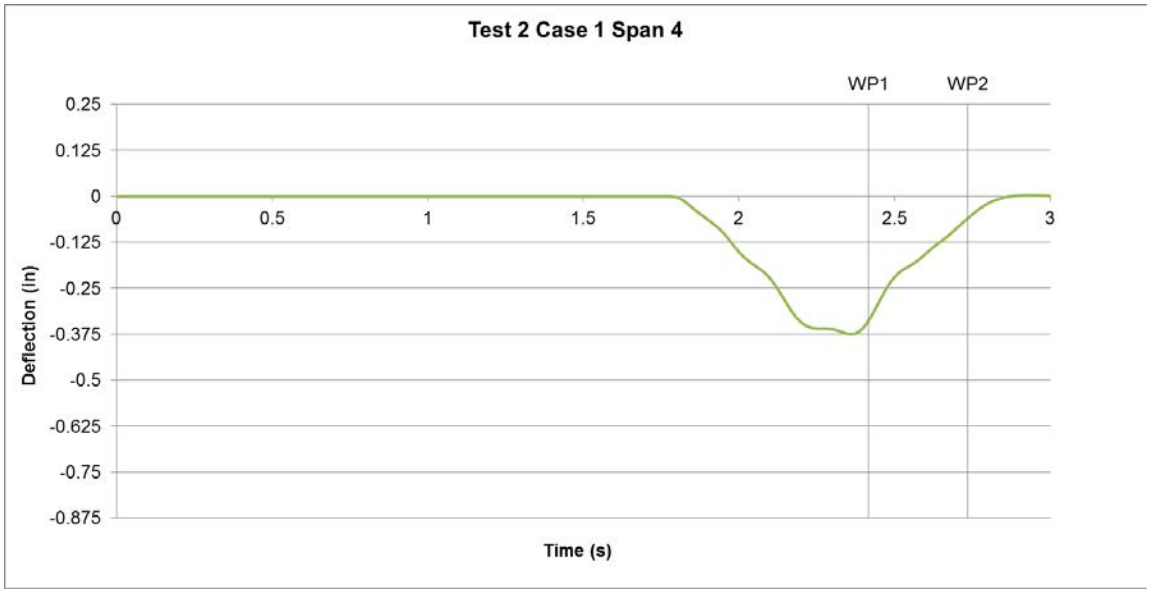
Test 2 Case 1 Span 4
WP1
WP2
0.25
0.125
0
-0.125
-0.25
-0.375
-0.5
-0.625
-0.75
-0.875
0
0.5
1
1.5
2
2.5
3
Deflection (in)
Time (s)

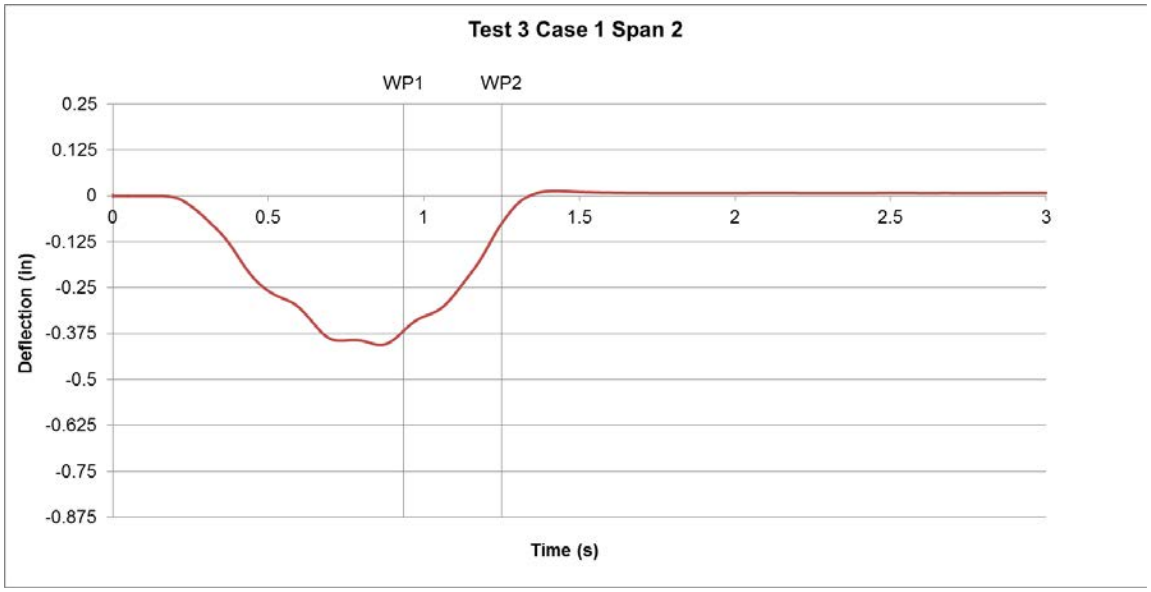
Test 3 Case 1 Span 2
WP1
WP2
0.25
0.125
0
-0.125
-0.25
-0.375
-0.5
-0.625
-0.75
-0.875
0
0.5
1
1.5
2
2.5
3
Deflection (in)
Time (s)

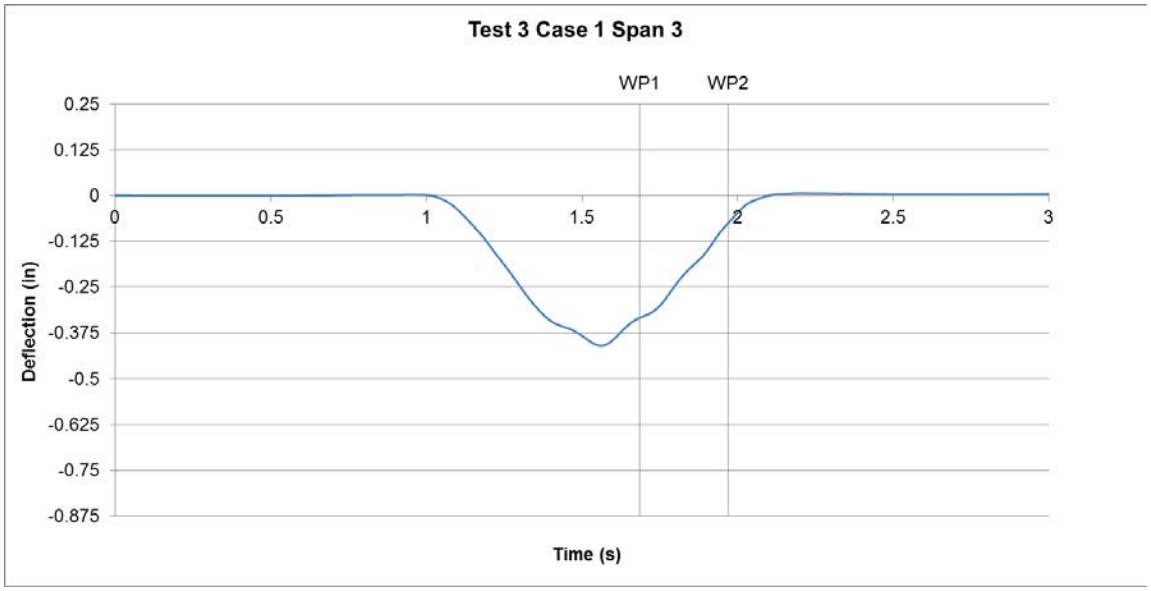
Test 3 Case 1 Span 3
WP1
WP2
0.25
0.125
0
-0.125
-0.25
-0.375
-0.5
-0.625
-0.75
-0.875
0
0.5
1
1.5
2
2.5
3
Deflection (in)
Time (s)

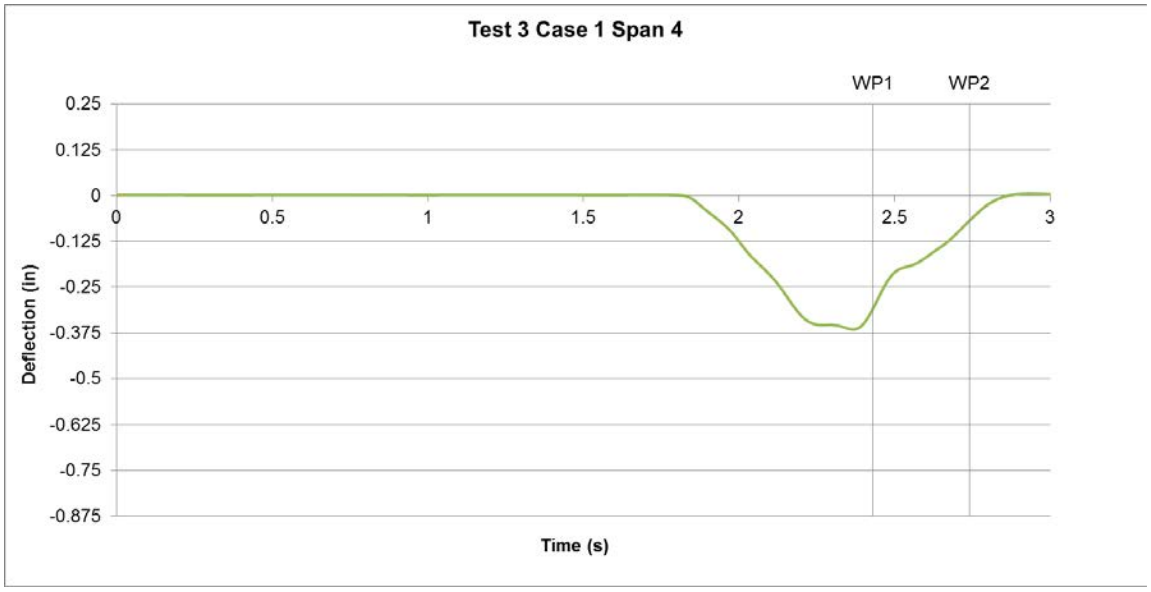
Test 3 Case 1 Span 4
WP1
WP2
0.25
0.125
0
-0.125
-0.25
-0.375
-0.5
-0.625
-0.75
-0.875
0
0.5
1
1.5
2
2.5
3
Deflection (in)
Time (s)

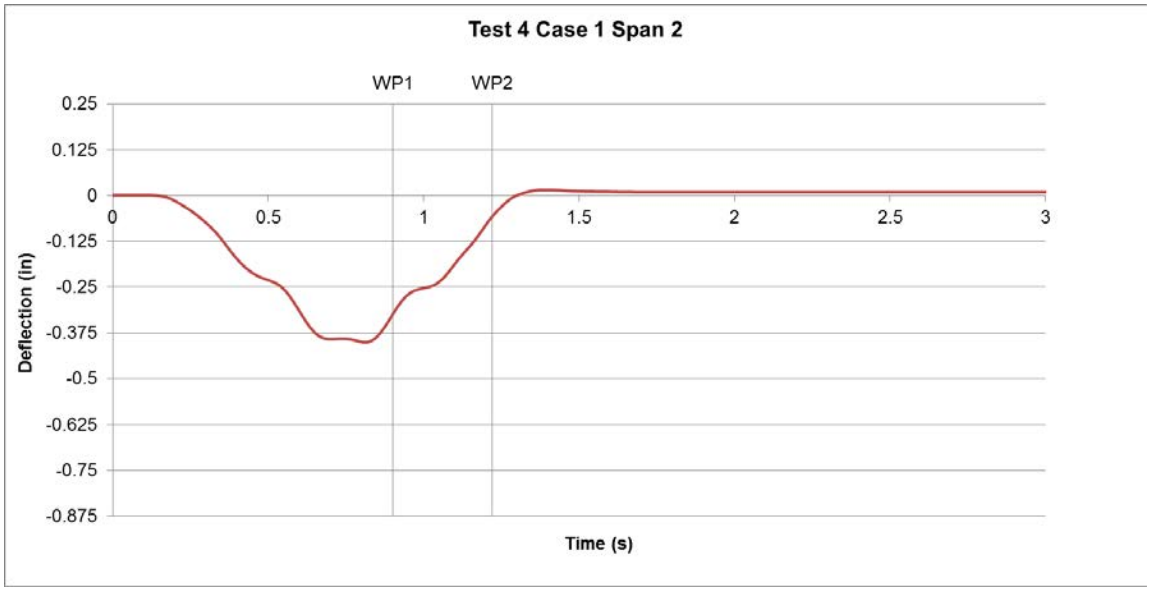
Test 4 Case 1 Span 2
WP1
WP2
0.25
0.125
0
-0.125
-0.25
-0.375
-0.5
-0.625
-0.75
-0.875
0
0.5
1
1.5
2
2.5
3
Deflection (in)
Time (s)

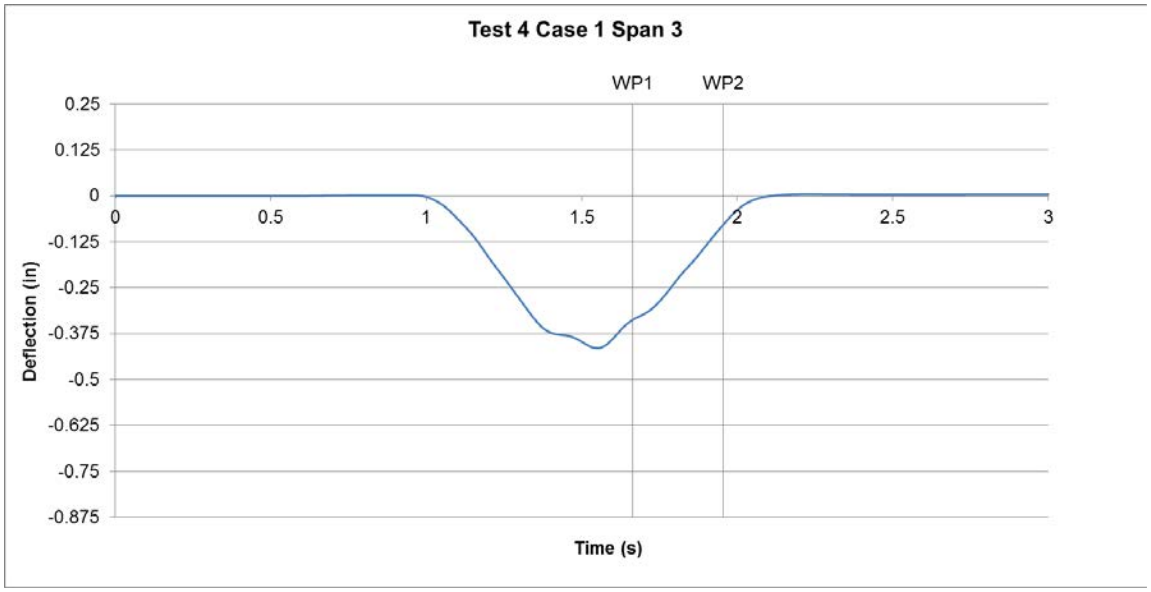
Test 4 Case 1 Span 3
WP1
WP2
0.25
0.125
0
-0.125
-0.25
-0.375
-0.5
-0.625
-0.75
-0.875
0
0.5
1
1.5
2
2.5
3
Deflection (in)
Time (s)

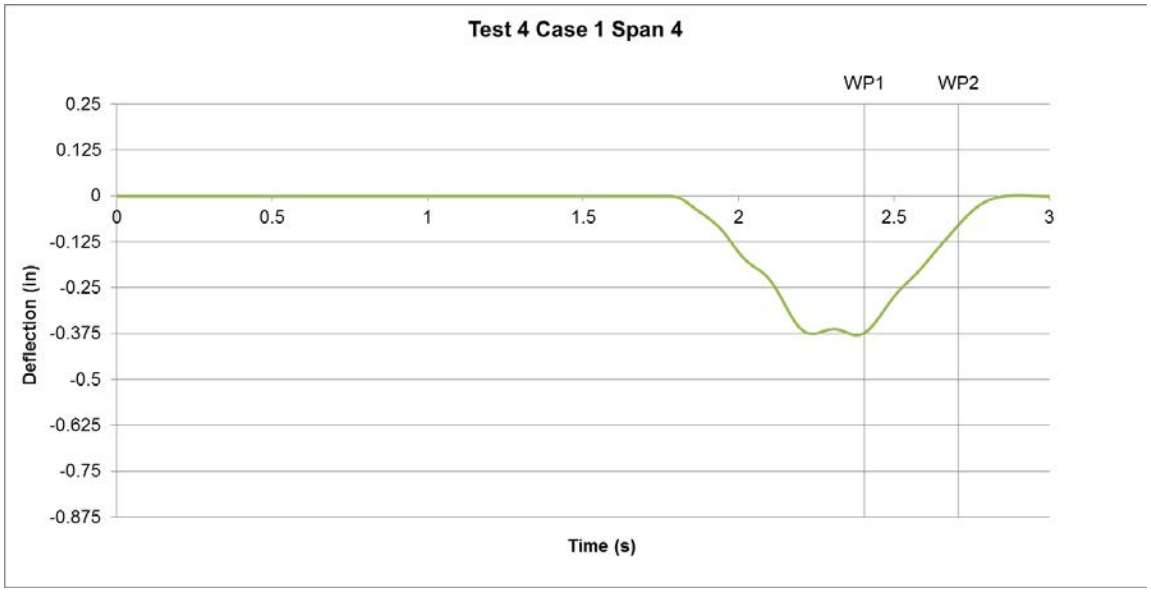
Test 4 Case 1 Span 4
WP1
WP2
0.25
0.125
0
-0.125
-0.25
-0.375
-0.5
-0.625
-0.75
-0.875
0
0.5
1
1.5
2
2.5
3
Deflection (in)
Time (s)

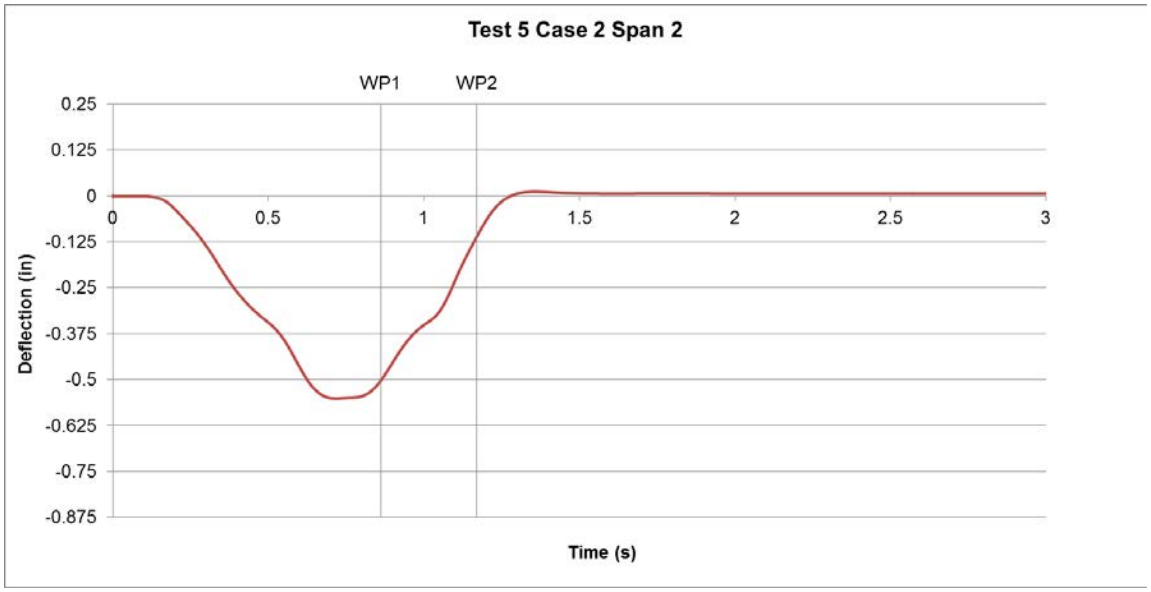
Test 5 Case 2 Span 2
WP1
WP2
0.25
0.125
0
-0.125
-0.25
-0.375
-0.5
-0.625
-0.75
-0.875
0
0.5
1
1.5
2
2.5
3
Deflection (in)
Time (s)

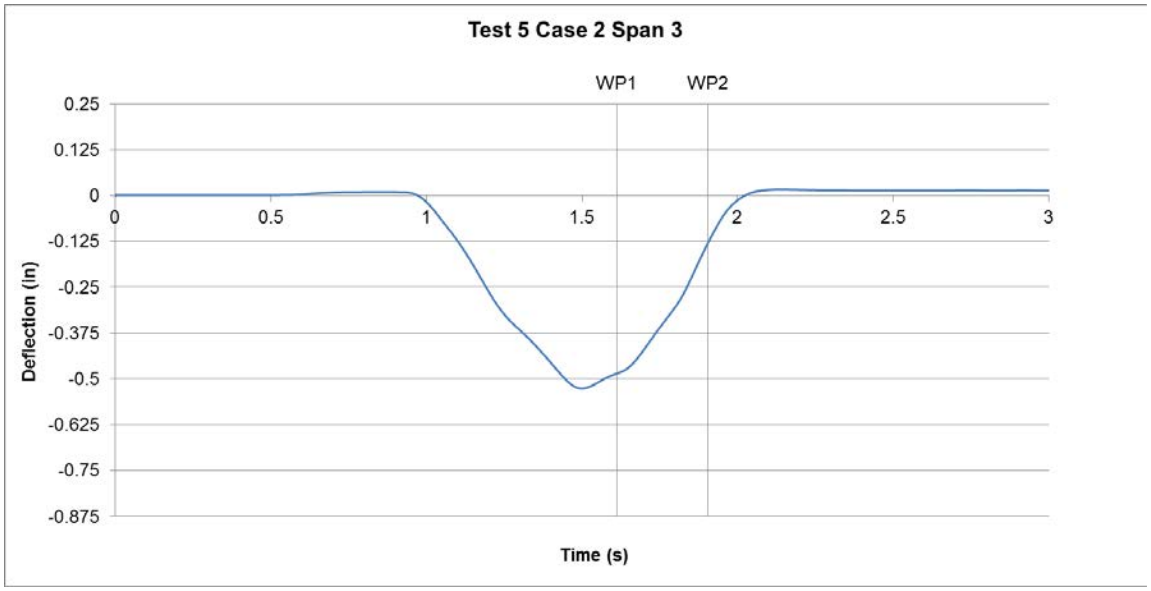
Test 5 Case 2 Span 3
WP1
WP2
0.25
0.125
0
-0.125
-0.25
-0.375
-0.5
-0.625
-0.75
-0.875
0
0.5
1
1.5
2
2.5
3
Deflection (in)
Time (s)

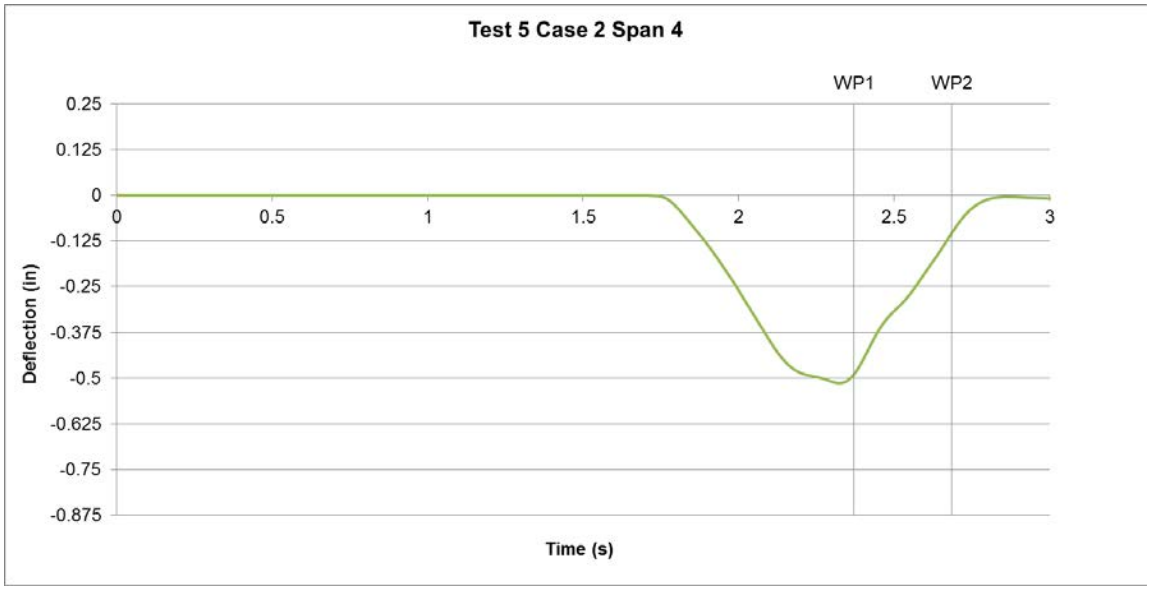
Test 5 Case 2 Span 4
WP1
WP2
0.25
0.125
0
-0.125
-0.25
-0.375
-0.5
-0.625
-0.75
-0.875
0
0.5
1
1.5
2
2.5
3
Deflection (in)
Time (s)

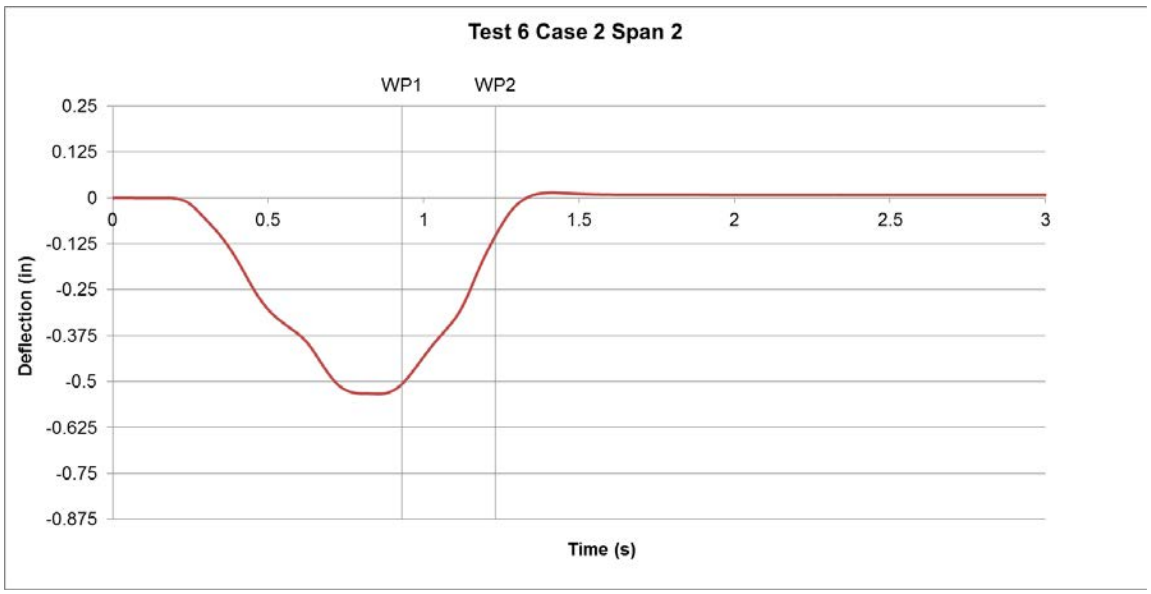
Test 6 Case 2 Span 2
WP1
WP2
0.25
0.125
0
-0.125
-0.25
-0.375
-0.5
-0.625
-0.75
-0.875
0
0.5
1
1.5
2
2.5
3
Deflection (in)
Time (s)

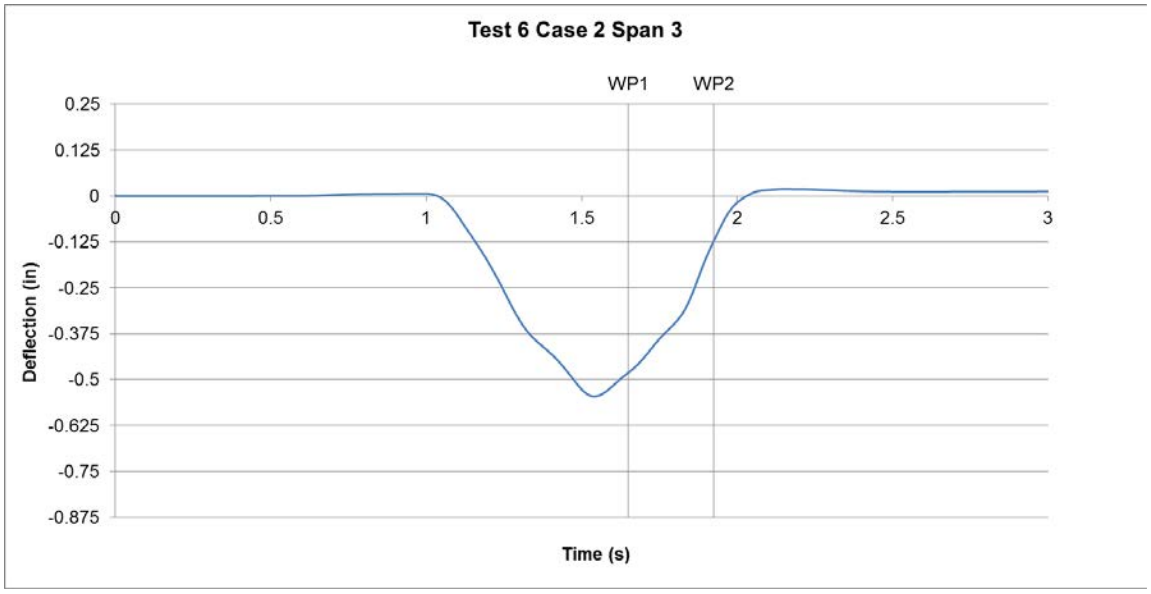
Test 6 Case 2 Span 3
WP1
WP2
0.25
0.125
0
-0.125
-0.25
-0.375
-0.5
-0.625
-0.75
-0.875
0
0.5
1
1.5
2
2.5
3
Deflection (in)
Time (s)

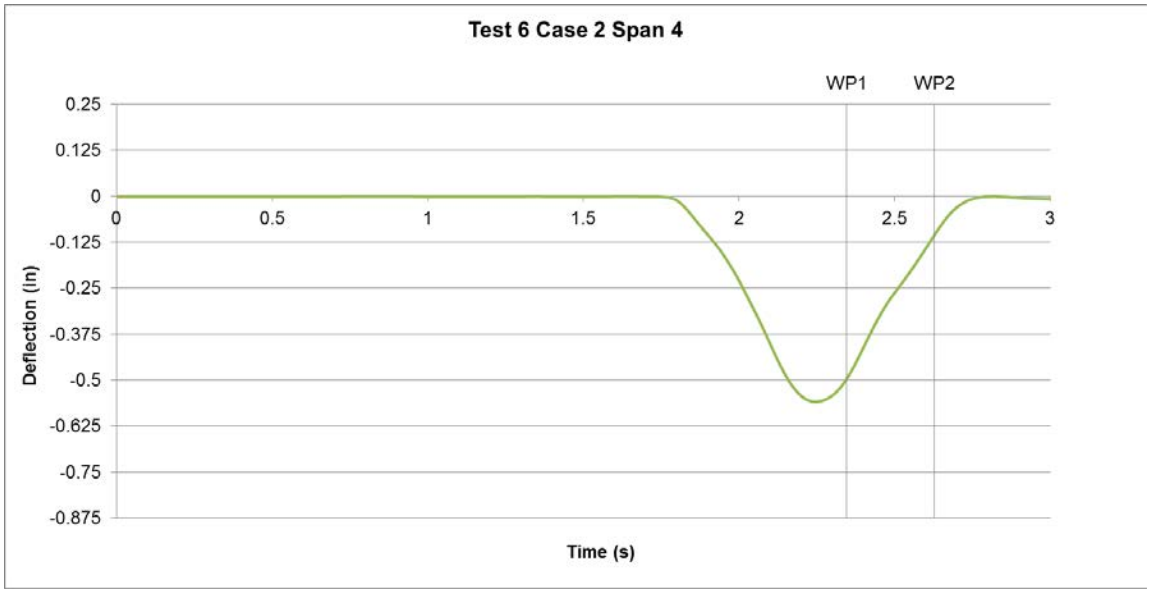
Test 6 Case 2 Span 4
WP1
WP2
0.25
0.125
0
-0.125
-0.25
-0.375
-0.5
-0.625
-0.75
-0.875
0
0.5
1
1.5
2
2.5
3
Deflection (in)
Time (s)

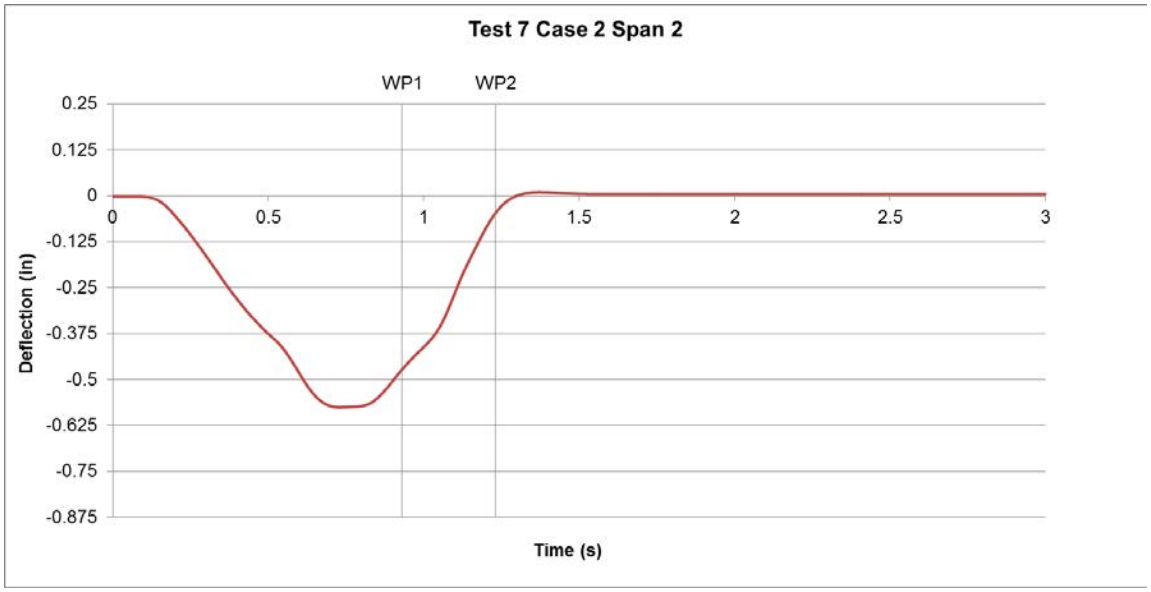
Test 7 Case 2 Span 2
WP1
WP2
0.25
0.125
0
-0.125
-0.25
-0.375
-0.5
-0.625
-0.75
-0.875
0
0.5
1
1.5
2
2.5
3
Deflection (in)
Time (s)

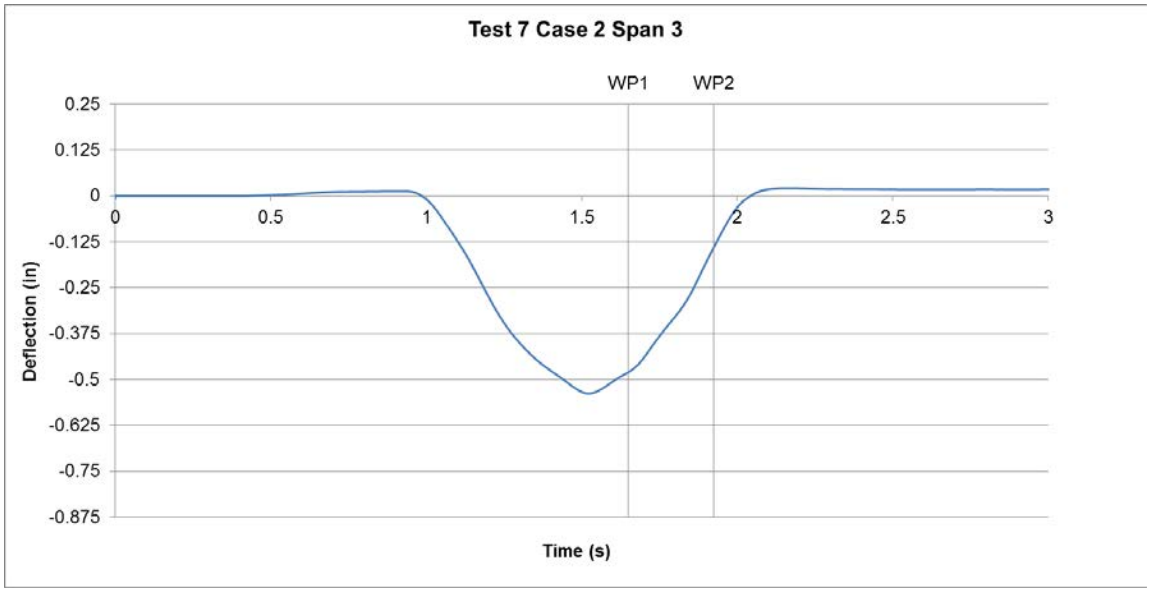
Test 7 Case 2 Span 3
WP1
WP2
0.25
0.125
0
-0.125
-0.25
-0.375
-0.5
-0.625
-0.75
-0.875
0
0.5
1
1.5
2
2.5
3
Deflection (in)
Time (s)

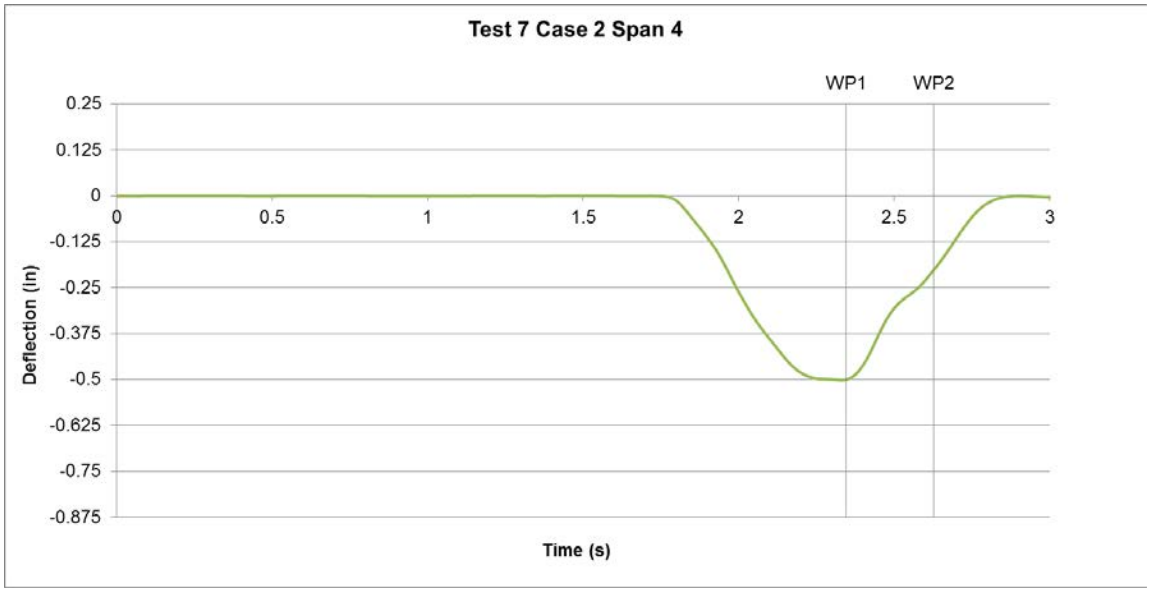
Test 7 Case 2 Span 4
WP1
WP2
0.25
0.125
0
-0.125
-0.25
-0.375
-0.5
-0.625
-0.75
-0.875
0
0.5
1
1.5
2
2.5
3
Deflection (in)
Time (s)

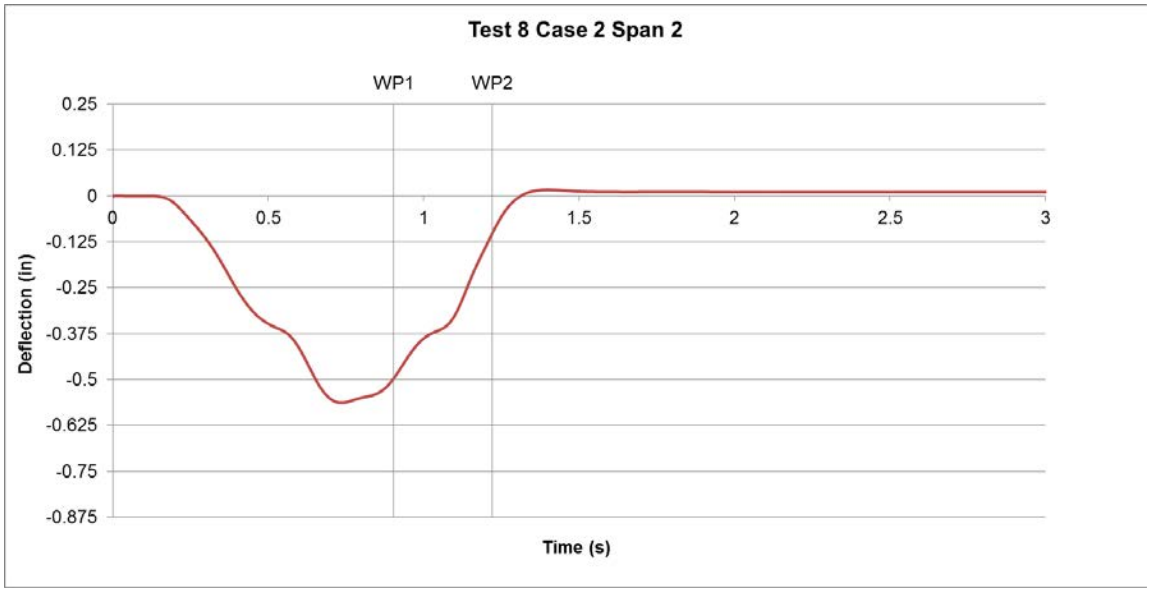
Test 8 Case 2 Span 2
WP1
WP2
0.25
0.125
0
-0.125
-0.25
-0.375
-0.5
-0.625
-0.75
-0.875
0
0.5
1
1.5
2
2.5
3
Deflection (in)
Time (s)

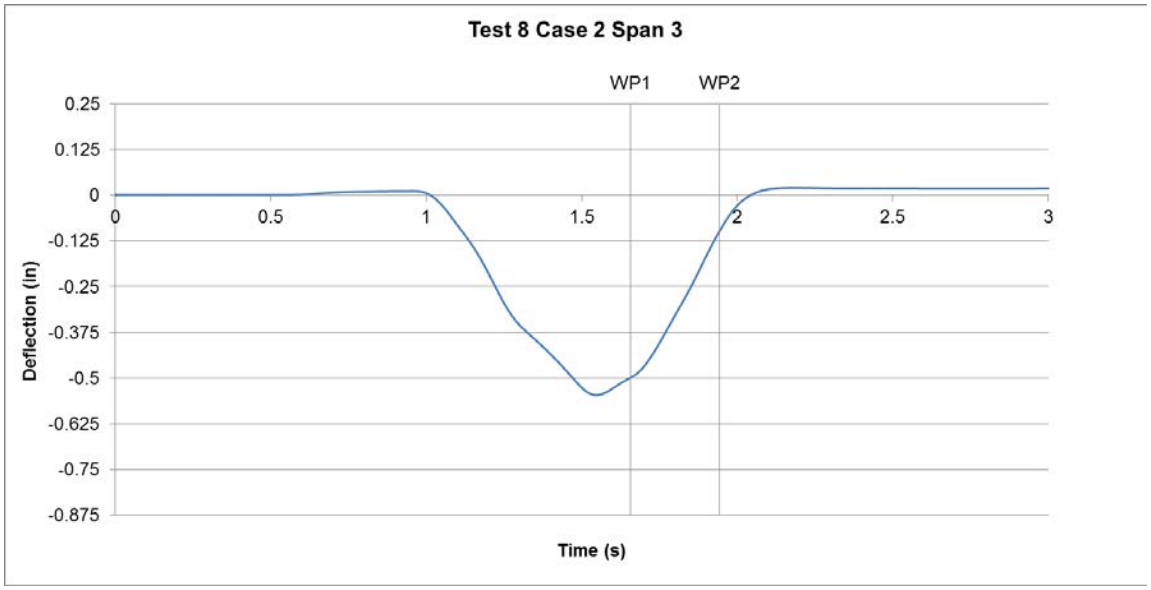
Test 8 Case 2 Span 3
WP1
WP2
0.25
0.125
0
-0.125
-0.25
-0.375
-0.5
-0.625
-0.75
-0.875
0
0.5
1
1.5
2
2.5
3
Deflection (in)
Time (s)

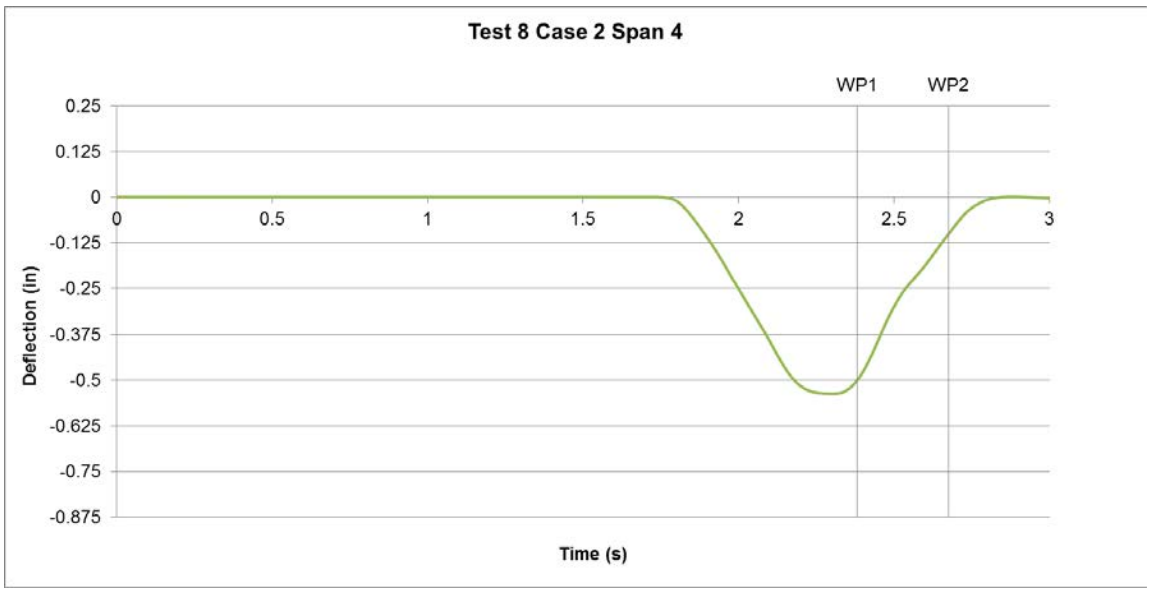
Test 8 Case 2 Span 4
WP1
WP2
0.25
0.125
0
-0.125
-0.25
-0.375
-0.5
-0.625
-0.75
-0.875
0
0.5
1
1.5
2
2.5
3
Deflection (in)
Time (s)

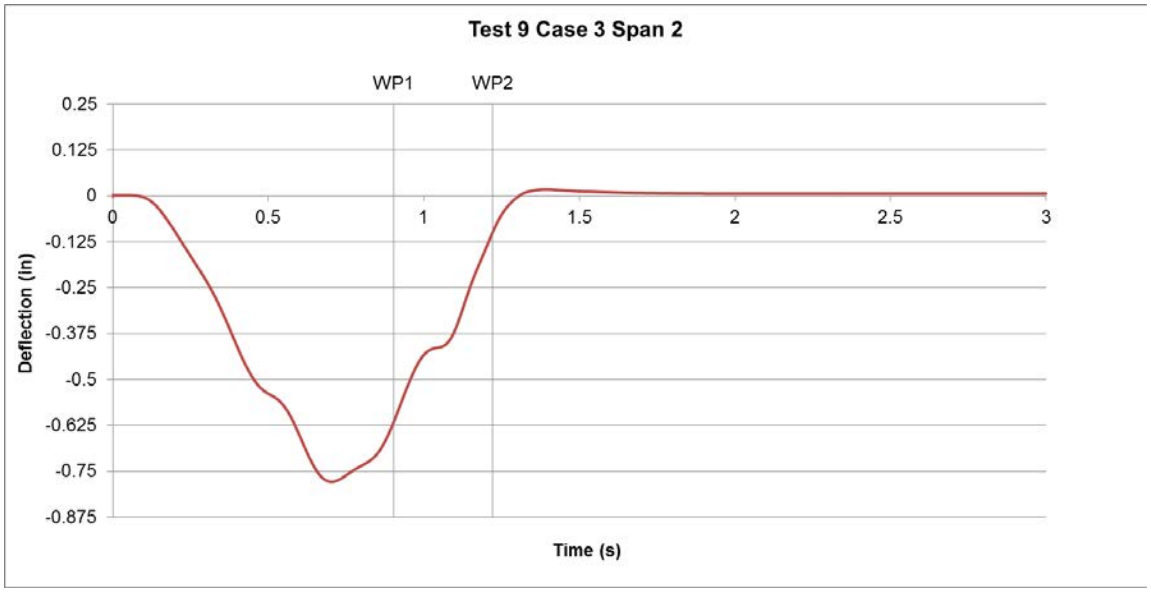
Test 9 Case 3 Span 2
WP1
WP2
0.25
0.125
0
-0.125
-0.25
-0.375
-0.5
-0.625
-0.75
-0.875
0
0.5
1
1.5
2
2.5
3
Deflection (in)
Time (s)

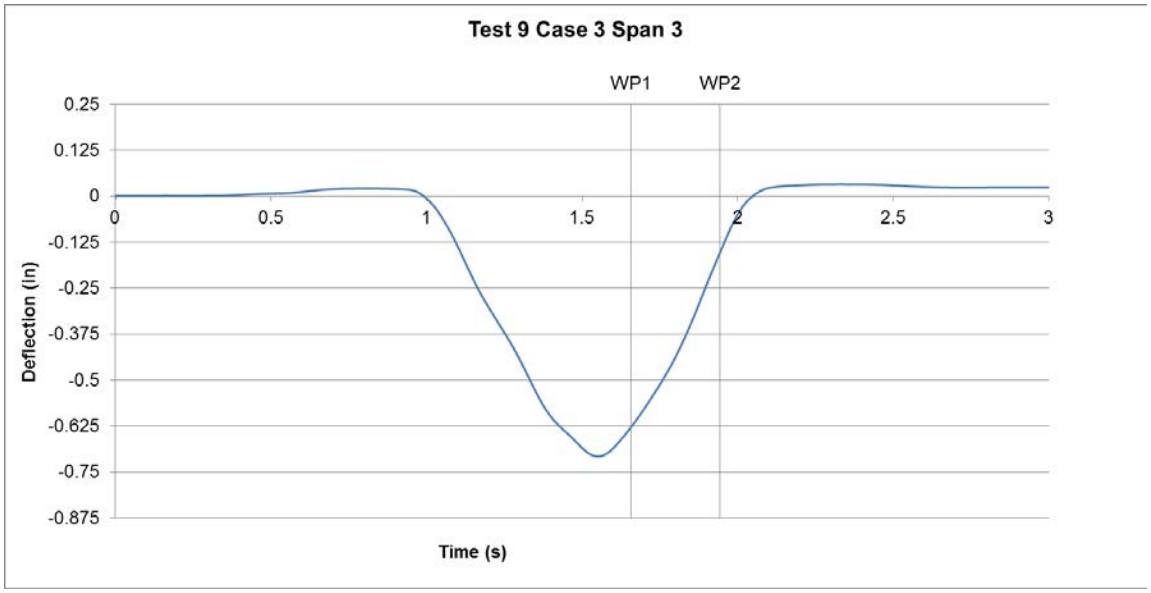
Test 9 Case 3 Span 3
WP1
WP2
0.25
0.125
0
-0.125
-0.25
-0.375
-0.5
-0.625
-0.75
-0.875
0
0.5
1
1.5
2
2.5
3
Deflection (in)
Time (s)

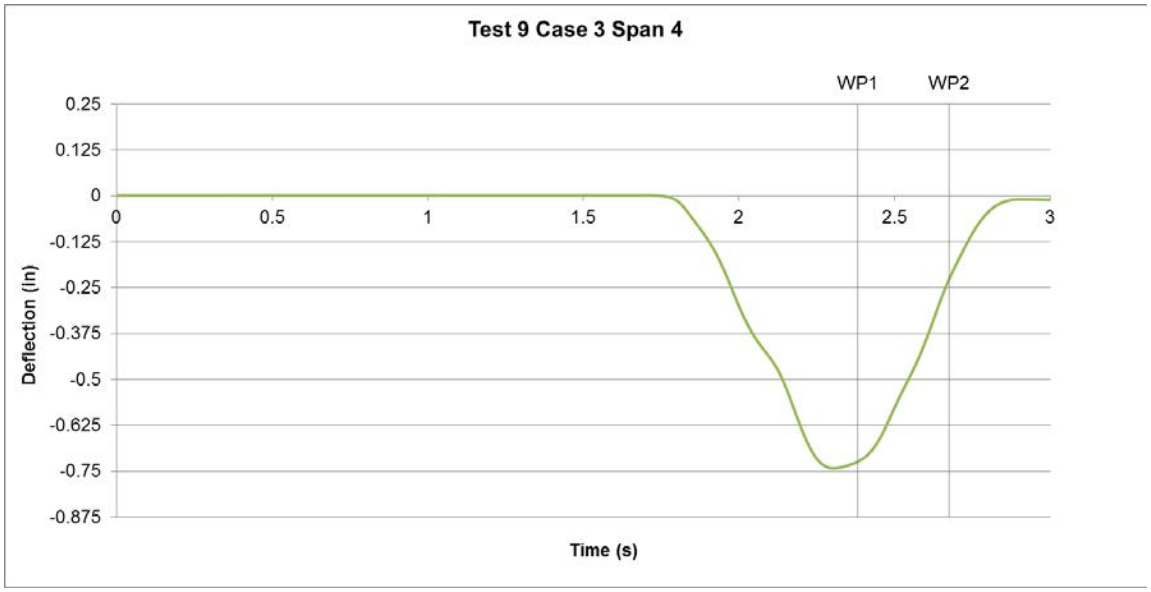
Test 9 Case 3 Span 4
WP1
WP2
0.25
0.125
0
-0.125
-0.25
-0.375
-0.5
-0.625
-0.75
-0.875
0
0.5
1
1.5
2
2.5
3
Deflection (in)
Time (s)

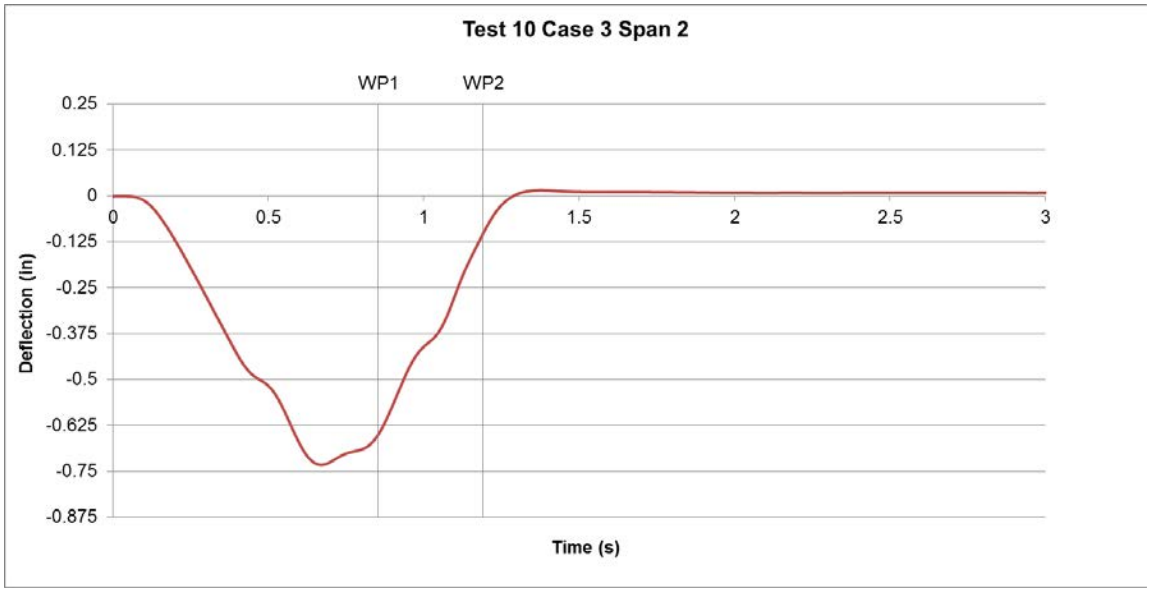
Test 10 Case 3 Span 2
WP1
WP2
0.25
0.125
0
-0.125
-0.25
-0.375
-0.5
-0.625
-0.75
-0.875
0
0.5
1
1.5
2
2.5
3
Deflection (in)
Time (s)

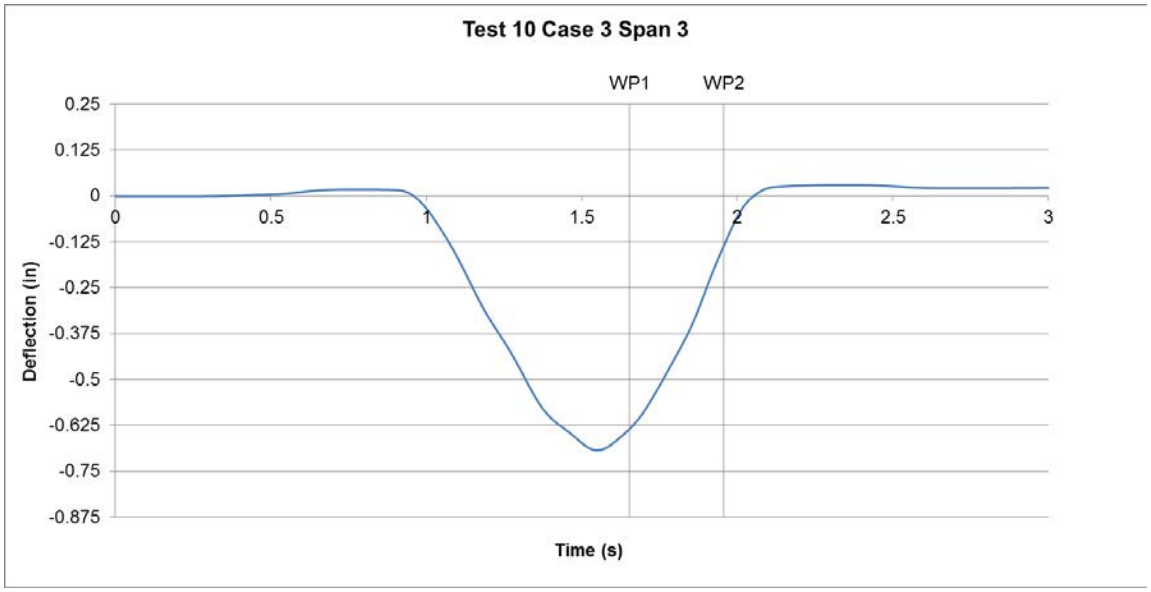
Test 10 Case 3 Span 3
WP1
WP2
0.25
0.125
0
-0.125
-0.25
-0.375
-0.5
-0.625
-0.75
-0.875
0
0.5
1
1.5
2
2.5
3
Deflection (in)
Time (s)

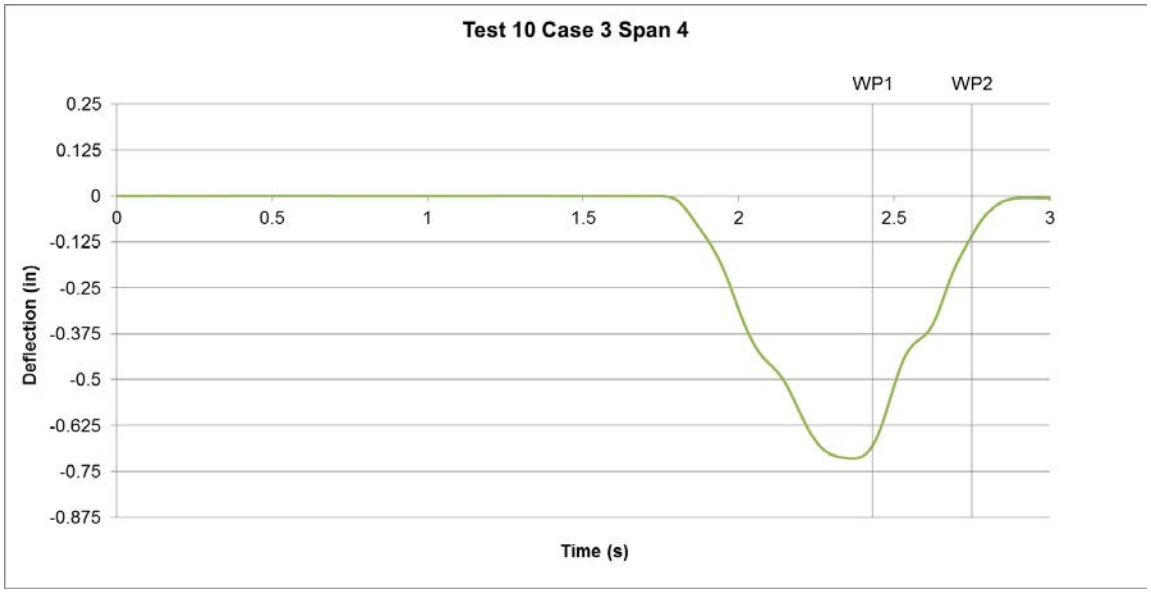
Test 10 Case 3 Span 4
WP1
WP2
0.25
0.125
0
-0.125
-0.25
-0.375
-0.5
-0.625
-0.75
-0.875
0
0.5
1
1.5
2
2.5
3
Deflection (in)
Time (s)

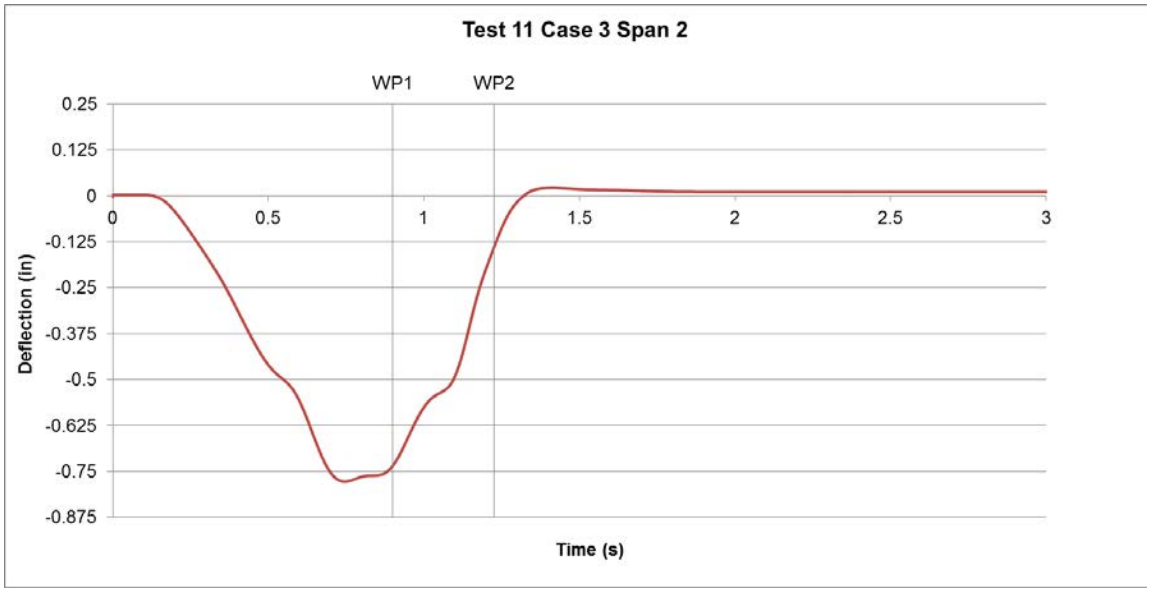
Test 11 Case 3 Span 2
WP1
WP2
0.25
0.125
0
-0.125
-0.25
-0.375
-0.5
-0.625
-0.75
-0.875
0
0.5
1
1.5
2
2.5
3
Deflection (in)
Time (s)

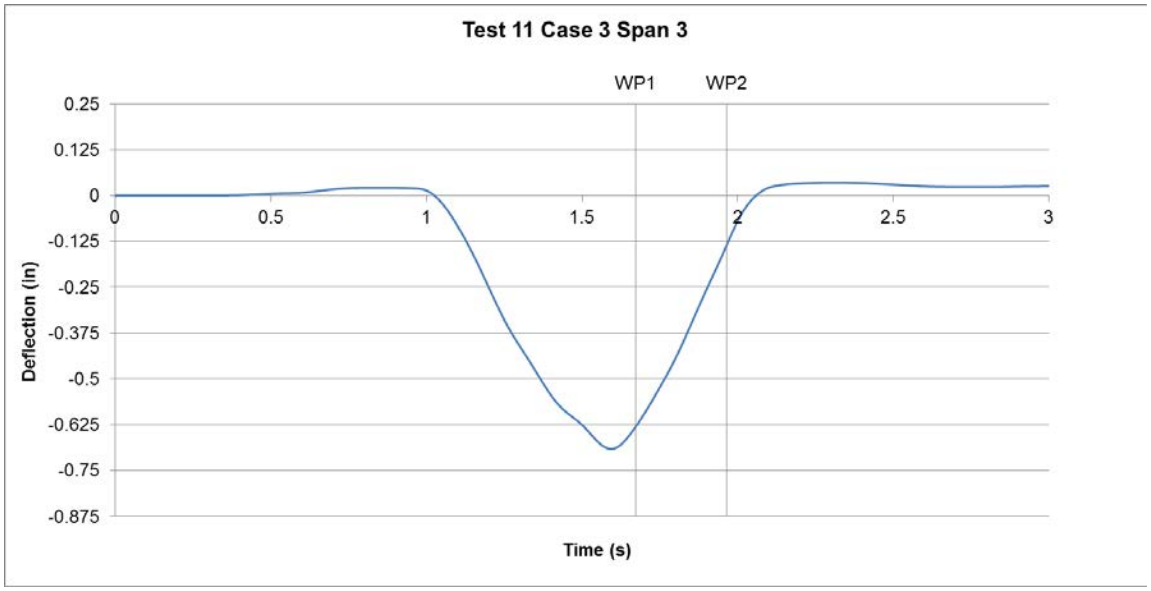
Test 11 Case 3 Span 3
WP1
WP2
0.25
0.125
0
-0.125
-0.25
-0.375
-0.5
-0.625
-0.75
-0.875
0
0.5
1
1.5
2
2.5
3
Deflection (in)
Time (s)

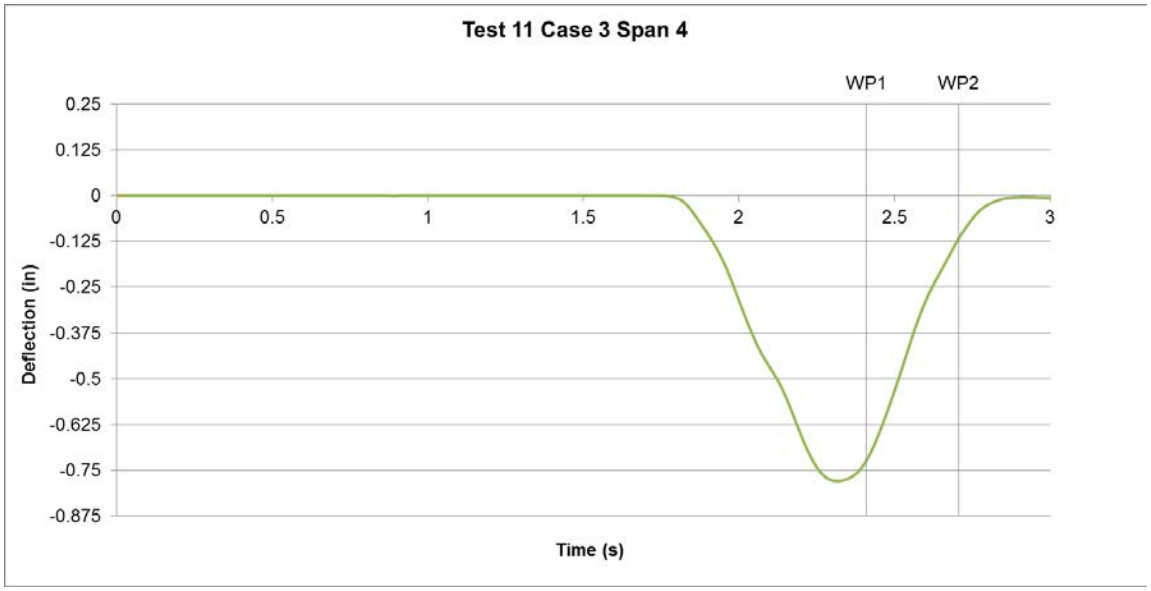
Test 11 Case 3 Span 4
WP1
WP2
0.25
0.125
0
-0.125
-0.25
-0.375
-0.5
-0.625
-0.75
-0.875
0
0.5
1
1.5
2
2.5
3
Deflection (in)
Time (s)

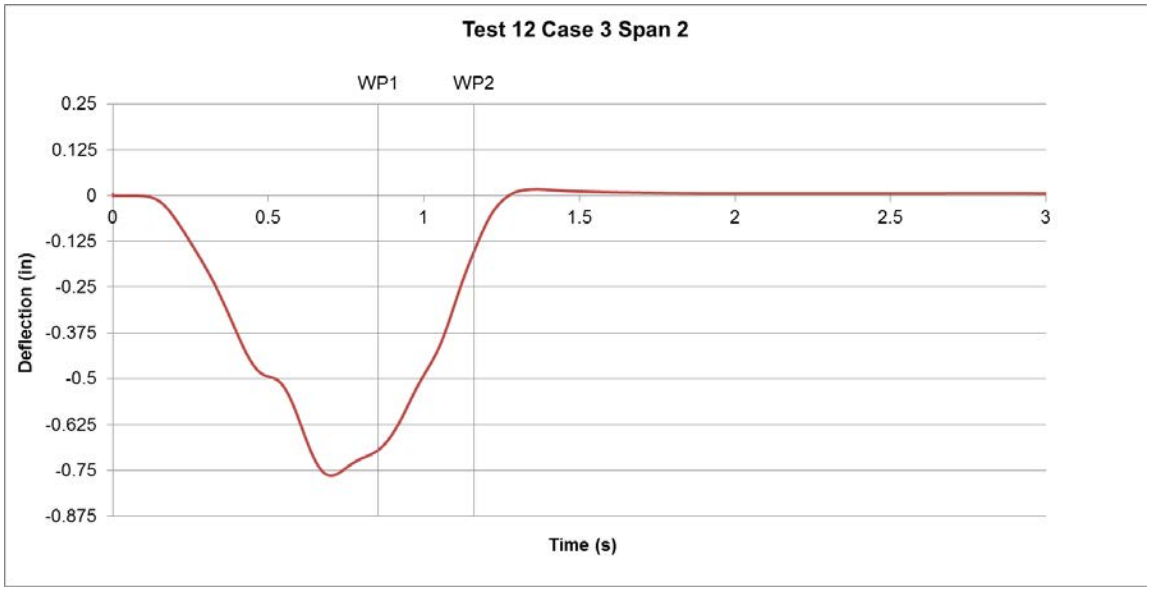
Test 12 Case 3 Span 2
WP1
WP2
0.25
0.125
0
-0.125
-0.25
-0.375
-0.5
-0.625
-0.75
-0.875
0
0.5
1
1.5
2
2.5
3
Deflection (in)
Time (s)

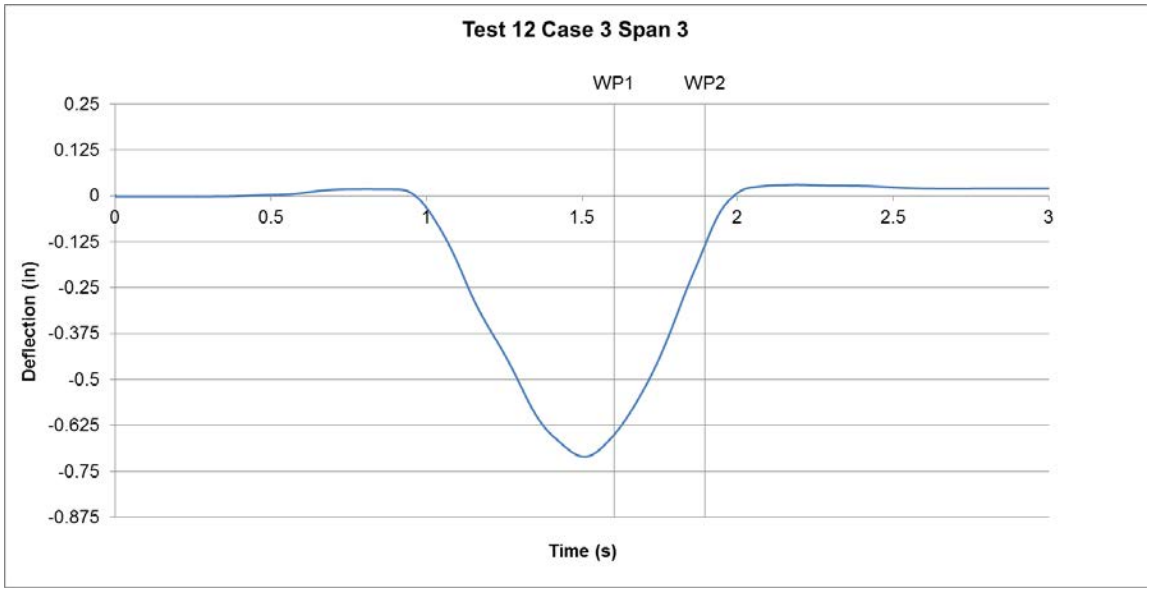
Test 12 Case 3 Span 3
WP1
WP2
0.25
0.125
0
-0.125
-0.25
-0.375
-0.5
-0.625
-0.75
-0.875
0
0.5
1
1.5
2
2.5
3
Deflection (in)
Time (s)

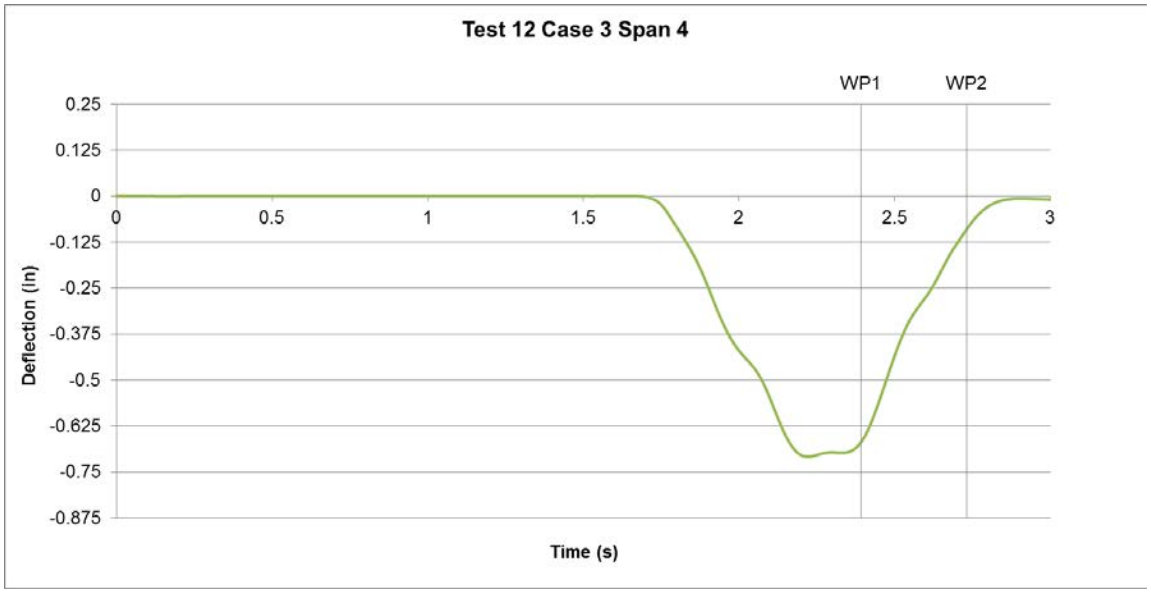
Test 12 Case 3 Span 4
WP1
WP2
0.25
0.125
0
-0.125
-0.25
-0.375
-0.5
-0.625
-0.75
-0.875
0
0.5
1
1.5
2
2.5
3
Deflection (in)
Time (s)

APPENDIX B

LARGE-SCALE OPEN DECK EXPERIMENT FREIGHT TRAIN PLOTS

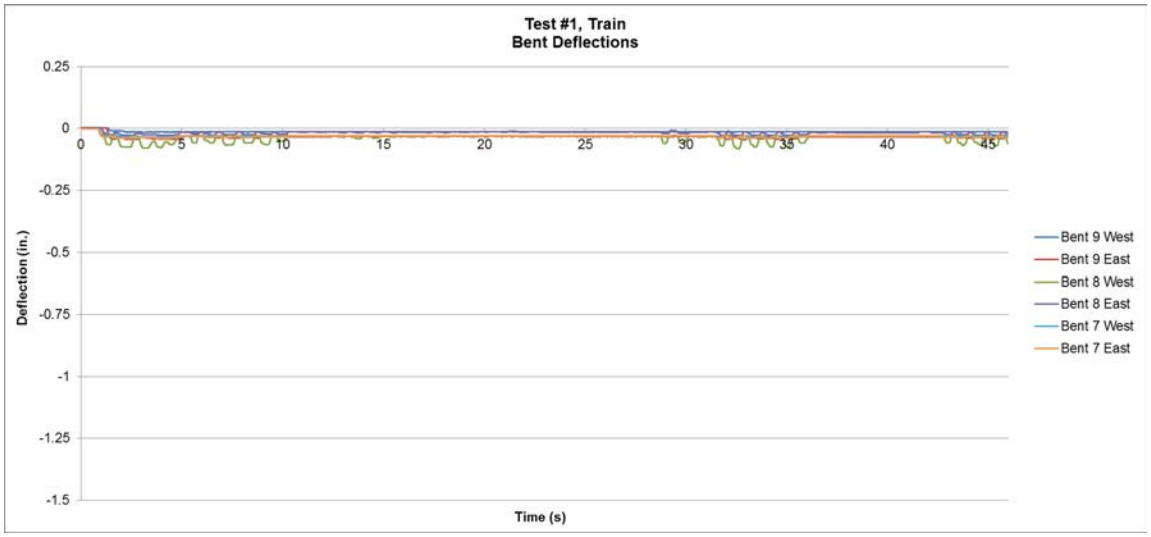

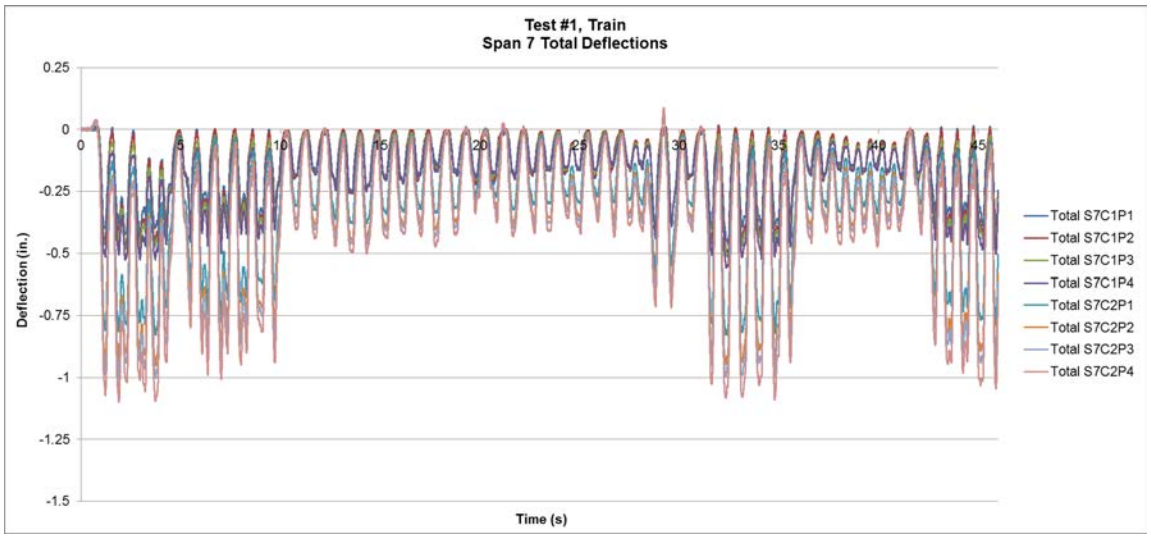

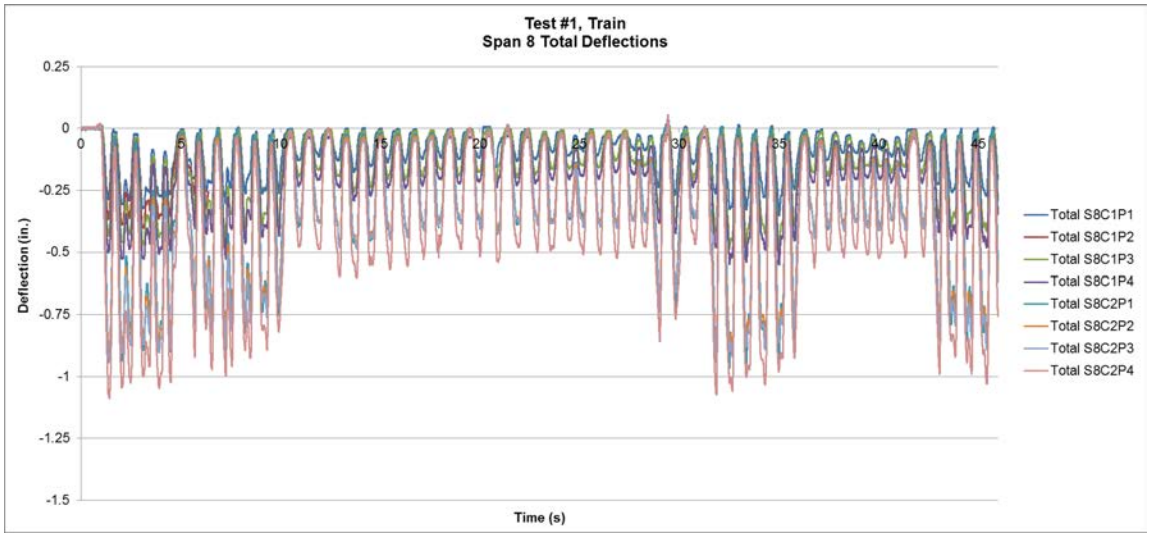
Test #1, Train
Span 8 Total Deflections
0.25
0
-0.25
-0.5
-0.75
-1
-1.25
-1.5
Deflection (in.)
0
5
10
15
20
25
30
35
40
45
Time (s)
Total S8C1P1
Total S8C1P2
Total S8C1P3
Total S8C1P4
Total S8C2P1
Total S8C2P2
Total S8C2P3
Total S8C2P4

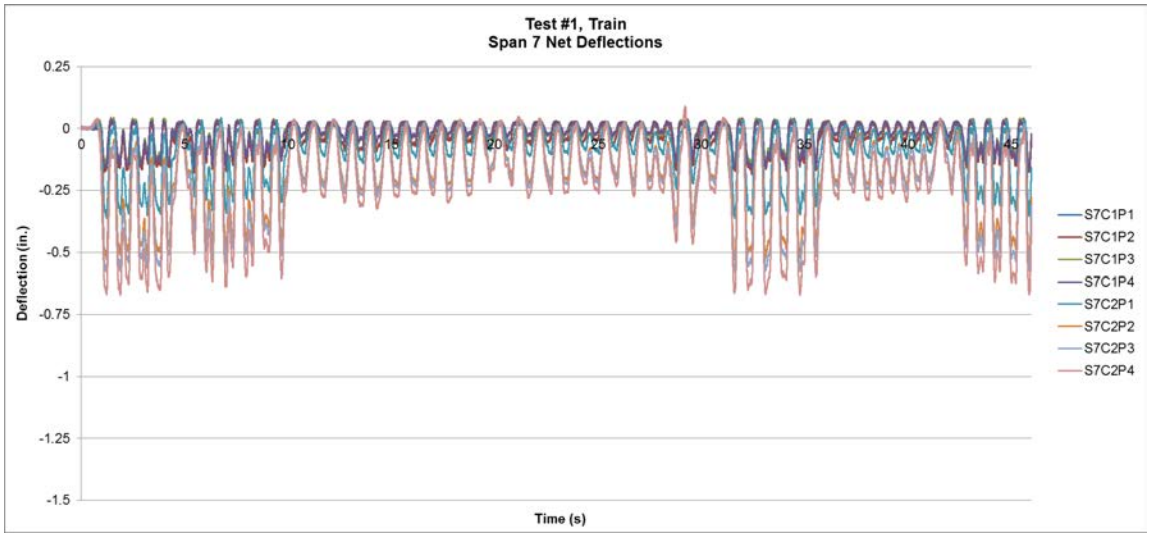
Test #1, Train
Span 7 Net Deflections
0.25
0
-0.25
-0.5
-0.75
-1
-1.25
-1.5
Deflection (in.)
0
5
10
15
20
25
30
35
40
45
Time (s)
S7C1P1
S7C1P2
S7C1P3
S7C1P4
S7C2P1
S7C2P2
S7C2P3
S7C2P4

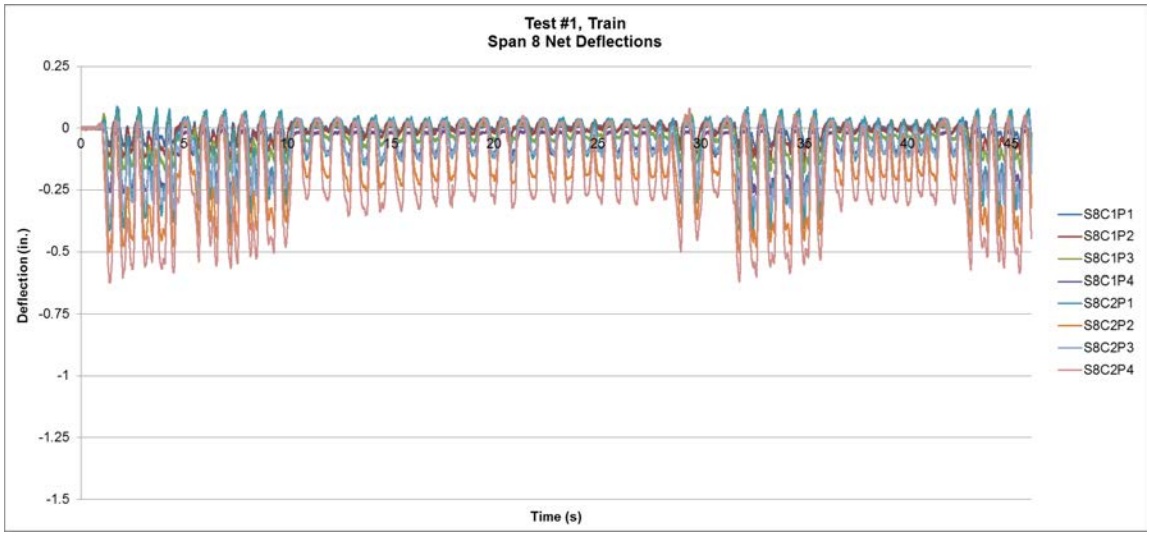
Test #1, Train
Span 8 Net Deflections
0.25
0
-0.25
-0.5
-0.75
-1
-1.25
-1.5
Deflection (in.)
0
5
10
15
20
25
30
35
40
45
Time (s)
S8C1P1
S8C1P2
S8C1P3
S8C1P4
S8C2P1
S8C2P2
S8C2P3
S8C2P4

APPENDIX C

LARGE-SCALE OPEN DECK EXPERIMENT BENT-CAP DEFLECTION PLOTS

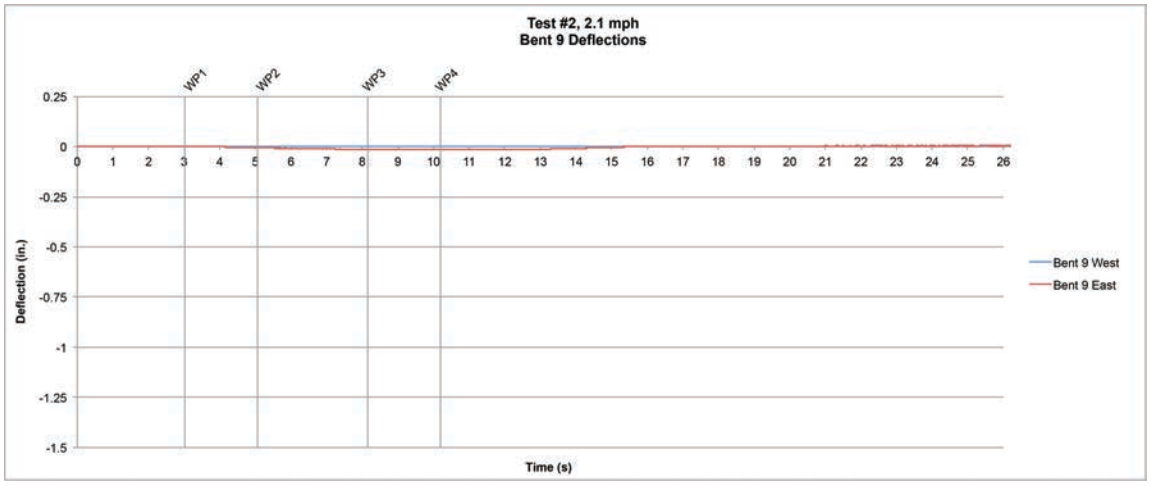

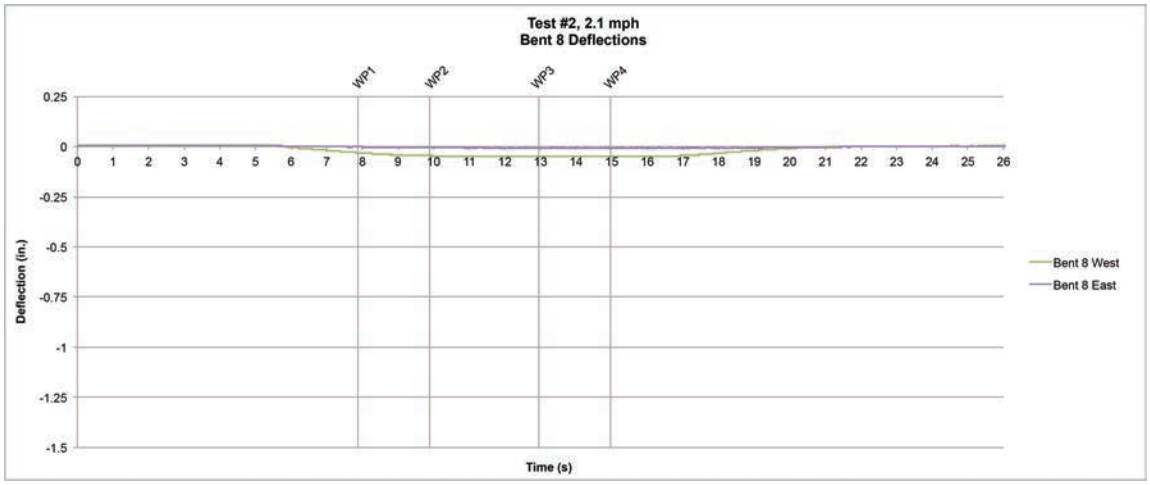

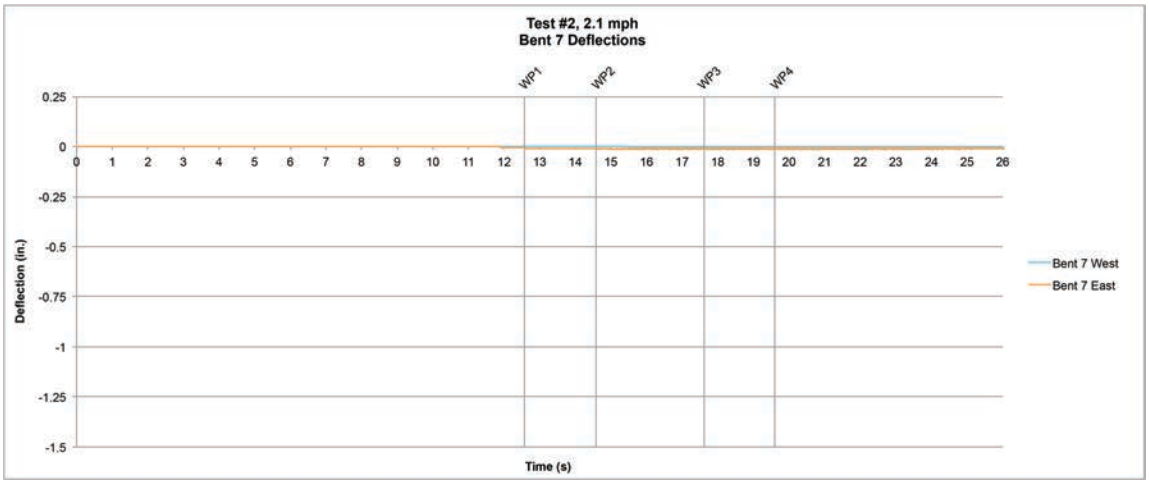
Test #2, 2.1 mph
Bent 7 Deflections
WP1
WP2
WP3
WP4
0.25
0
-0.25
-0.5
-0.75
-1
-1.25
-1.5
0 1 2 3 4 5 6 7 8 9 10 11 12 13 14 15 16 17 18 19 20 21 22 23 24 25 26
Deflection (in.)
Time (s)
Bent 7 West
Bent 7 East

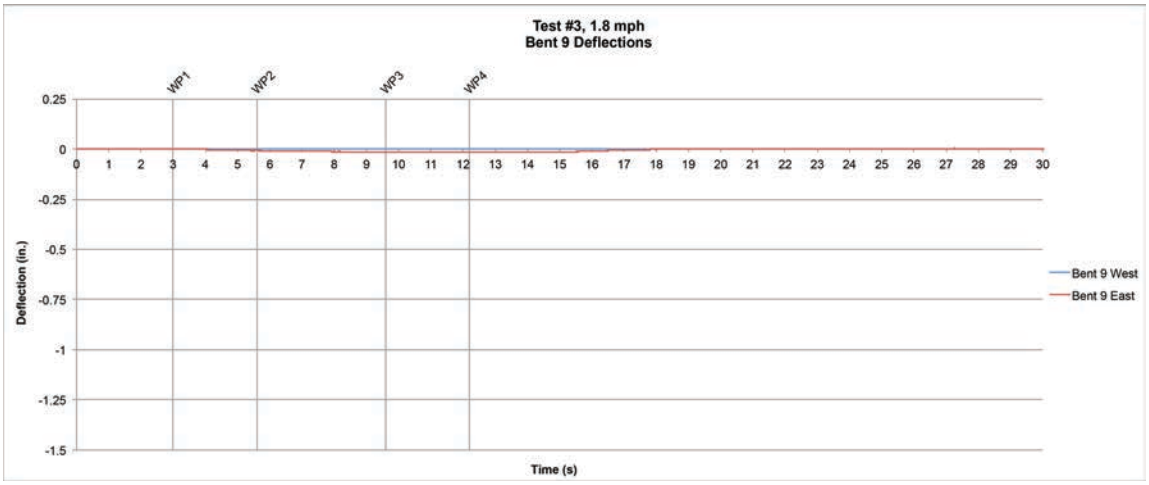
Test #3, 1.8 mph
Bent 9 Deflections
WP1
WP2
WP3
WP4
0.25
0
-0.25
-0.5
-0.75
-1
-1.25
-1.5
0 1 2 3 4 5 6 7 8 9 10 11 12 13 14 15 16 17 18 19 20 21 22 23 24 25 26 27 28 29 30
Deflection (in.)
Time (s)
Bent 9 West
Bent 9 East

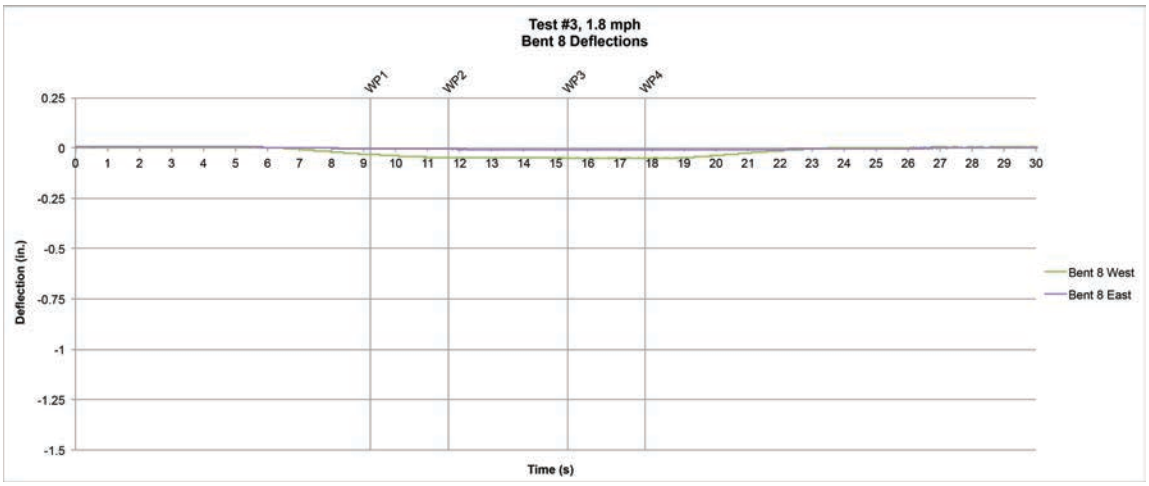
Test #3, 1.8 mph
Bent 8 Deflections
WP1
WP2
WP3
WP4
0.25
0
-0.25
-0.5
-0.75
-1
-1.25
-1.5
0 1 2 3 4 5 6 7 8 9 10 11 12 13 14 15 16 17 18 19 20 21 22 23 24 25 26 27 28 29 30
Deflection (in.)
Time (s)
Bent 8 West
Bent 8 East

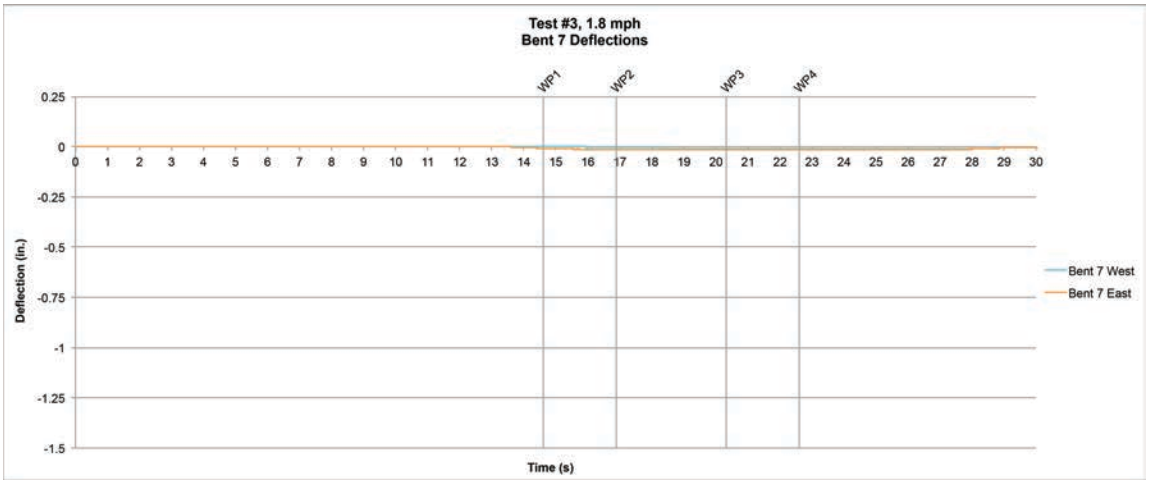
Test #3, 1.8 mph
Bent 7 Deflections
WP1
WP2
WP3
WP4
0.25
0
-0.25
-0.5
-0.75
-1
-1.25
-1.5
0 1 2 3 4 5 6 7 8 9 10 11 12 13 14 15 16 17 18 19 20 21 22 23 24 25 26 27 28 29 30
Deflection (in.)
Time (s)
Bent 7 West
Bent 7 East

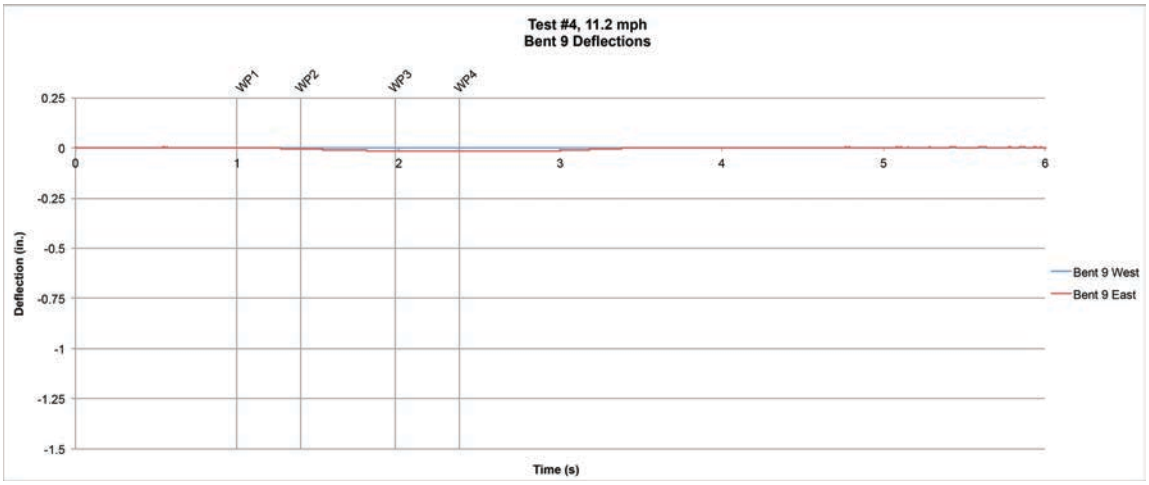
Test #4, 11.2 mph
Bent 9 Deflections
WP1
WP2
WP3
WP4
0.25
0
-0.25
-0.5
-0.75
-1
-1.25
-1.5
0 1 2 3 4 5 6
Deflection (in.)
Time (s)
Bent 9 West
Bent 9 East

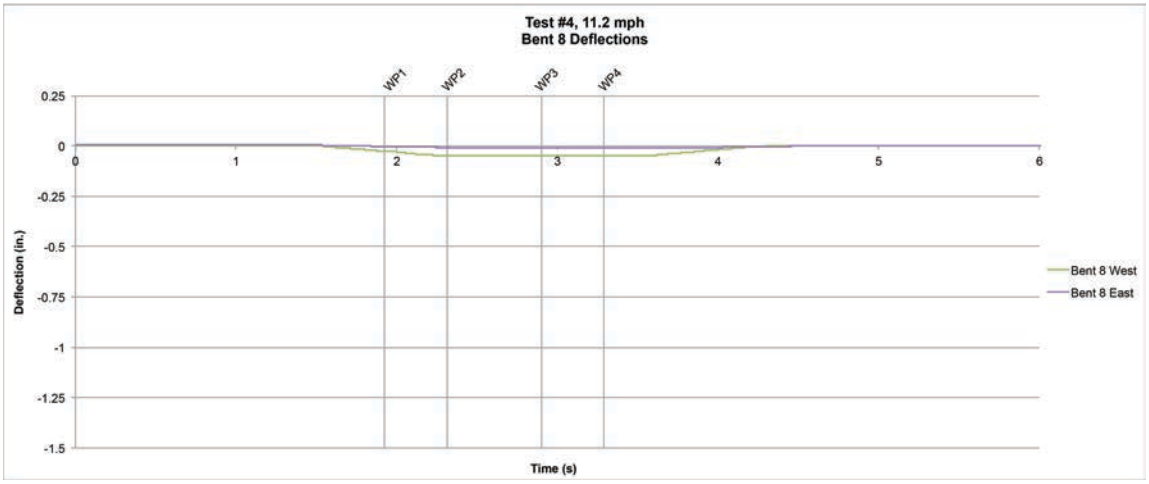
Test #4, 11.2 mph
Bent 8 Deflections
WP1
WP2
WP3
WP4
0.25
0
-0.25
-0.5
-0.75
-1
-1.25
-1.5
0 1 2 3 4 5 6
Deflection (in.)
Time (s)
Bent 8 West
Bent 8 East

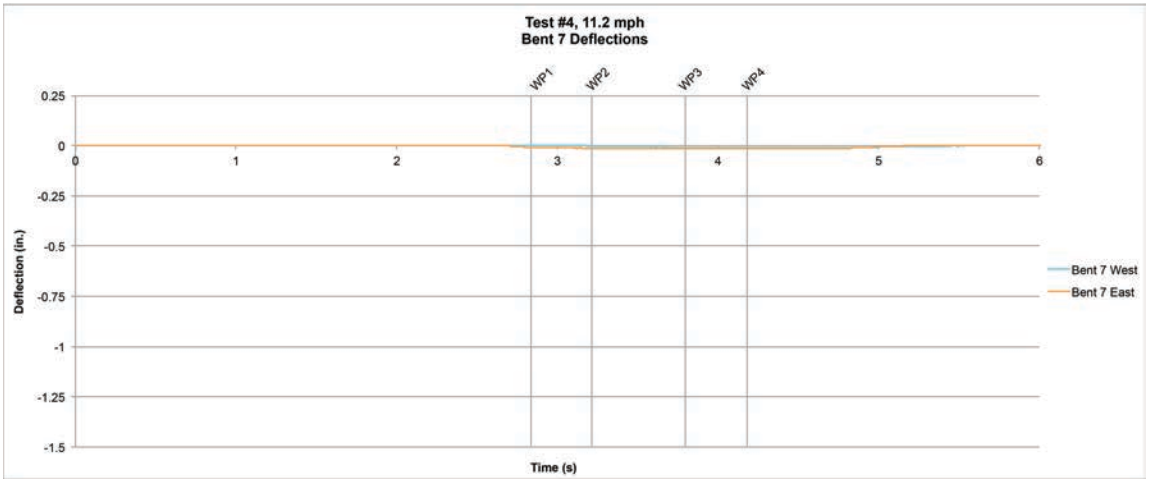
Test #4, 11.2 mph
Bent 7 Deflections
WP1
WP2
WP3
WP4
0.25
0
-0.25
-0.5
-0.75
-1
-1.25
-1.5
0
1
2
3
4
5
6
Deflection (in.)
Time (s)
Bent 7 West
Bent 7 East

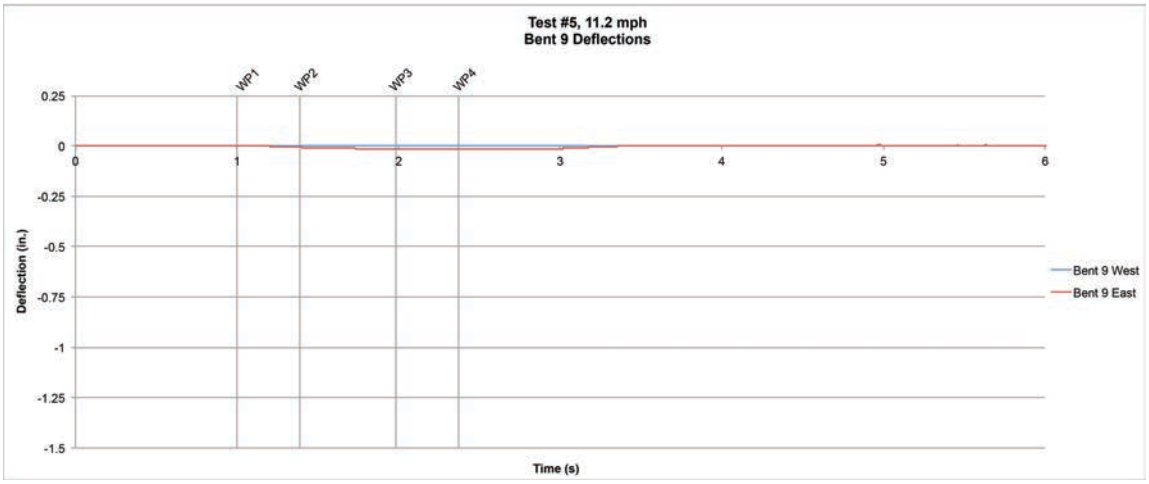
Test #5, 11.2 mph
Bent 9 Deflections
WP1
WP2
WP3
WP4
0.25
0
-0.25
-0.5
-0.75
-1
-1.25
-1.5
0
1
2
3
4
5
6
Deflection (in.)
Time (s)
Bent 9 West
Bent 9 East

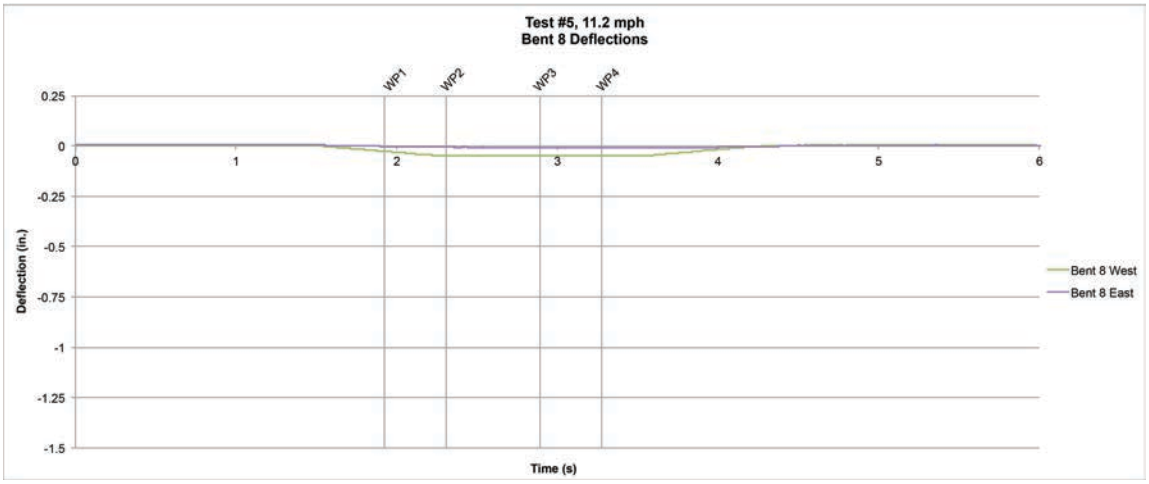
Test #5, 11.2 mph
Bent 8 Deflections
WP1
WP2
WP3
WP4
0.25
0
-0.25
-0.5
-0.75
-1
-1.25
-1.5
0
1
2
3
4
5
6
Deflection (in.)
Time (s)
Bent 8 West
Bent 8 East

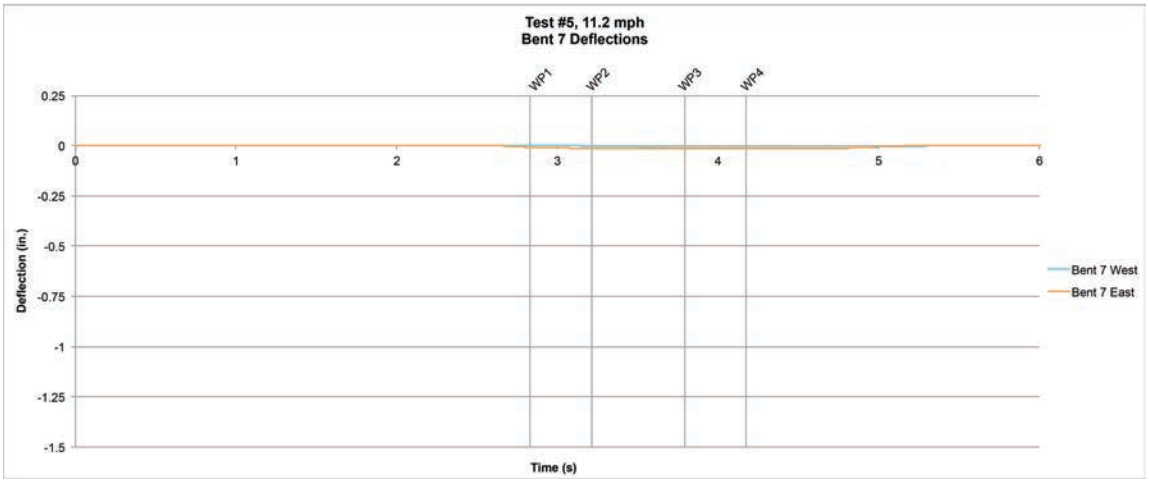
Test #5, 11.2 mph
Bent 7 Deflections
WP1
WP2
WP3
WP4
0.25
0
-0.25
-0.5
-0.75
-1
-1.25
-1.5
0
1
2
3
4
5
6
Deflection (in.)
Time (s)
Bent 7 West
Bent 7 East

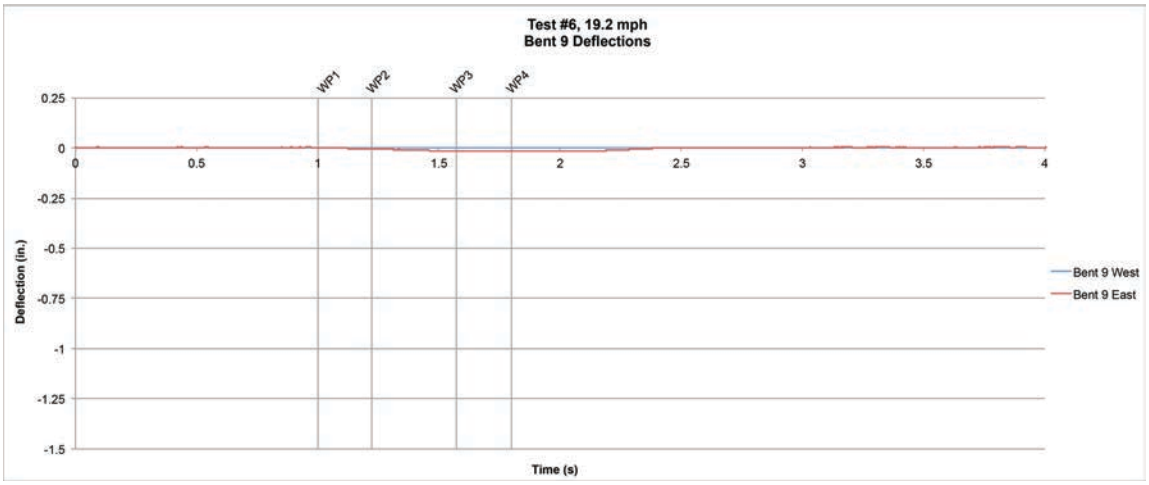
Test #6, 19.2 mph
Bent 9 Deflections
WP1
WP2
WP3
WP4
0.25
0
-0.25
-0.5
-0.75
-1
-1.25
-1.5
0
0.5
1
1.5
2
2.5
3
3.5
4
Deflection (in.)
Time (s)
Bent 9 West
Bent 9 East

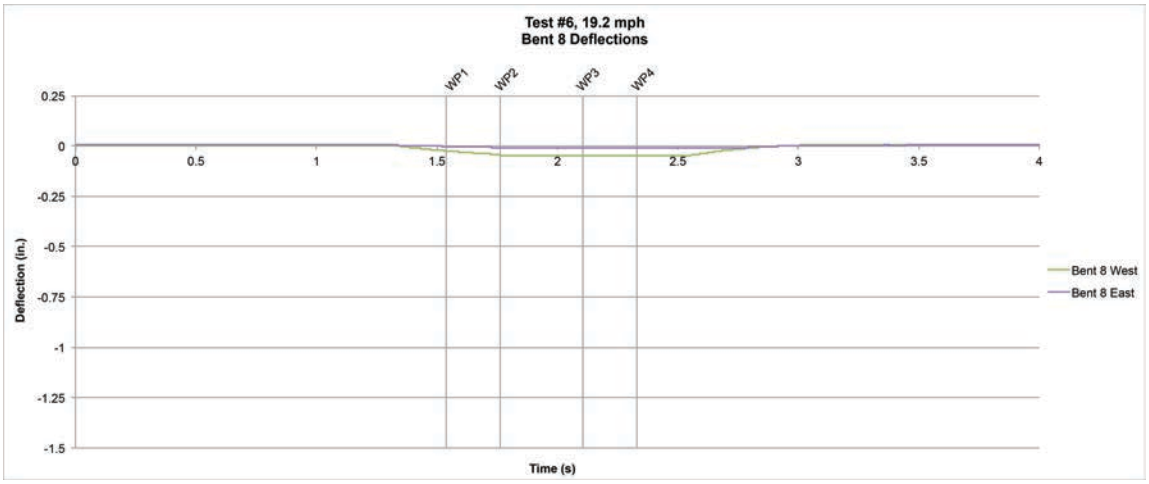
Test #6, 19.2 mph
Bent 8 Deflections
WP1
WP2
WP3
WP4
0.25
0
-0.25
-0.5
-0.75
-1
-1.25
-1.5
0
0.5
1
1.5
2
2.5
3
3.5
4
Deflection (in.)
Time (s)
Bent 8 West
Bent 8 East

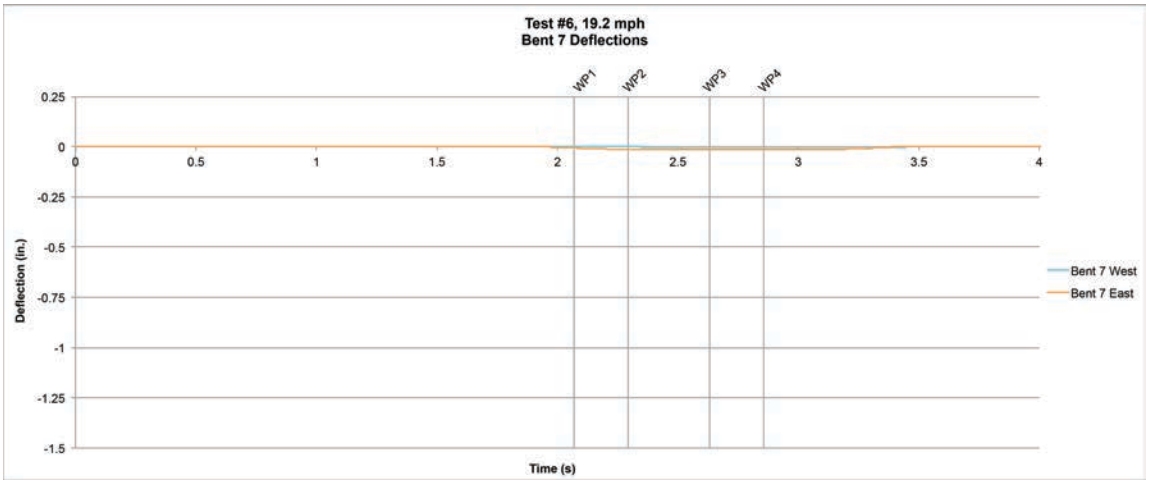
Test #6, 19.2 mph
Bent 7 Deflections
WP1
WP2
WP3
WP4
0.25
0
-0.25
-0.5
-0.75
-1
-1.25
-1.5
0
0.5
1
1.5
2
2.5
3
3.5
4
Deflection (in.)
Time (s)
Bent 7 West
Bent 7 East

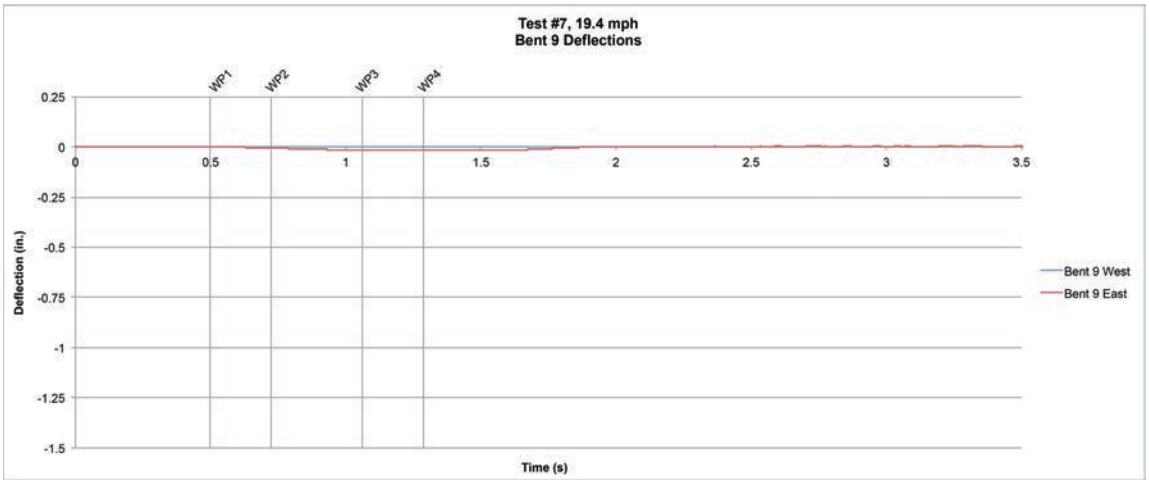
Test #7, 19.4 mph
Bent 9 Deflections
WP1
WP2
WP3
WP4
0.25
0
-0.25
-0.5
-0.75
-1
-1.25
-1.5
0
0.5
1
1.5
2
2.5
3
3.5
Deflection (in.)
Time (s)
Bent 9 West
Bent 9 East

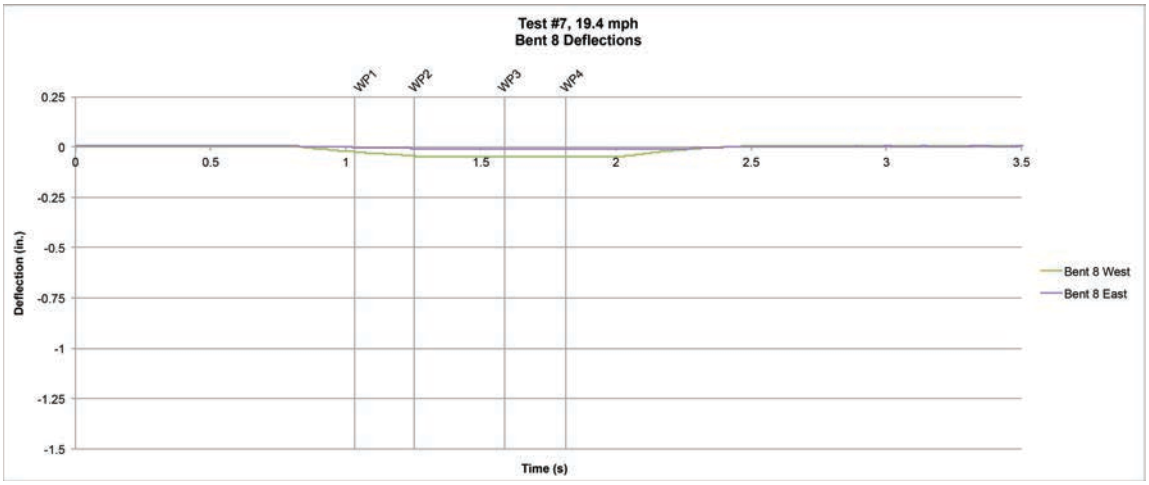
Test #7, 19.4 mph
Bent 8 Deflections
WP1
WP2
WP3
WP4
0.25
0
-0.25
-0.5
-0.75
-1
-1.25
-1.5
0
0.5
1
1.5
2
2.5
3
3.5
Deflection (in.)
Time (s)
Bent 8 West
Bent 8 East

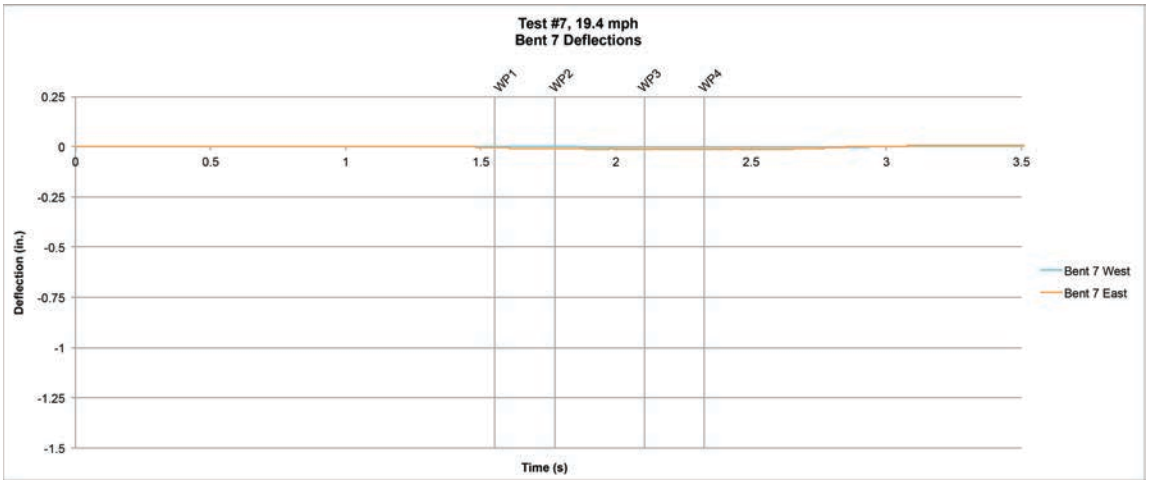
Test #7, 19.4 mph
Bent 7 Deflections
WP1
WP2
WP3
WP4
0.25
0
-0.25
-0.5
-0.75
-1
-1.25
-1.5
0
0.5
1
1.5
2
2.5
3
3.5
Deflection (in.)
Time (s)
Bent 7 West
Bent 7 East

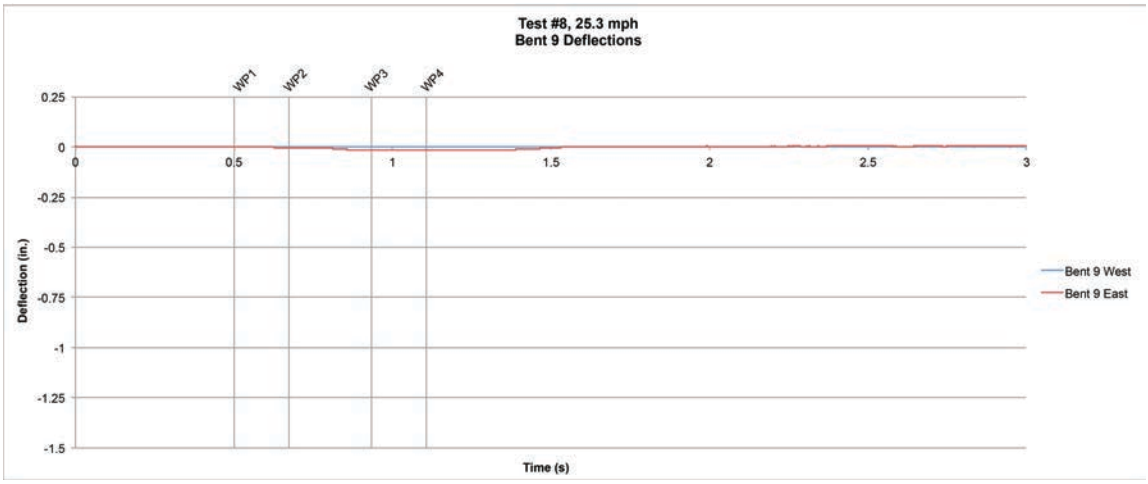
Test #8, 25.3 mph
Bent 9 Deflections
WP1
WP2
WP3
WP4
0.25
0
-0.25
-0.5
-0.75
-1
-1.25
-1.5
0
0.5
1
1.5
2
2.5
3
Deflection (in.)
Time (s)
Bent 9 West
Bent 9 East

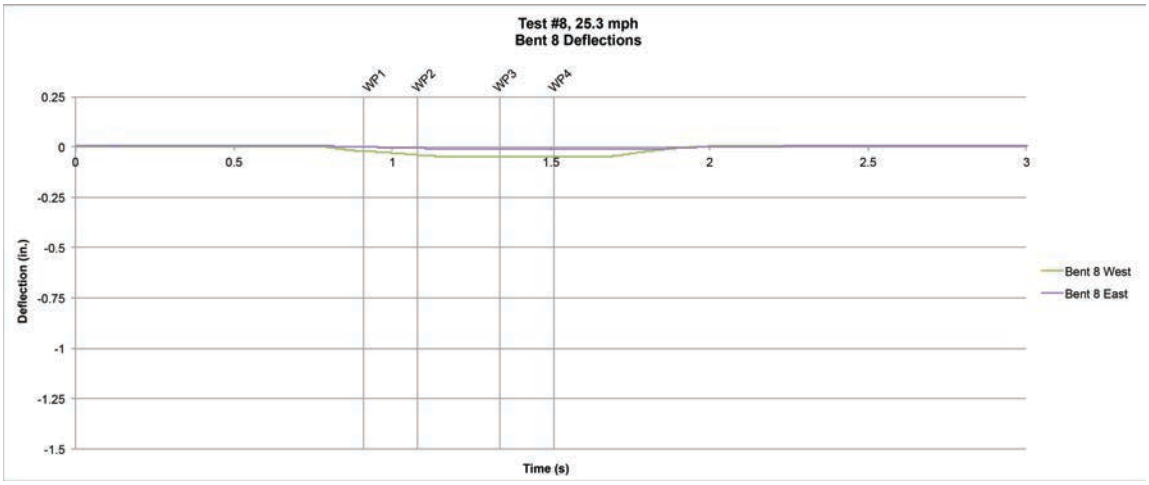
Test #8, 25.3 mph
Bent 8 Deflections
WP1
WP2
WP3
WP4
0.25
0
-0.25
-0.5
-0.75
-1
-1.25
-1.5
0
0.5
1
1.5
2
2.5
3
Deflection (in.)
Time (s)
Bent 8 West
Bent 8 East

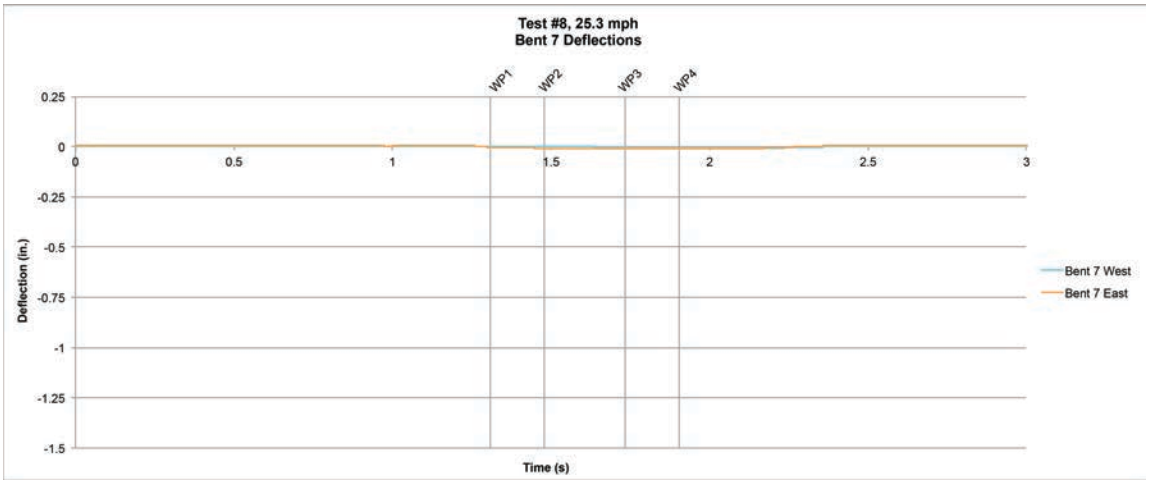
Test #8, 25.3 mph
Bent 7 Deflections
WP1
WP2
WP3
WP4
0.25
0
-0.25
-0.5
-0.75
-1
-1.25
-1.5
0
0.5
1
1.5
2
2.5
3
Deflection (in.)
Time (s)
Bent 7 West
Bent 7 East

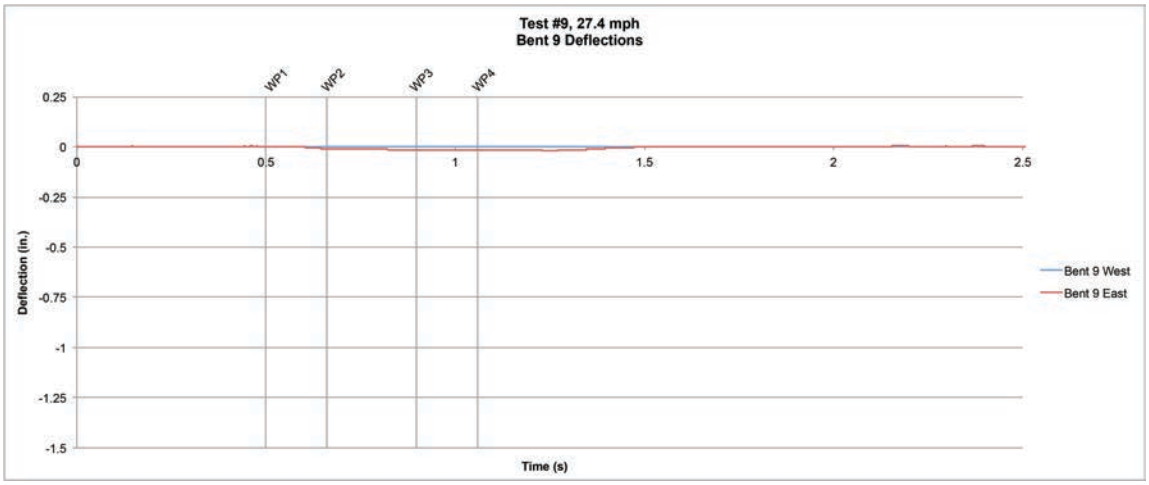
Test #9, 27.4 mph
Bent 9 Deflections
WP1
WP2
WP3
WP4
0.25
0
-0.25
-0.5
-0.75
-1
-1.25
-1.5
0
0.5
1
1.5
2
2.5
Deflection (in.)
Time (s)
Bent 9 West
Bent 9 East

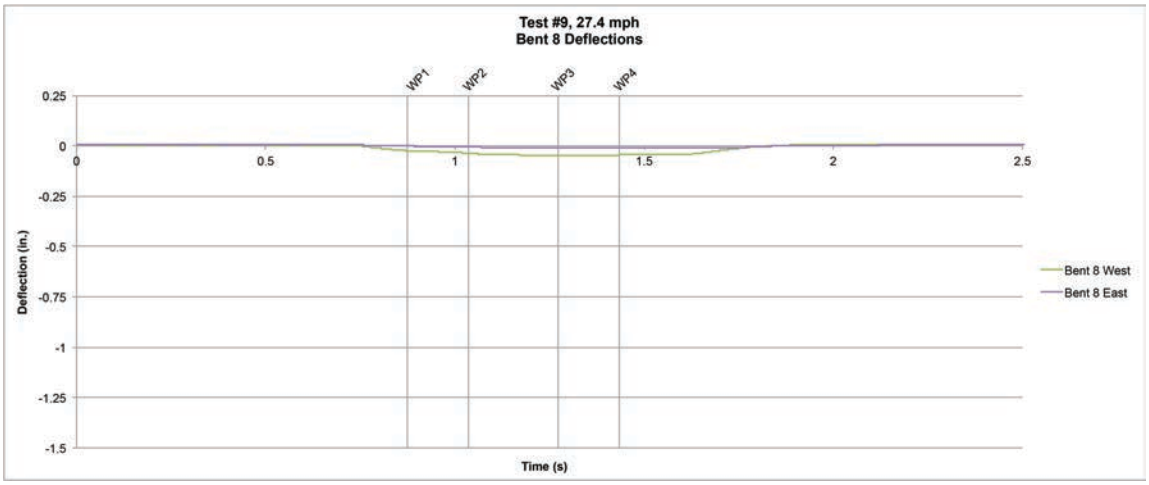
Test #9, 27.4 mph
Bent 8 Deflections
WP1
WP2
WP3
WP4
0.25
0
-0.25
-0.5
-0.75
-1
-1.25
-1.5
0
0.5
1
1.5
2
2.5
Deflection (in.)
Time (s)
Bent 8 West
Bent 8 East

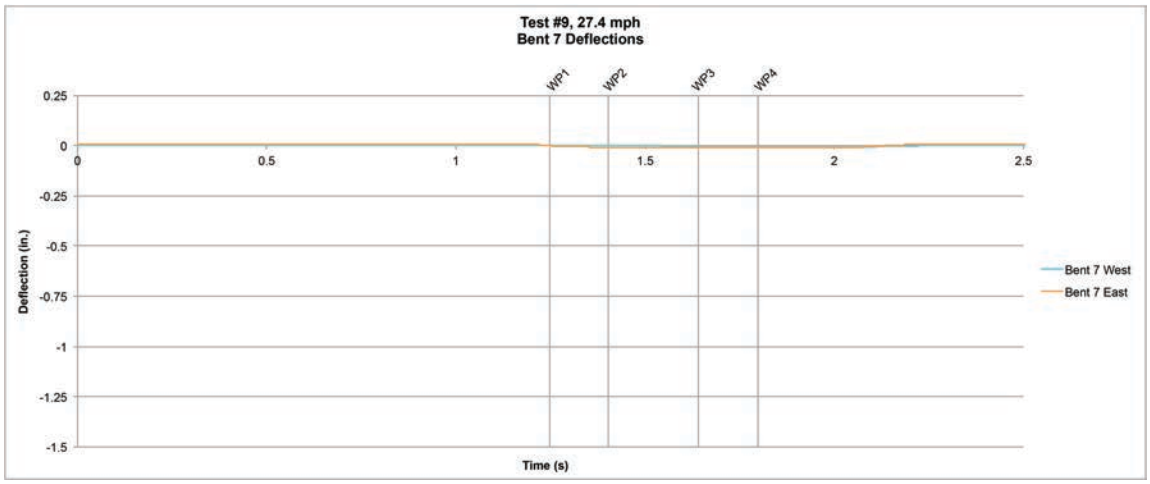
Test #9, 27.4 mph
Bent 7 Deflections
WP1
WP2
WP3
WP4
0.25
0
-0.25
-0.5
-0.75
-1
-1.25
-1.5
0
0.5
1
1.5
2
2.5
Deflection (in.)
Time (s)
Bent 7 West
Bent 7 East

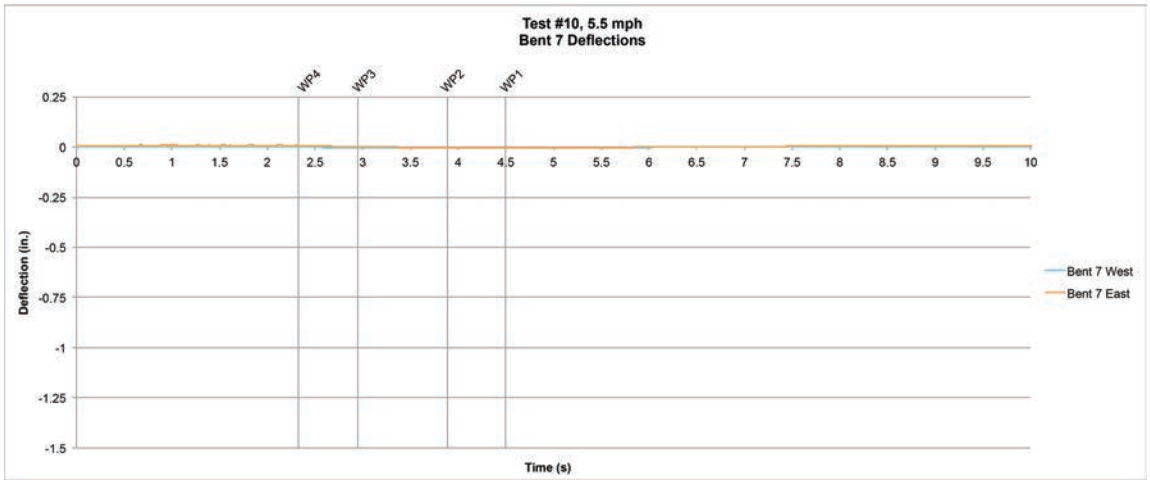
Test #10, 5.5 mph
Bent 7 Deflections
WP4
WP3
WP2
WP1
0.25
0
-0.25
-0.5
-0.75
-1
-1.25
-1.5
0
0.5
1
1.5
2
2.5
3
3.5
4
4.5
5
5.5
6
6.5
7
7.5
8
8.5
9
9.5
10
Deflection (in.)
Time (s)
Bent 7 West
Bent 7 East

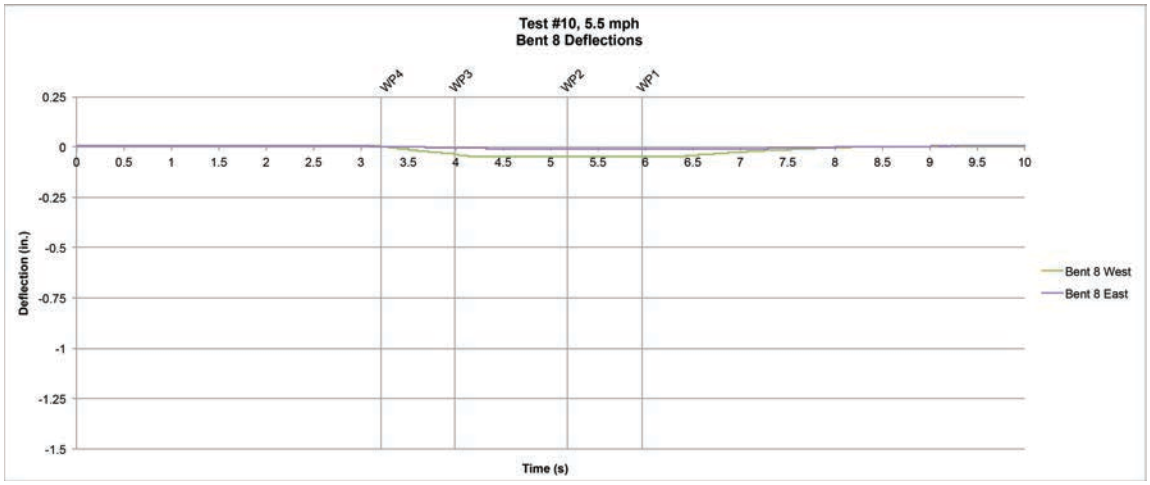
Test #10, 5.5 mph
Bent 8 Deflections
WP4
WP3
WP2
WP1
0.25
0
-0.25
-0.5
-0.75
-1
-1.25
-1.5
0
0.5
1
1.5
2
2.5
3
3.5
4
4.5
5
5.5
6
6.5
7
7.5
8
8.5
9
9.5
10
Deflection (in.)
Time (s)
Bent 8 West
Bent 8 East

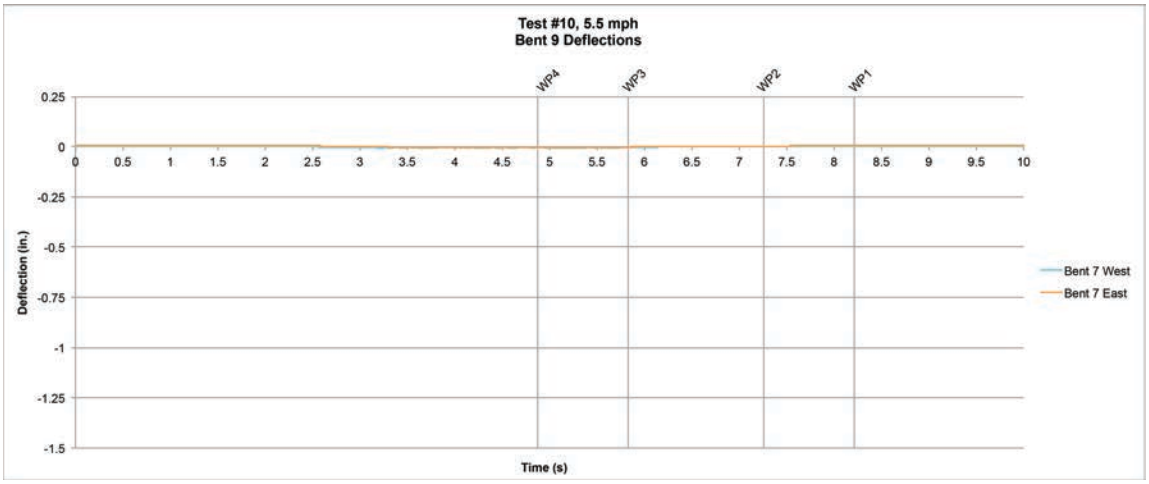
Test #10, 5.5 mph
Bent 9 Deflections
WP4
WP3
WP2
WP1
0.25
0
-0.25
-0.5
-0.75
-1
-1.25
-1.5
0
0.5
1
1.5
2
2.5
3
3.5
4
4.5
5
5.5
6
6.5
7
7.5
8
8.5
9
9.5
10
Deflection (in.)
Time (s)
Bent 7 West
Bent 7 East

APPENDIX D

LARGE-SCALE OPEN DECK EXPERIMENT TOTAL STRINGER DEFLECTION PLOTS

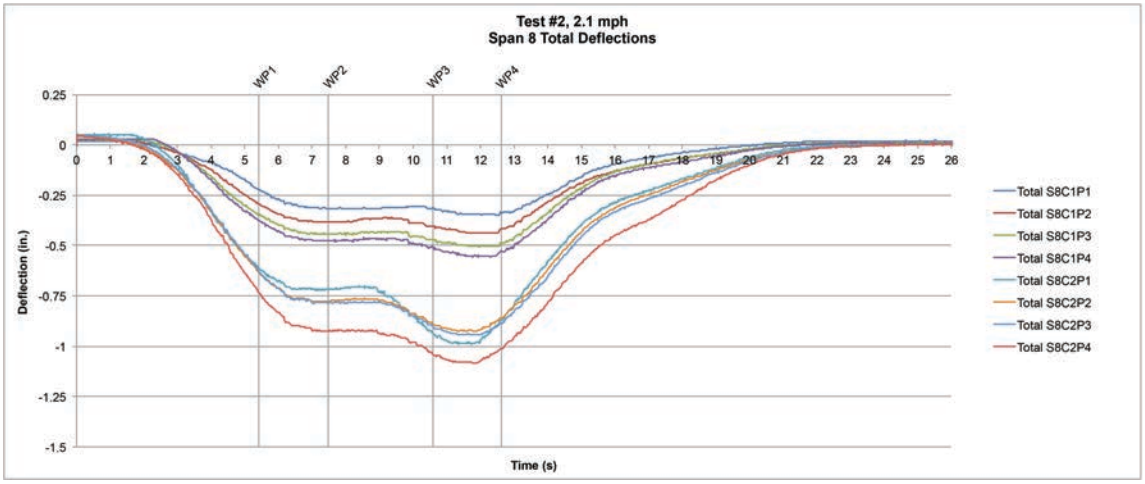

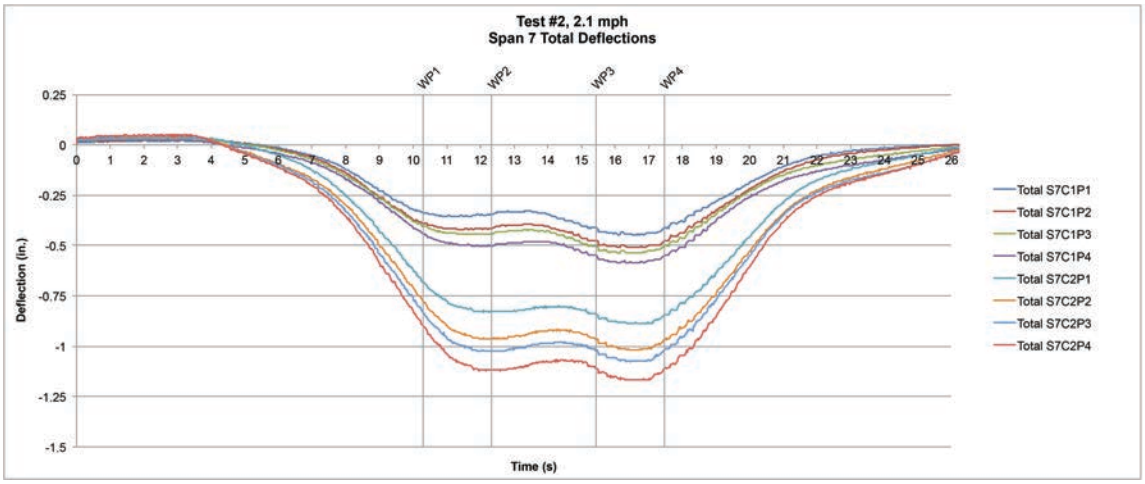

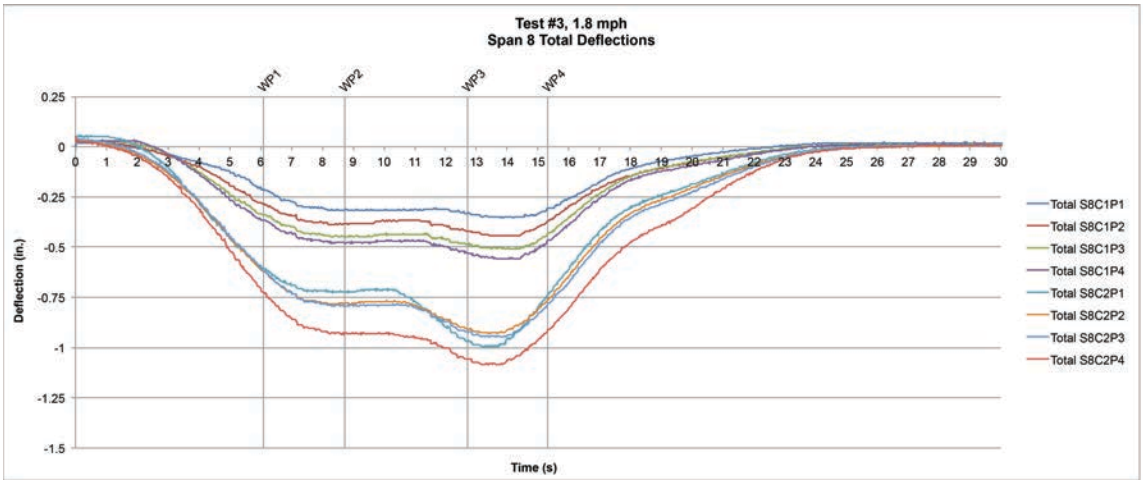
Test #3, 1.8 mph
Span 8 Total Deflections
WP1
WP2
WP3
WP4
Deflection (in.)
Time (s)
Total S8C1P1
Total S8C1P2
Total S8C1P3
Total S8C1P4
Total S8C2P1
Total S8C2P2
Total S8C2P3
Total S8C2P4

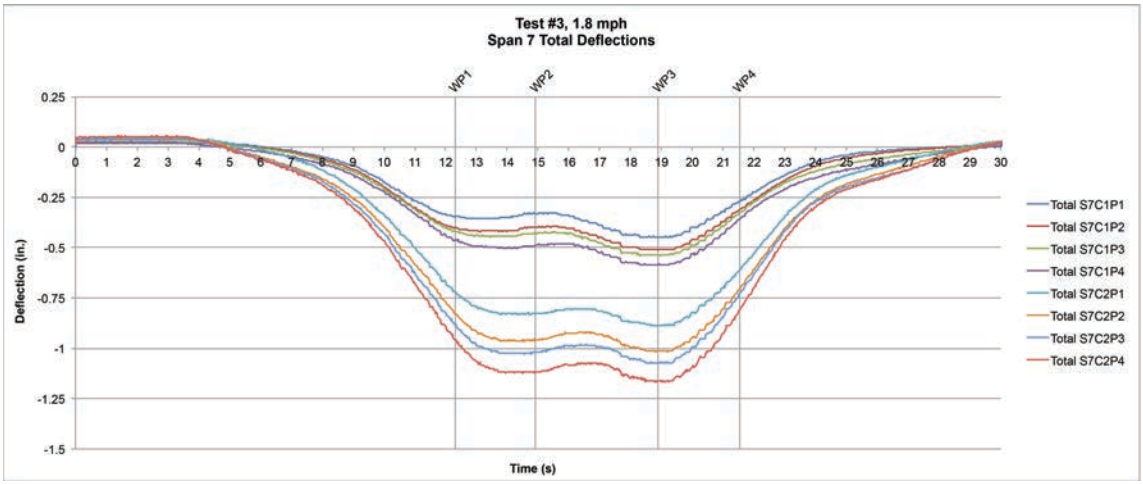
Test #3, 1.8 mph
Span 7 Total Deflections
WP1
WP2
WP3
WP4
Deflection (in.)
Time (s)
Total S7C1P1
Total S7C1P2
Total S7C1P3
Total S7C1P4
Total S7C2P1
Total S7C2P2
Total S7C2P3
Total S7C2P4

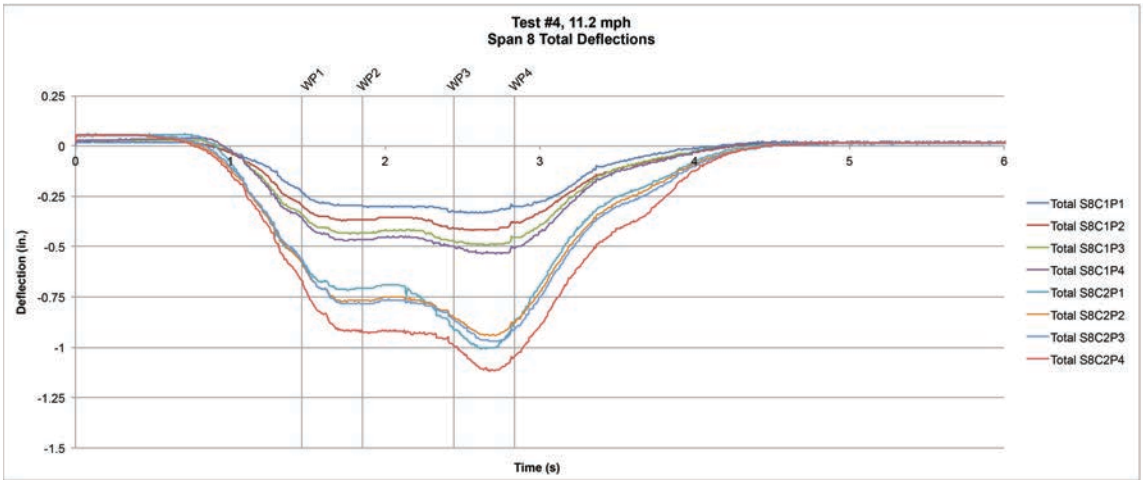
Test #4, 11.2 mph
Span 8 Total Deflections
WP1
WP2
WP3
WP4
Deflection (in.)
Time (s)
Total S8C1P1
Total S8C1P2
Total S8C1P3
Total S8C1P4
Total S8C2P1
Total S8C2P2
Total S8C2P3
Total S8C2P4

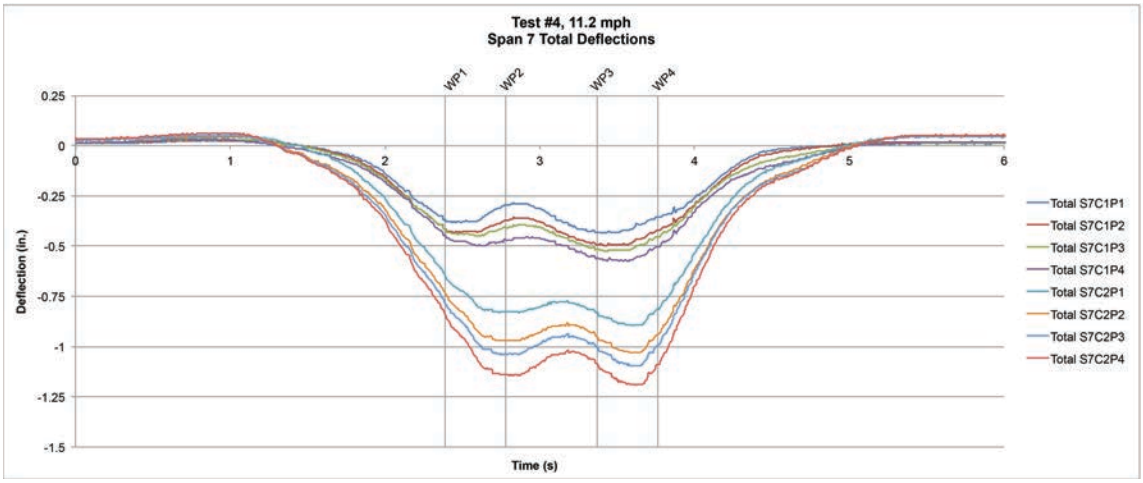
Test #4, 11.2 mph
Span 7 Total Deflections
WP1
WP2
WP3
WP4
0.25
0
-0.25
-0.5
-0.75
-1
-1.25
-1.5
Deflection (in.)
0
1
2
3
4
5
6
Time (s)
Total S7C1P1
Total S7C1P2
Total S7C1P3
Total S7C1P4
Total S7C2P1
Total S7C2P2
Total S7C2P3
Total S7C2P4

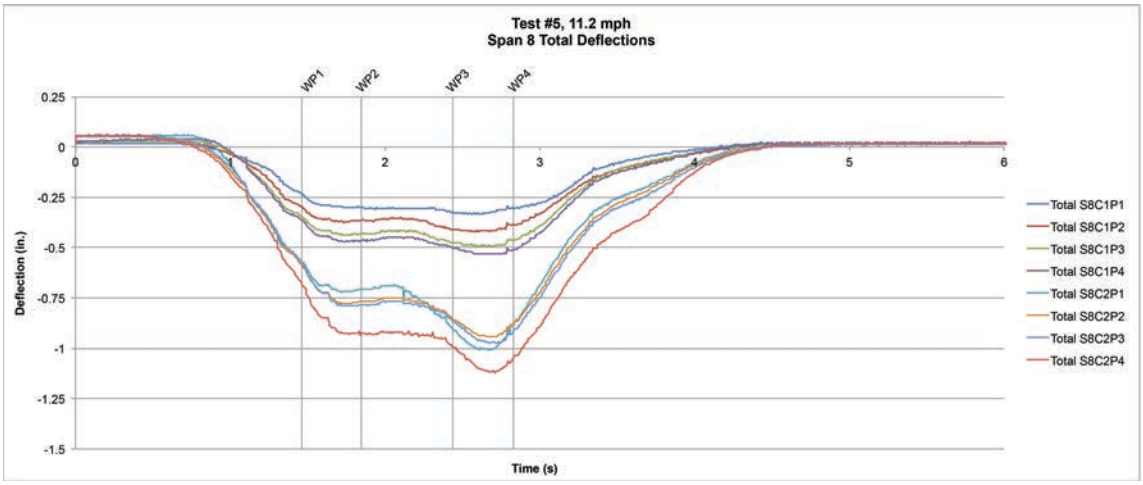
Test #5, 11.2 mph
Span 8 Total Deflections
WP1
WP2
WP3
WP4
0.25
0
-0.25
-0.5
-0.75
-1
-1.25
-1.5
Deflection (in.)
0
1
2
3
4
5
6
Time (s)
Total S8C1P1
Total S8C1P2
Total S8C1P3
Total S8C1P4
Total S8C2P1
Total S8C2P2
Total S8C2P3
Total S8C2P4

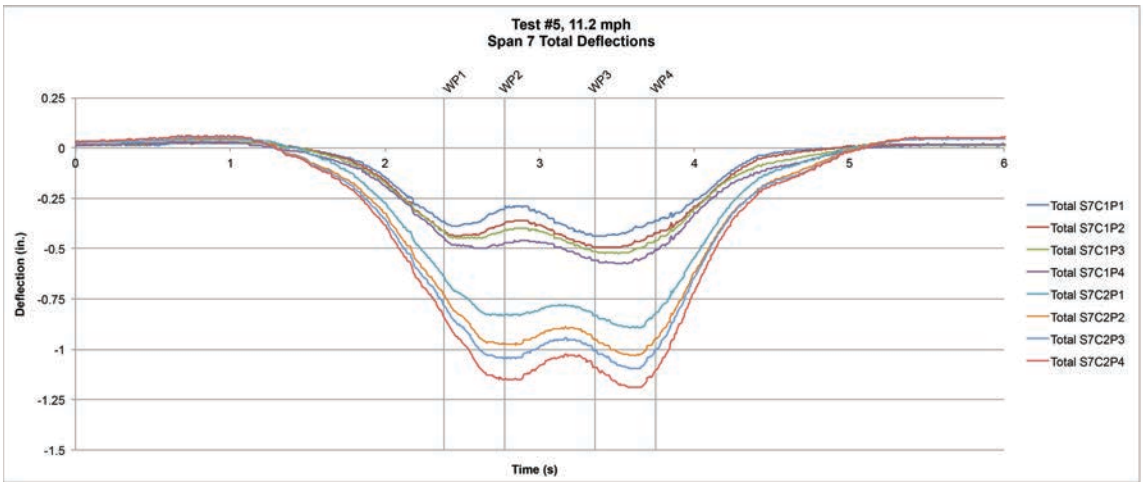
Test #5, 11.2 mph
Span 7 Total Deflections
WP1
WP2
WP3
WP4
0.25
0
-0.25
-0.5
-0.75
-1
-1.25
-1.5
Deflection (in.)
0
1
2
3
4
5
6
Time (s)
Total S7C1P1
Total S7C1P2
Total S7C1P3
Total S7C1P4
Total S7C2P1
Total S7C2P2
Total S7C2P3
Total S7C2P4

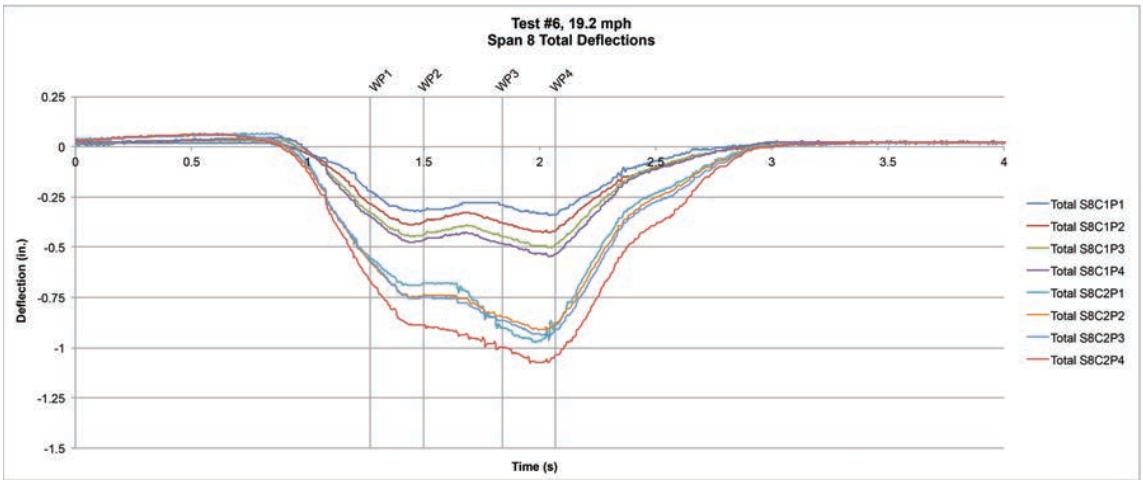
Test #6, 19.2 mph
Span 8 Total Deflections
WP1
WP2
WP3
WP4
Deflection (in.)
Time (s)
Total S8C1P1
Total S8C1P2
Total S8C1P3
Total S8C1P4
Total S8C2P1
Total S8C2P2
Total S8C2P3
Total S8C2P4

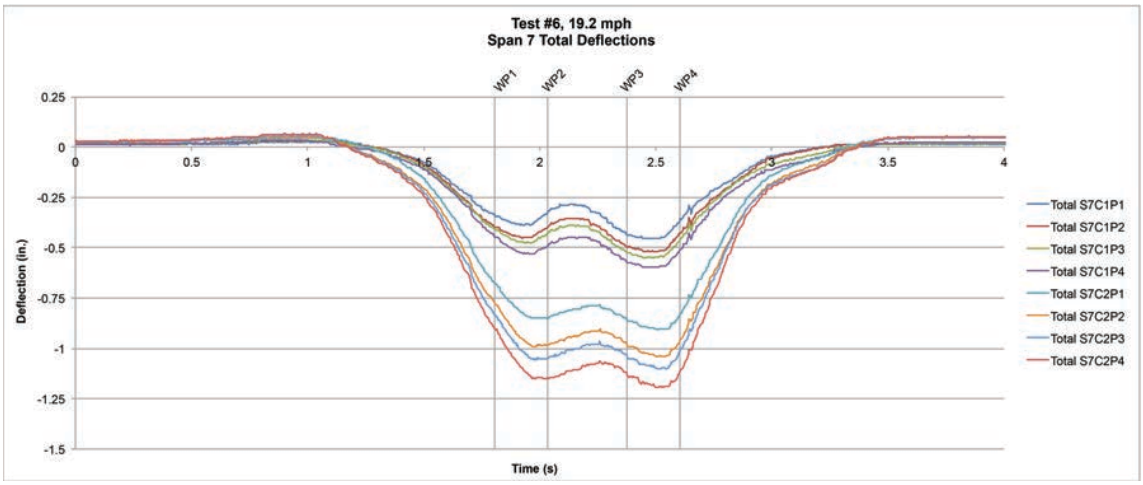
Test #6, 19.2 mph
Span 7 Total Deflections
WP1
WP2
WP3
WP4
Deflection (in.)
Time (s)
Total S7C1P1
Total S7C1P2
Total S7C1P3
Total S7C1P4
Total S7C2P1
Total S7C2P2
Total S7C2P3
Total S7C2P4

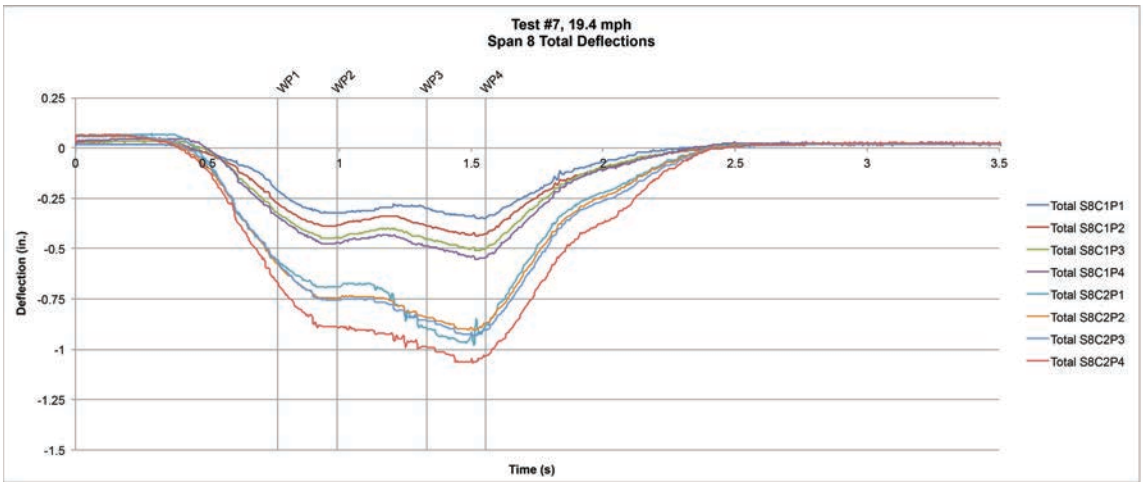
Test #7, 19.4 mph
Span 8 Total Deflections
WP1
WP2
WP3
WP4
Deflection (in.)
Time (s)
Total S8C1P1
Total S8C1P2
Total S8C1P3
Total S8C1P4
Total S8C2P1
Total S8C2P2
Total S8C2P3
Total S8C2P4

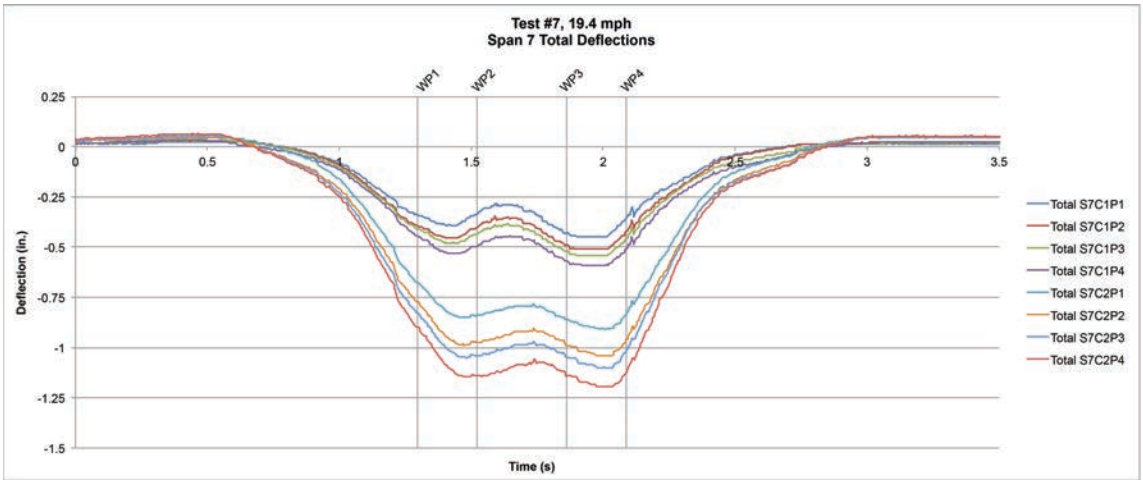
Test #7, 19.4 mph
Span 7 Total Deflections
WP1
WP2
WP3
WP4
0.25
0
-0.25
-0.5
-0.75
-1
-1.25
-1.5
0
0.5
1
1.5
2
2.5
3
3.5
Deflection (in.)
Time (s)
Total S7C1P1
Total S7C1P2
Total S7C1P3
Total S7C1P4
Total S7C2P1
Total S7C2P2
Total S7C2P3
Total S7C2P4

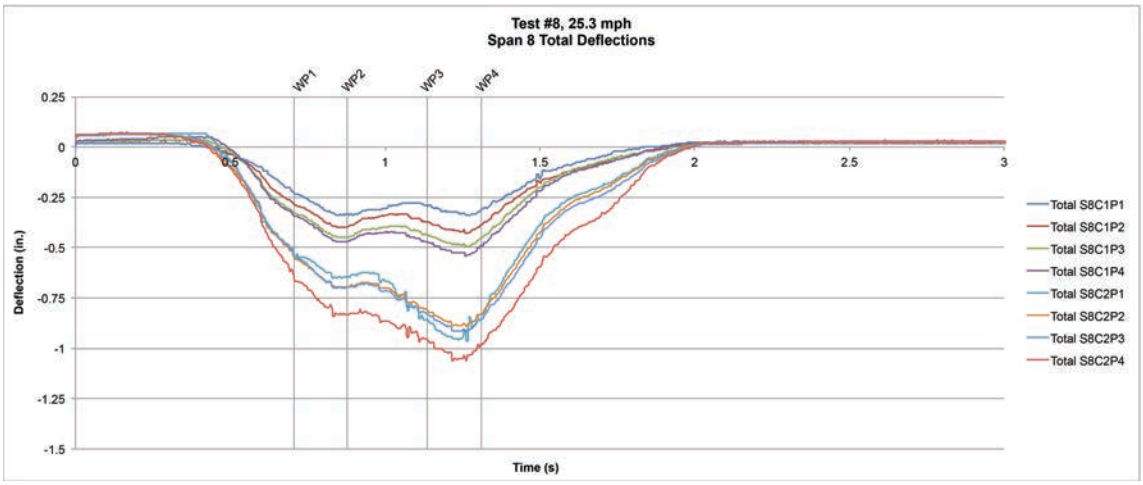
Test #8, 25.3 mph
Span 8 Total Deflections
WP1
WP2
WP3
WP4
0.25
0
-0.25
-0.5
-0.75
-1
-1.25
-1.5
0
0.5
1
1.5
2
2.5
3
Deflection (in.)
Time (s)
Total S8C1P1
Total S8C1P2
Total S8C1P3
Total S8C1P4
Total S8C2P1
Total S8C2P2
Total S8C2P3
Total S8C2P4

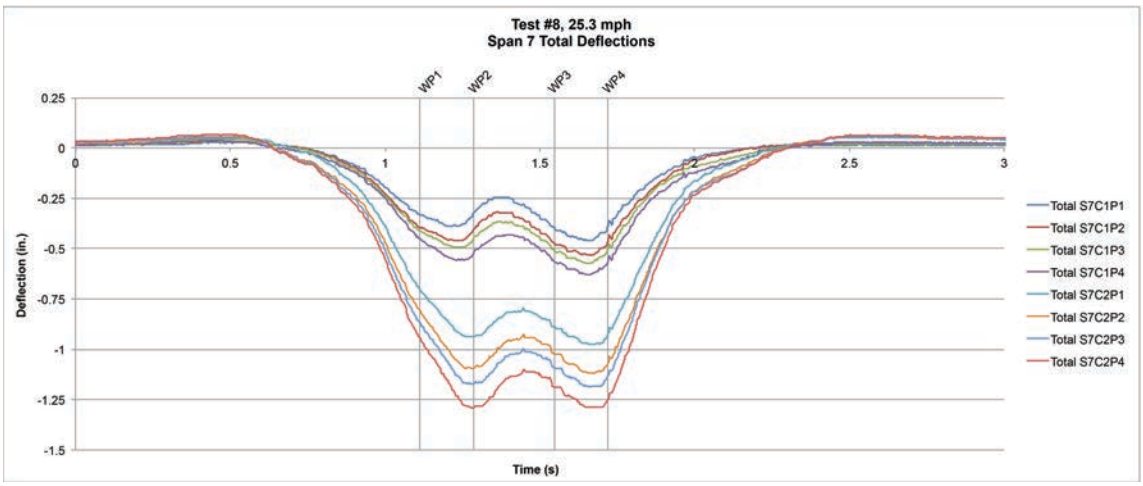
Test #8, 25.3 mph
Span 7 Total Deflections
WP1
WP2
WP3
WP4
0.25
0
-0.25
-0.5
-0.75
-1
-1.25
-1.5
0
0.5
1
1.5
2
2.5
3
Deflection (in.)
Time (s)
Total S7C1P1
Total S7C1P2
Total S7C1P3
Total S7C1P4
Total S7C2P1
Total S7C2P2
Total S7C2P3
Total S7C2P4

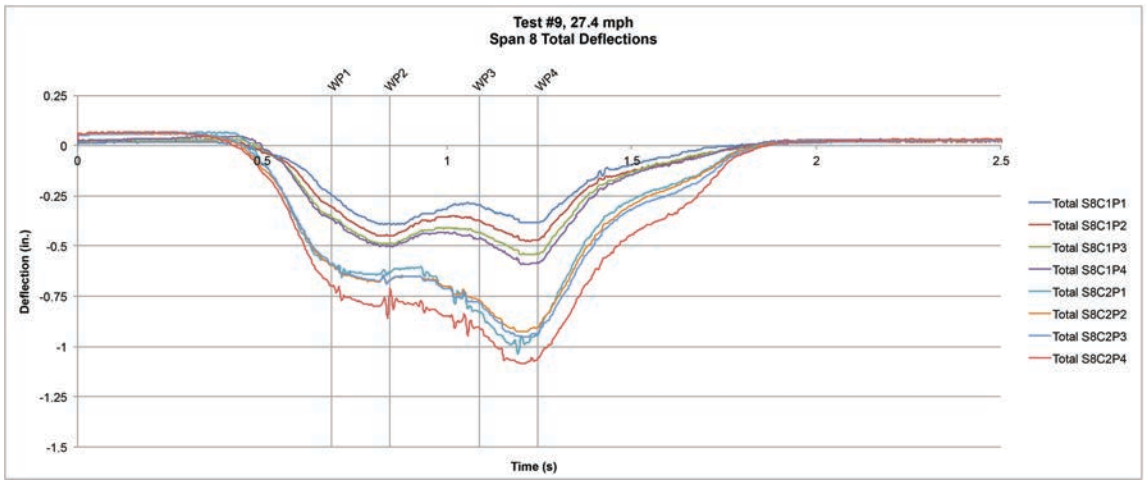
Test #9, 27.4 mph
Span 8 Total Deflections
WP1
WP2
WP3
WP4
0.25
0
-0.25
-0.5
-0.75
-1
-1.25
-1.5
0
0.5
1
1.5
2
2.5
Deflection (in.)
Time (s)
Total S8C1P1
Total S8C1P2
Total S8C1P3
Total S8C1P4
Total S8C2P1
Total S8C2P2
Total S8C2P3
Total S8C2P4

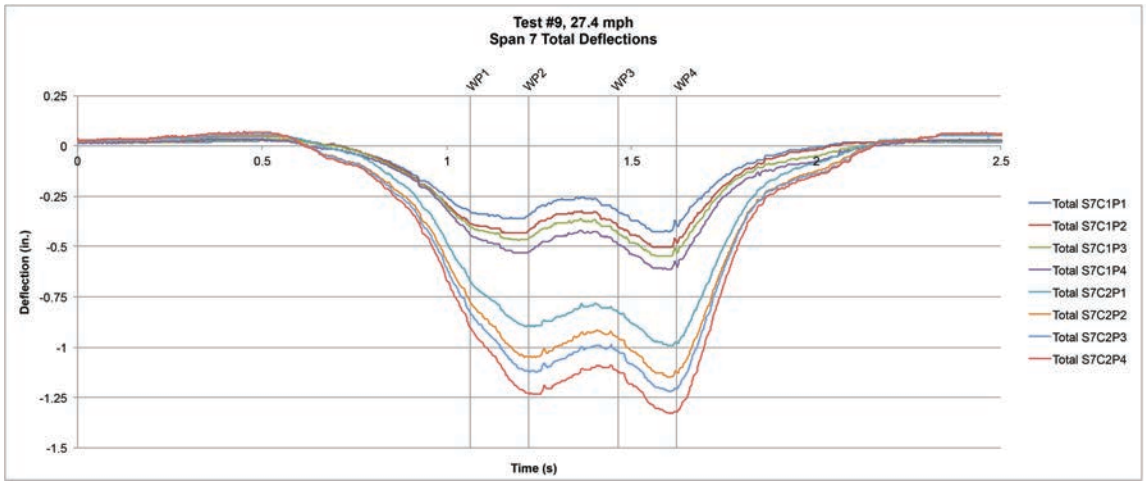
Test #9, 27.4 mph
Span 7 Total Deflections
WP1
WP2
WP3
WP4
0.25
0
-0.25
-0.5
-0.75
-1
-1.25
-1.5
0
0.5
1
1.5
2
2.5
Deflection (in.)
Time (s)
Total S7C1P1
Total S7C1P2
Total S7C1P3
Total S7C1P4
Total S7C2P1
Total S7C2P2
Total S7C2P3
Total S7C2P4

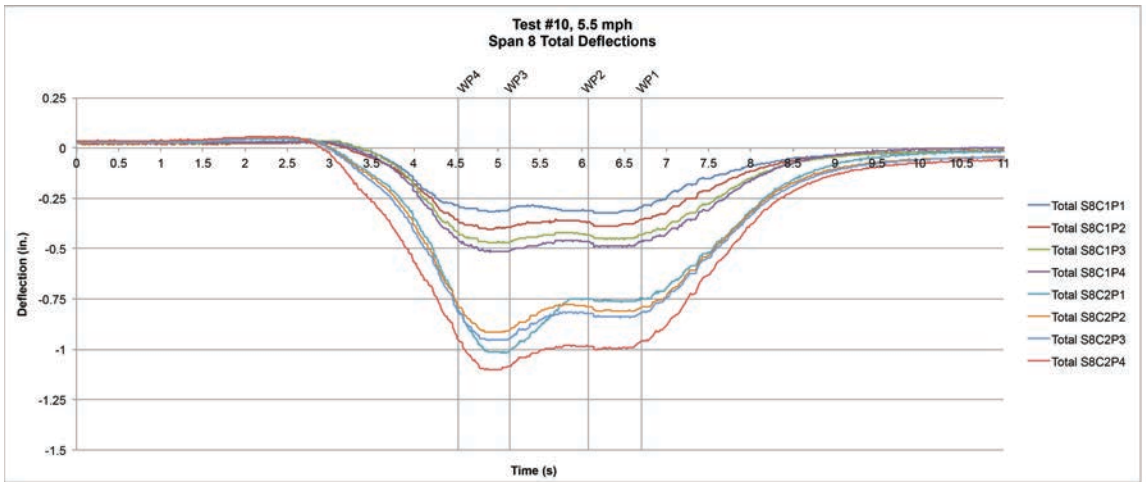
Test #10, 5.5 mph
Span 8 Total Deflections
WP4
WP3
WP2
WP1
0.25
0
-0.25
-0.5
-0.75
-1
-1.25
-1.5
0
0.5
1
1.5
2
2.5
3
3.5
4
4.5
5
5.5
6
6.5
7
7.5
8
8.5
9
9.5
10
10.5
11
Deflection (in.)
Time (s)
Total S8C1P1
Total S8C1P2
Total S8C1P3
Total S8C1P4
Total S8C2P1
Total S8C2P2
Total S8C2P3
Total S8C2P4

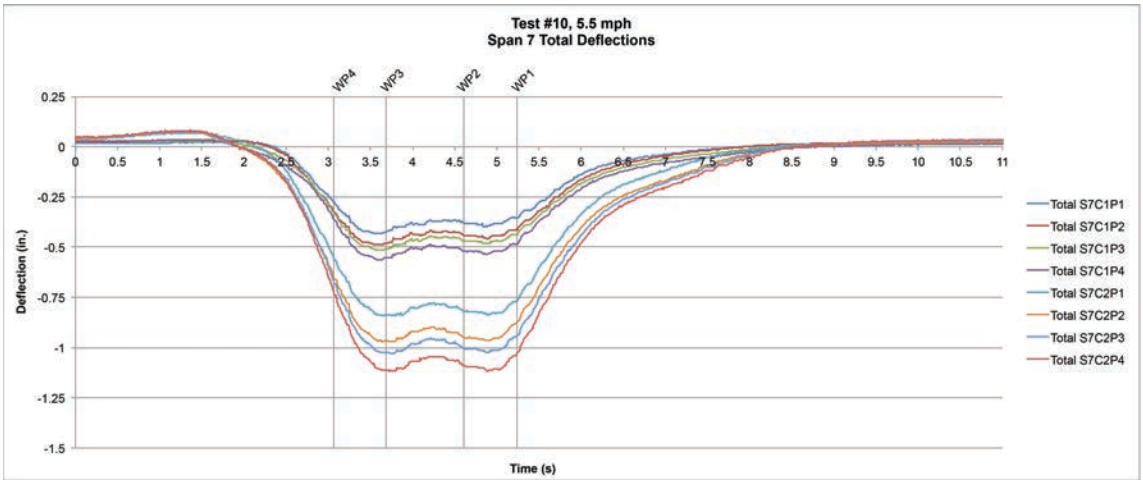
Test #10, 5.5 mph
Span 7 Total Deflections
WP4
WP3
WP2
WP1
0.25
0
-0.25
-0.5
-0.75
-1
-1.25
-1.5
Deflection (in.)
0
0.5
1
1.5
2
2.5
3
3.5
4
4.5
5
5.5
6
6.5
7
7.5
8
8.5
9
9.5
10
10.5
11
Time (s)
Total S7C1P1
Total S7C1P2
Total S7C1P3
Total S7C1P4
Total S7C2P1
Total S7C2P2
Total S7C2P3
Total S7C2P4

APPENDIX E
LARGE-SCALE OPEN DECK EXPERIMENT NET STRINGER DEFLECTION PLOTS

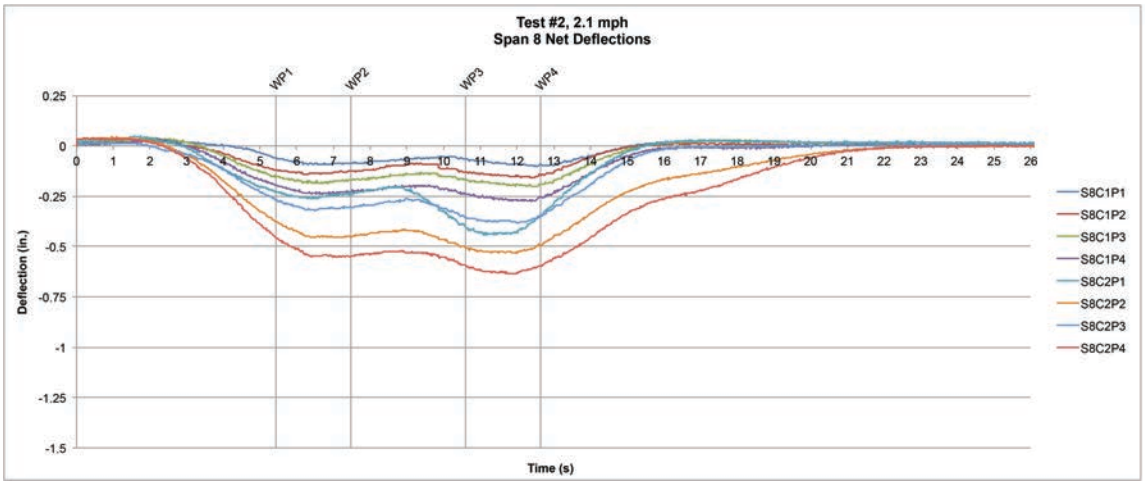

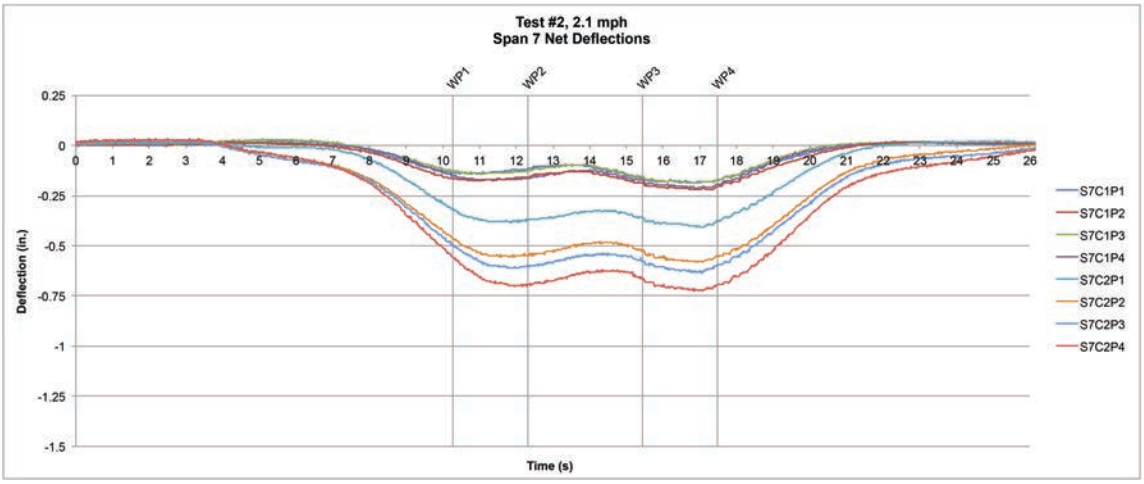

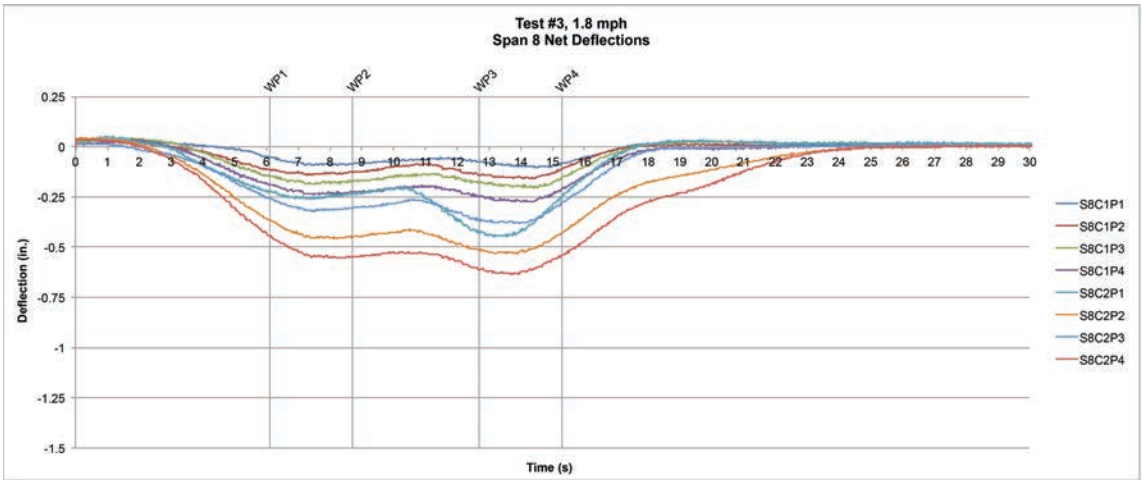
Test #3, 1.8 mph
Span 8 Net Deflections
WP1
WP2
WP3
WP4
Deflection (in.)
Time (s)
S8C1P1
S8C1P2
S8C1P3
S8C1P4
S8C2P1
S8C2P2
S8C2P3
S8C2P4

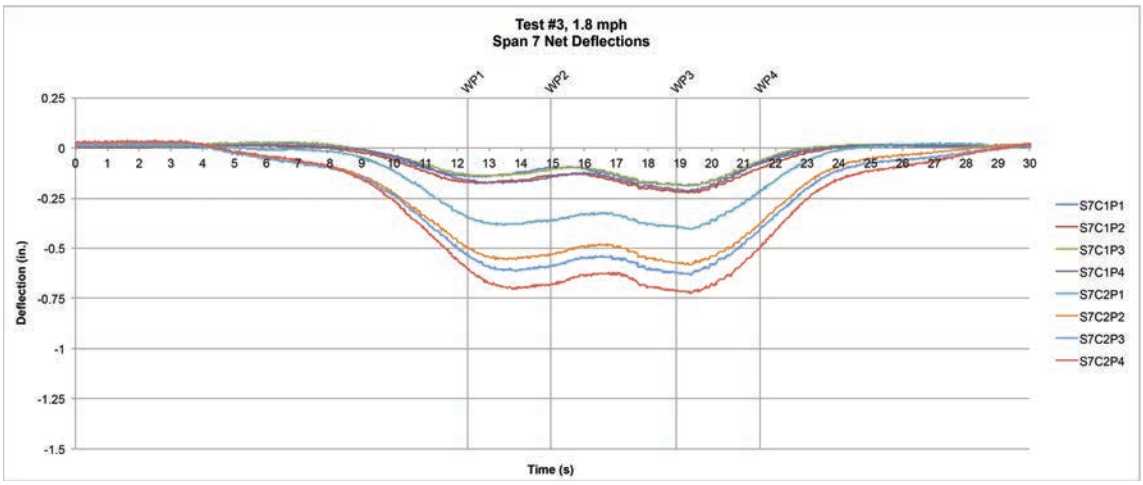
Test #3, 1.8 mph
Span 7 Net Deflections
WP1
WP2
WP3
WP4
Deflection (in.)
Time (s)
S7C1P1
S7C1P2
S7C1P3
S7C1P4
S7C2P1
S7C2P2
S7C2P3
S7C2P4

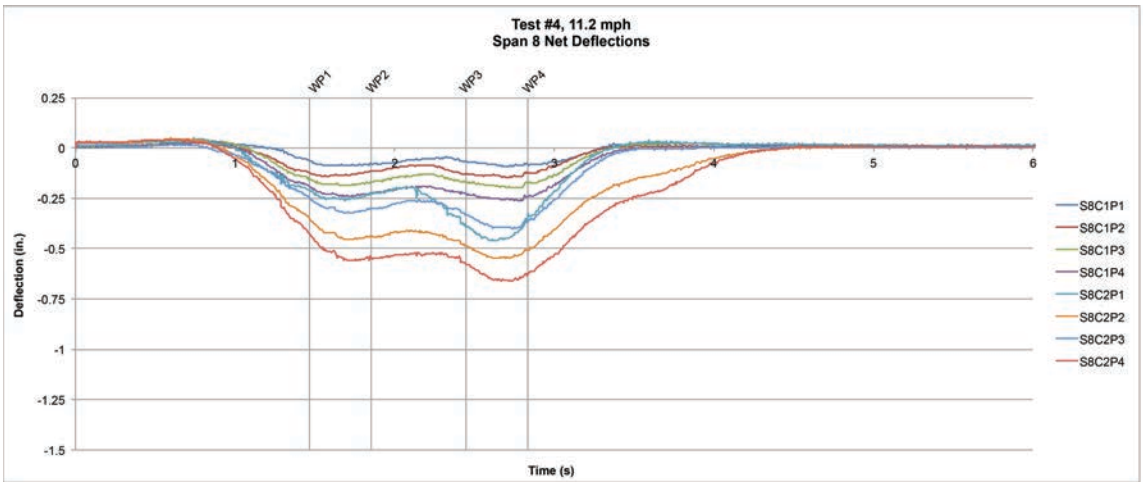
Test #4, 11.2 mph
Span 8 Net Deflections
WP1
WP2
WP3
WP4
Deflection (in.)
Time (s)
S8C1P1
S8C1P2
S8C1P3
S8C1P4
S8C2P1
S8C2P2
S8C2P3
S8C2P4

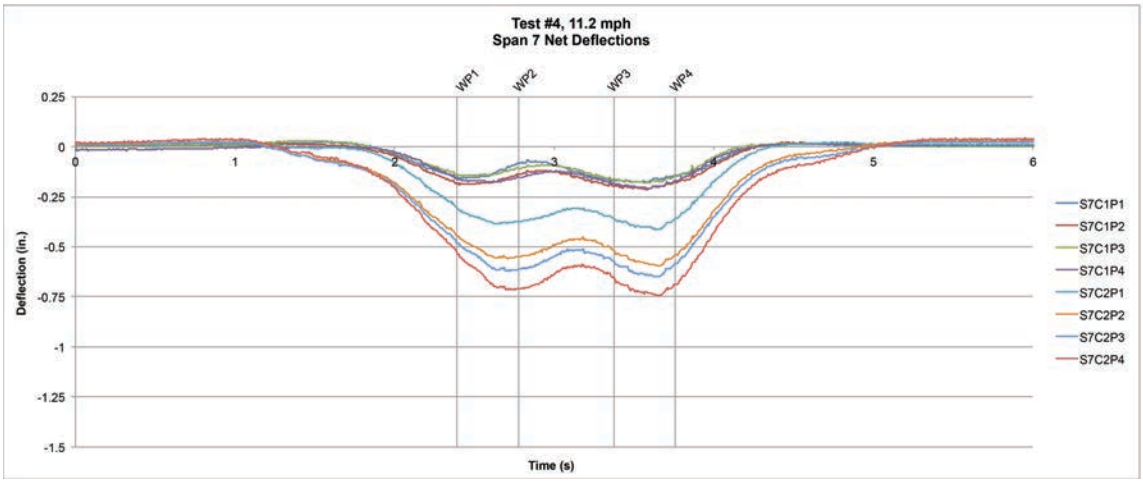
Test #4, 11.2 mph
Span 7 Net Deflections
WP1
WP2
WP3
WP4
0.25
0
-0.25
-0.5
-0.75
-1
-1.25
-1.5
0
1
2
3
4
5
6
Deflection (in.)
Time (s)
S7C1P1
S7C1P2
S7C1P3
S7C1P4
S7C2P1
S7C2P2
S7C2P3
S7C2P4

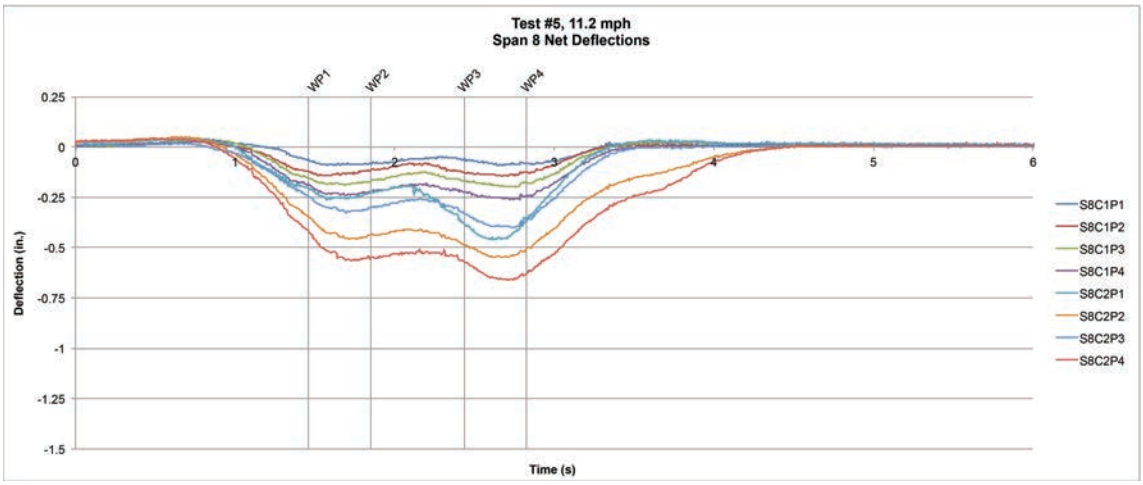
Test #5, 11.2 mph
Span 8 Net Deflections
WP1
WP2
WP3
WP4
0.25
0
-0.25
-0.5
-0.75
-1
-1.25
-1.5
0
1
2
3
4
5
6
Deflection (in.)
Time (s)
S8C1P1
S8C1P2
S8C1P3
S8C1P4
S8C2P1
S8C2P2
S8C2P3
S8C2P4

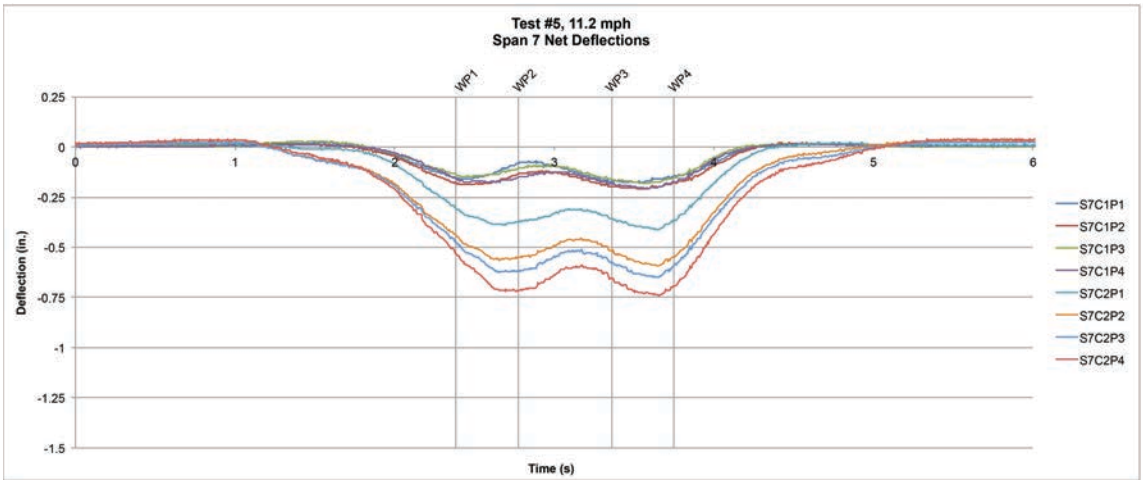
Test #5, 11.2 mph
Span 7 Net Deflections
WP1
WP2
WP3
WP4
0.25
0
-0.25
-0.5
-0.75
-1
-1.25
-1.5
0
1
2
3
4
5
6
Deflection (in.)
Time (s)
S7C1P1
S7C1P2
S7C1P3
S7C1P4
S7C2P1
S7C2P2
S7C2P3
S7C2P4

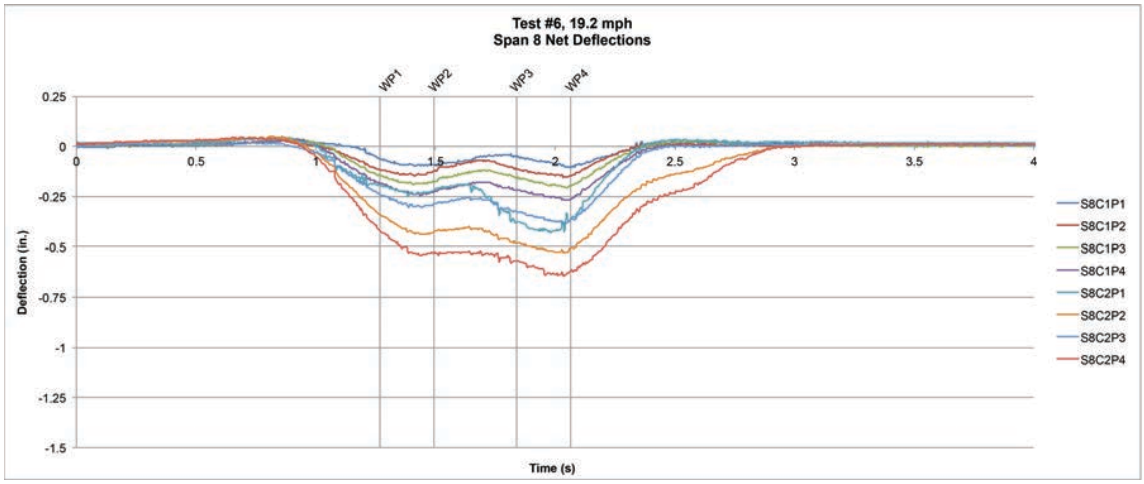
Test #6, 19.2 mph
Span 8 Net Deflections
WP1
WP2
WP3
WP4
0.25
0
-0.25
-0.5
-0.75
-1
-1.25
-1.5
0
0.5
1
1.5
2
2.5
3
3.5
4
Deflection (in.)
Time (s)
S8C1P1
S8C1P2
S8C1P3
S8C1P4
S8C2P1
S8C2P2
S8C2P3
S8C2P4

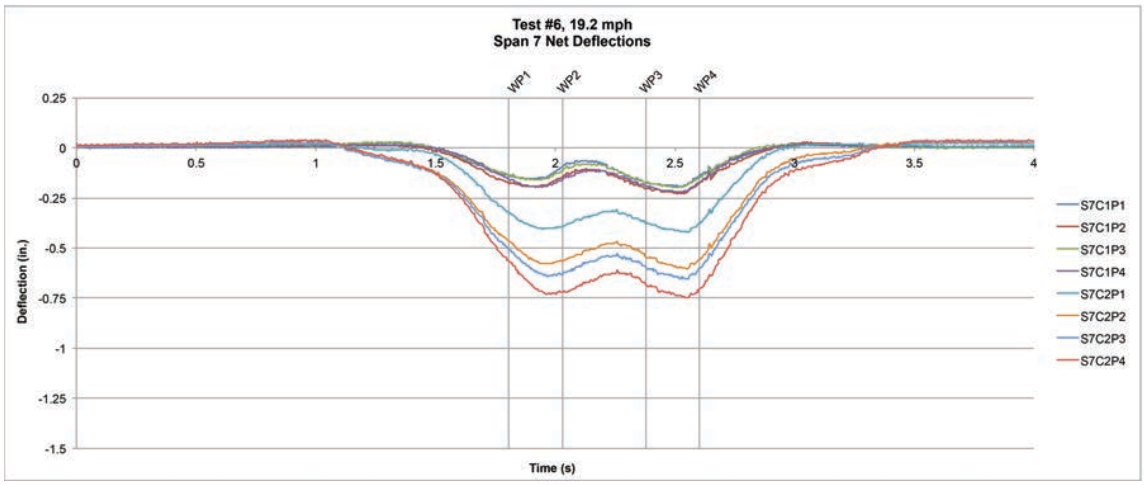
Test #6, 19.2 mph
Span 7 Net Deflections
WP1
WP2
WP3
WP4
0.25
0
-0.25
-0.5
-0.75
-1
-1.25
-1.5
0
0.5
1
1.5
2
2.5
3
3.5
4
Deflection (in.)
Time (s)
S7C1P1
S7C1P2
S7C1P3
S7C1P4
S7C2P1
S7C2P2
S7C2P3
S7C2P4

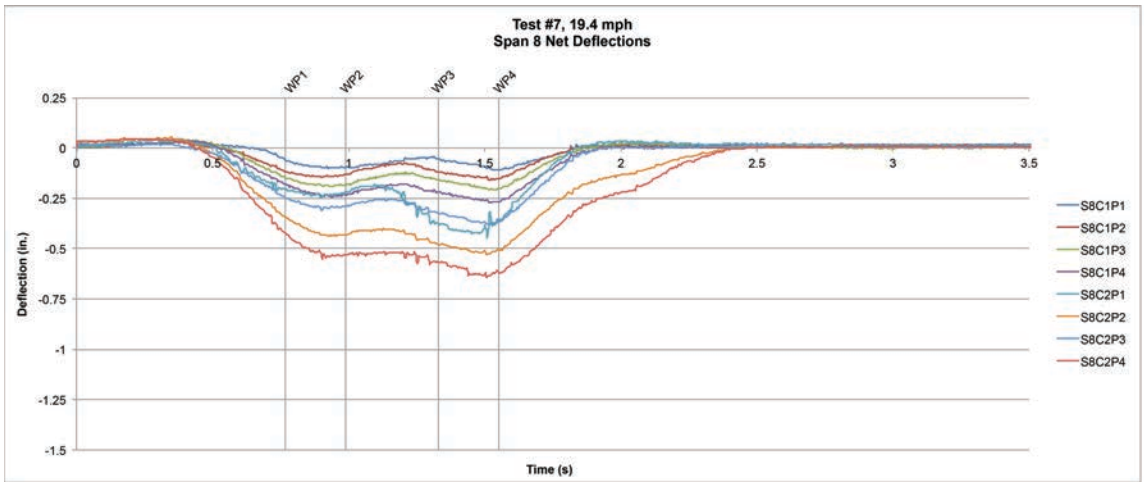
Test #7, 19.4 mph
Span 8 Net Deflections
WP1
WP2
WP3
WP4
0.25
0
-0.25
-0.5
-0.75
-1
-1.25
-1.5
0
0.5
1
1.5
2
2.5
3
3.5
Deflection (in.)
Time (s)
S8C1P1
S8C1P2
S8C1P3
S8C1P4
S8C2P1
S8C2P2
S8C2P3
S8C2P4

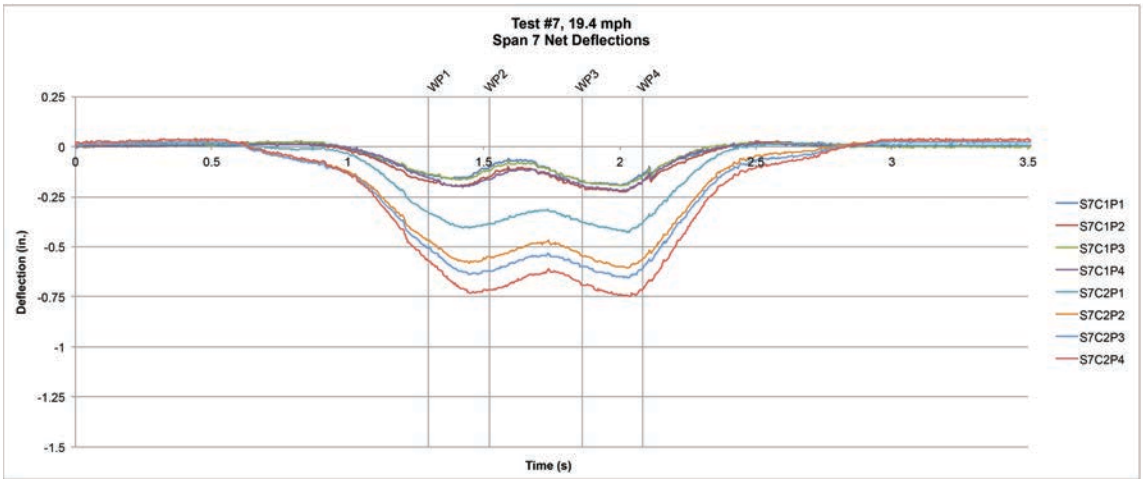
Test #7, 19.4 mph
Span 7 Net Deflections
WP1
WP2
WP3
WP4
0.25
0
-0.25
-0.5
-0.75
-1
-1.25
-1.5
0
0.5
1
1.5
2
2.5
3
3.5
Deflection (in.)
Time (s)
S7C1P1
S7C1P2
S7C1P3
S7C1P4
S7C2P1
S7C2P2
S7C2P3
S7C2P4

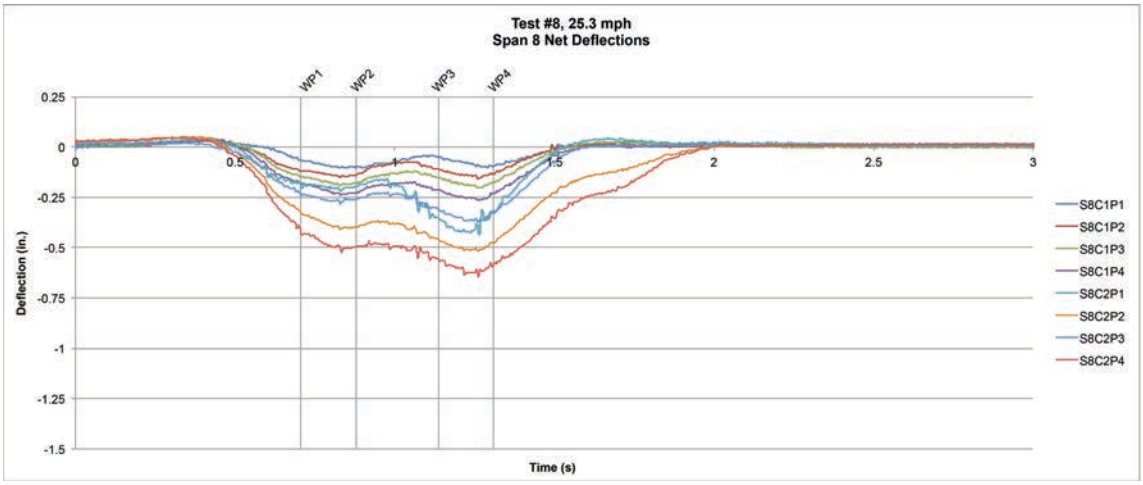
Test #8, 25.3 mph
Span 8 Net Deflections
WP1
WP2
WP3
WP4
0.25
0
-0.25
-0.5
-0.75
-1
-1.25
-1.5
0
0.5
1
1.5
2
2.5
3
Deflection (in.)
Time (s)
S8C1P1
S8C1P2
S8C1P3
S8C1P4
S8C2P1
S8C2P2
S8C2P3
S8C2P4

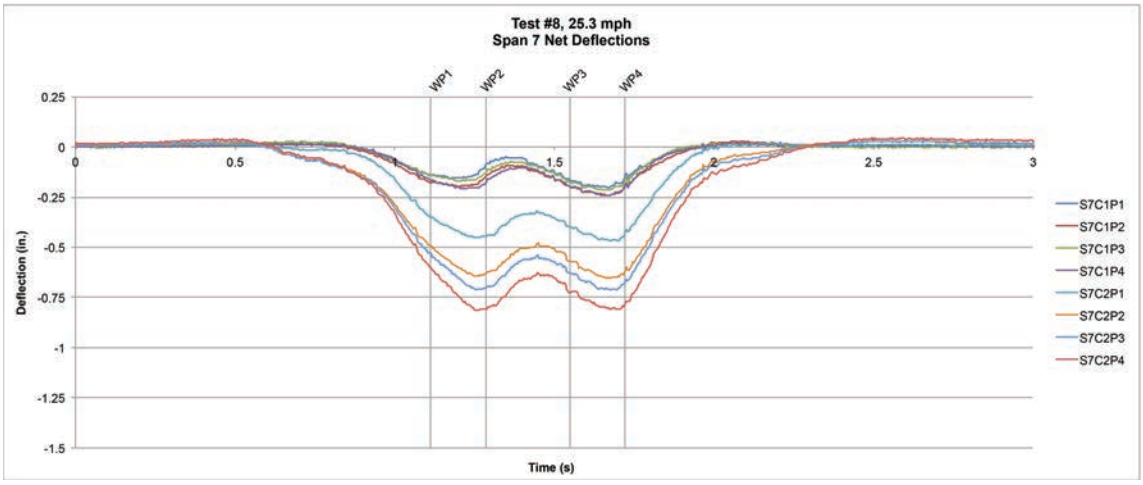
Test #8, 25.3 mph
Span 7 Net Deflections
WP1
WP2
WP3
WP4
0.25
0
-0.25
-0.5
-0.75
-1
-1.25
-1.5
0
0.5
1
1.5
2
2.5
3
Deflection (in.)
Time (s)
S7C1P1
S7C1P2
S7C1P3
S7C1P4
S7C2P1
S7C2P2
S7C2P3
S7C2P4

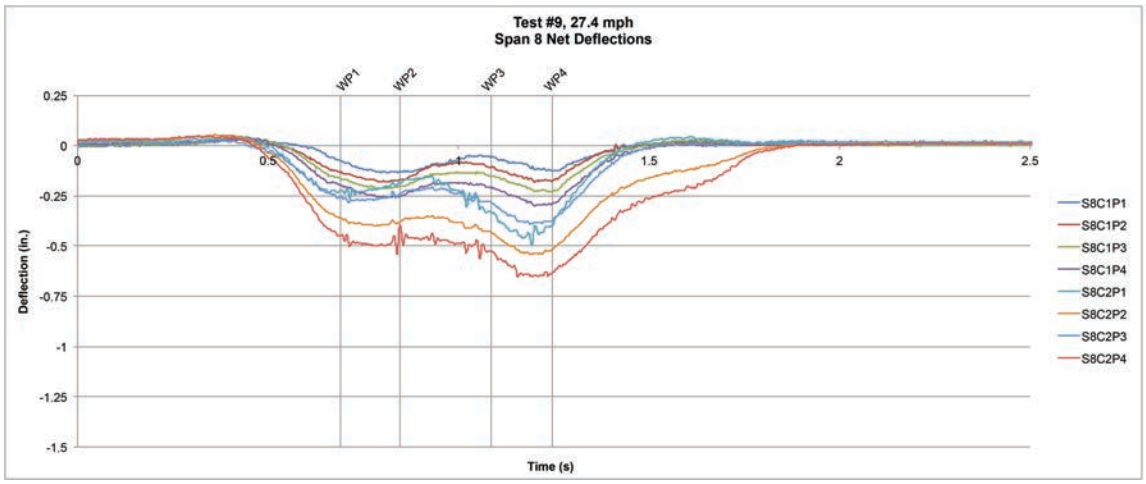
Test #9, 27.4 mph
Span 8 Net Deflections
WP1
WP2
WP3
WP4
0.25
0
-0.25
-0.5
-0.75
-1
-1.25
-1.5
0
0.5
1
1.5
2
2.5
Deflection (in.)
Time (s)
S8C1P1
S8C1P2
S8C1P3
S8C1P4
S8C2P1
S8C2P2
S8C2P3
S8C2P4

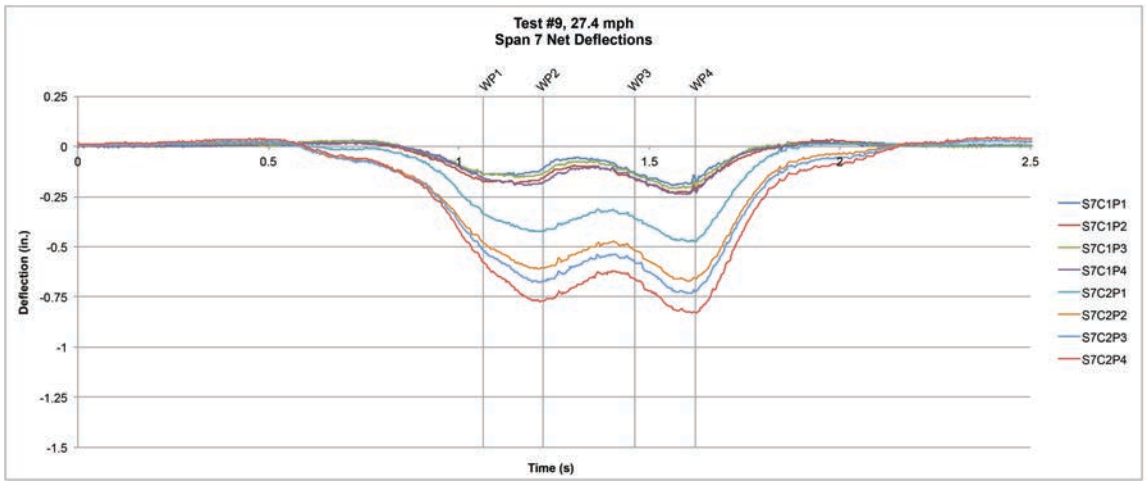
Test #9, 27.4 mph
Span 7 Net Deflections
WP1
WP2
WP3
WP4
0.25
0
-0.25
-0.5
-0.75
-1
-1.25
-1.5
0
0.5
1
1.5
2
2.5
Deflection (in.)
Time (s)
S7C1P1
S7C1P2
S7C1P3
S7C1P4
S7C2P1
S7C2P2
S7C2P3
S7C2P4

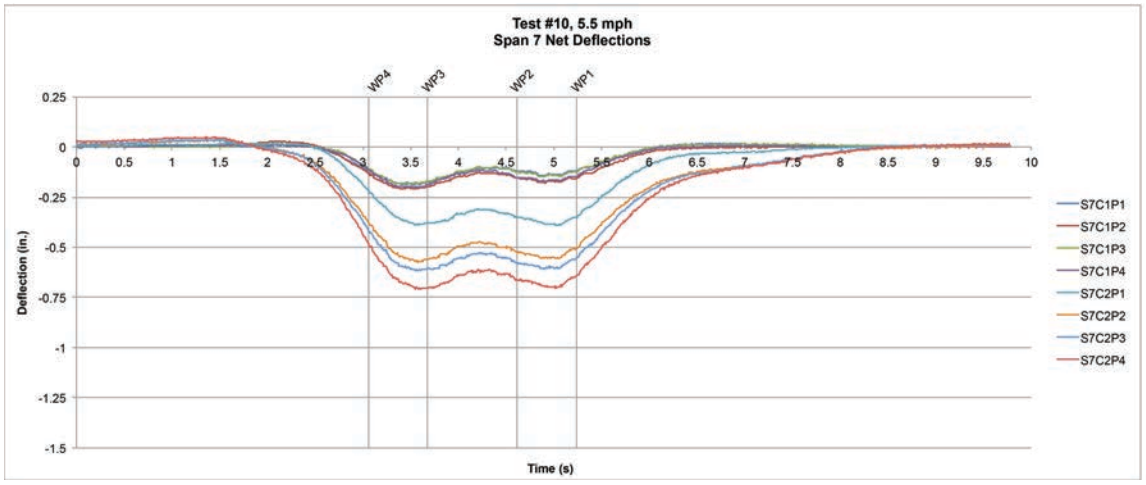
Test #10, 5.5 mph
Span 7 Net Deflections
WP4
WP3
WP2
WP1
0.25
0
-0.25
-0.5
-0.75
-1
-1.25
-1.5
0
0.5
1
1.5
2
2.5
3
3.5
4
4.5
5
5.5
6
6.5
7
7.5
8
8.5
9
9.5
10
Deflection (in.)
Time (s)
S7C1P1
S7C1P2
S7C1P3
S7C1P4
S7C2P1
S7C2P2
S7C2P3
S7C2P4

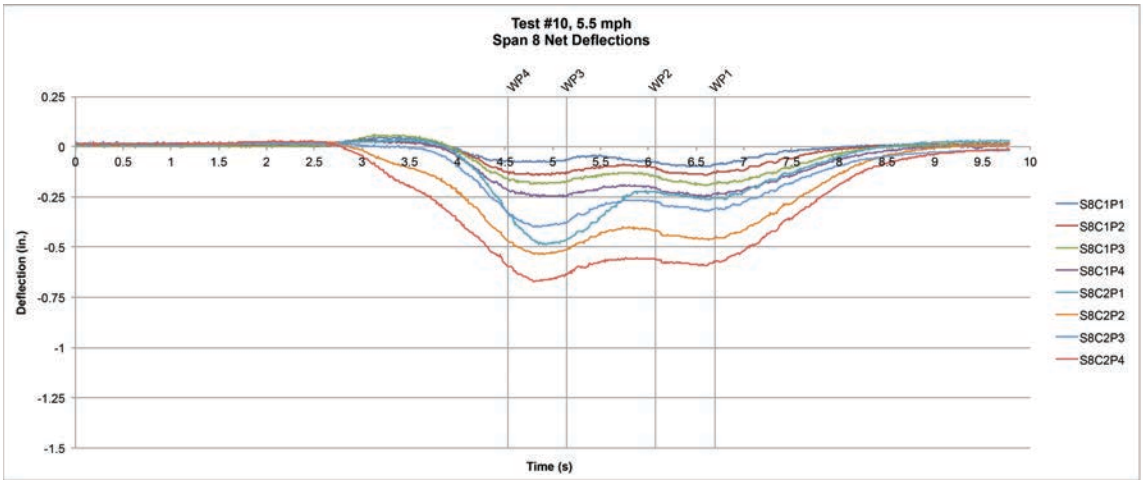
Test #10, 5.5 mph
Span 8 Net Deflections
WP4
WP3
WP2
WP1
0.25
0
-0.25
-0.5
-0.75
-1
-1.25
-1.5
Deflection (in.)
0
0.5
1
1.5
2
2.5
3
3.5
4
4.5
5
5.5
6
6.5
7
7.5
8
8.5
9
9.5
10
Time (s)
S8C1P1
S8C1P2
S8C1P3
S8C1P4
S8C2P1
S8C2P2
S8C2P3
S8C2P4

APPENDIX F

LARGE-SCALE BALLAST DECK EXPERIMENT FREIGHT TRAIN AND PASSENGER TRAIN PLOTS

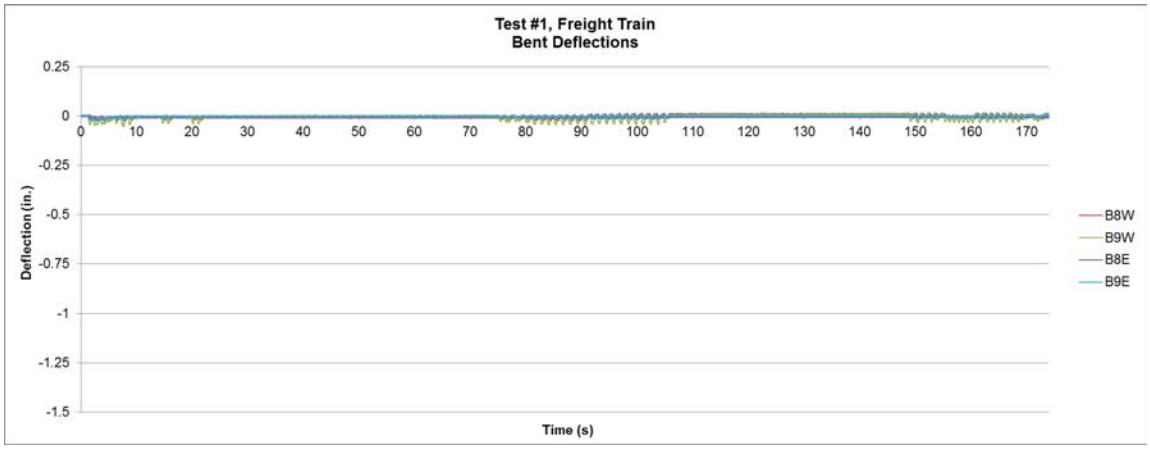

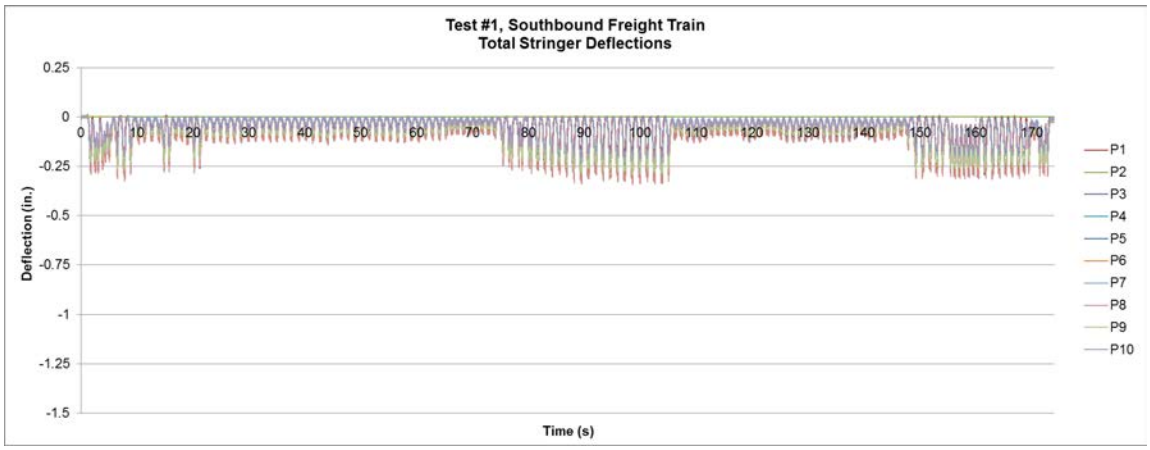

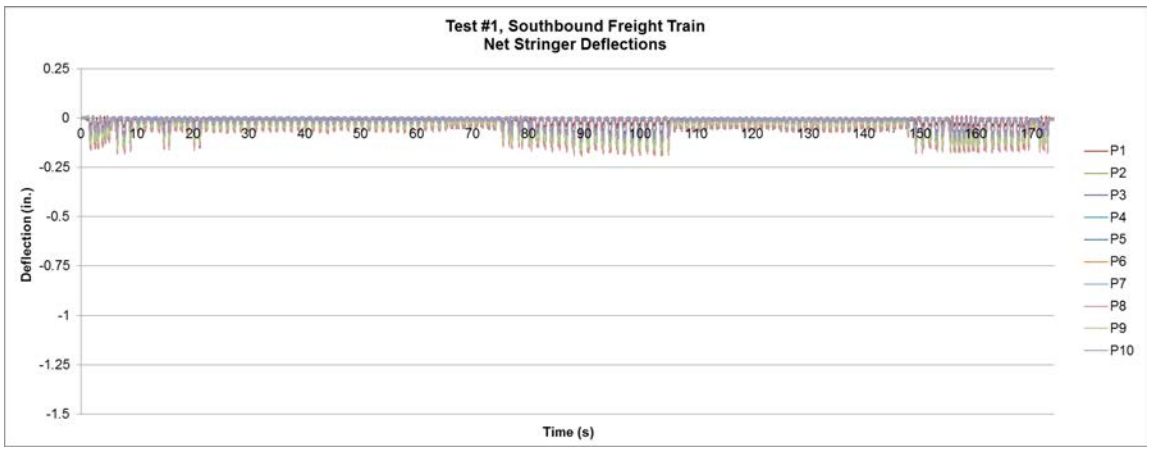

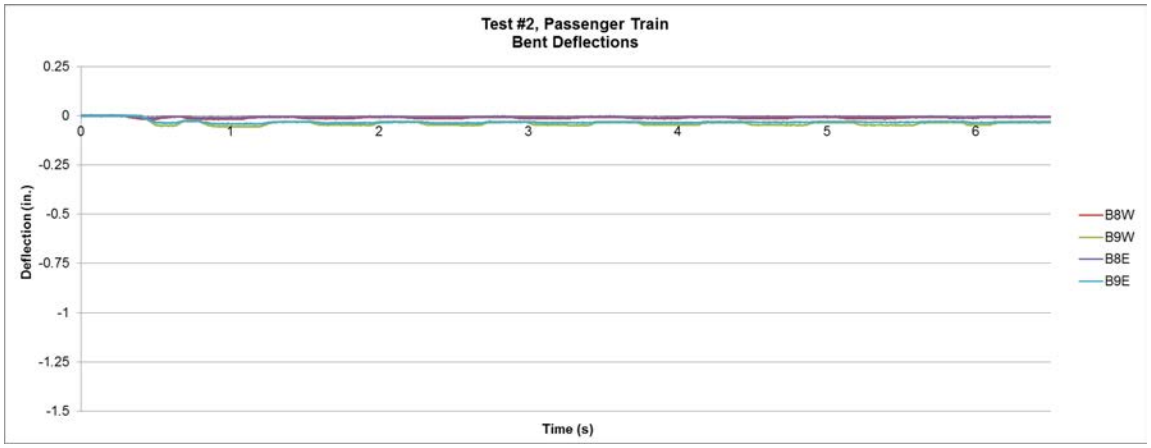
Test #2, Passenger Train
Bent Deflections
0.25
0
-0.25
-0.5
-0.75
-1
-1.25
-1.5
0
1
2
3
4
5
6
Deflection (in.)
Time (s)
B8W
B9W
B8E
B9E

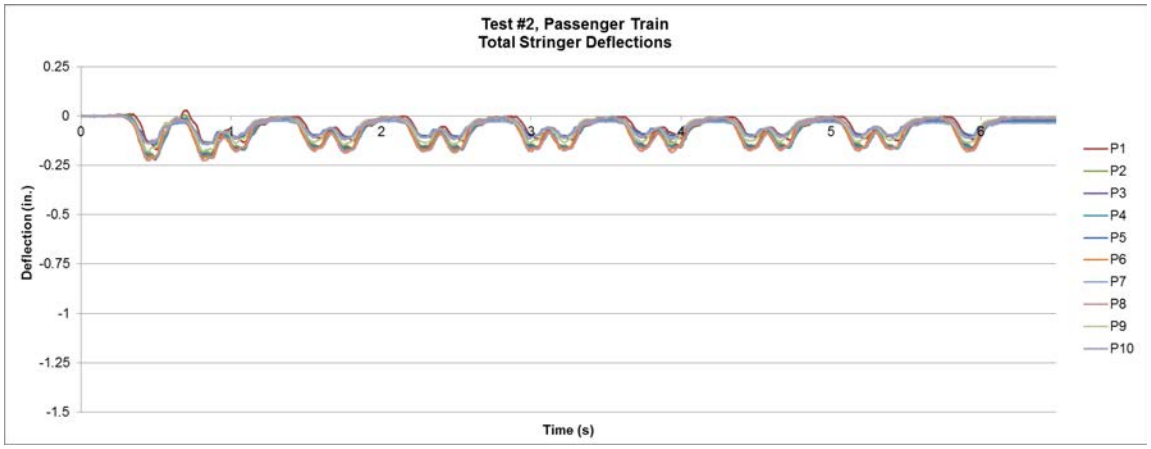
Test #2, Passenger Train
Total Stringer Deflections
0.25
0
-0.25
-0.5
-0.75
-1
-1.25
-1.5
0
1
2
3
4
5
6
Deflection (in.)
Time (s)
P1
P2
P3
P4
P5
P6
P7
P8
P9
P10

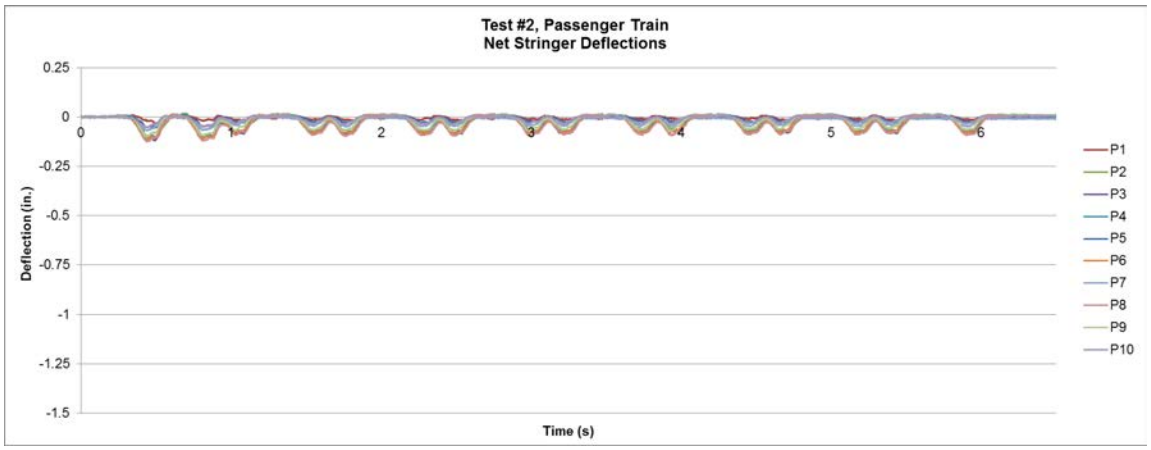
Test #2, Passenger Train
Net Stringer Deflections
0.25
0
-0.25
-0.5
-0.75
-1
-1.25
-1.5
0
1
2
3
4
5
6
Deflection (in.)
Time (s)
P1
P2
P3
P4
P5
P6
P7
P8
P9
P10

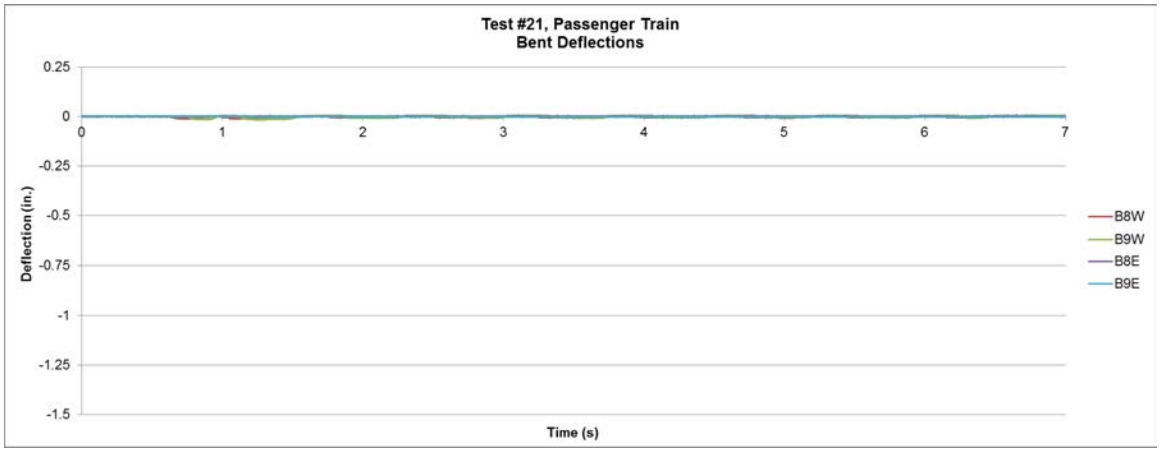
Test #21, Passenger Train
Bent Deflections
0.25
0
-0.25
-0.5
-0.75
-1
-1.25
-1.5
0
1
2
3
4
5
6
7
Deflection (in.)
Time (s)
B8W
B9W
B8E
B9E

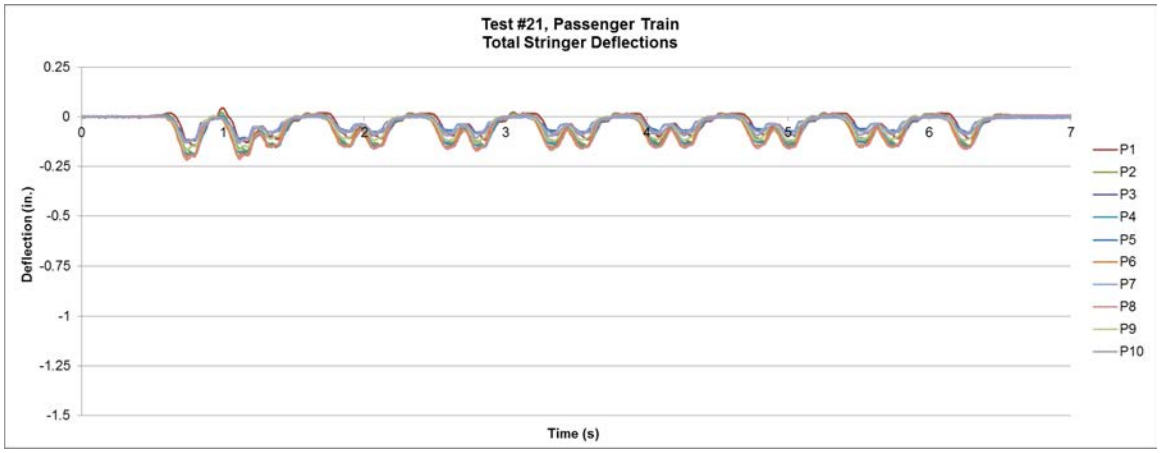
Test #21, Passenger Train
Total Stringer Deflections
0.25
0
-0.25
-0.5
-0.75
-1
-1.25
-1.5
0
1
2
3
4
5
6
7
Deflection (in.)
Time (s)
P1
P2
P3
P4
P5
P6
P7
P8
P9
P10

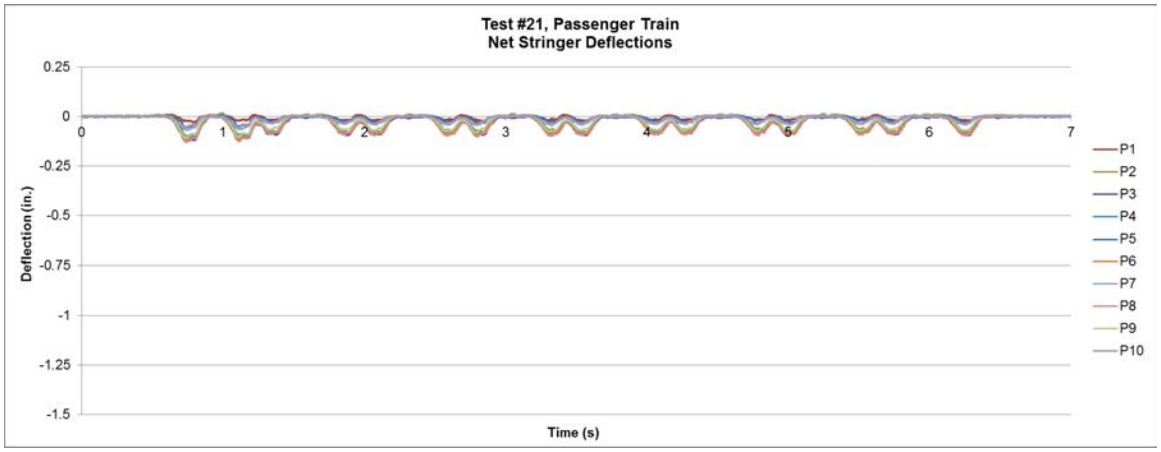
Test #21, Passenger Train
Net Stringer Deflections
0.25
0
-0.25
-0.5
-0.75
-1
-1.25
-1.5
0
1
2
3
4
5
6
7
Deflection (in.)
Time (s)
P1
P2
P3
P4
P5
P6
P7
P8
P9
P10

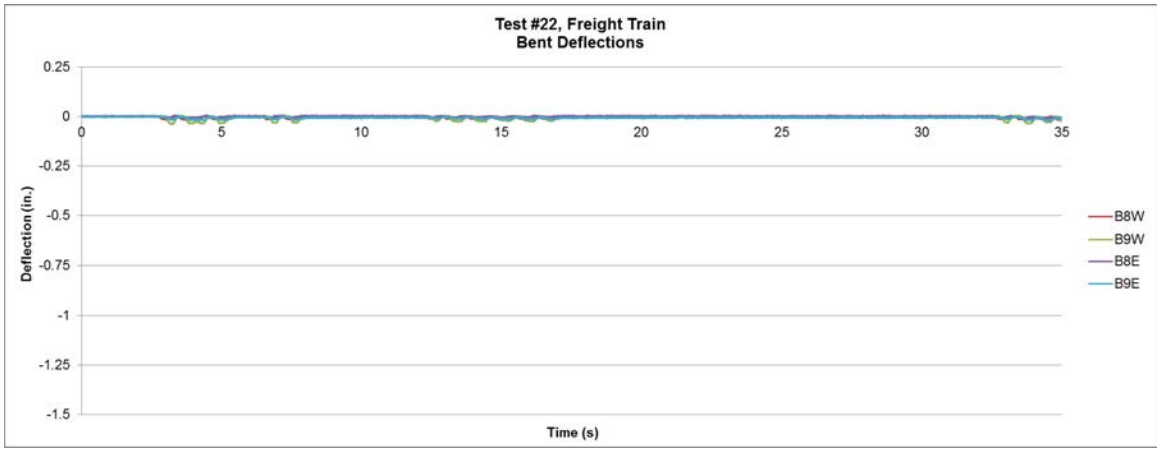
Test #22, Freight Train
Bent Deflections
Deflection (in.)
Time (s)
B8W
B9W
B8E
B9E

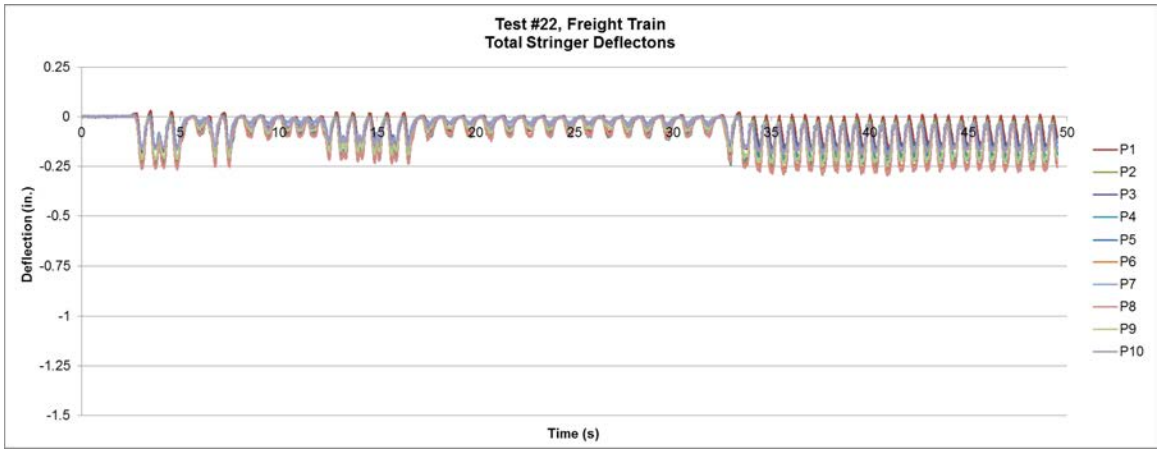
Test #22, Freight Train
Total Stringer Deflectons
Deflection (in.)
Time (s)
P1
P2
P3
P4
P5
P6
P7
P8
P9
P10

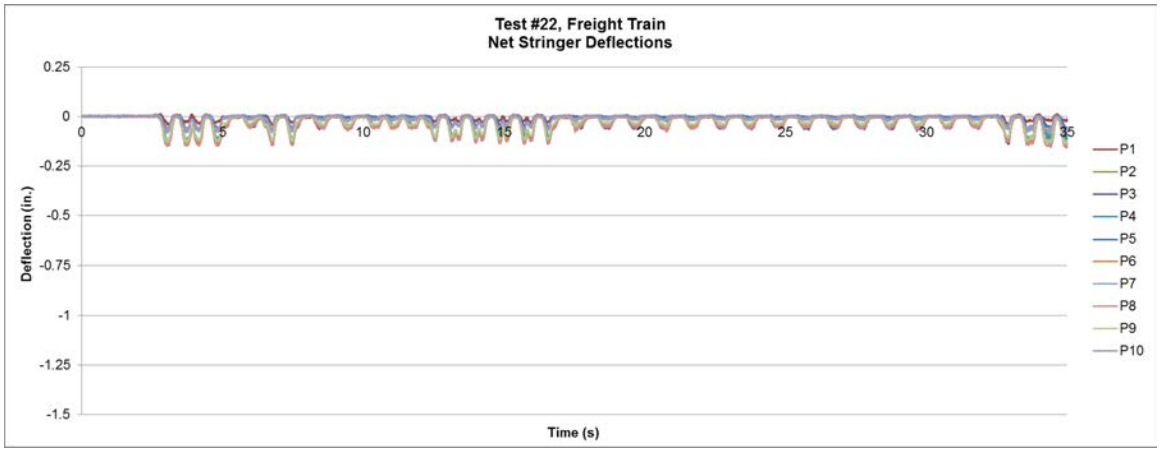
Test #22, Freight Train
Net Stringer Deflections
Deflection (in.)
Time (s)
P1
P2
P3
P4
P5
P6
P7
P8
P9
P10

APPENDIX G
LARGE-SCALE BALLAST DECK EXPERIMENT BENT-CAP DEFLECTION PLOTS

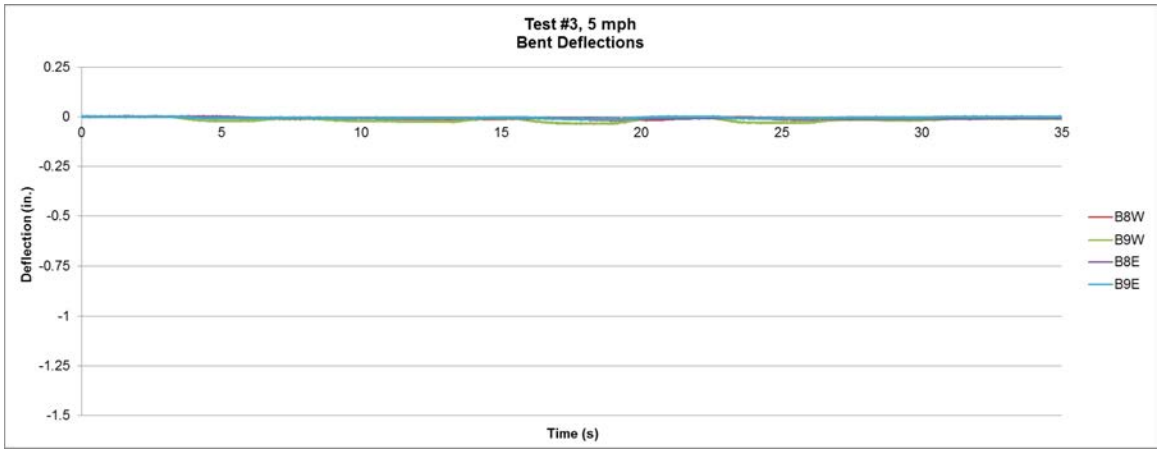

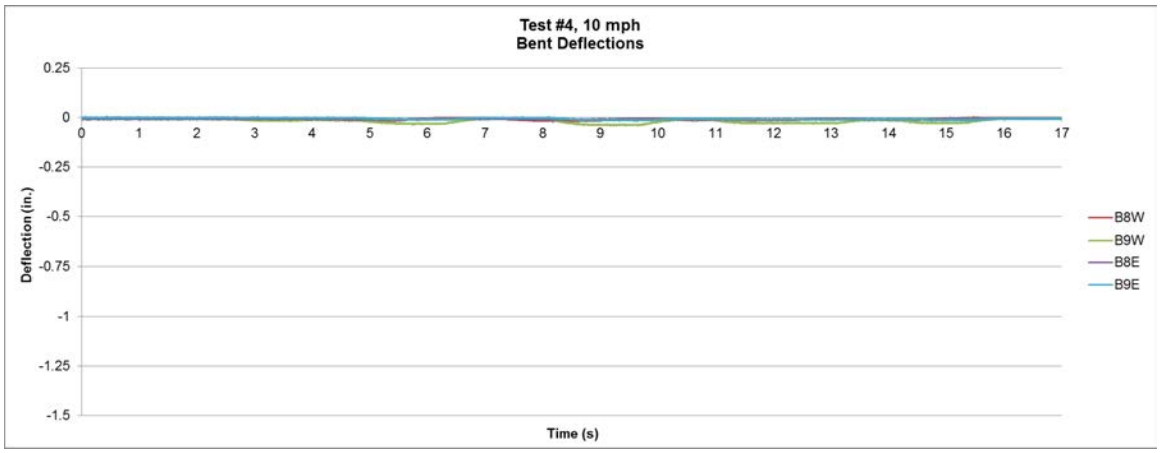

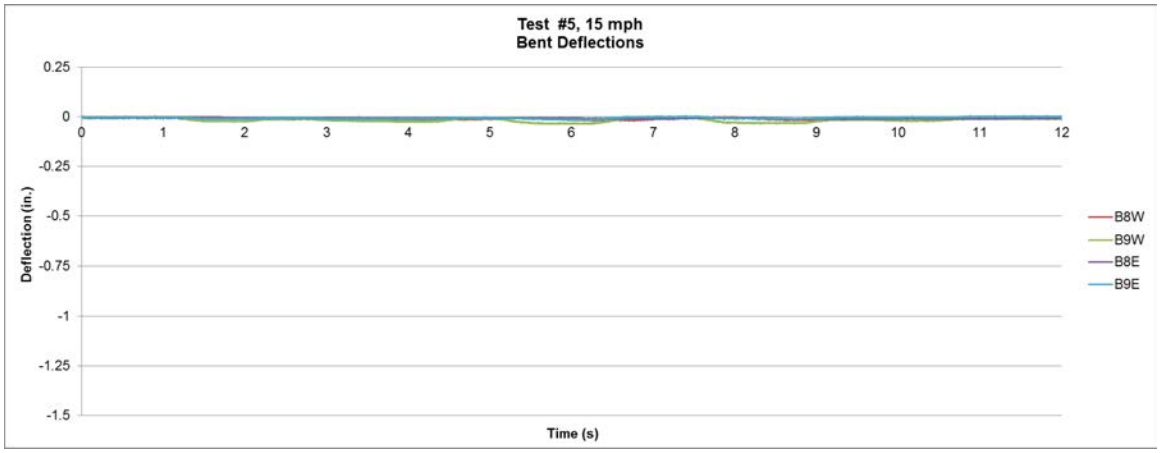

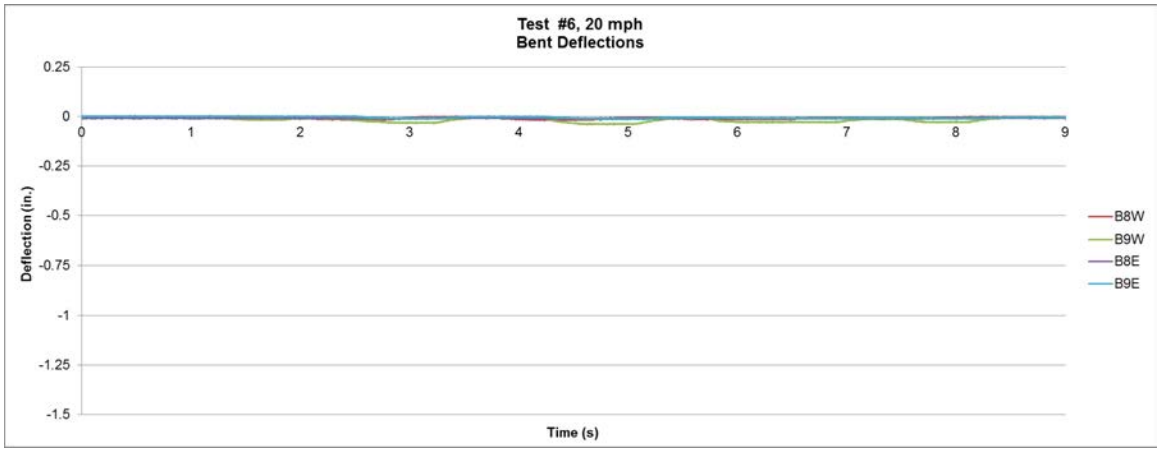
Test #6, 20 mph
Bent Deflections
0.25
0
-0.25
-0.5
-0.75
-1
-1.25
-1.5
Deflection (in.)
0
1
2
3
4
5
6
7
8
9
Time (s)
B8W
B9W
B8E
B9E

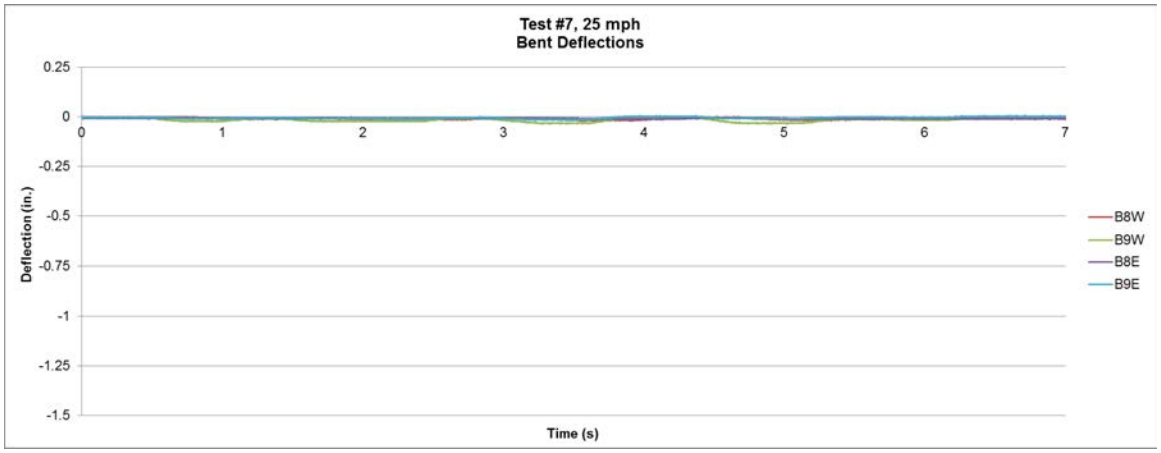
Test #7, 25 mph
Bent Deflections
0.25
0
-0.25
-0.5
-0.75
-1
-1.25
-1.5
Deflection (in.)
0
1
2
3
4
5
6
7
Time (s)
B8W
B9W
B8E
B9E

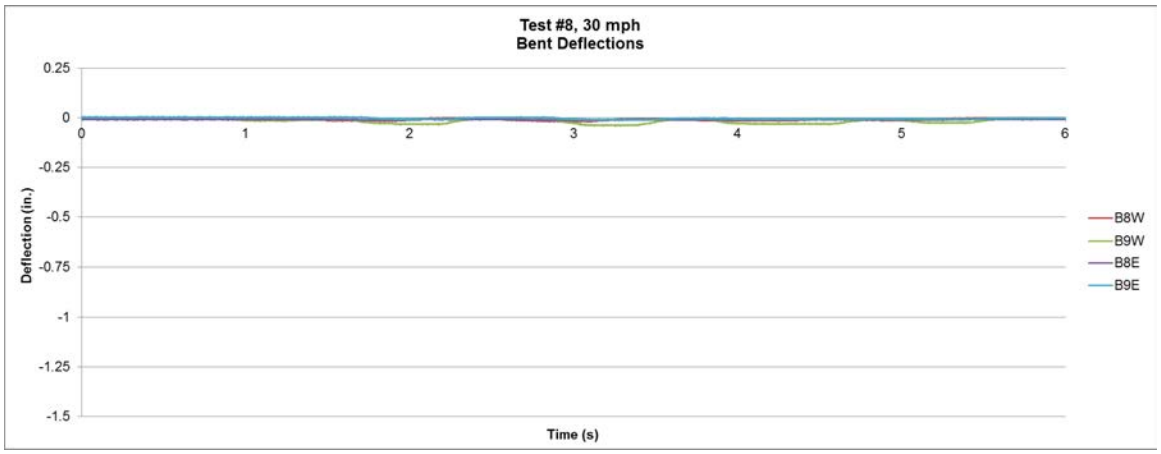
Test #8, 30 mph
Bent Deflections
0.25
0
-0.25
-0.5
-0.75
-1
-1.25
-1.5
Deflection (in.)
0
1
2
3
4
5
6
Time (s)
B8W
B9W
B8E
B9E

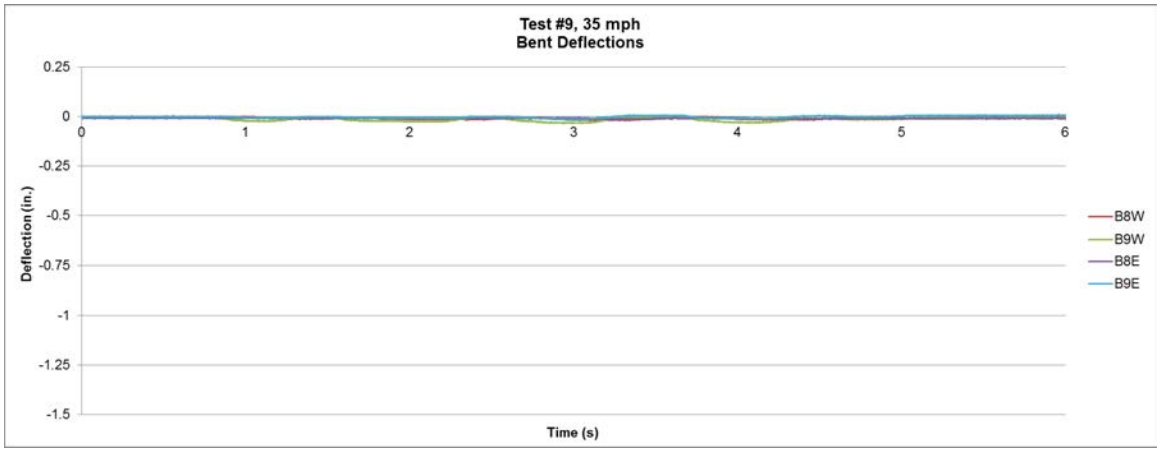
Test #9, 35 mph
Bent Deflections
0.25
0
-0.25
-0.5
-0.75
-1
-1.25
-1.5
Deflection (in.)
0
1
2
3
4
5
6
Time (s)
B8W
B9W
B8E
B9E

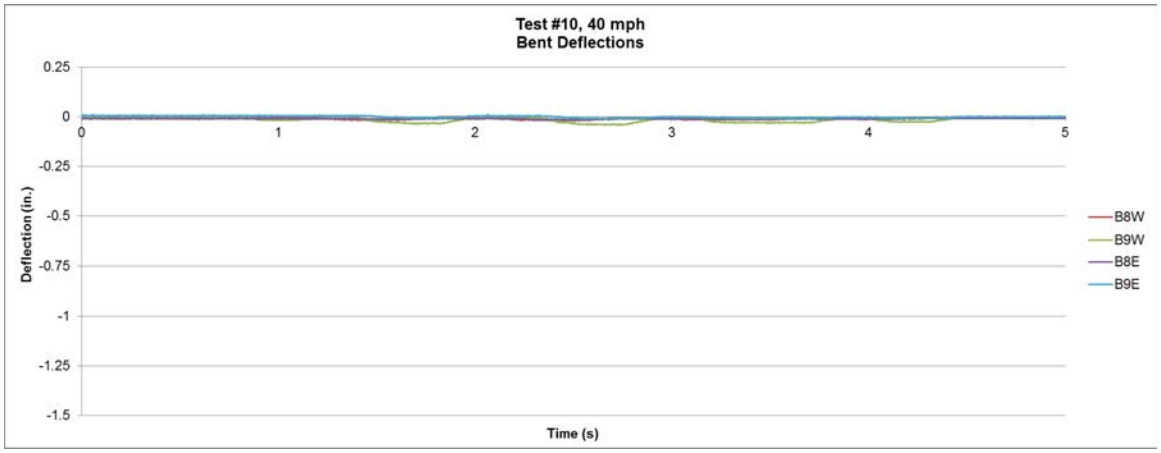
Test #10, 40 mph
Bent Deflections
0.25
0
-0.25
-0.5
-0.75
-1
-1.25
-1.5
Deflection (in.)
0
1
2
3
4
5
Time (s)
B8W
B9W
B8E
B9E

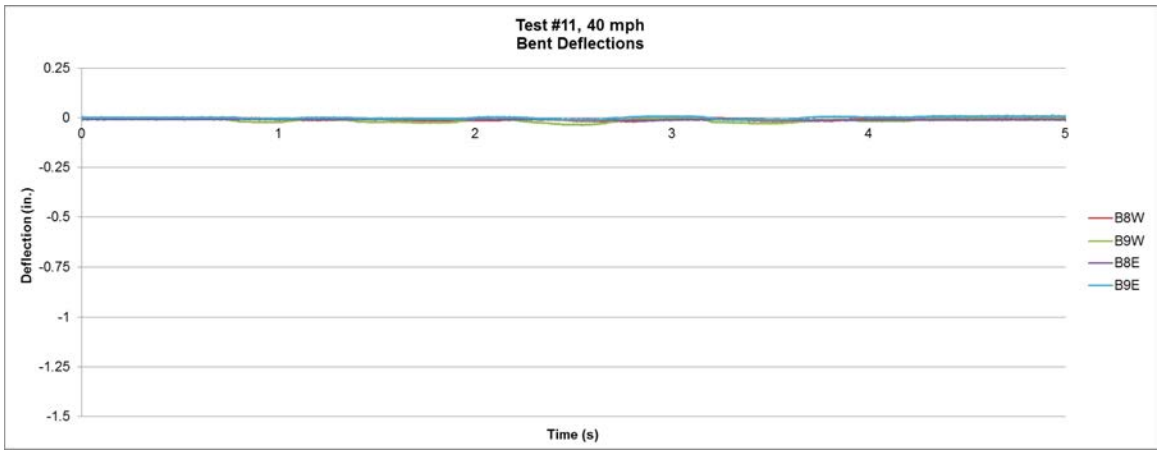
Test #11, 40 mph
Bent Deflections
0.25
0
-0.25
-0.5
-0.75
-1
-1.25
-1.5
Deflection (in.)
0
1
2
3
4
5
Time (s)
B8W
B9W
B8E
B9E

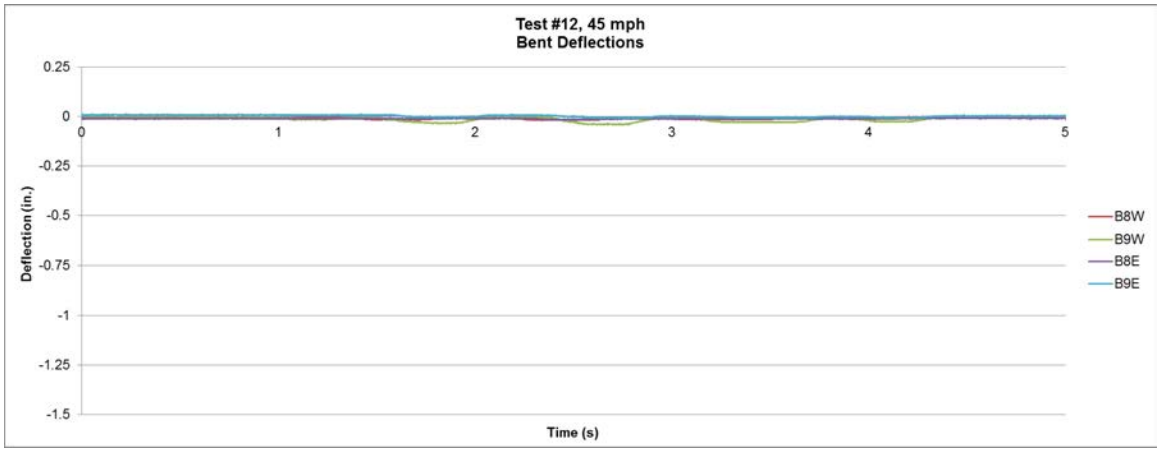
Test #12, 45 mph
Bent Deflections
0.25
0
-0.25
-0.5
-0.75
-1
-1.25
-1.5
Deflection (in.)
0
1
2
3
4
5
Time (s)
B8W
B9W
B8E
B9E

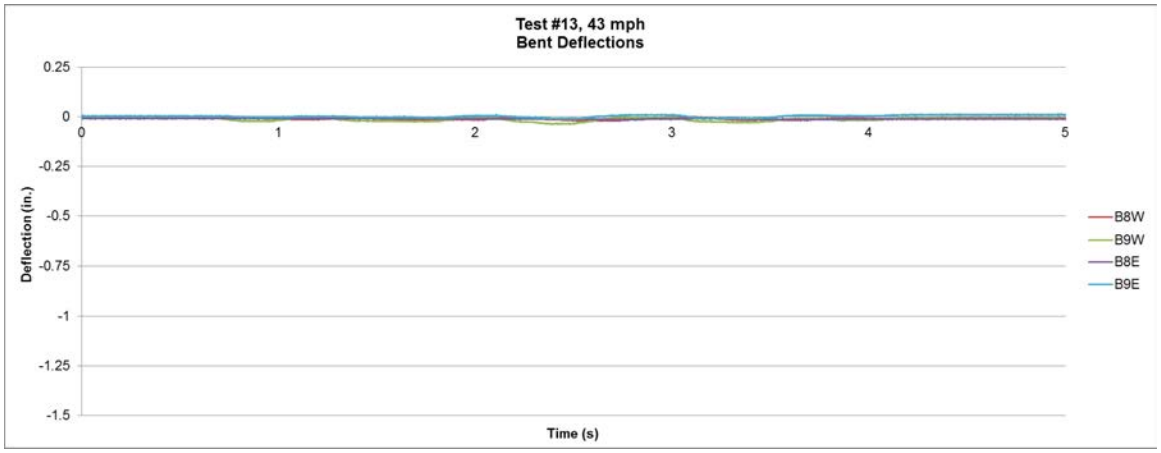
Test #13, 43 mph
Bent Deflections
0.25
0
-0.25
-0.5
-0.75
-1
-1.25
-1.5
Deflection (in.)
0
1
2
3
4
5
Time (s)
B8W
B9W
B8E
B9E

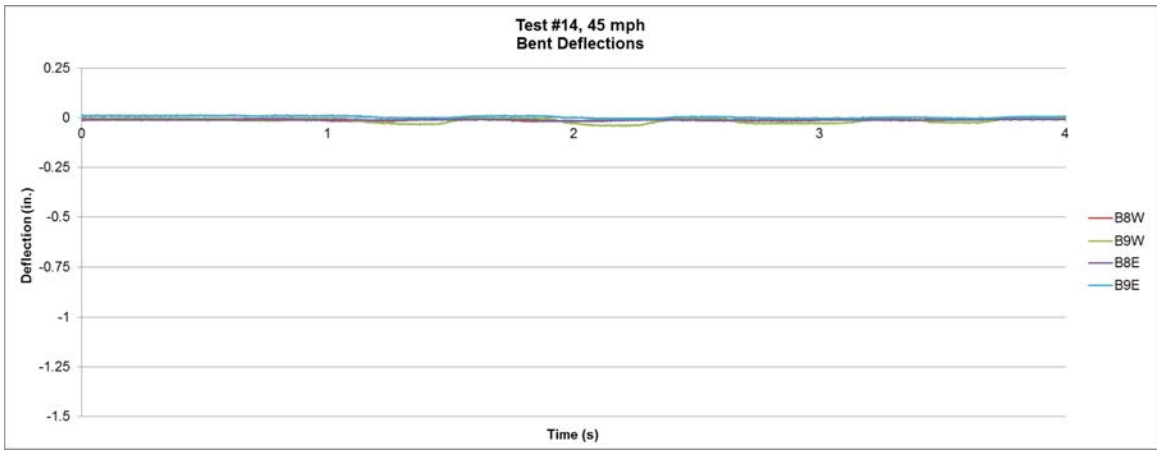
Test #14, 45 mph
Bent Deflections
0.25
0
-0.25
-0.5
-0.75
-1
-1.25
-1.5
Deflection (in.)
0
1
2
3
4
Time (s)
B8W
B9W
B8E
B9E

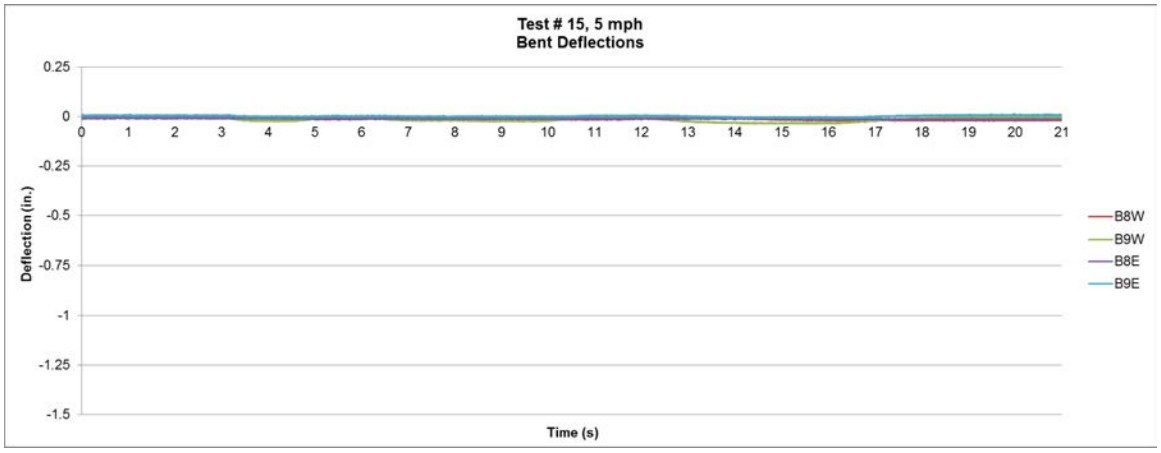
Test # 15, 5 mph
Bent Deflections
Deflection (in.)
Time (s)
B8W
B9W
B8E
B9E

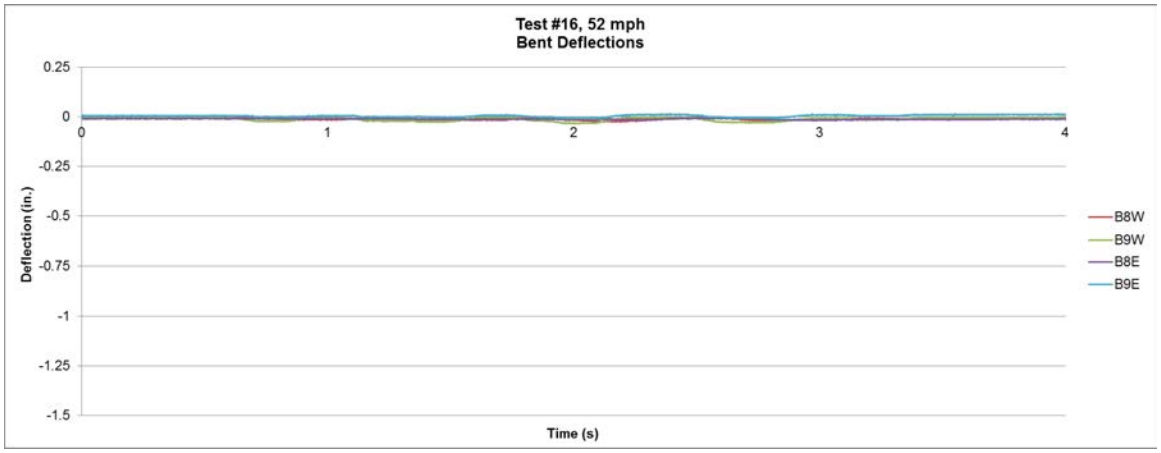
Test #16, 52 mph
Bent Deflections
Deflection (in.)
Time (s)
B8W
B9W
B8E
B9E

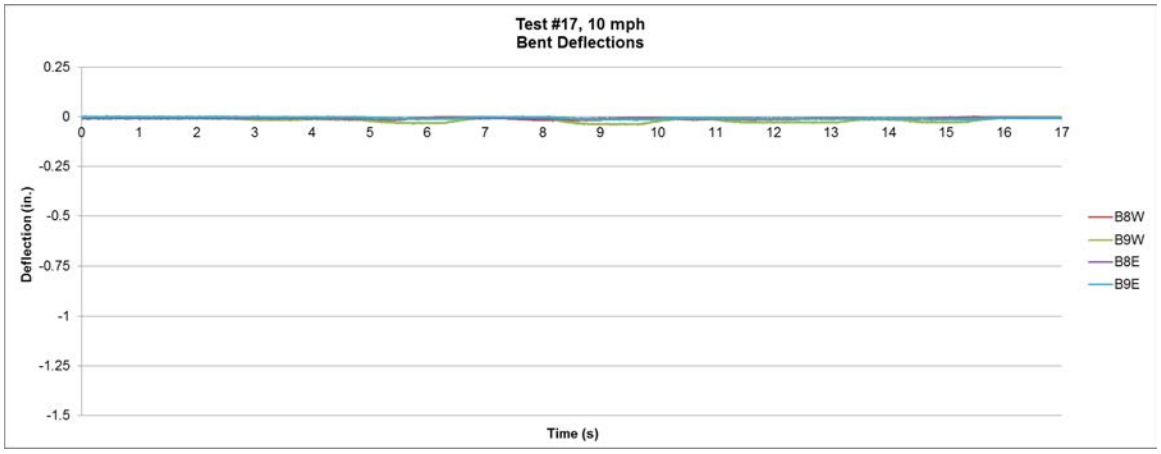
Test #17, 10 mph
Bent Deflections
Deflection (in.)
Time (s)
B8W
B9W
B8E
B9E

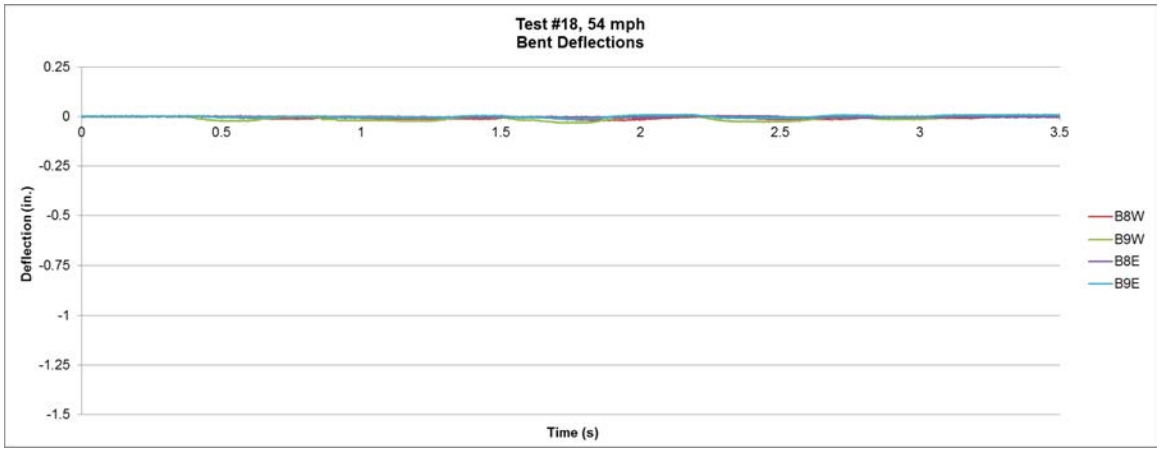
Test #18, 54 mph
Bent Deflections
Deflection (in.)
Time (s)
B8W
B9W
B8E
B9E

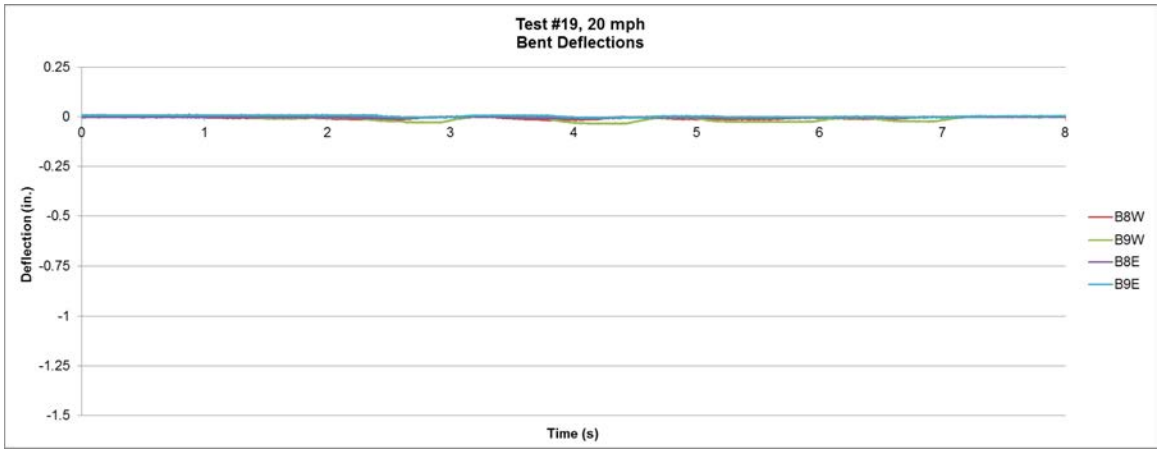
Test #19, 20 mph
Bent Deflections
Deflection (in.)
Time (s)
B8W
B9W
B8E
B9E

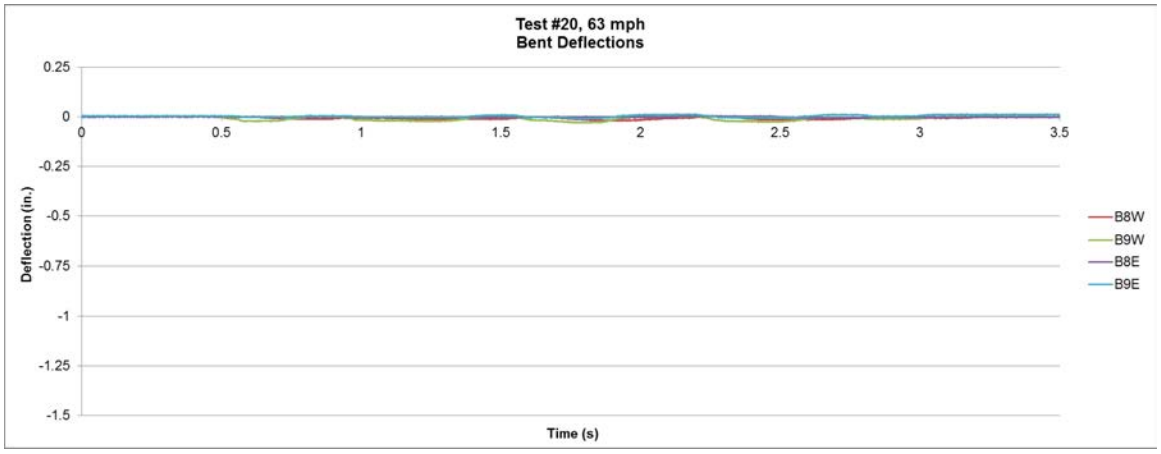
Test #20, 63 mph
Bent Deflections
Deflection (in.)
Time (s)
B8W
B9W
B8E
B9E

APPENDIX H

LARGE-SCALE BALLAST DECK EXPERIMENT TOTAL STRINGER DEFLECTION PLOTS

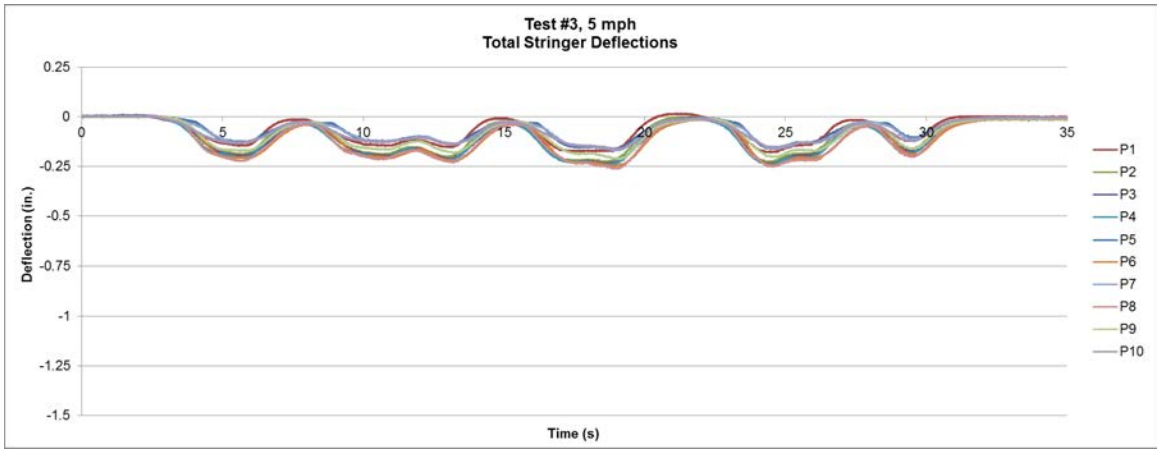

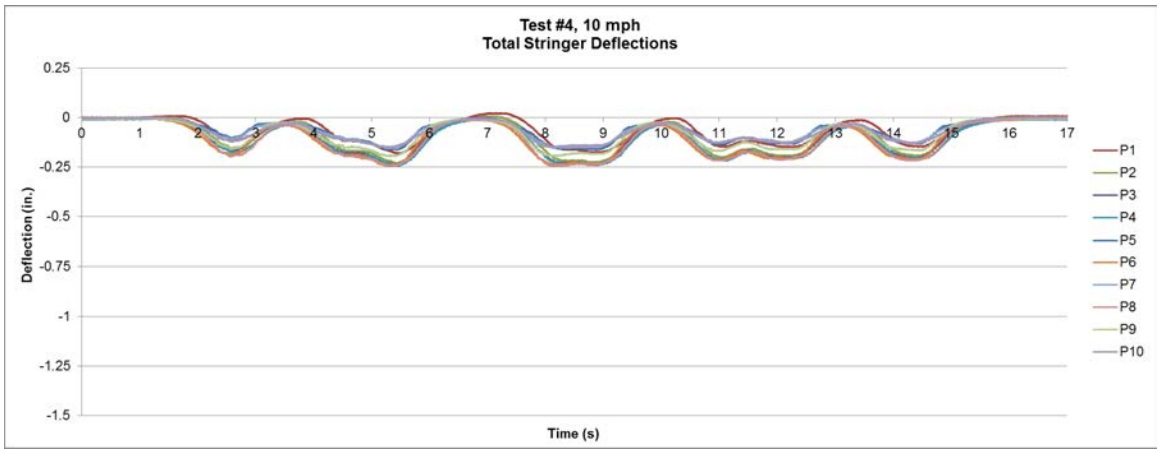

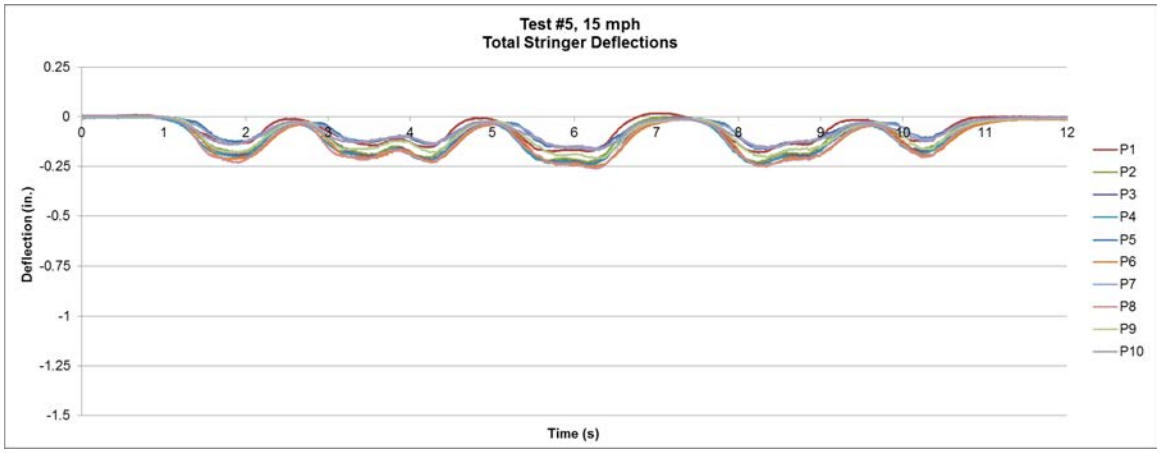

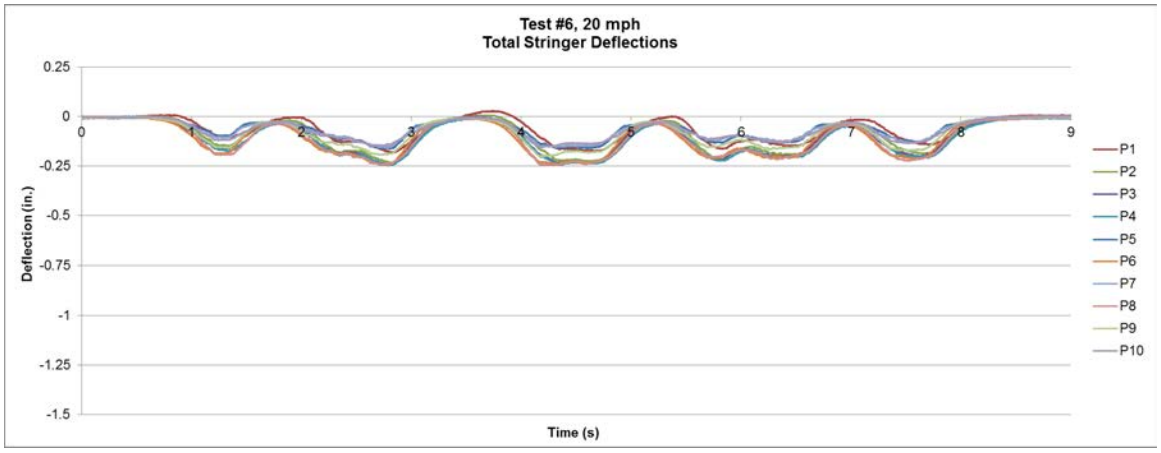
Test #6, 20 mph
Total Stringer Deflections
Deflection (in.)
Time (s)
P1
P2
P3
P4
P5
P6
P7
P8
P9
P10

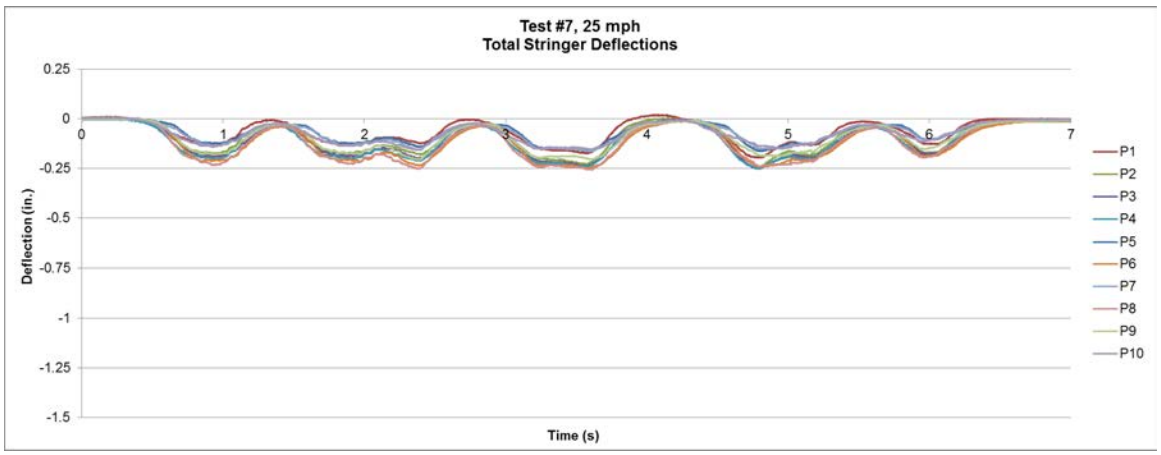
Test #7, 25 mph
Total Stringer Deflections
Deflection (in.)
Time (s)
P1
P2
P3
P4
P5
P6
P7
P8
P9
P10

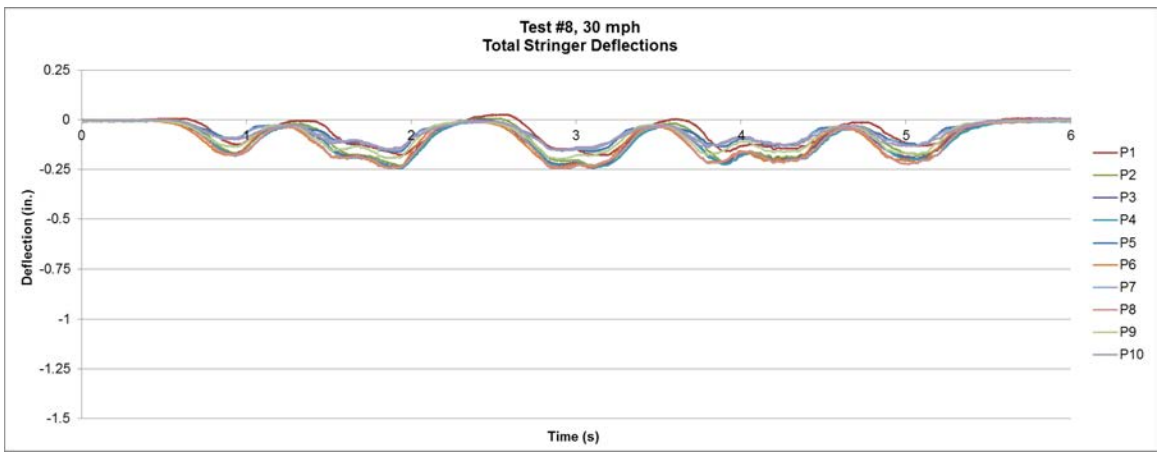
Test #8, 30 mph
Total Stringer Deflections
Deflection (in.)
Time (s)
P1
P2
P3
P4
P5
P6
P7
P8
P9
P10

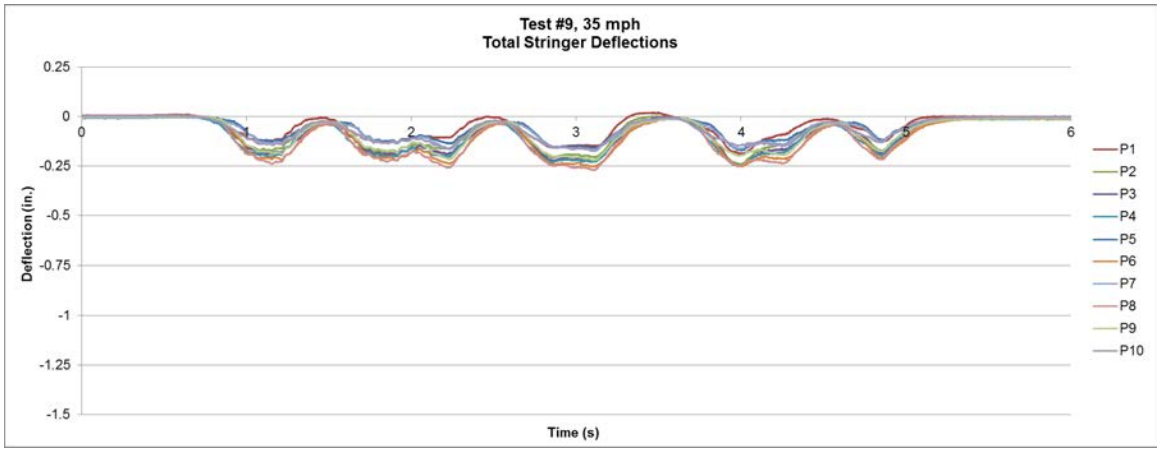
Test #9, 35 mph
Total Stringer Deflections
Deflection (in.)
Time (s)
P1
P2
P3
P4
P5
P6
P7
P8
P9
P10

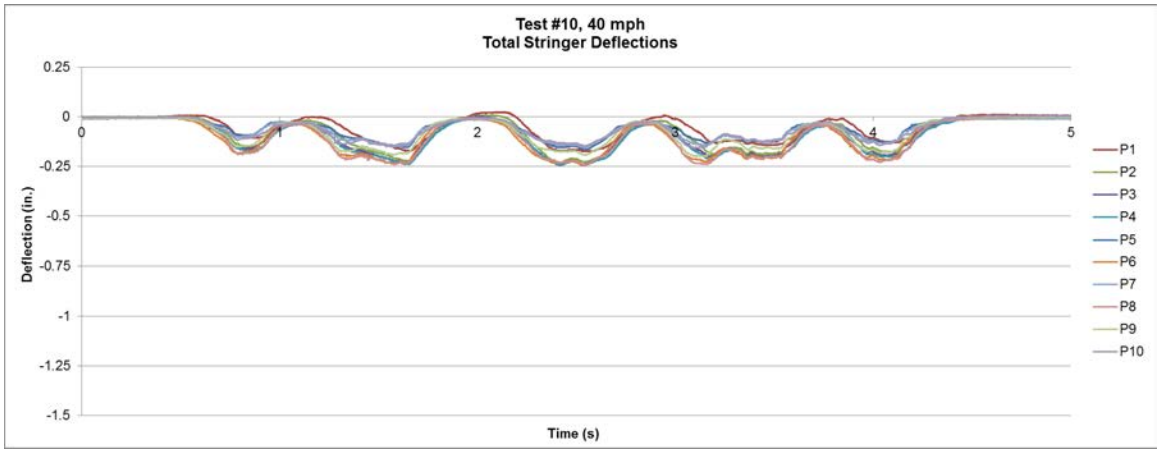
Test #10, 40 mph
Total Stringer Deflections
Deflection (in.)
Time (s)
P1
P2
P3
P4
P5
P6
P7
P8
P9
P10

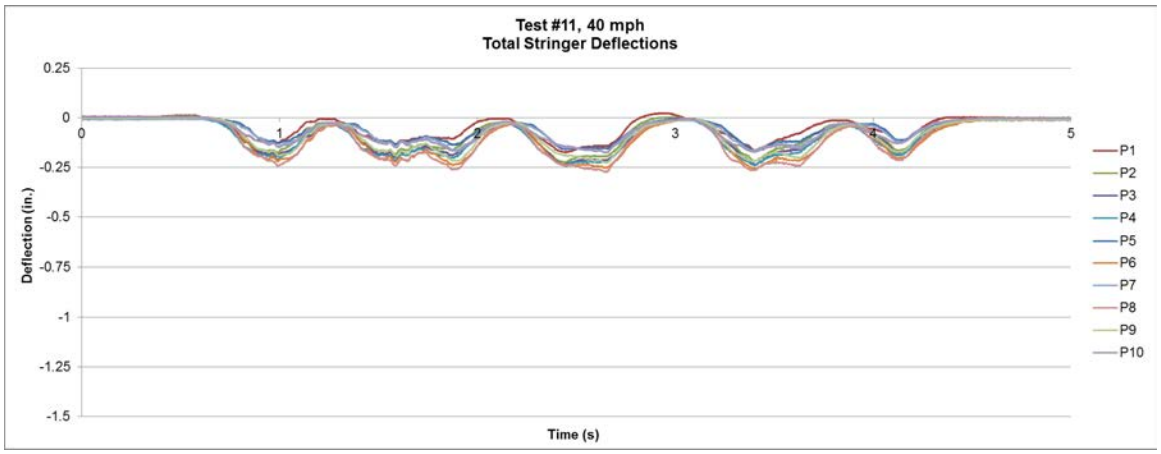
Test #11, 40 mph
Total Stringer Deflections
Deflection (in.)
Time (s)
P1
P2
P3
P4
P5
P6
P7
P8
P9
P10

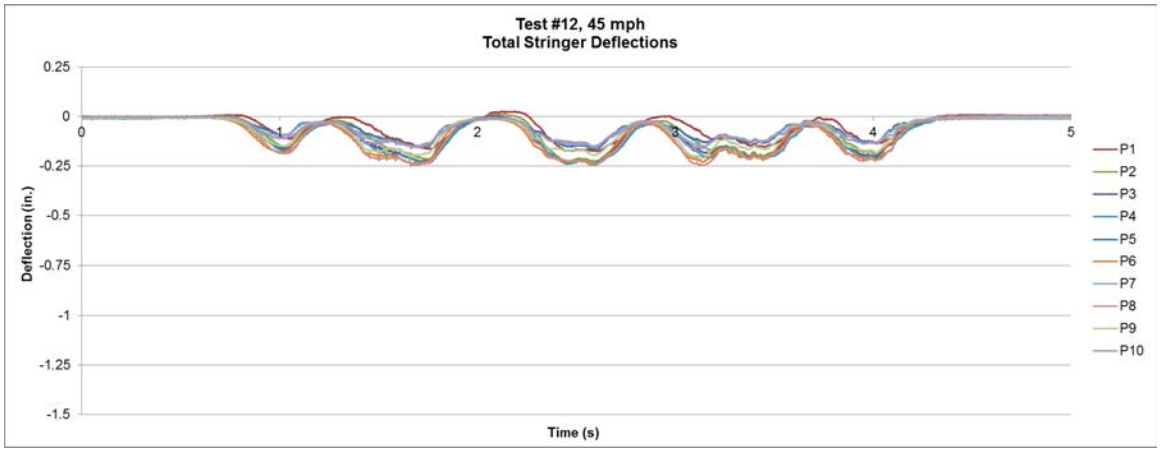
Test #12, 45 mph
Total Stringer Deflections
Deflection (in.)
Time (s)
P1
P2
P3
P4
P5
P6
P7
P8
P9
P10

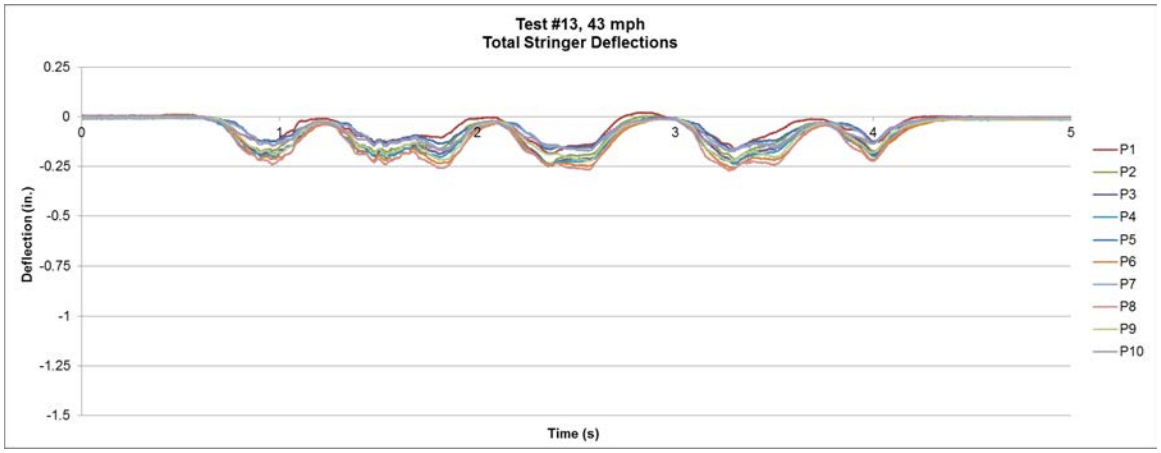
Test #13, 43 mph
Total Stringer Deflections
Deflection (in.)
Time (s)
P1
P2
P3
P4
P5
P6
P7
P8
P9
P10

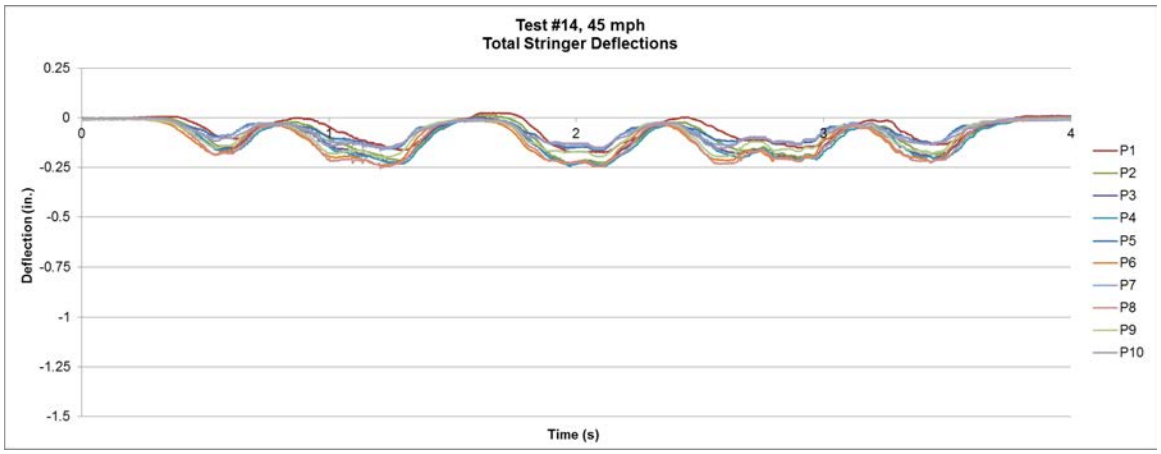
Test #14, 45 mph
Total Stringer Deflections
Deflection (in.)
Time (s)
P1
P2
P3
P4
P5
P6
P7
P8
P9
P10

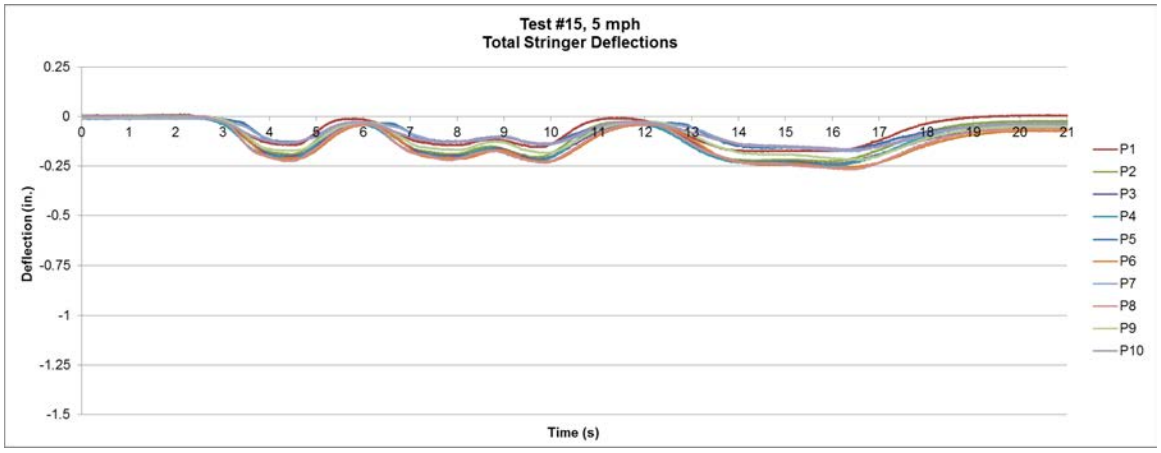
Test #15, 5 mph
Total Stringer Deflections
Deflection (in.)
Time (s)
P1
P2
P3
P4
P5
P6
P7
P8
P9
P10

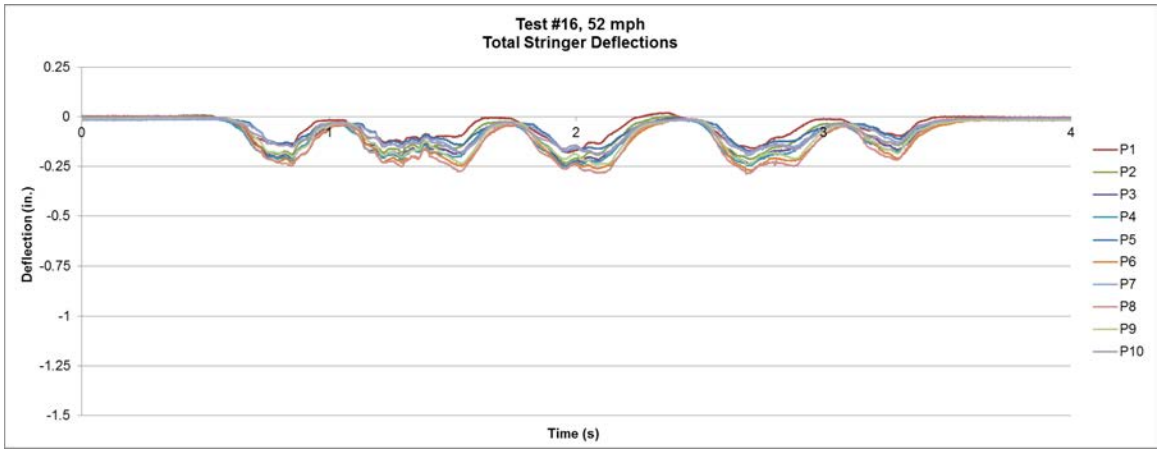
Test #16, 52 mph
Total Stringer Deflections
Deflection (in.)
Time (s)
P1
P2
P3
P4
P5
P6
P7
P8
P9
P10

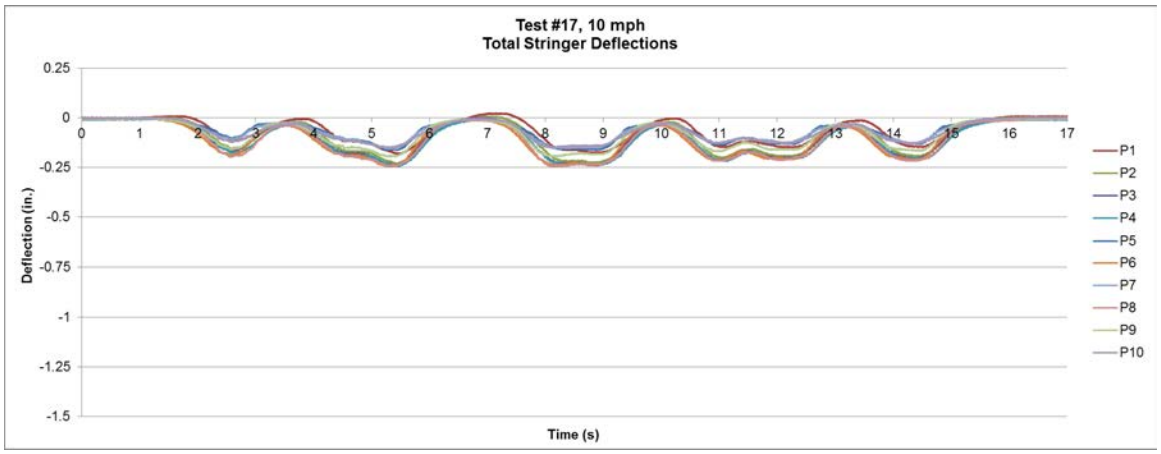
Test #17, 10 mph
Total Stringer Deflections
Deflection (in.)
Time (s)
P1
P2
P3
P4
P5
P6
P7
P8
P9
P10

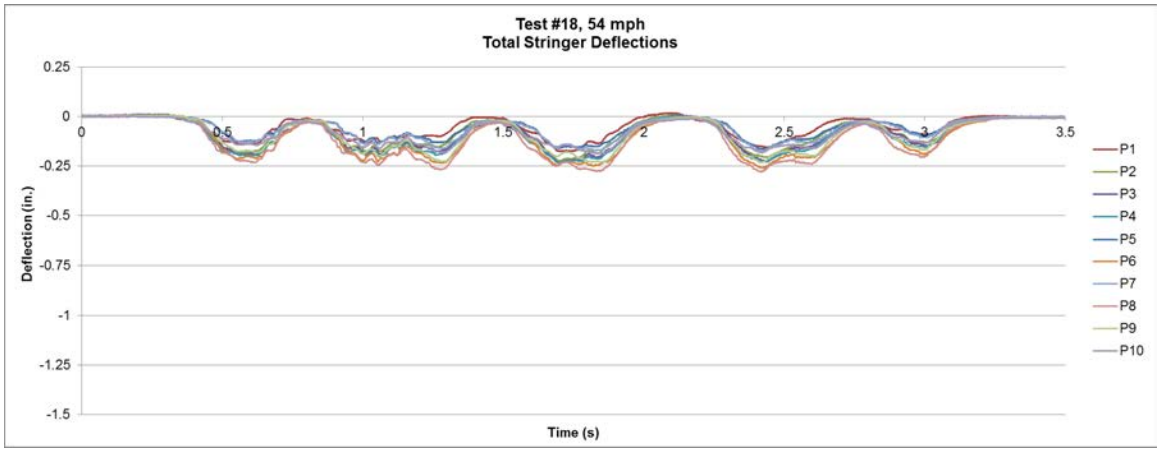
Test #18, 54 mph
Total Stringer Deflections
Deflection (in.)
Time (s)
P1
P2
P3
P4
P5
P6
P7
P8
P9
P10

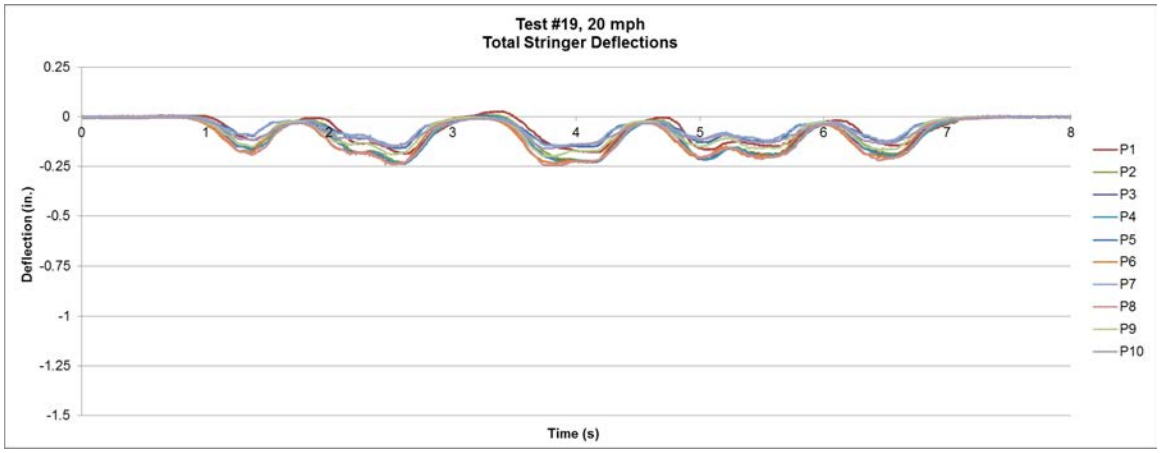
Test #19, 20 mph
Total Stringer Deflections
Deflection (in.)
Time (s)
P1
P2
P3
P4
P5
P6
P7
P8
P9
P10

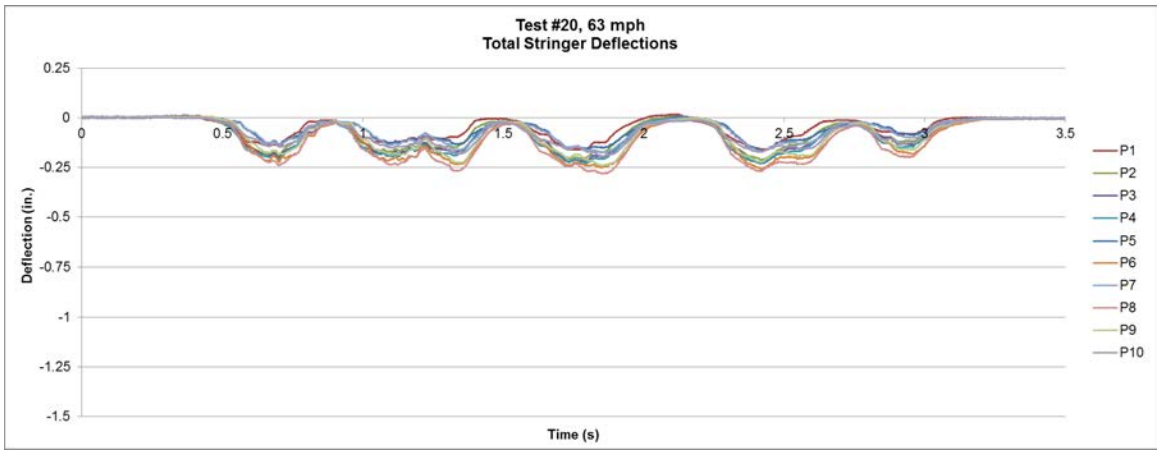
Test #20, 63 mph
Total Stringer Deflections
Deflection (in.)
Time (s)
P1
P2
P3
P4
P5
P6
P7
P8
P9
P10

APPENDIX I

LARGE-SCALE BALLAST DECK EXPERIMENT NET STRINGER DEFLECTION PLOTS

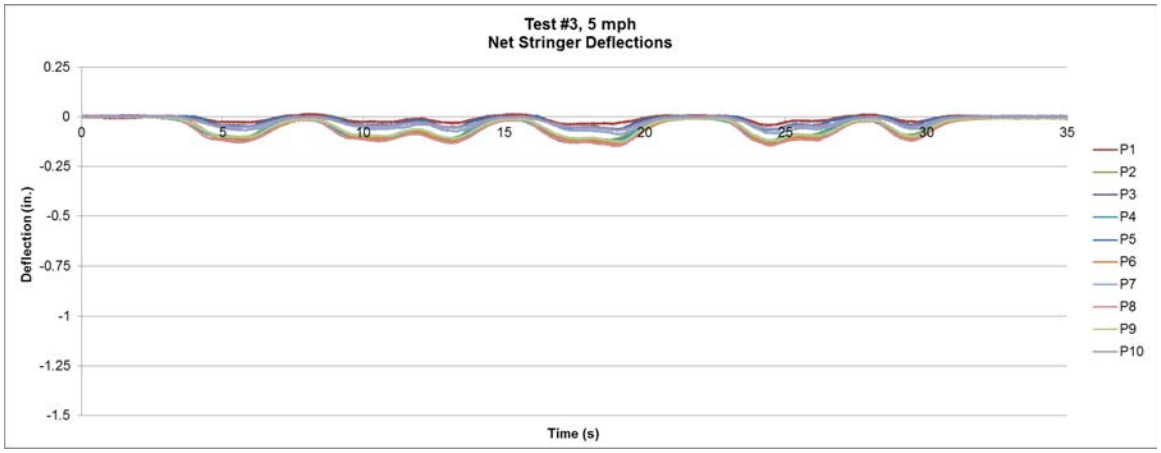

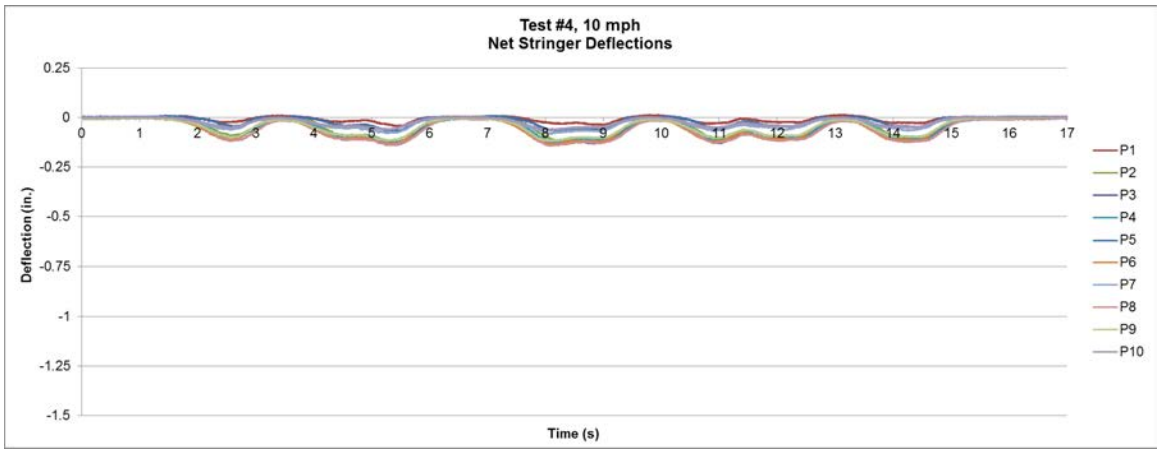

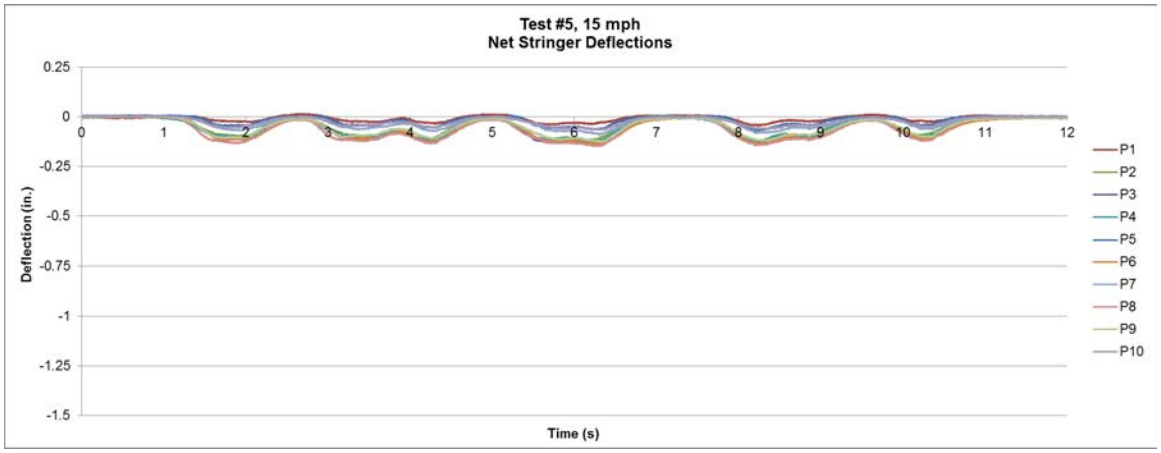

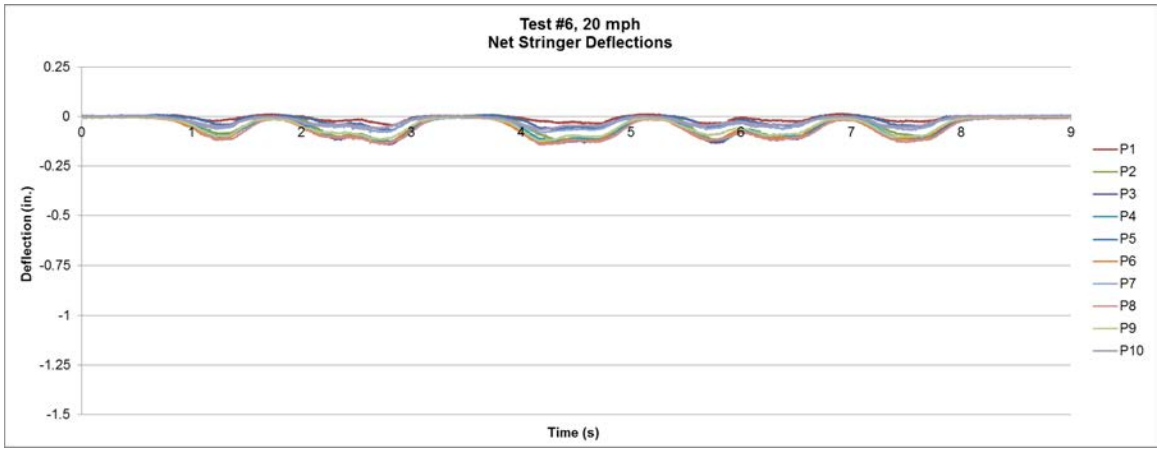
Test #6, 20 mph
Net Stringer Deflections
0.25
0
-0.25
-0.5
-0.75
-1
-1.25
-1.5
Deflection (in.)
0
1
2
3
4
5
6
7
8
9
Time (s)
P1
P2
P3
P4
P5
P6
P7
P8
P9
P10

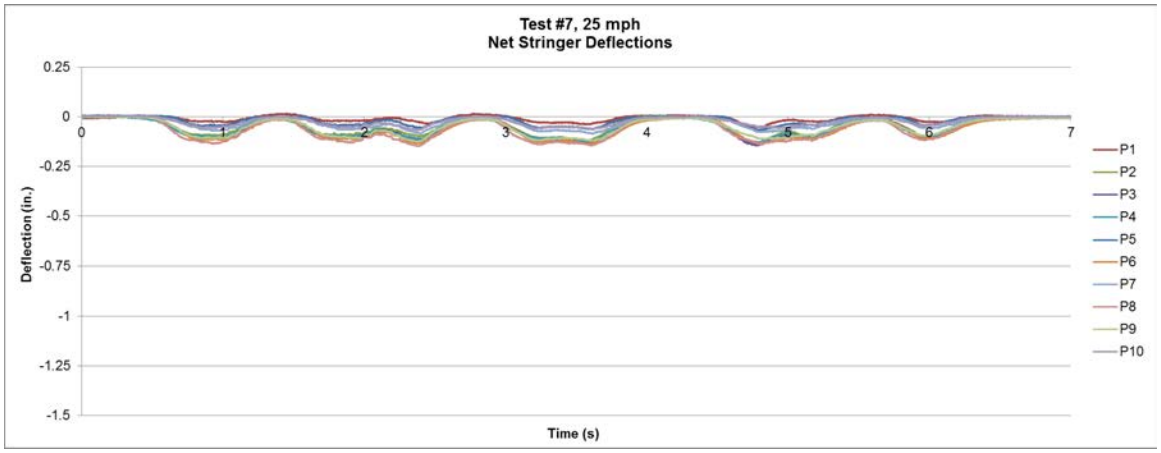
Test #7, 25 mph
Net Stringer Deflections
0.25
0
-0.25
-0.5
-0.75
-1
-1.25
-1.5
Deflection (in.)
0
1
2
3
4
5
6
7
Time (s)
P1
P2
P3
P4
P5
P6
P7
P8
P9
P10

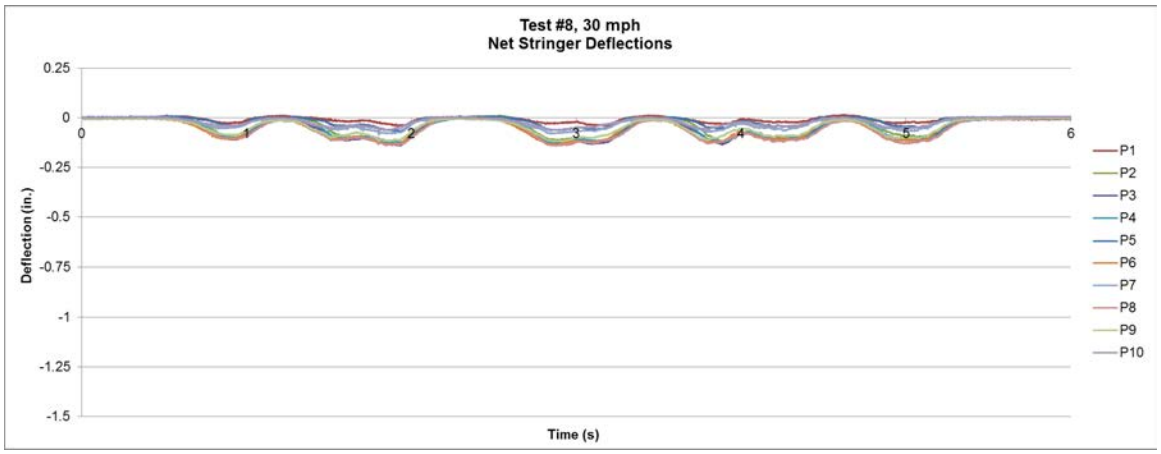
Test #8, 30 mph
Net Stringer Deflections
0.25
0
-0.25
-0.5
-0.75
-1
-1.25
-1.5
Deflection (in.)
0
1
2
3
4
5
6
Time (s)
P1
P2
P3
P4
P5
P6
P7
P8
P9
P10

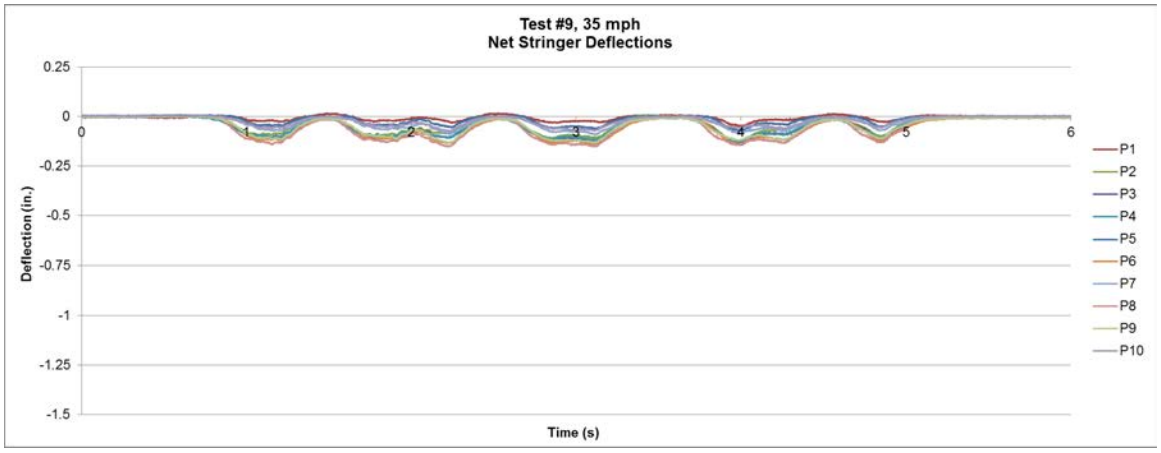
Test #9, 35 mph
Net Stringer Deflections
0.25
0
-0.25
-0.5
-0.75
-1
-1.25
-1.5
Deflection (in.)
0
1
2
3
4
5
6
Time (s)
P1
P2
P3
P4
P5
P6
P7
P8
P9
P10

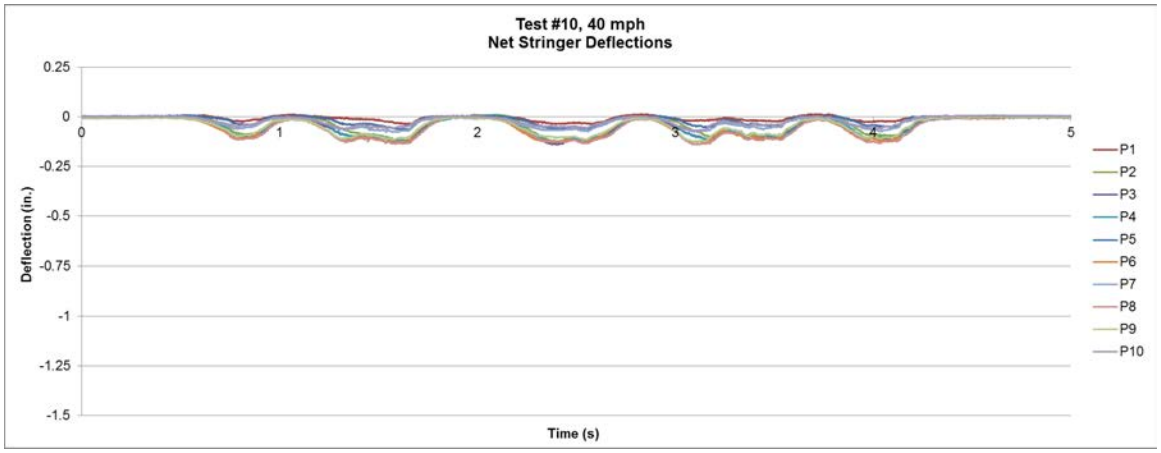
Test #10, 40 mph
Net Stringer Deflections
0.25
0
-0.25
-0.5
-0.75
-1
-1.25
-1.5
Deflection (in.)
0
1
2
3
4
5
Time (s)
P1
P2
P3
P4
P5
P6
P7
P8
P9
P10

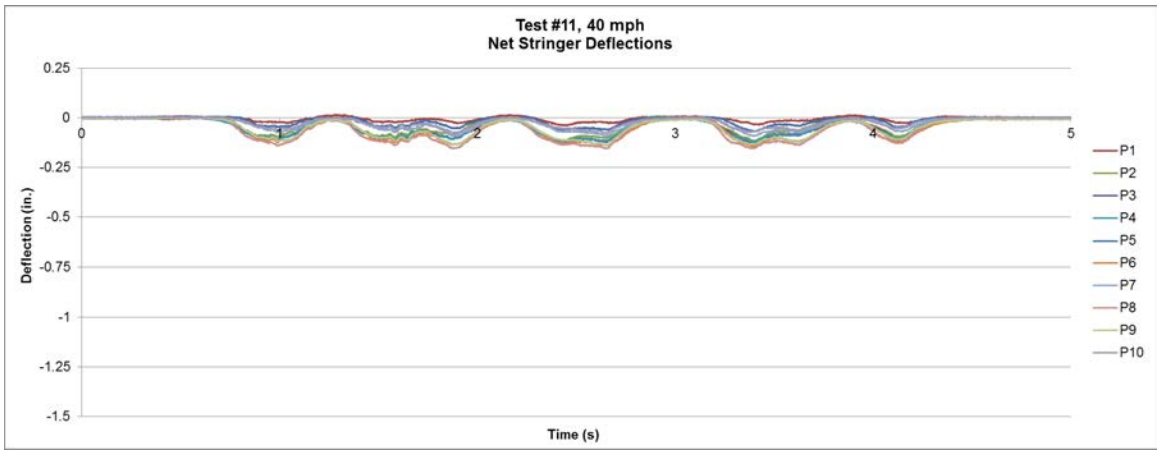
Test #11, 40 mph
Net Stringer Deflections
0.25
0
-0.25
-0.5
-0.75
-1
-1.25
-1.5
Deflection (in.)
0
1
2
3
4
5
Time (s)
P1
P2
P3
P4
P5
P6
P7
P8
P9
P10

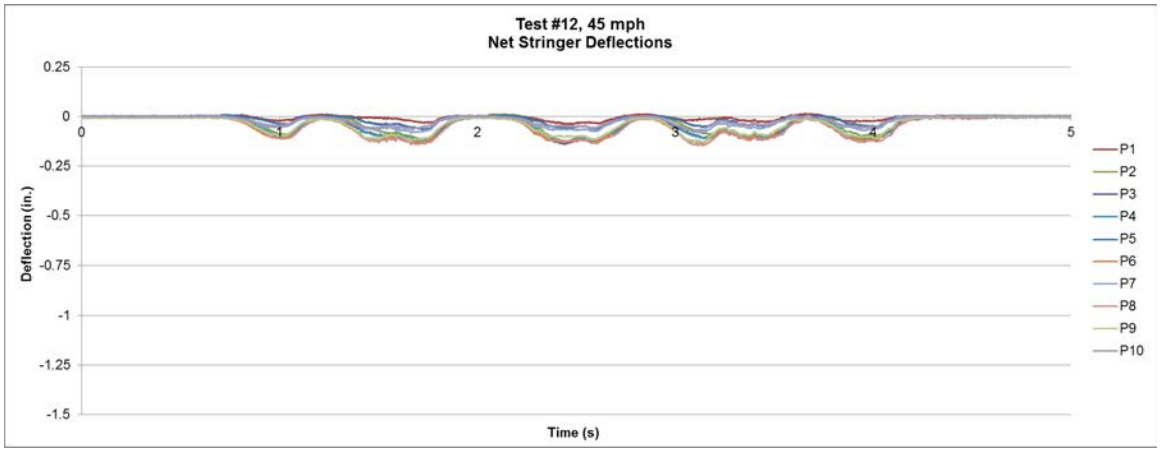
Test #12, 45 mph
Net Stringer Deflections
0.25
0
-0.25
-0.5
-0.75
-1
-1.25
-1.5
Deflection (in.)
0
1
2
3
4
5
Time (s)
P1
P2
P3
P4
P5
P6
P7
P8
P9
P10

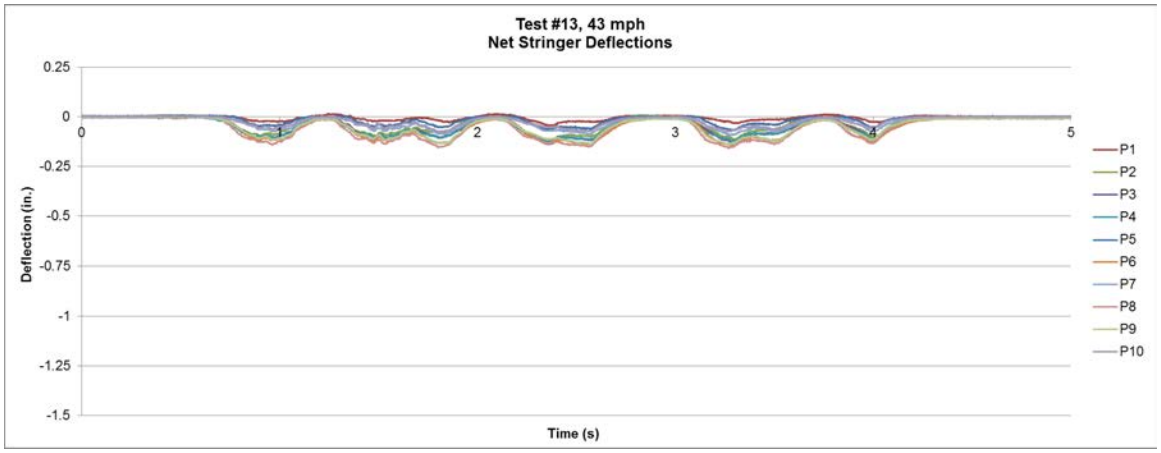
Test #13, 43 mph
Net Stringer Deflections
0.25
0
-0.25
-0.5
-0.75
-1
-1.25
-1.5
Deflection (in.)
0
1
2
3
4
5
Time (s)
P1
P2
P3
P4
P5
P6
P7
P8
P9
P10

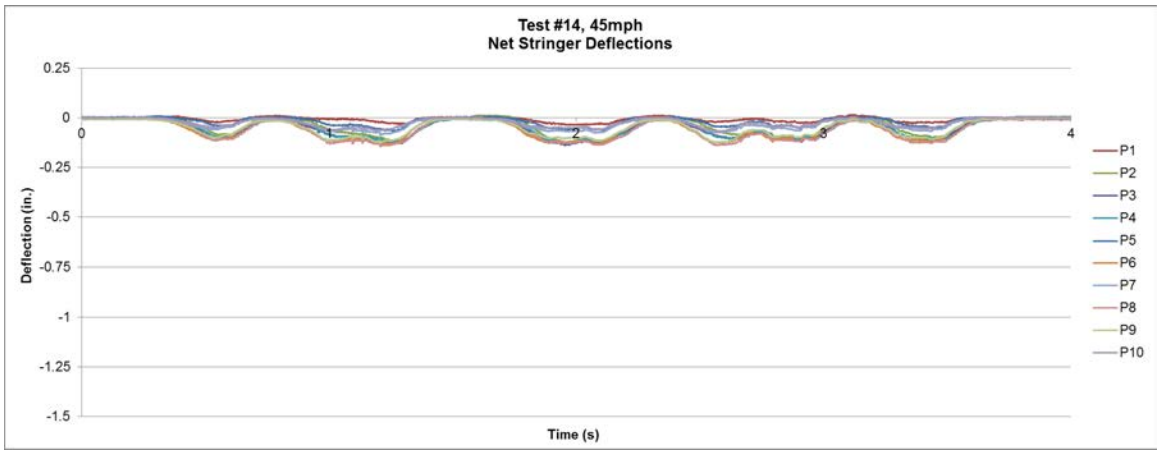
Test #14, 45mph
Net Stringer Deflections
0.25
0
-0.25
-0.5
-0.75
-1
-1.25
-1.5
Deflection (in.)
0
1
2
3
4
Time (s)
P1
P2
P3
P4
P5
P6
P7
P8
P9
P10

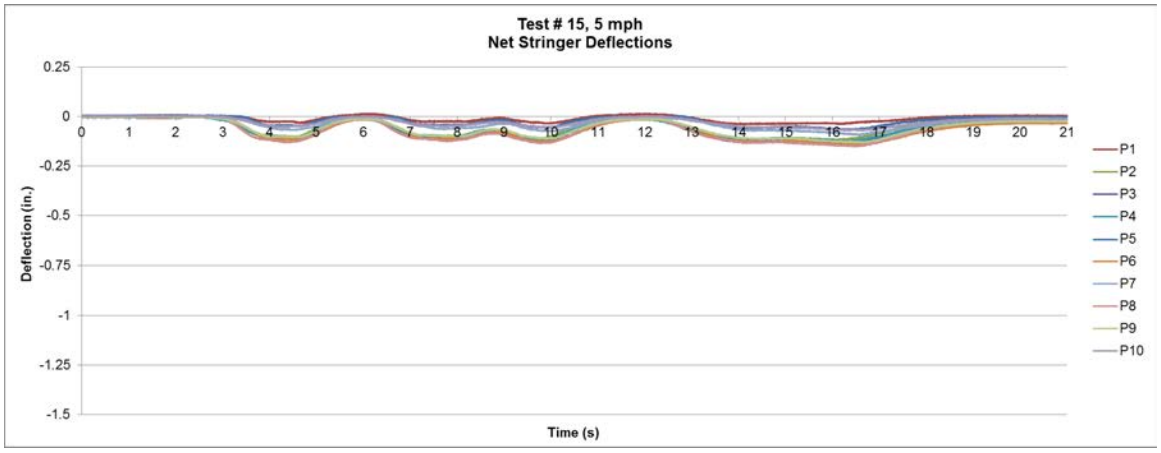
Test # 15, 5 mph
Net Stringer Deflections
Deflection (in.)
Time (s)
P1
P2
P3
P4
P5
P6
P7
P8
P9
P10

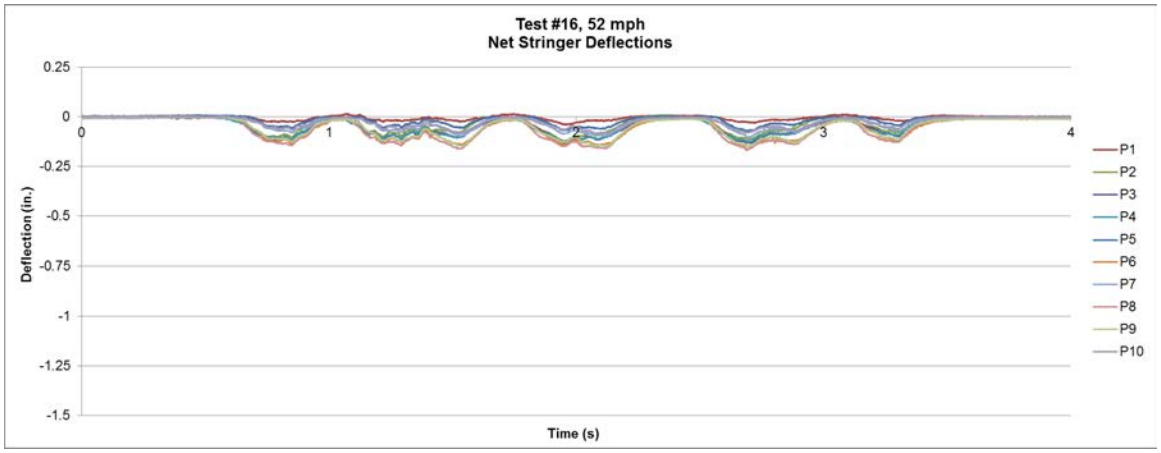
Test #16, 52 mph
Net Stringer Deflections
Deflection (in.)
Time (s)
P1
P2
P3
P4
P5
P6
P7
P8
P9
P10

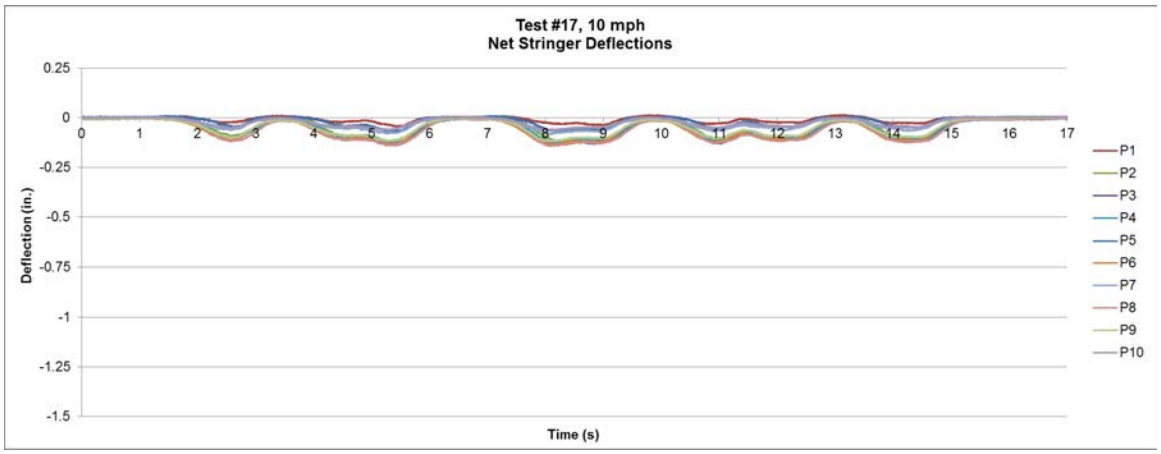
Test #17, 10 mph
Net Stringer Deflections
Deflection (in.)
Time (s)
P1
P2
P3
P4
P5
P6
P7
P8
P9
P10

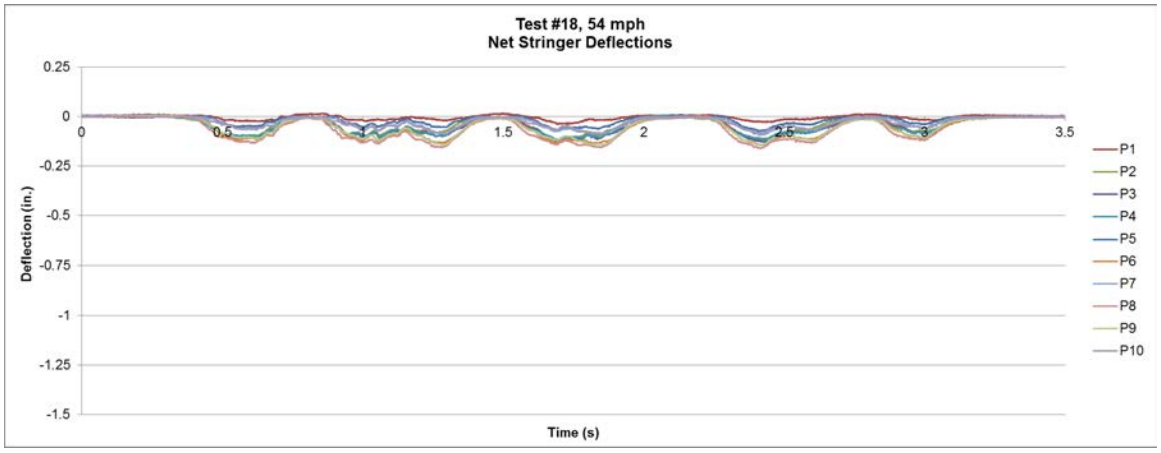
Test #18, 54 mph
Net Stringer Deflections
0.25
0
-0.25
-0.5
-0.75
-1
-1.25
-1.5
Deflection (in.)
0
0.5
1
1.5
2
2.5
3
3.5
Time (s)
P1
P2
P3
P4
P5
P6
P7
P8
P9
P10

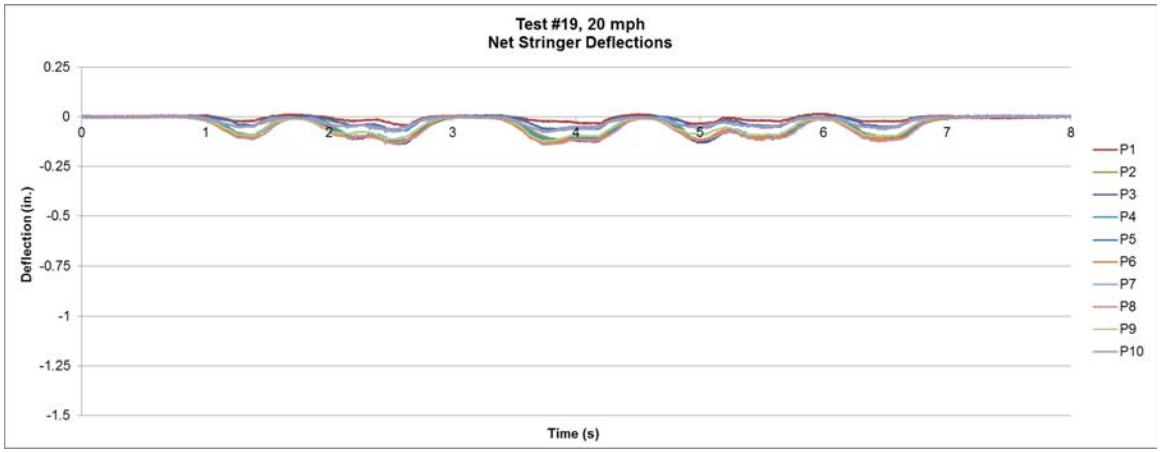
Test #19, 20 mph
Net Stringer Deflections
0.25
0
-0.25
-0.5
-0.75
-1
-1.25
-1.5
Deflection (in.)
0
1
2
3
4
5
6
7
8
Time (s)
P1
P2
P3
P4
P5
P6
P7
P8
P9
P10

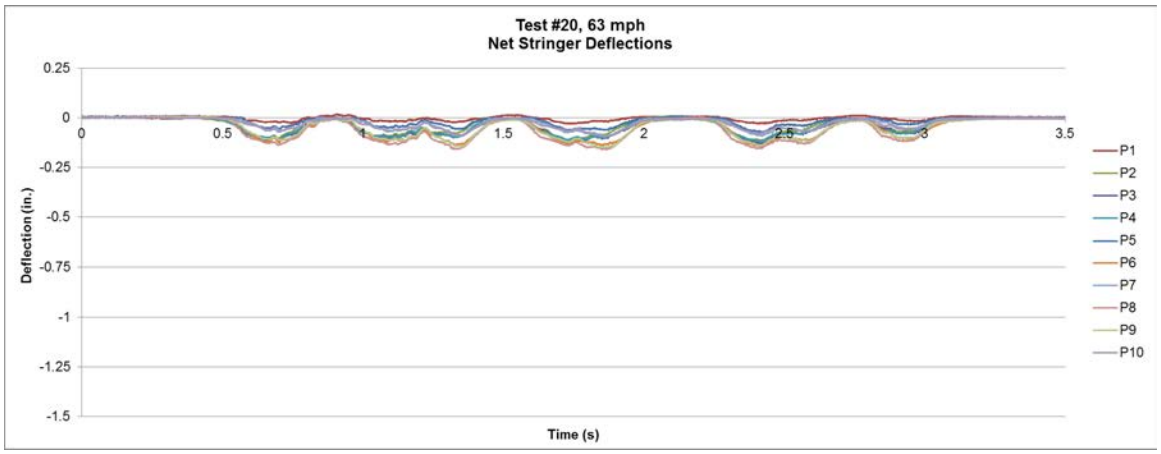
Test #20, 63 mph
Net Stringer Deflections
0.25
0
-0.25
-0.5
-0.75
-1
-1.25
-1.5
Deflection (in.)
0
0.5
1
1.5
2
2.5
3
3.5
Time (s)
P1
P2
P3
P4
P5
P6
P7
P8
P9
P10